Physics of Column Stability

Mazlumolhosseini, Ali Asghar

1975

LUND INSTITUTE OF TECHNOLOGY · LUND · SWEDEN · 1975
DIVISION OF STRUCTURAL MECHANICS AND CONCRETE CONSTRUCTION · BULLETIN 38

Ali Asghar Mazlumolhosseini

PHYSICS OF COLUMN STABILITY

PHYSICS OF COLUMN STABILITY

av

ALI ASGHAR MAZLUMOLHOSSEINI

AKADEMISK AVHANDLING

som med tillstånd av dekanus vid sektionen för väg- och vattenbyggnad vid Tekniska Högskolan i Lund framlägges till offentlig granskning för teknisk doktorsgrads vinnande tisdagen den 3 juni 1975 kl 09.00 å hörsal A, byggnaden för väg- och vatten, John Ericssons väg 1, Lund

LUND 1975

PHYSICS OF COLUMN STABILITY

Ali Asghar Mazlumolhosseini

DIVISION OF STRUCTURAL MECHANICS AND CONCRETE CONSTRUCTION,

LUND INSTITUTE OF TECHNOLOGY,

LUND, SWEDEN

Particular thanks are due my brother's wife Virginia Mazlumol-hosseini for her determination and her devotion to help completing this work by spending all her free time in typing the manuscript; Miss Tarja Aunola and Miss Lisbeth Henning for helpful assistance in typing parts of the manuscript; Mrs. Ann Schollin for skillfully drawing the diagrams; My brother Mahmood Mazlumolhosseini for proof reading the manuscript and checking the derivations of the equations in some parts; and Tekn. Dr. Erik Plem for checking the derivations of the equations in Appendix C.

CONDENSED OUTLINE

This dissertation reexamines the fundamental concepts of column stability and develops a general theory on the basis of a dynamic approach. Special attention is paid to exploring the buckling behaviour of an inelastic column with arbitrary stress strain diagram. The introductory part of the dissertation is devoted to a review of the well-known concepts of elastic stability for the twofold objective of partly renewing a knowledge of the fundamental principles and partly gaining a clear understanding of the significance of the dynamic concept. The general arguments presented herein are connected in a sequential chain with the attention predominantly focused on the physics of the problem. Numerical examples based on the study of simple columns are presented in order to illustrate the general discussion. Each column is studied during two distinct phases: 1) the buckling behaviour simultaneous with the increase of axial load (buckling phase 1); and 2) behaviour under the influence of a constant axial load (buckling phase 2).

Three column models are used in the study of inelastic buckling, the first two of which are assumed to be initially perfect columns with bilinear stress strain diagram, whereas the third model simulates an initially imperfect column with arbitrary stress strain diagram. The first model analyzes the load-deflection behaviour of a simple perfect inelastic column loaded above the tangent modulus load, up to a stage where either strain reversal begins to occur in the column, or the reduced modulus load is attained before the occurrence of strain reversal; the analysis of this model shows that for certain parameter combinations, the axial load can increase considerably above the tangent modulus load without the occurrence of strain reversal.

The second model studies the complete process of lateral deflection of the simple column for axial loads between the tangent modulus and the reduced modulus loads, taking into account the possibility of strain reversal simultaneous with loading; the buckling behaviour of this model under the influence of constant axial load (during buckling phase 2), and below the reduced modulus load level, may be characterized by a dynamically stable oscillatory behaviour which turns into a simple harmonic motion after three motion reversal positions subsequent to the end of buckling phase 1 (just at the time the axial load ceases to increase). The amplitude of this simple harmonic motion is usually small.

The third model thcroughly studies the buckling properties of an imperfect inelastic column with arbitrary stress strain diagram. This model can simulate all the buckling phenomena analyzed by the first two models; furthermore, this model is capable of determining the influence of variations of column parameters on the size of the maximum column load.

Three column types shown in Fig. I are utilized in the development of the stability concepts.

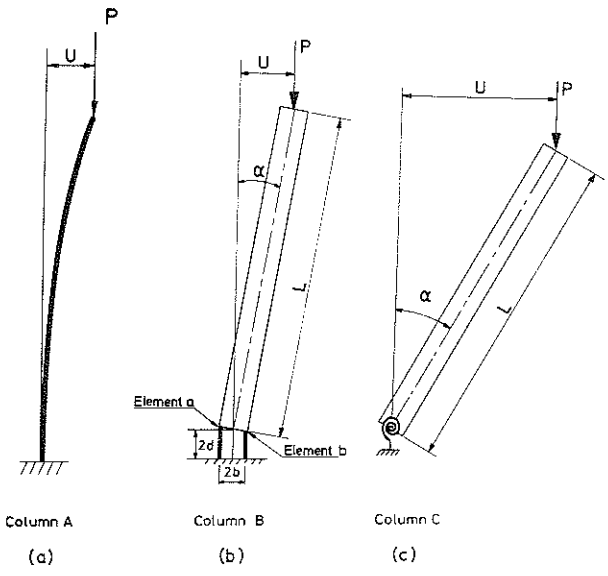

THREE COLUMN TYPES USED IN THE PRESENT WORK

FIG. I

Column A is solely used for clarifying the description of fundamental ideas. Column B is used for obtaining numerical results in the illustrations taken from various places in the main body of the dissertation and appearing in this summary in Figs. III through XIV. Column C is used for evaluation of the buckling behaviour depicted in Fig. II below. The results described in the following illustrations are obtained by computations based on 8 computer programs developed in this dissertation.

The following notations are used in the description of Column B:

A = area of one hinge element; b = half the width of the hinge; d = half the depth of the hinge; L = column length; M = total column mass; E_o = the initial modulus of elasticity; E_t = the tangent modulus; U_o = initial end deflection; V_o = initial end velocity; X_o = eccentricity; and c = loading rate.

Fig. II reveals the complete buckling behaviour of a perfect elastic column with the following data (see Column C):

L = 2.5 m; C = proportionality constant between internal moment and spring rotation = 25 000 Newton-meters; M = 100 kg; c = 2 000 Newtons/sec.; U_o = .001 cm; and V_o = 0 cm/sec.

Figs. II(a) and (b) show the static load deflection behaviour according to the Small and Large Deflection Theories respectively. Figs. II(c) and

(d) show the corresponding dynamic behaviour. When the axial load ceases to increase, the dynamically unstable column would move towards the equilibrium position according to the Large Displacement Theory. According to the Small Displacement Theory, no lateral equilibrium position above the Euler load exists in which case the column would continue to bow indefinitely forwards. Fig. II(b) shows that excessive lateral deflections are required for the slight increases of the axial load above the Euler load, whereby in subsequent illustrations the Small Displacement Theory is considered to be satisfactorily valid.

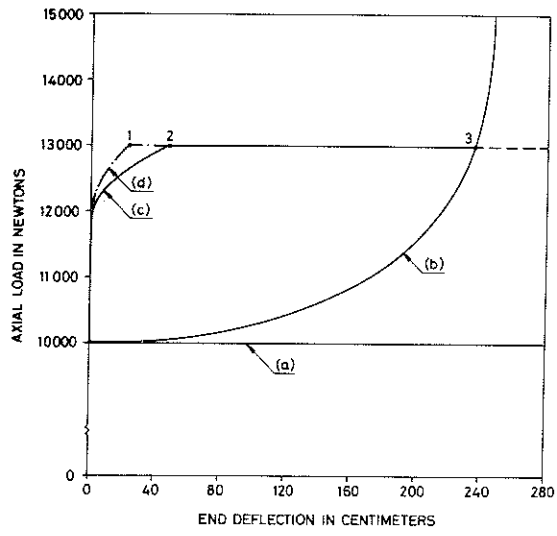

LOAD DEFLECTION BEHAVIOUR OF SIMPLE ELASTIC COLUMN (COLUMN C): (a) ACCORDING TO THE STATIC SMALL DISPLACEMENT THEORY; (b) ACCORDING TO THE STATIC LARGE DISPLACEMENT THEORY; (c) AND (d) THE UNSTABLE BEHAVIOUR SIMULTANEOUS WITH LOADING FOR LOADS ABOVE THE EULER LOAD ACCORDING TO THE DYNAMIC SMALL AND LARGE DISPLACEMENT THEORIES RESPECTIVELY

FIG. II

Fig. III depicts the buckling behaviour of the imperfect elastic column with the following data:

$A = 5\ cm^2$; $b = 5$ cm; $d = 10$ cm; $L = 5$ m; $M = 500$ kg; $E_o = 10^{10}$ Newtons/m^2; $U_o = V_o = 0$; $X_o = .1$ cm; $c = 5\,000$ Newtons/sec. for Fig.III(b), and $c = 2\,000$ Newtons/sec. for Fig.III(a).

From a study of Figs. II and III it follows that the temporary dynamic position of the column may considerably deviate from the corresponding static position. This physical phenomenon, which does not influence the final position of an elastic column without energy losses, may become significant for an inelastic column whose behaviour may be affected by the deformation and strain reversal history. The significance of this phenomenon will now be explored for an inelastic column with bilinear or arbitrary stress strain diagram, see Figs. IV(a) and (b).

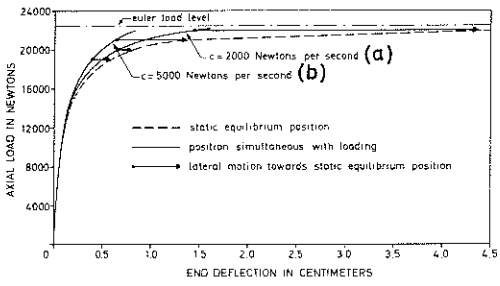

LOAD DEFLECTION BEHAVIOUR OF ECCENTRICALLY LOADED SIMPLE ELASTIC COLUMN FOR THE GIVEN DATA

FIG. III

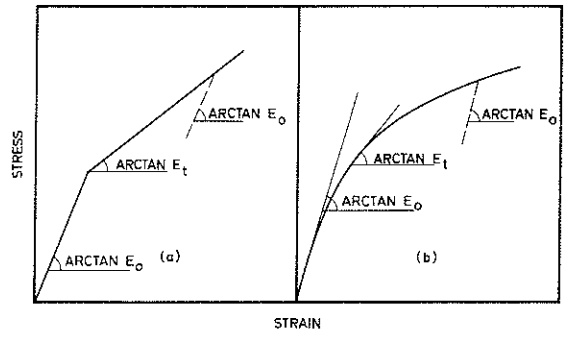

STRESS STRAIN DIAGRAM, (a) BILINEAR CURVE; (b) ARBITRARY CURVE

FIG. IV

The partial load deflection behaviour of the simple initially perfect inelastic column with bilinear stress strain diagram for the increase of axial load, ΔP, above the tangent modulus load is shown in Fig. V. The reference column marked in Fig. V has the following numerical data:

$A = 5\ cm^2$; $b = 5$ cm; $d = 10$ cm; $L = 5$ m; $M = 500$ kg; $E_o = 2 \times 10^{10}$ Newtons/m^2; $E_t = 10^{10}$ Newtons/m^2; $U_o = .001$ cm; $V_o = X_o = 0$; and $c = 1\ 000$ Newtons/sec.

The heavy dots in Fig. V indicate the points at which strain reversal begins to occur in the columns. Thus, some deviation is shown to emerge between the present approach and the static theory which assumes the occurrence of strain reversal from the tangent modulus load level.

If possible strain reversal simultaneous with loading is taken into account and if subsequent lateral motion of the column under constant axial load is analyzed at various load levels, the illustration in Fig. VI would be obtained.[1] Fig. VI shows that as the loading rate gets larger, the deviation between the present approach and Shanley Theory becomes increasingly more pronounced. Furthermore, as the loading rate gets smaller values, the lateral deflection zone according to the present approach gets narrower and nearer to the positions predicted by Shanley theory.

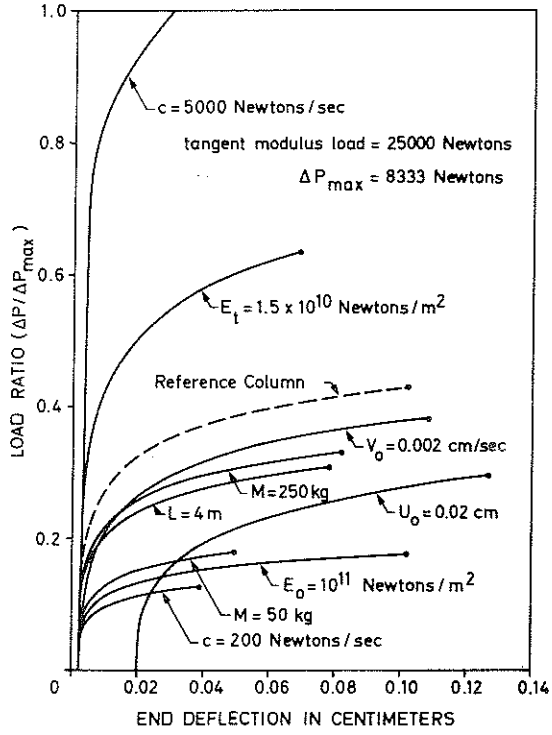

PARTIAL LOAD DEFLECTION CURVES FOR VARIOUS PARAMETER VARIATIONS CORRESPONDING TO THE GIVEN DATA

FIG. V

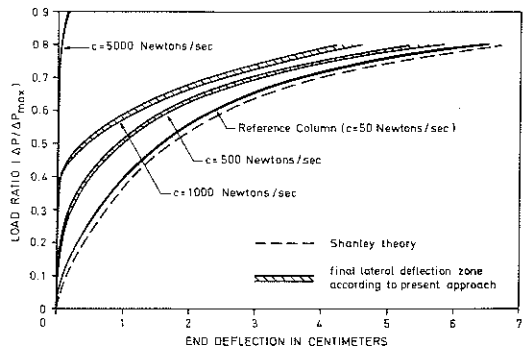

FINAL LATERAL DEFLECTION ZONE ACCORDIN TO THE PRESENT APPROACH FOR VARIOUS LOADING RATES COMPARED WITH THE LATERA EQUILIBRIUM POSITIONS ACCORDING TO SHANLEY THEORY

FIG. VI

1. With the exception of the loading rate, the reference column in Fig. VI has the same data as that of Fig. V

Fig. VII shows the relative shape of the σ-ε curve used in the illustrations in Figs. VIII - XIV. The relative shape implies that all the tangent moduli are fixed in relation to the initial modulus of elasticity, E_o. The stress axis is subdivided into 79 equal intervals where the tangent moduli may change, such that the reduced modulus load would occur at the 60th stress level.

Fig. VIII shows the variation of the maximum column load as a function of the loading rate for various values of initial end deflection, U_o. The column used in Fig. VIII has the following numerical data:

$A = 5\ cm^2$; $b = 5$ cm; $d = 10$ cm; $L = 5$ m; $M = 500$ kg; $E_o = 10^{10}$ Newtons/m^2; and $V_o = X_o = 0$.

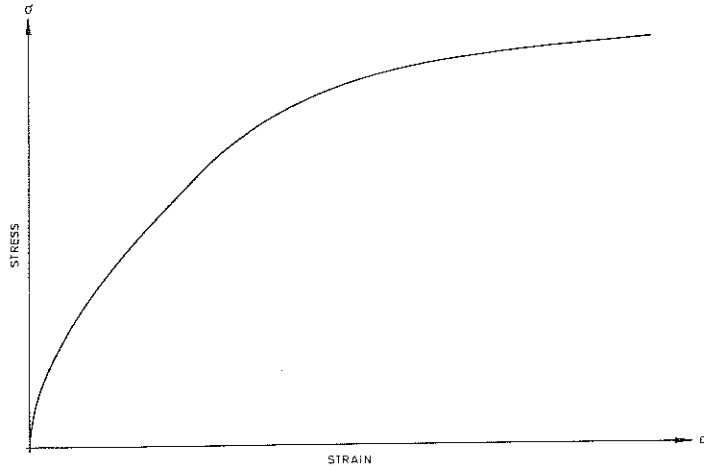

RELATIVE SHAPE OF THE STRESS STRAIN DIAGRAM USED IN THE COMPUTATIONS OF MODEL 3

FIG. VII

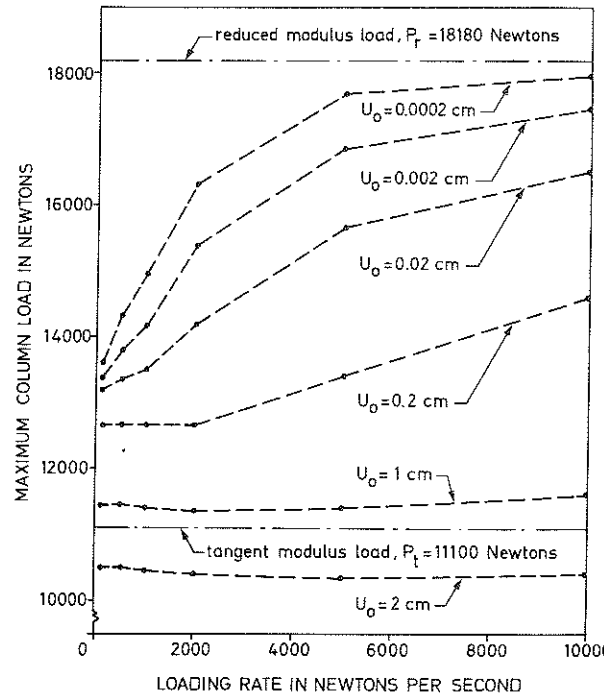

MAXIMUM COLUMN LOAD VERSUS LOADING RATE FOR VARIOUS INITIAL DEFLECTIONS

FIG. VIII

Fig. VIII shows that the influence of the loading rate on the size of the maximum column load becomes more pronounced for small initial deflections.

Two remarkable buckling phenomena are observed in Figs. IX and X, indicating the possibility of failure in reverse direction for a column originally deflected in another direction. Columns with such properties are called herein "backwards-inclined" in contrast to the normal or forwards-inclined columns. This property may be induced by a velocity disturbance as in Fig. IX, or self-induced in the absence of velocity disturbances as in Fig. X. The column corresponding to Fig. IX has the following data:

$A = 5\ cm^2$; $b = d = 5$ cm; $L = 2.5$ m; $M = 100$ kg; $E_o = 10^{10}$ Newtons/m^2; $U_o = .001$ cm; $V_o = .2$ cm/sec.; $X_o = 0$ cm; and $c = 5\ 000$ Newtons/sec.

The column corresponding to Fig. X has the same data except that $U_o = .0001$ cm; $V_o = 0$ cm/sec; and $c = 1\ 000$ Newtons/sec with the axial load applied as 10 Newton-increments at intervals of .01 seconds.

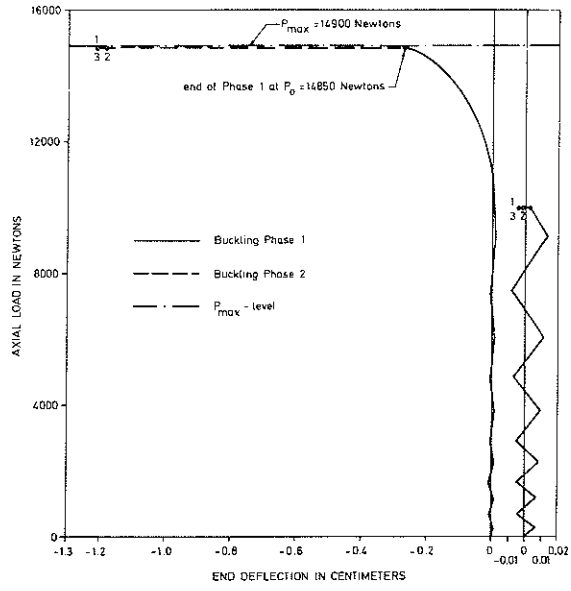

BUCKLING BEHAVIOUR OF INDUCED BACKWARDS-INCLINED COLUMN FOR THE GIVEN DATA

FIG. IX

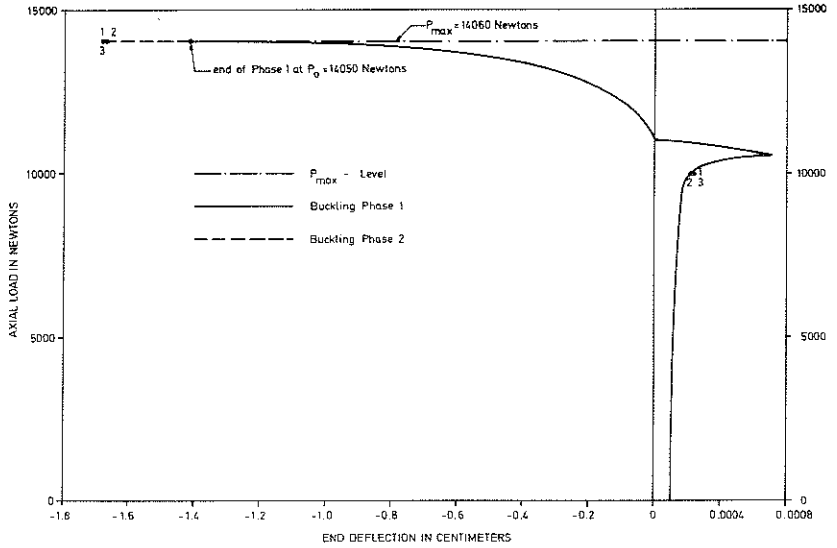

BUCKLING BEHAVIOUR OF SELF-INDUCED BACKWARDS-INCLINED COLUMN FOR THE GIVEN DATA

FIG. X

The phenomenon depicted in Fig.IX may appear frequently while the phenomenon illustrated in Fig. X happens quite rarely and is sensitively dependent on the manner the axial load is applied.

Fig. XI corresponds to a column with the following data:

$A = 5\ cm^2$; $b = d = 5$ cm; $L = 2.5$ m; $E_o = 10^{10}$ Newtons/m^2; $M = 100$ Kg; $V_o = .2$ cm/sec.; $c = 5\ 000$ Newtons/sec.

This diagram illustrates the remarkable abnormal column behaviour, namely that increasing the initial end deflection of backwards-inclined columns may result in an increase of the axial load. The transition zone, where the column turns from backwards-inclined to forwards-inclined behaviour, marks the uncertainty zone where slight changes in the value of the initial end deflection may change the direction of failure of the column.

Fig. XII corresponds to a column with the following data:

$A = 5\ cm^2$; $b = d = 5$ cm; $L = 2.5$ m; $E_o = 10^{10}$ Newtons/m^2; $M = 100$ Kg; $U_o = .001$ cm; $c = 5\ 000$ Newtons/sec.

This illustration shows the dependence of the maximum column load on the variation of velocity disturbances at the start of both buckling phases.

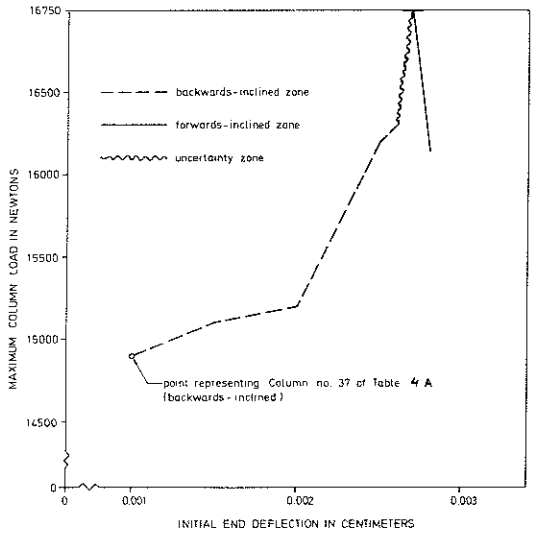

ILLUSTRATION OF THE ABNORMAL BEHAVIOUR OF BACKWARDS-INCLINED COLUMNS

FIG. XI

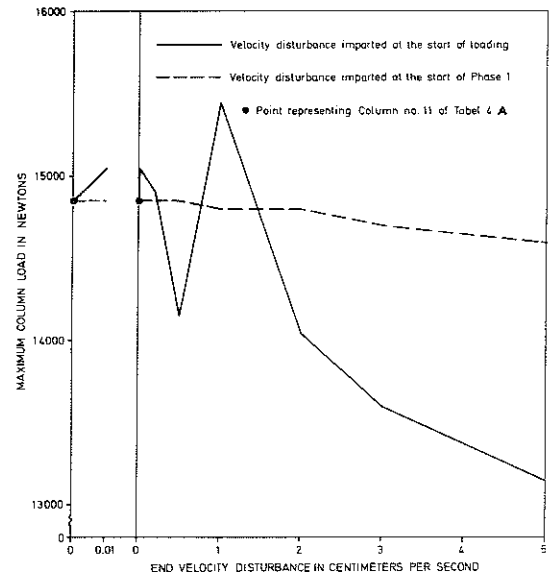

VARIATION OF MAXIMUM COLUMN LOAD AS A FUNCTION OF VELOCITY DISTURBANCES AT THE BEGINNING OF EITHER OF THE TWO BUCKLING PHASES

FIG. XII

The influence of gravitational force and the effect of nonconservative axial load is examined for a column with the following data:

$A = 5\ cm^2$; $b = d = 5$ cm; $L = 2.5$ m; $M = 100$ kg; $E_o = 10^{10}$ Newtons/m^2; $U_o = .1$ cm; $V_o = X_o = 0$; and $c = 5\ 000$ Newtons/sec.

It should be observed that the effect of gravitational force with $g = 10\ m/sec^2$ in Fig. XIII has resulted in a lowering of the maximum column load. However, for a nonconservative axial load with changes in the same direction as the end tangent to the deflection curve, the maximum column load is shown to increase above the conservative axial load level, see Fig. XIV. It should be noted that the points marked by 1, 2 and 3 in Figs. IX and X as well as in Figs. XIII and XIV indicate the first three positions of motion reversal in the course of oscillations of the column under the influence of constant axial load.

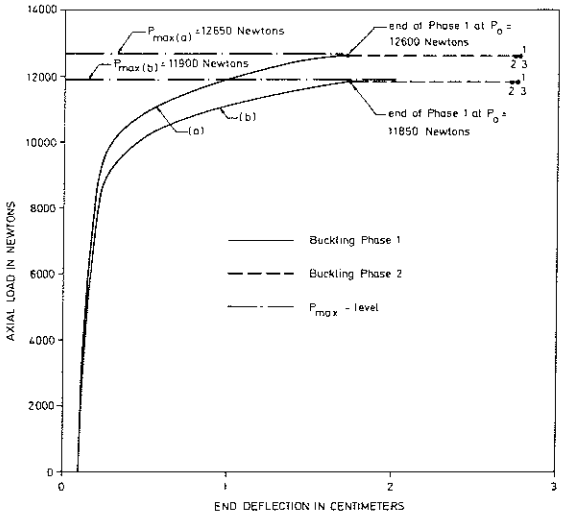

COMPARISON OF BUCKLING BEHAVIOUR: (a) THE GIVEN COLUMN WITH g = 0; (b) IDENTICAL COLUMN WITH g = 10 METERS PER SECOND SQUARE

FIG. XIII

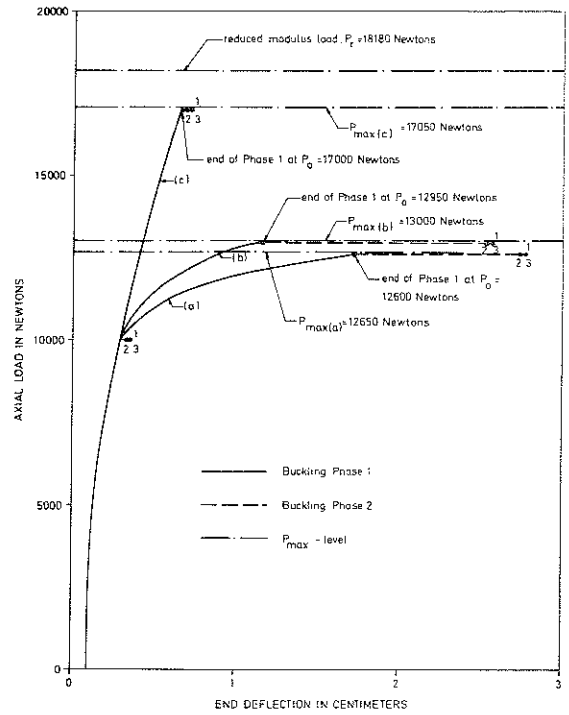

COMPARISON OF CONSERVATIVE AND NONCONSERVATIVE BUCKLING BEHAVIOUR: (a) THE GIVEN COLUMN; (b) IDENTICAL COLUMN WITH NONCONSERVATIVE AXIAL LOAD DURING PART OF PHASE 1; (c) IDENTICAL COLUMN WITH NONCONSERVATIVE AXIAL LOAD DURING PART OF PHASE 1 AND THROUGHOUT PHASE 2

FIG. XIV

To sum up, in the course of development of the present dissertation, a general theory of column stability has been developed which can explain the various buckling phenomena on the basis of predominantly physical arguments, and, furthermore, it provides the methodology and the analytical tools to evaluate the influence of variations of various parameters including the loading rate, on the size of the maximum column load and on the lateral equilibrium configurations of an inelastic column with arbitrary stress strain relationship.

CONTENTS

Page

PART IV: APPENDICES

NOTATIONS

The following notations are used throughout the main parts of the present work in the equations, in the diagrams and in the exposition of the main text. However, the symbols adopted for use in the 8 computer programs which accompany the main text are explained in respective places in Appendix D.

A	=	Cross sectional area corresponding to one hinge element (Fig. 12)
$A(...)$	=	One dimensional array containing the tangent moduli of the multilinear stress strain diagram (Fig. 33)
A_1	=	Integer controlling the current number of limiting stress levels corresponding to compressive stress in element a of column B (see Figs. 1, 32 and 33)
A_2	=	Integer controlling the current number of limiting stress levels corresponding to compressive stress in element b of column B (see Figs. 1, 32 and 33)
A_3	=	Integer controlling the current number of limiting stress levels corresponding to possible tensile stress in element a of column B (see Figs. 1, 32 and 33)
B_o	=	Integer controlling the current number of limiting stress levels corresponding to possible tensile stress in element b of column B (see Figs. 1, 32 and 33)
b	=	Half the width of the hinge (Fig. 12)
C	=	Bending rigidity defined by Eq.(101); set of column cross sections (see Sec. 2.1)
C_1	=	Variable defined by Eq. (112)
C_2	=	Variable defined by Eq. (113)
c	=	Loading rate
D	=	Ratio of axial load at disturbance time to the maximum column load
d	=	Half the depth of the hinge (Fig. 12)
E_o	=	Initial elastic modulus

E_a, E_b, E_j = Tangent moduli corresponding to column element, a, b and j respectively

E_{as}, E_{bs}, E_{js} = Tangent moduli at unloading time corresponding to elements a, b and j respectively

E_i = Tangent modulus at the i:th stress level (Fig. 32)

E_t = Tangent modulus

F = Variable defined by Eq. (142)

f = Load increment ratio defined by Eq. (69)

f_c = Critical load increment ratio defined by Eq. (74)

g = Gravitational acceleration

H = Variable defined by Eq. (141)

H_a, H_b = Horizontally applied external forces (Fig. 3)

I = Mass moment of inertia of the column

i = Index corresponding to the stress level

J = Symbol corresponding to cross section J of the column ;moment of inertia in Eq.(1)

j = Index corresponding to column element, j

K = Ratio defined by Eq. (C4)

L = Column length

M = Total mass of the column

M_e = External moment; set of external moments (see Sec. 2.1)

M_i = Internal moment; set of internal moments (see Sec. 2.1)

M_{io} = Initial internal moment

N = Number of stress levels on the linearized stress strain diagram (Fig. 32)

P = Axial load

P_o = Constant load level during buckling phase 2

P_a = An arbitrary axial load greater than the maximum column load

P_d, P_o^* = Axial load corresponding to velocity disturbance level; last desired constant axial load below maximum level

P_{n1}, P_{n2} = Initial and terminal axial loads in between which the axial load is non-conservative

P_r = Reduced modulus load

P_t = Tangent modulus load

P_{max} = Maximum column load

S = Variable defined by Eq. (53); set of maximum cross sectional strain (see Sec. 2.1)

saf, sbb = Strain reversal identifiers in elements a and b respectively (see Sec. 6.2)

saf_0, sbb_o = Initial values of Saf and Sbb (see Sec. 6.2)

t = Time

t_c = Time corresponding to the next consecutive limiting stress level (see Sec. 8.5)

t_r = Return time (see Sec. 7.3)

t_1 = Time at the end of phase 1

t_{m1}, t_{m2}, t_{m3} = Times corresponding to motion reversal positions 1, 2 and 3 respectively

t_{min}, t_{max} = Times corresponding to two consecutive maximum and minimum motion reversal positions

U = Current end deflection of the column; set of deflections along the whole length of the column (see Sec. 2.1)

U_o = Initial end deflection of the column

U_1 = End deflection at the end of phase 1

U_a = End deflection of the column (Fig. 3)

U_{m1}, U_{m2}, U_{m3} = End deflection corresponding to motion reversal positions 1, 2 and 3

U_{max}, U_{min} = End deflection corresponding to two consecutive motion reversal positions under constant axial load

V, V_o = Current and initial end velocity

V_1 = Disturbance velocity corresponding to any arbitrary load level

X = Longitudinal axis of the column (Fig. 3)

X_o = Eccentricity in the application of loading

α, α_o	=	Current and initial deflection angle
α_c	=	Deflection angle corresponding to the next consecutive limiting stress level (see Sec. 8.5)
$\dot{\alpha}$, $\dot{\alpha}_o$	=	Current and initial angular velocity
β_i	=	Ratio of the tangent modulus at the i:th stress level to the initial elastic modulus (Fig. 32)
Δ	=	Symbol for "increment of ..."
ΔM	=	Surplus moment increment
ΔM_{ia}	=	Axially induced internal bending moment increment
ΔM_{ib}	=	Laterally induced bending moment increment
ΔP_{max}	=	Maximum axial load increment defined by Eq. (60)
Δt	=	Time step corresponding to one computation cycle (see Appendix C)
$\Delta\alpha_c$, $\Delta\sigma_c$	=	Deflection angle increment respective stress increment corresponding to the next consecutive limiting stress level (see Sec. 8.5)
$\Delta\varepsilon_{axial}$	=	Axial strain increment defined by Eq. (117)
$\Delta\theta$	=	Increment deviation angle θ defined below
$\Delta\sigma$	=	Stress interval on the multilinear stress strain diagram (Fig. 32)
$\Delta\sigma_{cg}$	=	Stress increment corresponding to the next limiting stress level due to column deflection under the influence of gravitational force
$\Delta\sigma_{eg}$	=	Stress increment corresponding to column equilibrium in the last stress interval due to deflection under the influence of the gravitational force
δ	=	Symbol for "increment of ...", symbol for "partial derivative of ..."
ε_a, ε_b, ε_j	=	Strains in elements a, b and j respectively
ε_{aa}, ε_{ab}	=	Axial strain in elements a and b respectively
ε_{ba}, ε_{bb}	=	Bending strain in elements a and b respectively
ε_{axial}	=	Axial strain increment defined by Eq. (49 a)
$\varepsilon_{bending}$	=	Bending strain increment defined by Eq. (49 b)

θ	=	Deviation of non-conservative axial load from its original axial direction
Σ	=	Operator "summation"
σ_a, σ_b, σ_j	=	Stresses in elements a, b and j respectively
σ_c	=	Stress corresponding to the next limiting stress level (see Sec 8.5)
σ_{aa}, σ_{ab}	=	Axial stress in elements a and b respectively
σ_{ba}, σ_{bb}	=	Bending stresses in elements a and b respectively
ω	=	Variable defined by Eq. (107)

KEY WORDS

The following key words are either familiar terms found elsewhere in the technical literature, or words newly employed in the description of the concepts developed herein.

AXIALLY INDUCED BENDING MOMENT INCREMENT (see Sec. 7.3)

BACK SIDE OF THE COLUMN (opposite to the front side of the column, see the description below)

BACKWARDS-INCLINED COLUMN (see Sec. 10.1)

BUCKLING PHASE 1 (the time-dependent bending behaviour of the column simultaneous with the increase of axial load)

BUCKLING PHASE 2 (the time-dependent bending behaviour of the column under the influence of a constant axial load)

DEFORMATION MODULUS (a term interchangeably used for either the tangent modulus or the unloading modulus of elasticity as the case may be)

DYNAMICALLY STABLE COLUMN (a column whose lateral motion as a function of time always remains within finite bounds)

DYNAMIC STATE (see Sec. 6.1)

FORWARDS-INCLINED COLUMN (opposite to backwards-inclined column, see Sec. 10.1)

θ	=	Deviation of non-conservative axial load from its original axial direction
Σ	=	Operator "summation"
σ_a, σ_b, σ_j	=	Stresses in elements a, b and j respectively
σ_c	=	Stress corresponding to the next limiting stress level (see Sec 8.5)
σ_{aa}, σ_{ab}	=	Axial stress in elements a and b respectively
σ_{ba}, σ_{bb}	=	Bending stresses in elements a and b respectively
ω	=	Variable defined by Eq. (107)

KEY WORDS

The following key words are either familiar terms found elsewhere in the technical literature, or words newly employed in the description of the concepts developed herein.

AXIALLY INDUCED BENDING MOMENT INCREMENT (see Sec. 7.3)

BACK SIDE OF THE COLUMN (opposite to the front side of the column, see the description below)

BACKWARDS-INCLINED COLUMN (see Sec. 10.1)

BUCKLING PHASE 1 (the time-dependent bending behaviour of the column simultaneous with the increase of axial load)

BUCKLING PHASE 2 (the time-dependent bending behaviour of the column under the influence of a constant axial load)

DEFORMATION MODULUS (a term interchangeably used for either the tangent modulus or the unloading modulus of elasticity as the case may be)

DYNAMICALLY STABLE COLUMN (a column whose lateral motion as a function of time always remains within finite bounds)

DYNAMIC STATE (see Sec. 6.1)

FORWARDS-INCLINED COLUMN (opposite to backwards-inclined column, see Sec. 10.1)

FRONT SIDE OF THE COLUMN (the zone of the column situated on the front side with respect to the direction of motion including the whole zone which is currently subjected to increasing bending stresses caused due to purely bending effect)

LATERAL DEFLECTION ZONE (see Sec. 6.6)

LATERALLY INDUCED BENDING MOMENT INCREMENT (see Sec 7.2)

LIMITING STRESS LEVEL (see Sec. 8.2)

MAXIMUM COLUMN LOAD (see Secs. 7.6 and 7.8)

MOTION REVERSAL (see Sec. 7.5)

MULTILINEAR STRESS STRAIN DIAGRAM (see Sec. 8.2)

SELF-INDUCED BACKWARDS-INCLINED COLUMN (see Sec. 10.2)

STATE SPACE VARIABLES (see Sec. 6.1)

STRAIN REVERSAL PHENOMENON (strain reversal in a certain point of the column takes place when the total strain at that point begins to decrease)

SURPLUS MOMENT INCREMENT (see Sec. 7.1)

TANGENT MODULUS (local derivative of the stress strain diagram)

TOTAL INTERNAL MOMENT SURPLUS (see Sec. 7.4)

PHYSICS OF COLUMN STABILITY

1. INTRODUCTION

1.1 Aims and Scope

The subject of column stability has been frequently discussed eversince Euler presented his first study of this problem in the field of elastic stability in 1744. By the end of the last century and the beginning of the present one, the attention was paid to find out the buckling behaviour of a column with inelastic material properties. As a result of this development the concepts of the tangent modulus and the double modulus (reduced modulus) loads were proposed consecutively (1,2,3,4). A significant development occurred when Shanley presented his two papers (5,6).

Because of their remarkable simplicity and intuitive reasoning, Shanley's papers arose a great interest in the concepts of inelastic buckling and soon afterwards many papers appeared which were devoted to further explanations and applications of the principles envisaged by Shanley (7,8,9,10,11,12,13,14). Despite the intuitive approach which had characterized the development of the concepts of inelastic buckling, starting with the presentation of the tangent modulus load by Engesser and up to the exposition of inelastic buckling by Shanley, in recent studies of this problem mathematics has played the dominant role (15,16).

This work, which is written in four main parts, aims to achieve the following two main objectives:

1. to reexamine the most fundamental concepts of column stability by means of simple ideas in physics and geometry; and

2. to gain additional insight into the nature of column stability by attempting to explore and further increase the extent of knowledge in this field with emphasis on disclosing further significant properties of an inelastic column with arbitrary stress strain diagram.

In Part I, some general concepts of elastic stability are examined and illustrated herein in order to acquire sufficient analytical tools to cope with the problem of instability of an inelastic column. In Part II, the complete buckling behaviour of perfect inelastic column is analyzed herein for the range of loading between the tangent modulus and the reduced modulus loads. In Part III, the instability of imperfect inelastic column is treated and originally new buckling properties are disclosed. Although Part I is developed on the basis of well-known concepts, the sequence of arguments and the corresponding illustrations, herein, are intended to pave the way for further progress in the field of column stability in Parts II and III of this dissertation. Part IV consists of a collection of appendices including a preliminary discussion of Shanley Theory in Appendix A; an exact partial solution of the lateral motion of a simple inelastic column in Appendix B; development of an approximate complete solution on the basis of a multi-cycle computation technique in Appendix C; description of 8 computer programs in Appendix D; and the flow diagrams for the largest computer program developed herein in Appendix E.

The following material has been prepared with the awareness that, in addition to new contributions of this paper, even some fraction of the existing knowledge reexamined herein has been the subject of numerous papers in the field some of which are mentioned above. Even such knowledge as the existence of a finite buckling load, well-known

eversince Euler time, is treated herein on the basis of purely physical arguments.

The present goal is to achieve novelty in both simplicity of exposition and richness of new concepts. However, the reader is entreated not to initially worry about the feasibility of this predetermined goal. Two salient features of the present work should be particularly noted:

1. With the exception of some preliminary discussion on the existence of buckling load, all the ideas are linked in a sequential chain; and

2. the dynamic analysis of the column in the present paper is not a matter of choise; on the contrary, the arguments presented herein are intended to show that the emergence of a dynamic theory is unavoidable if the aim is to adequately describe column behaviour and to acquire new knowledge in the field of column stability.

1.2 Description of the Column Models

Three column models are used in the development of the ideas in the present work. Column A in Fig. 1(a) is solely used for illustrating the description of fundamental ideas.

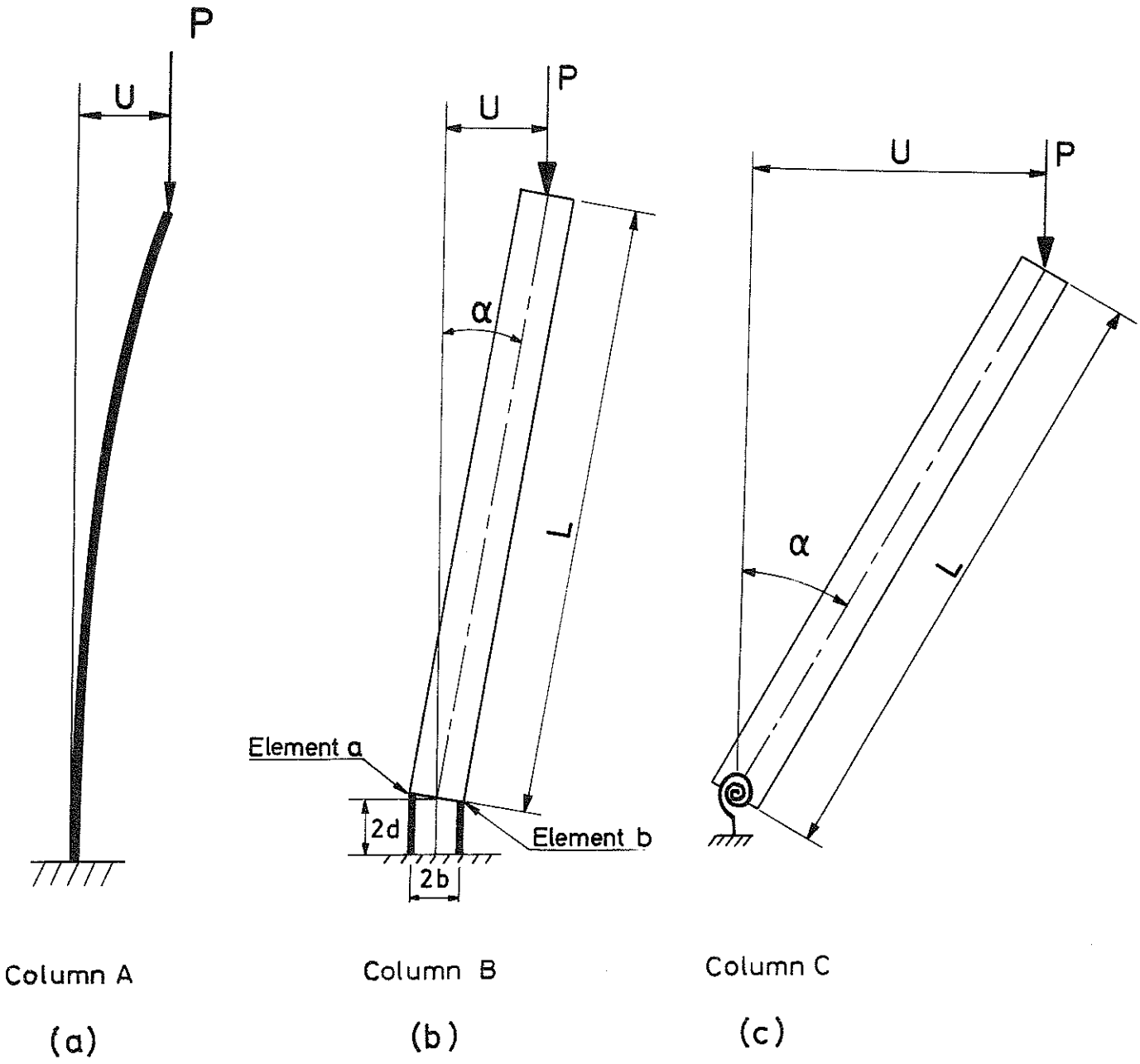

FIG. 1. THREE COLUMN MODELS USED IN THE PRESENT WORK

Although the general arguments are intended to be applicable to any arbitrary model, Column A is used whenever a simple pictorial illustration is considered to enhance understanding of a certain fundamental discussion. Column A is assumed to be a built-in cantilever column with arbitrary cross sectional area. Bending of the column is assumed to take place in the plane of the paper.

Column B in Fig. 1(b) is mostly used for the quantitative analysis of elastic or inelastic dynamic models. This column consists of an infinitely rigid leg connected to an inelastic hinge. The hinge is made up of two identical deformable elastic or inelastic elements of equal area and of equal initial length, placed at the two extreme sides of the hinge. Column B is of the same type used by Shanley for illustrating the inelastic buckling in Ref. 6. This type of simple column has proved to be highly successful for simulating various complex buckling phenomena with less complicated mathematics (18). Pearson, who has in Ref. 12 analyzed the simple model as well as columns of more realistic type, confirms the usefullness of the simple column by stating that "... it may be remarked that this column follows the behaviour of more conventional columns more closely than might be expected".

Since the two hinge elements can be made of any material, Column B can efficiently simulate any desirable elastic or inelastic material properties. Besides, due to the nondeformability of the column leg, considerable mathematical simplification is achieved in the numerical evaluation of various complicated buckling phenomena. Thus, Column B is an ideal model in cases where the disclosure of fundamentally new column behaviour demands simple and easily understandable illustrations before applications to more realistic columns. The only difference be-

tween Column B and a more conventional model is that the former deflects linearly, Fig. 1(b), whereas the latter bows laterally in a curved form, Fig. 1(a).

Column C in Fig. 1(c) is similar to Column B with a hinge consisting of a deformable elastic spring. This model is merely used in Chapter 2, for illustrating large deflections of an elastic column loaded above the Euler load.

1.3 Historical Review of Various Column Theories

Since the development of the concepts of column stability in the present work starts in Chapter 2 right from the question of the existence of buckling load, the reader is not supposed to possess specialized knowledge in this field in order to follow the course of arguments. However, some elementary concepts such as the Euler load, tangent modulus load, reduced modulus (double modulus) load, will be freely used herein throughout the main text. Thus, the objective of this section is twofold:

1. To provide an easy reference for the explanation of the above elementary concepts; and

2. to make a short review of the development of various column theories in their historical order.

Fig. 2 illustrates the difference in various column theories, in which Column A in Fig. 1(a) is assumed to be applicable. The relation, $1/\rho = d^2U/dX^2$, for the curvature of the column is supposed to be true for all lateral deflections, in accordance with the small displacement theory[1] (Coordinates U and X are indicated in Fig. 2(b)).

Fig. 2(a) shows the equilibrium position of the initially straight centrally loaded column up to the critical load, P_c. The critical load is defined as the load above which an ideal column, subjected to the slightest disturbances, cannot remain in the straight position, as shown in Fig. 2(b). It should be noted that in the relation, $P \geq P_c$, appearing in Fig. 2(b), the equality sign holds for all the theories discussed below with the exception of Shanley Theory for which the axial

---

1. The difference between the small and large displacemen theories is explained in greater detail in Sec. 2.1.

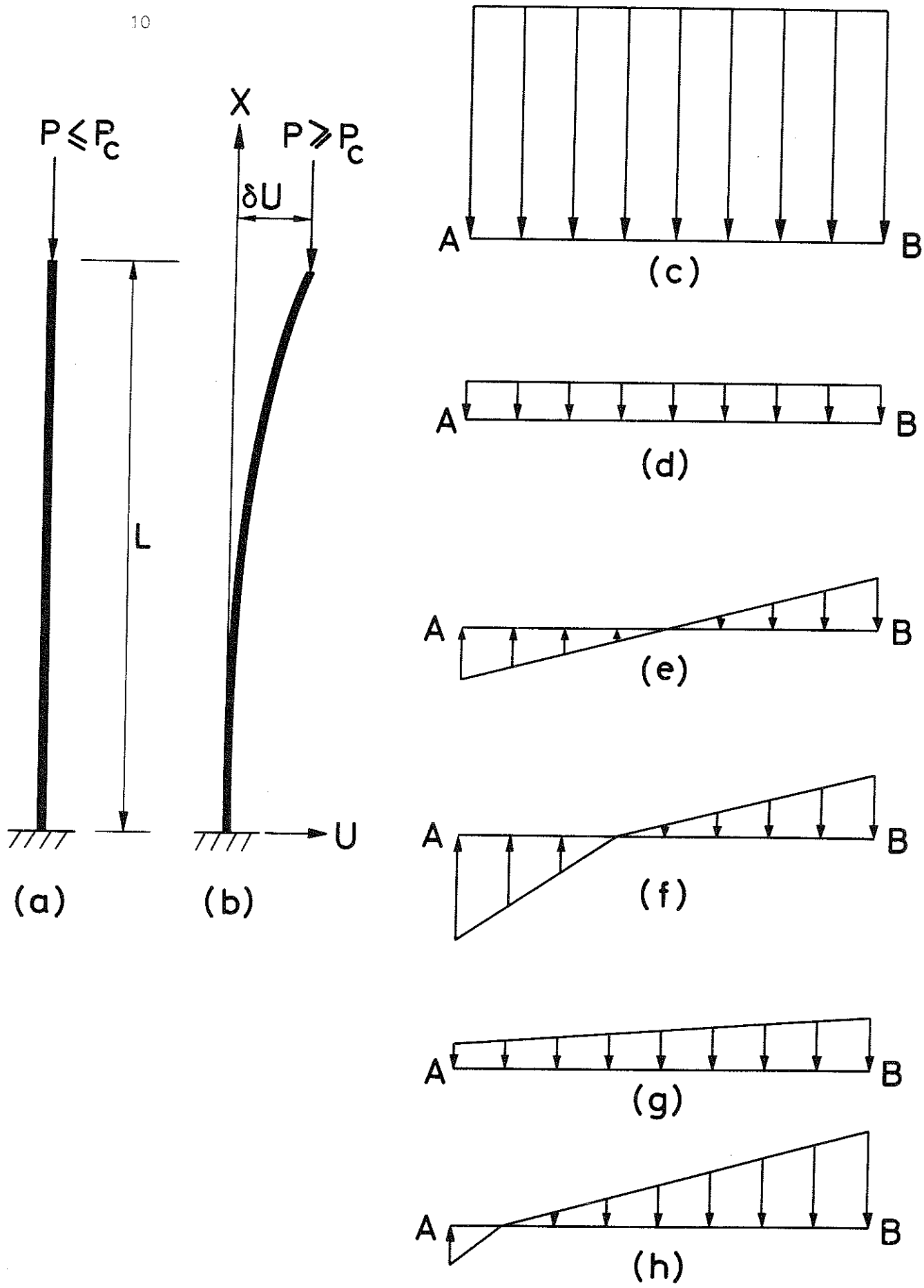

FIG. 2. COMPARISON OF VARIOUS COLUMN THEORIES

load, P, may exceed the tangent modulus load which is considered to be the lowest critical load. Figs. 2(c) and (d) show the stress distribution just before reaching the critical load, due to the total axial load, P, and due to an increment of axial load, ΔP, respectively. Figs. 2(e)-(h) show incremental stress distributions according to the various column theories described below.

Euler Theory. - For an elastic column with equal loading and unloading moduli, the critical load of the column is a unique load given by the following formula derived by Euler in 1744 (22).

$$P_E = \frac{\pi^2 EJ}{4L^2} \tag{1}$$

where P_E represents the critical Euler load; E, the modulus of elasticity; L, the length of the column; J, moment of inertia of the cross section about the main axis perpendicular to the plane of bending. Fig. 2(e) shows the distribution of bending stresses over a cross section of the column due to an infinitesimal lateral deflection, δU, after reaching the Euler load. It should be noted that according to small displacement theory, lateral deflection of the column for loads above or equal to the Euler load are not defined and just at the Euler load, the column can have any lateral deflection.

Tangent Modulus Theory. - The concept of buckling at the tangent modulus load for an inelastic column was first proposed by Engesser in 1889 in a few notes in Z. Architek. U. Ing. Ver., Vol. 35, p 455, The tangent modulus load, P_t, is obtained by replacing the modulus of elasticity, E, in the Euler formula by the local derivative of the stress strain diagram denoted by E_t:

$$P_t = \frac{\pi^2 E_t J}{4L^2} \qquad (2)$$

Fig. 2(e) shows the distribution of bending stresses over a cross section of an inelastic column due to an infinitesimal lateral deflection, δU, beyond the tangent modulus load according to the tangent modulus theory.

Double Modulus Theory. - The well-known contradiction in the tangent modulus theory may be realized by Fig. 2(f), which shows that in the unloading zone (convex side) of a cross section of the column, the unloading modulus has to be applied instead of the tangent modulus. Since the unloading modulus is always greater than the tangent modulus, then E_t, in Eq. (2) has to be replaced by a greater modulus, E_r, according to the double modulus theory. Thus reduced modulus load, P_r, would be given by the formula

$$P_r = \frac{\pi^2 E_r J}{4L^2} \qquad (3)$$

The modulus, E_r, called the reduced modulus is a function of the tangent modulus, the unloading modulus and the cross sectional form of the column. The concept of the reduced modulus was first envisaged by Considère (1) in 1889, a few months after the appearance of the tangent modulus theory. The contradiction in the tangent modulus theory was first pointed out by Felix Jasinski in 1895, who referred to Considère's concept as the correct alternative (see Ref. 2). A month later, Engesser acknowledged the incorrectness of his theory and calculated an expression for the reduced modulus, E_r, in the general form (see Ref. 3). The exact determination of the reduced modulus for a column of rectangular cross section and a column of idealized I-section with negligible web area

and infinitely thin flanges was given by T.V. Kármán in 1910 (see Ref. 4).

Shanley Theory. - Shanley has explained the paradox of the reduced modulus theory in the following way (see Refs. 5 and 6): The double modulus theory assumes that the column remains straight up to the reduced modulus load, P_r, after which the column buckles, Fig. 2(f). However, at the tangent modulus load, while the axial load is increasing and the tangent modulus applies to the whole cross section, there is nothing except the column's flexural rigidity to prevent bending of the column simultaneous with increase of axial load according to Fig. 2(g) or Fig. 2(h). Fig. 2(g) would still be a paradox since the tangent modulus still applies to the entire cross section and thus the axial load cannot increase above the tangent modulus load. If the column load is to exceed the tangent modulus load, the flexural rigidity of the column must increase, that is to say, some strain reversal must occur at the column, beginning with a cross section of the column with greatest bending stresses, Fig. 2(h). For each subsequent increase of axial load, there would be a further propagation of the unloading zone as determined by a simultaneous equality between the internal and external moments.

Thus, the Shanley Theory is crucially dependent on the occurrence of some strain reversal as soon as bending starts at the tangent modulus load. Although this assumption is correct in the context of the static theory, the preliminary discussion herein in Appendix A and the results obtainted in the course of development of the stability concepts in this paper show that the question of stability of an inelastic column cannot adequately be described by means of the static theory. It should be noted

that although the tangent modulus and the reduced modulus theories are also based on static considerations, they differ from Shanley Theory on the following fundamental question: the tangent modulus and the reduced modulus loads are calculated on the basis of equilibrium of the column in an aribitrarily chosen infinitesimal lateral position under the influence of a constant axial load. Thus, the question of duration of loading or duration of the lateral deflection have no relevance to the determination of the tangent modulus and the reduced modulus loads.

On the other hand, Shanley Theorey predicts a bending process during which the column starts bending from initially straight position at the tangent modulus load to infinetely large lateral deflection at the maximum column load. Furthermore, the bending process envisaged by Shanley is sensitively dependent on the question of the simultaneous increase of axial load. Thus, when it is desired to develop principles which may estabilish a general theory, the question of a finite bending of the column simultaneous with a finite increase of axial load cannot be dissociated from the question of the time element. This statement is particulary relevant to an inelastic column for which the deformation and strain reversal history may have a pronounced influence on the buckling behaviour. The duration of loading and the size of initial disturbances are two significant factors which may considerably affect the size of the maximum column load and influence other buckling properties of an inelastic column with arbitrary stress strain diagram. In a dynamic consideration of the problem, the following two situations may arise:

1. For a given initial imperfection and lateral disturbance, the dynamically unstable column may approximately approach the position envisaged by Shanley Theory provided that the loading rate becomes sufficiently small; and

2. on the other hand, for a given loading rate, a sufficiently small initial imperfection and lateral disturbance may lead to considerably large discrepancy between the actual column behaviour and that predicted by Shanley Theory.

The objective of the present work is to develop a general theory which can take into account all the pertinent variables, including the time factor, which may influence the buckling behaviour of an inelastic column with arbitrary stress strain diagram.

PART I

ANALYSIS OF ELASTIC COLUMN

2. BEHAVIOUR OF PERFECT ELASTIC COLUMN

2.1 Existence of Buckling Load

According to the classical concept of elastic stability, the buckling load is the smallest central load at which an initially straight column may stay in equilibrium at various small lateral deflections. The concepts of elastic stability are well known and are fully described in the existing classical works (17). However, it may prove useful to begin this discussion with a fundamental insight into the nature of column stability. The existence of a buckling load with a finite value could be shown by a simple geometrical reasoning.

Although the following discussion does not enter as a sequential chain in the development of later concepts in the paper, it is included in order to increase understanding of the essential elementary physical aspects of the problem. Euler's original solution of this problem consists of setting up the differential equation describing equilibrium between internal and external moments. Although a numerical evaluation of buckling load still requires the solution of such a differential equation in each particular case, the qualitative understanding of the problem could be enhanced by the following analysis.

Fig. 3 illustrates an elastic column of arbitrary cross sectional area with one end fixed and the other end free. All dimensions of the column are considered to have finite values. Bending of the column is assumed to take place in the plane of the paper.

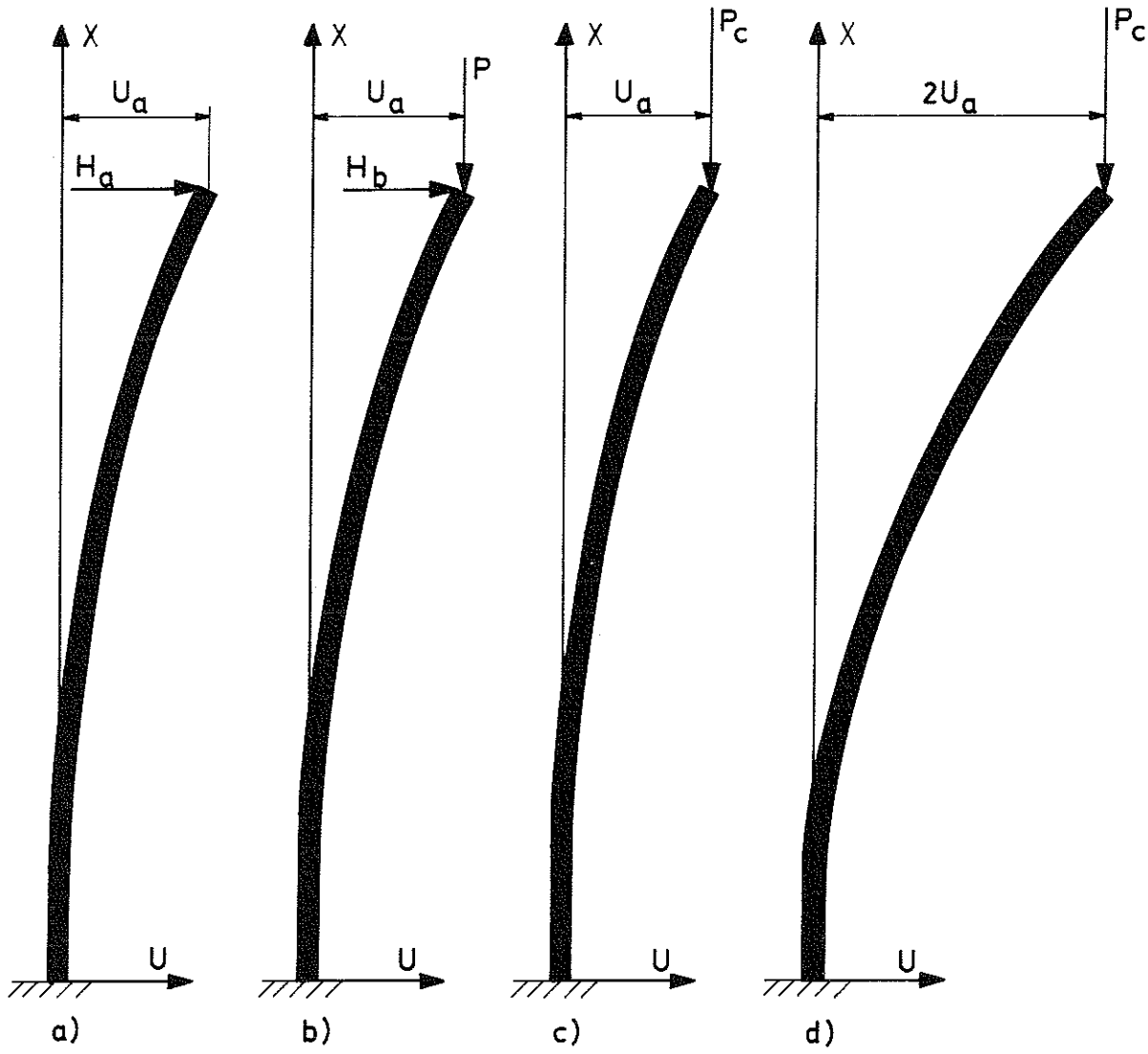

FIG. 3. ELASTIC COLUMN DEFLECTED TO AN EQUILIBRIUM POSITION: (a) DUE TO A HORIZONTAL FORCE; (b) DUE TO THE SIMULTANEOUS ACTION OF A HORIZONTAL FORCE AND AN AXIAL LOAD; (c), AND (d) DUE TO THE CRITICAL AXIAL LOAD.

The column in Fig. 3(a) is deflected by a horizontal force, H_a, applied at the free end of the column. This external force causes external moments at every cross section of the column while the subsequent distortion of the column causes corresponding internal moments. If the column is assumed to be in a state of equilibrium at the deflected position, the external and internal moments would be equalized at every cross section. This state of equilibrium will now be studied in two different situations: (a) when the end deflection has a finite value; and (b) when its value is infinitesimal.

In order to make the argument precise, we may think of the column in Fig. 3(a), or any other column model, as comprising five infinite sets: set of cross sections, C, set of internal moments, M_i, set of external moments, M_e, set of deflections, U, and set of maximum strains, S. This last set is entirely built up of members each of which corresponds to the maximum strain which occurs at a particular cross section. Each member of the set C is associated with a corresponding member of each of the other four sets.

Now, there are two requirements for the existence of equilibrium configuration in Fig. 3(a): 1) the internal and external moments must be equal at each given cross section; and 2) the finite dimensional geometry of the column requires that the member of the set S with greatest absolute value be of the same order of magnitude as the highest valued member of the set U. This means, specifically, that if the maximum strain at the cross section of maximum strain - fixed end in Fig. 3(a) - has a finite value, then the lateral bowing at the cross section of maximum deflection - free end in Fig. 3(a) - must also have a finite value. On the other hand, if the highest-

valued member of S is infinitesimal, then the highest-valued member of U would also be infinitesimal of the same order of magnitude (two infinitesimal values are defined to be of the same order of magnitude if and only if their quotient remains finite).

Since each two matching members of M_i and M_e are of the same order of magnitude as the corresponding member of S, it follows immediately that the highest-valued members of M_i and M_e are also of the same order of magnitude as the highest-valued member of U.

Now, if the horizontal force, H_a, in Fig. 3(a) is reduced to a smaller value, H_b, the end deflection, U_a, would likewise decrease unless a compensating external moment is caused in the column by additional external agency such as a centrally applied axial load, Fig. 3(b). It is significant to observe, that although the axial load in Fig. 3(b) is chosen sufficiently large to cause the same end deflection as in Fig. 3(a), the distortion of the column as a whole, is not expected to be identical for the two cases. Now, if the force, H_b, is reduced to zero, the axial load, P, has to further increase in order to maintain the same end deflection, U_a, see Fig. 3(c). Now, it is our aim to prove that the axial load in Fig. 3(c) has a finite value, regardless of whether the end deflection, U_a, is finite or infinitesimal.

According to the above discussion, the deflection of the free end of the column in Fig. 3(the highest-valued member of U) is of the same order of magnitude as the highest valued members of M_e and M_i which occur at the fixed end of the column. This implies that in the relation

$$P = \frac{M}{U_a} \qquad (4)$$

where M represents the moment ($M = M_e = M_i$) at the fixed end of the column, since U_a and M are of the same order of magnitude, their quotient, P, would always remain finite, regardless of the size of U_a.

The generality of the geometric argument given above has the following inherent advantages:

1. The proof avoided making any specific assumptions regarding the relative significance of various internal column factors such as the effect of shearing forces. This implies that the argument does not discard the significance of such parameters as shearing forces in the numerical value of the buckling load.

2. The proof asserts the existence of a finite buckling load for any predetermined finite or infinitesimal end deflection of the column. This means that the argument does not rule out the possibility that as the end deflection changes, the actual value of the axial load in Fig. 3(c) may also change. In other words the given proof includes both the small deflection and the large deflection classical theories.

A question of theoretical interest is under what physically simplifying assumptions the axial load in Fig. 3(c) would maintain constant value for all possible values of lateral deflections. This situation is illustrated in Fig. 3(d) where the free end of the column is deflected twice the corresponding value in Fig. 3(c); the axial load, P_c, however, is assumed to remain unchanged. The configuration depicted in Fig. 3(d) is statically stable provided that the column can stay in equilibrium in the new position, i.e., only if the external and internal moments are equalised. This is possible only if it is assumed that the increase in internal moment in all the cross sections of the column due to

additional distortion, in moving from one deflected position to another, is exactly balanced by the corresponding increase in the external moment due to additional deflection. This simplifying assumption corresponds to the classical small displacement theory where the curvature of the column is approximated by the expression d^2U/dX^2, where $\underline{U}$ denotes deflection, and $\underline{X}$ the length measured along the initially undeflected straight longitudinal axis of the column, see Fig. 3 for the definition of X and U.

The large displacement theory, on the other hand, corresponds to the use of the exact mathematical expression for the curvature of the column. The classical theory shows that according to the large displacement theory, static equilibrium positions exist for the deflected column loaded above the critical load. However, excessive lateral deflections are caused due to slight increases in the axial load above the critical level, see Ref. 17 and the illustration in Sec. 2.4 herein. The behaviour of an elastic column for loads above the critical load is illustrated herein in Sec. 2.4 according to both small and large displacements theories. It is noteworthy that the proof of the existence of the critical load in the above discussion conforms with both the approximate and the exact classical approaches.

2.2 Illustration of the Existence of Buckling Load

Fig. 4 shows the deformed configuration of the elastic hinge corresponding to Column B in Fig. 1(b). The central line of the column is deflected by angle, α, from its initial straight position under the influence of an axial load, P, which will now be shown - using the line of arguments above - to be finite regardless of the size of the end deflection, U, assuming that all dimensions of the column are finite. The column is furthermore assumed to be in equilibrium in the deflected position under the influence of an axial load, P, alone. We now prove that this P is always finite.

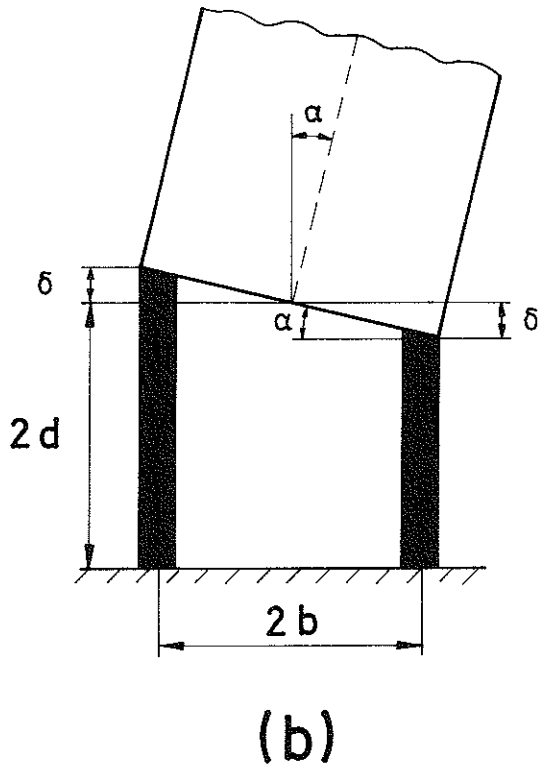

FIG. 4. DEFORMATION OF THE ELASTIC HINGE CORRESPONDING TO COLUMN B

The strain increment, ε, in each hinge element is found from the equatic

$$\varepsilon = \frac{\delta}{2d} = \frac{b \sin \alpha}{2d} \tag{5a}$$

From geometry, see Fig. 1(b),

$$\sin \alpha = \frac{U}{L} \tag{5b}$$

Substitution of Eq. (5b) into Eq. (5a) gives

$$\varepsilon = \frac{b}{2dL} \cdot U \tag{6}$$

Eq. (6) shows the validity of the first statement above that for a column of finite dimensions, the highest-valued mumber of the set S (the strain, ε, in this case) is of the same order of magnitude as the highest-valued member of the set U (the end deflection, U, in the present case).

The internal moment developed due to the current deformation of the hinge is obtained by taking the moment of the internal stresses with respect to the center of the hinge. This leads to

$$M_i = 2bAE \cdot \varepsilon \tag{7}$$

in which b = half the width of the hinge; A = area of each hinge element; E = the modulus of elasticity; and ε = the strain given by Eq. (6).

Eq. (7) shows the validity of the second statement above that

each two matching members of M_i and M_e ($M_i = M_e$ due to equilibrium) are of the same order of magnitude as the corresponding member of the set S (the strain ε in this case).

From the discussion of the above mentioned two statements, it follows that the highest-valued members of M_i and M_e are necessarily of the same order of magnitude as the highest-valued member of U. This conclusion becomes mathematically obvious by substituting Eq. (6) into Eq. (7):

$$M_i = \frac{b^2 AE}{dL} \cdot U = \text{a finite value times } U \qquad (8)$$

Now, since $M_i = M_e$ and since M_i and U are of the same order of magnitude, it follows that the ratio, M_e/U, that is to say the axial load, which alone keeps the column in equilibrium, must remain finite regardless of the size of U.

The finiteness of the critical axial load could most easily have been established by equating the expression for the internal moment with the corresponding expression for the external moment. However, the present sequence of arguments, used in proving the elementary concept of a finite buckling load in this section, shows a technique which may turn out powerful in applications to more involved problems where a set of simple and intrinsically true physical facts may be utilized to explore complicated physical phenomena.

2.3 Dynamic Concept

The fact, that according to small displacement theory an additional deflection of the column under the critical load causes equal increments of internal and external moments leads to the following two distinct situations:

1. For axial loads below the critical load, any distortion of the column causes internal moments in excess of the corresponding external moments due to the axial load and therefore as soon as the external cause of the disturbance is removed, the column moves towards the initial straight equilibrium configuration. The kinetic energy thus attained by the column in passing the straight position results in a vibratory motion. The column in this situation is defined to be dynamically stable.

2. For loads above the critical load, any distortion of the column causes external moments due to axial load in excess of the corresponding internal moments due to distortion and therefore the column tends to move further away from the straight configuration. Once the motion of the column begins in this manner, there are no additional increments of internal moment to impede the motion and thus the lateral deflection of the column will grow indefinitely with time. The column in this situation is obviously dynamically unstable according to the small deflection theory. This straightforward conclusion agrees with the classical mathematical result that the frequency of vibration of a column loaded by its critical load, tends to zero, that is to say the period of vibration of the column tends to infinity as its amplitude attains very large values.

2.4 Illustration of the Dynamic Concept

The dynamic behaviour of the simple initially straight, centrally loaded elastic column, simultaneous with the increase of axial load below and/or above the critical load, according to both small and large displacement theories, is examined herein (see Fig. 5 below).

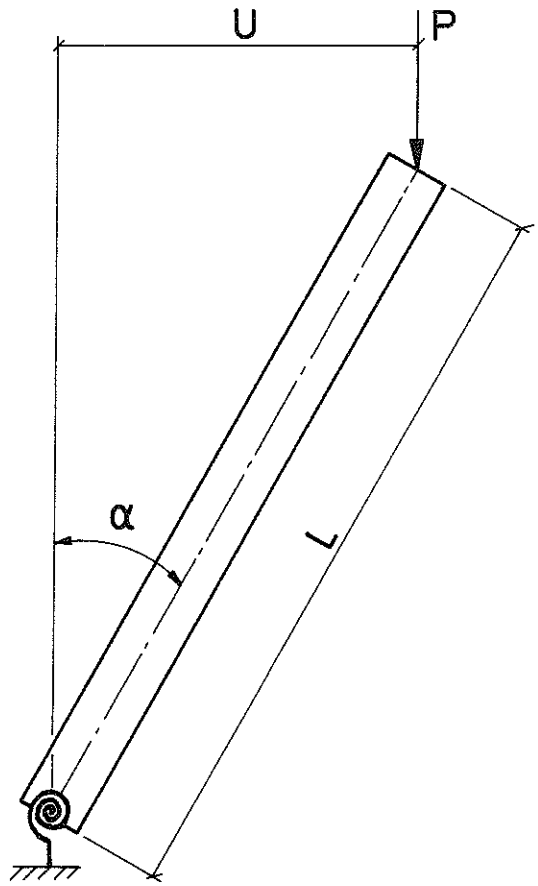

FIG. 5. DEFLECTED CONFIGURATION OF SIMPLE ELASTIC COLUMN

The column in Fig. 5 is the same as Column C presented in Fig. 1 (c). The axial load is assumed to be conservative, i.e., the direction of the applied force does not change during lateral deflection. Furthermore, it is assumed that the moment developed in the elastic hinge is always proportional to the deflection angle, α. The deflected configu-

ration shown in Fig. 5 may either represent a lateral equilibrium position, or it may depict a configuration of the dynamically unstable column at a certain instant of time during lateral motion. In the dynamic treatment of this problem the effect of axial inertia is assumed to be negligible. The validity of this last assumption is more closely examined in the next chapter.

a. Analysis according to Small Displacement Theory

The problem of numerical analysis of the dynamic behaviour of the column simultaneous with the increase of axial load below or above the critical load is solved according to the following procedure: All the column variables are assumed to be initially known at a certain axial load. The column load is then increased by an increment, ΔP, the equations of lateral motion of the column is set up under the influence of a constant axial load. During the computation cycle corresponding to Δt, the new state of the column is found at the end of the cycle. The axial load is then increased by a new increment and the state of the column at the end of the previous computation cycle is considered as the initial state for a new computation cycle. In this manner, the whole loading period may be divided into a number of time intervals, the size of which depends on the desired degree of accuracy. The state of the column may then successively be found at consecutive computation cycles simultaneous with loading.

The state of the column in the above discussion implies all the column variables which together uniquely determine the dynamic behaviour of the column. It should be observed that the increments ΔP and Δt in the above discussion are dependent on each other, i.e., the choice

of the time step, Δt, corresponding to a computation cycle, together with the specified loading rate determine the value of the axial load increment, ΔP.

The above procedure for the determination of the dynamic state of the column simultaneous with the increase of axial load is used throughout this work for both elastic and inelastic columns. Appendix C fully develops the above procedure according to the small displacement theory by treating the time dependent lateral and axial motion of a simple column, Column B in Fig. 1(b), with an arbitrary stress strain diagram, taking into account initial deflection, initial eccentricity, and possible deviation in the direction of application of the axial load.

The derivations in Appendix C are easily applicable to an elastic column by setting the values of tangent moduli anywhere and during any computation cycle equal to a constant modulus of elasticity, E. Furthermore, the formulas in Appendix C are equally valid to Column C, Fig. 5, by observing that the bending rigidity of Column C is given by a single constant, C, whereas the bending rigidity of Column B in Appendix C is more closely specified by Eq. (C 15).[1]

Thus, considering that for the present case, the bending rigidity, C_c, at the critical load is equal to the corresponding value, C, during any computation cycle, and noting that for an elastic column the axially

---

1. Since Appendix C is referenced, hereafter, from many places in this work, the reader is advised to review that appendix after reading the present illustration.

induced moment increment, ΔM_{ia}, is always equal to zero, see Eqs. (C 4), (C 6a), (C 6b), and (C 7), and observing that, the internal moment, $M_{io} = C \cdot \alpha_o$, where the index o corresponds to initial state at the beginning of the current computation cycle, then Eq. (C 58) of Appendix C reduces to the following form[1]

$$\ddot{\alpha} \pm \frac{\Delta PL}{I} \alpha = 0 \tag{9}$$

in which $\ddot{\alpha}$ = the second derivative of the deflection angle with respect to time; and I = the column's mass moment of inertia, which for a slender column of the type shown in Fig. 5 may be expressed by the formula

$$I = \frac{ML^2}{3} \tag{10}$$

For an increment of load, ΔP, below the critical load, Eq. (9) reduces to the equation

$$\ddot{\alpha} + \frac{\Delta PL}{I} \alpha = 0 \tag{11}$$

and for a load increment, ΔP, above the critical load, Eq. (9) is reduced to the form

$$\ddot{\alpha} - \frac{\Delta PL}{I} \alpha = 0 \tag{12}$$

Using the notations

$$\Delta M = \Delta PL \tag{13}$$

---

1. The gravitational force does not enter in the equation of motion of this column (see Appendix C, Sec. d).

and $$\omega^2 = \frac{|\Delta M|}{I} \tag{14}$$

in which $|\Delta M|$ = the absolute value of ΔM; the following solutions of the problem are obtained:

When the axial load is below the critical load, Eq. (11) leads to the solutions

$$\alpha = C_1 \sin \omega t + C_2 \cos \omega t \tag{15}$$

and $$\dot{\alpha} = C_1 \omega \cos \omega t - C_2 \omega \sin \omega t \tag{16}$$

in which $\dot{\alpha}$ = the angular velocity; and C_1, C_2 = two constants determined from the initial conditions of the problem at time, $t = 0$:

$$C_1 = \frac{\dot{\alpha}_o}{\omega} \tag{17}$$

$$C_2 = \alpha_o \tag{18}$$

Since the value of ΔM approaches zero as ΔP approaches zero, it follows that the value of ω also approaches zero. This verifies the assertion that as long as the axial load lies below the critical level, the column may develop oscillatory motion. However, as the axial load approaches the critical load, the frequency of motion approaches zero and the lateral bowing of the column would increase continuously with time. Furthermore, if the axial load remains at a constant level below the critical load, then the values of ΔM and ω from Eqs. (13) and (14) would be constant, whereupon Eqs. (15) - (16) would represent a simple harmonic motion.

If the axial load is just equal to the critical load, the value of ΔP would be zero, whereupon, Eq. (9) results in the following expression for α and $\dot{\alpha}$:

$$\alpha = \dot{\alpha}_o \cdot t + \alpha_o \tag{19}$$

$$\dot{\alpha} = \dot{\alpha}_o \tag{20}$$

If the axial load is above the critical load, Eq. (12) leads to the following solutions:

$$\alpha = C_1 \sinh \omega t + C_2 \cosh \omega t \tag{21}$$

and

$$\dot{\alpha} = C_1 \omega \cosh \omega t + C_2 \omega \sinh \omega t \tag{22}$$

in which C_1 and C_2 are determined by Eqs. (17) and (18) respectively.

Eqs. (19) - (22) show that for axial loads equal to or above the critical load, the lateral deflection of the column would continue to grow indefinitely with time.

b. Analysis According to Large Displacement Theory

The internal moment, M_i, is always governed by the equation

$$M_i = C \cdot \alpha \tag{23}$$

according to both small and large deflection theories. However, the external moment according to the large displacement theory is found

from the following equation:

$$M_e = (P + \frac{M \cdot g}{2}) L \sin \alpha \qquad (24)$$

Substitution of Eqs. (23) and (24) into the general equation of lateral motion of the simple column,

$$M_e - M_i = I\ddot{\alpha} \qquad (25)$$

leads to the following differential equation for the determination of the lateral motion of the column:

$$\ddot{\alpha} - (P + \frac{M \cdot g}{2}) \cdot \frac{L \cdot \sin \alpha}{I} + \frac{C \cdot \alpha}{I} = 0 \qquad (26)$$

in which P is an arbitrary function of time, and may be assumed to be constant during a short time step, Δt, corresponding to one computation cycle.

Equating the expressions for internal and external moments from Eqs. (23) and (24) leads to the following expression for the critical load, P_{cg}, with due consideration to the gravitational force:

$$P_{cg} = \frac{C}{L} \cdot \frac{\alpha}{\sin\alpha} - \frac{Mg}{2} \qquad (27)$$

Substitution of Eq. (27) into the following equation, Eq. (28),

$$P = P_{cg} + \Delta P \qquad (28)$$

in which P = the current axial load exceeding the critical load by an

increment, ΔP, and subsequent substitution of Eq. (28) into Eq. (26) results in the following equation for the lateral motion of the column above the critical load, according to large displacement theory:

$$\ddot{\alpha} - \frac{\Delta P \cdot L}{I} \cdot \sin \alpha = 0 \qquad (29)$$

Eq. (29) again shows that for a certain increment of axial load above the critical load, the equation of lateral motion is independent of the gravitational force, in the present case.

Without an actual solution of Eq. (29), significant properties of this equation of lateral motion could be disclosed as compared with Eq. (12). It should be noted that the fundamental equation, Eq. (25), is in general applicable to the simple column both according to small and large displacement theories. The expression for internal moment, M_i, is common for both theories. However, for the same angular deflection, α, the expression for external moment corresponding to small displacement theory is found from the following equation

$$M_e = (P + \frac{M \cdot g}{2})L \cdot \alpha \qquad (30)$$

Since the external moment, M_e, obtained from Eq. (30) is always larger than the corresponding value according to large displacement theory from Eq. (24), it follows that for the same angular deflection, α, Eq. (25) leads to a greater angular acceleration for the small displacement theory as compared with the value obtained from the large displacement theory.

Thus, starting from the same initial state, the angular deflection

and velocity of the column simultaneous with loading above the Euler load derived from Eq. (29) would always be less than the corresponding values from Eq. (12). Furthermore, since the axial load is conservative, and there are no energy losses during the process of lateral motion, the column under a constant axial load above the Euler load would develop an oscillatory motion around a position of static equilibrium. This static deflected configuration is determined according to Eq. (27). Thus, the above concepts lead to the diagrammatic representation shown in Fig. 6. This diagram is obtained by using the formulas in the above analysis in a computer program, (see program 1, Appendix D), with the following numerical data applied to Column C (see Fig. 5):

L = 2.5 meters; C = bending rigidity = 25000 Newton-meters; M = 100 kilogramms; c = loading rate = 2000 Newtons per second; U_o = initial end deflection = .001 centimeters with zero velocity disturbances; and Δt = the chosen time step corresponding to one computation cycle = .01 seconds.[1]

Fig. 6(a) depicts the static load deflection behaviour according to the small displacement theory. This line which is parallel to the deflection axis shows that at the critical load, the equilibrium of the column at a deflected configuration is indifferent, i.e., it can maintain equilibrium at any lateral deflection. Fig. 6(b) shows the static load deflection behaviour calculated for the simple column according to large displacement theory. This curve indicates that although the column can, in reality, attain lateral equilibrium positions above the critical load, considerable lateral bowing of the column is caused due to a slight increase of the axial load above the critical level.

Figs. 6(c) and (d) show the actual dynamic load deflection behaviour

---

1. The choice Δt = .01 seconds leads to good results. This fact is illustrated in Sec. 5.5 and Sec. 8.9.

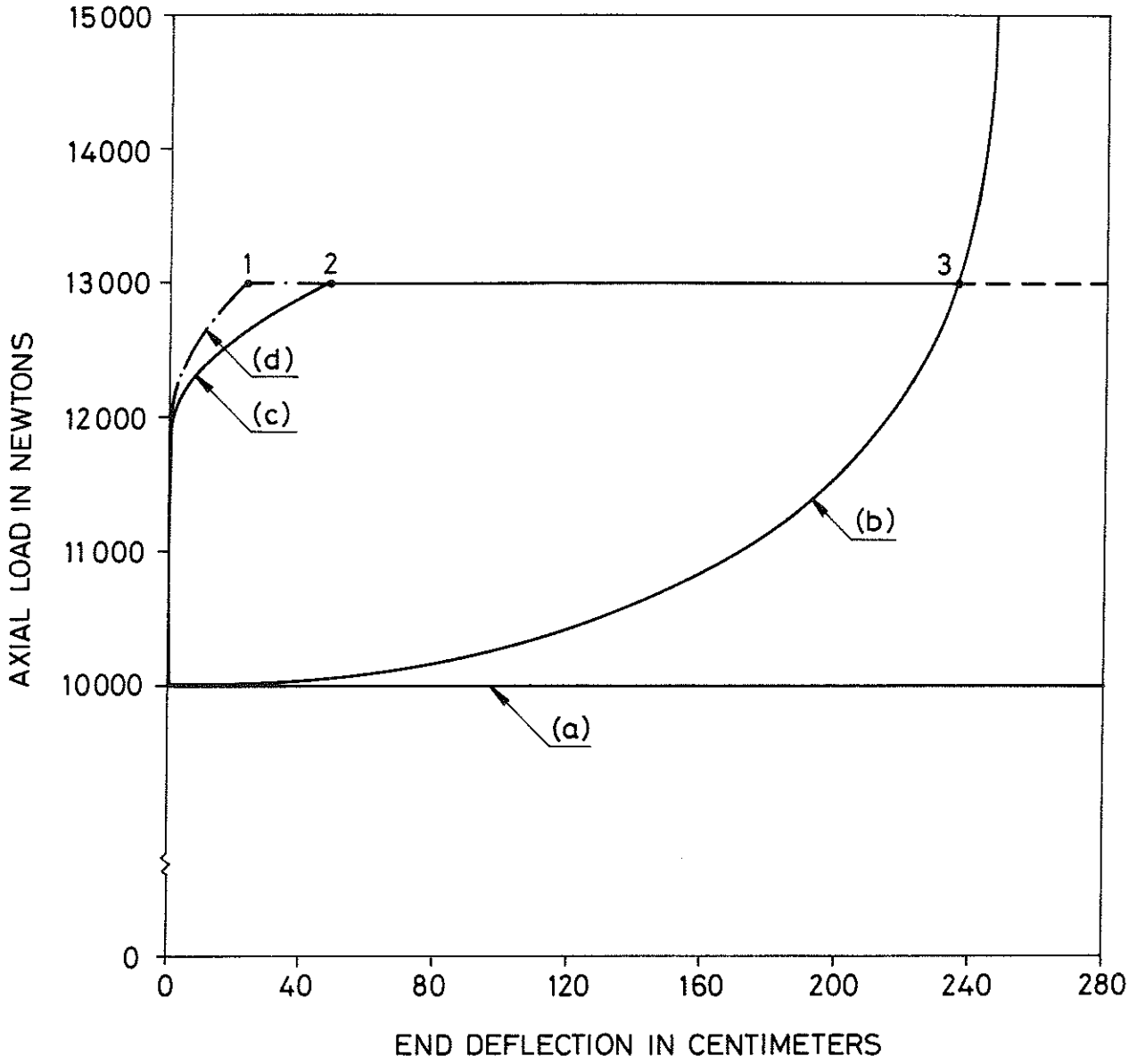

FIG. 6. LOAD DEFLECTION BEHAVIOUR OF SIMPLE ELASTIC COLUMN (COLUMN C): (a) ACCORDING TO THE STATIC SMALL DISPLACEMENT THEORY; (b) ACCORDING TO THE STATIC LARGE DISPLACEMENT THEORY; (c) AND (d) THE UNSTABLE BEHAVIOUR SIMULTANEOUS WITH LOADING FOR LOADS ABOVE THE EULER LOAD ACCORDING TO THE DYNAMIC SMALL AND LARGE DISPLACEMENT THEORIES RESPECTIVELY.

of the column simultaneous with the increase of axial load above the critical level, according to the small respective large displacement theories.

Fig. 6(d) shows the assumed load deflection behaviour simultaneous with loading above the critical load according to the large displacement theory. Although the shape of the curve in Fig. 6(d) is assumed, its position in relation to Fig. 6(c) is correctly indicated, due to the fact that the lateral deflection of the column according to large displacement theory is always smaller than the corresponding value according to the small displacement theory, see the previous discussion above.

When the axial load ceases to increase, the lateral positions of the column at points 1 and 2 in Fig. 6, corresponding to the large and small displacement theories respectively are unstable. Thus, the column continues to move laterally until it reaches point 3 which corresponds to a position of static equilibrium according to the large displacement theory. The column would then begin to oscillate around this position, according to the large displacement theory, until it comes to rest in the neighbourhood of this point due to unavoidable damping forces not treated herein. According to the small displacement theory, no equilibrium position exists above the critical load, whereupon the lateral deflection of the column would continue to grow indefinitely with time.

Since the gravitational force is shown above not to influence the motion of the perfect column under consideration, it is altogether, omitted from the calculations in this illustration.

Fig. 6 clearly shows that if the column is to attain a deflected equilibrium position according to large displacement theory, the column must suffer large lateral deflections for small initial increases in the axial load above the critical level. Thus, hereafter in the present work, we assume that the Small Displacement Theory is valid throughout the following chapters. The results of the numerical calculations in the following sections would eventually show that the small displacement theory is a good approximation for the purpose of the present study, due to the fact that we shall never or seldom encounter such large lateral displacement which would warrant the use of more complicated techniques by means of the large displacement theory.

3. BEHAVIOUR OF IMPERFECT ELASTIC COLUMN

3.1 Applicability of Dynamic Principles

Application of dynamic principles discussed herein to a perfect elastic column is intrinsically obvious, since in this case the column would find itself in a state of complete instability throughout the increase of axial load above the critical level, according to the small displacement theory. The nature of dynamic instability in this case is too dominant to be ignored. A question of profound importance is whether it is equally important to tackle the problem of an imperfect column dynamically. It is true that an imperfect column would start to bend right from the start of loading. However, it is far from obvious that a static approach - that is to say assuming the existence of continuous equality between external and internal moments - would lead to reliable results. A way out of this dilemma would be to formulate the problem dynamically and compare the results of a quantitative analysis with the corresponding figures found according to the static method. Nevertheless, before trying to analyze a model quantitatively, our present aim is to gain a qualitative appreciation of the relative significance of the dynamic approach. Thus, we cope with this problem heuristically.

When a column is subjected to time dependent loading, it would be computationally more exact to take into account both axial and bending inertia. Nevertheless, the present question is whether it would be a good approximation to ignore the inertia effects. These effects are considered negligible by implication whenever we treat the problem statically.

Since for most engineering materials, small axial deformations give rise to large axial stresses, one may safely assume that in the axial direction, the column material responds immediately to the external axial load. Obviously, if a very large load is applied transiently, then a relatively large axial deformation may be required to create sufficient internal stresses. In such case the axial inertia may have to be taken into account.

It would be instructive to realize the significance of bending inertia by means of a simple illustration. Fig. 7 is intended to clarify the idea. In Fig. 7, an axial load, P, has been applied to an imperfect column during an interval of time, Δt. If we were to apply the static theory, then the condition of equilibrium between internal and external moments at each cross section would require a shortening, δ, of the concave side of the shaded element, relative to its convex side, in order to create an internal moment sufficiently large to balance the external moment due to P. Although this relative axial deformation, δ, is small and finite, the lateral deflection, U, has a relatively large finite value. This is due to the fact that linear deflection, $\delta \cdot L/b$, where L is the length and b is the width of the column, is usually much larger than δ (the length is assumed to be many times the width of the column). As the geometry of the bent column shows, the actual deflection, U, is still larger than the linear deflection, $\delta \cdot L/b$.

Now, we arrive at the decisive question whether it is possible for the column to bend laterally the relatively large deflection, U, during the loading interval of time, Δt. The answer to this naturally depends on the simultaneous influence of all the dynamic parameters

of the column. If the loading rate, for instance, is sufficiently rapid, the answer to the question is negative. Even if the loading rate is assumed to be slow, the required synchronization that the column must deflect just the amount, U, in the period of time, Δt, would not physically be realizable as a general rule.

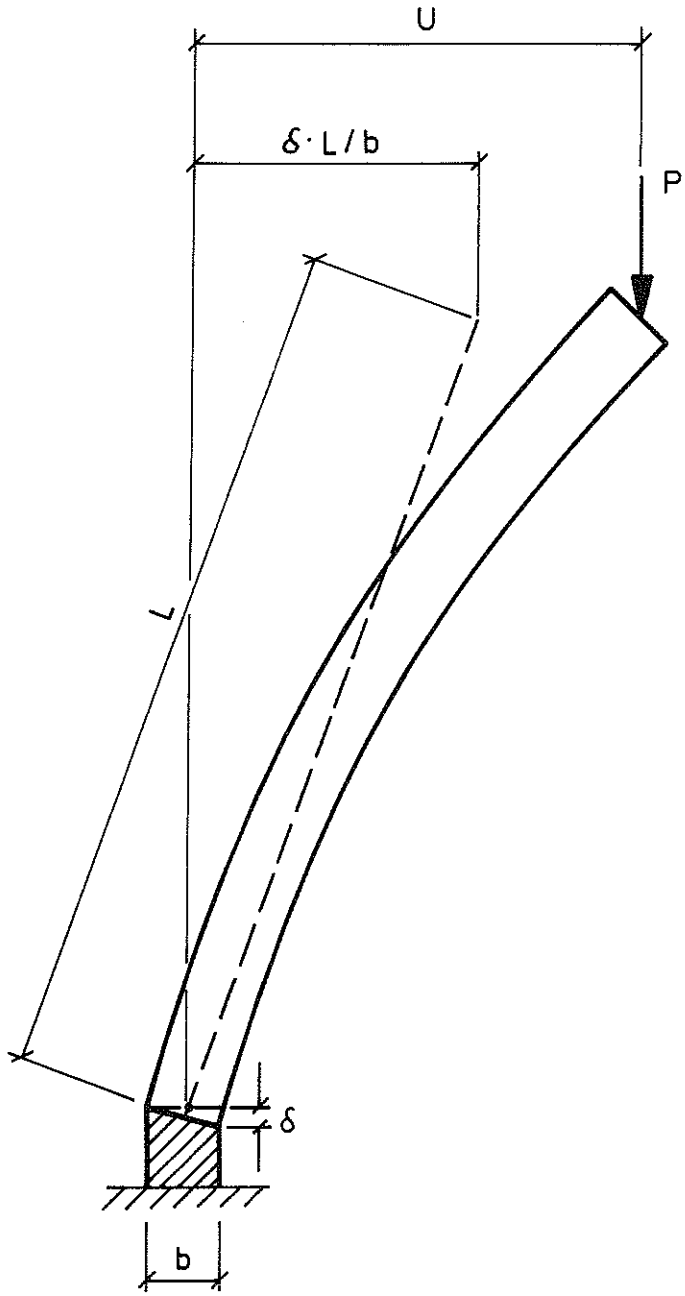

FIG. 7. RELATIONSHIP BETWEEN BENDING STRAIN AND LATERAL DEFLECTION

The difference between the lateral deflection required according to the static theory and the actual deflection developed simultaneous with the increase of axial load may get accentuated as the axial load approaches the critical level. This may be shown by the following argument:

As the axial load of the imperfect column approaches the maximum load, successively larger increments of lateral deflection are required in order to balance the additional increments of external moments caused by a certain increment of axial load. This is due to the physical fact that an increase of lateral deflection from U to U + ΔU, due to an increase of the axial load from P to P + ΔP would cause an additional external moment with two significant terms, $\Delta P \cdot U$ and $P \cdot \Delta U$: At the maximim column load, the second external moment increment, $P \cdot \Delta U$, would just be balanced by the corresponding increment of internal moment at the cross section of maximum strain. Thus, at the vicinity of the maximum load, the first external moment increment, $\Delta P \cdot U$, tends to become unbalanced, whereupon even small increments of axial loading may require increasingly larger lateral deflections.

The above discussion indicates the possibility that if the loading rate is sufficiently large and if the other dynamic parameters are favourable, the axial load may attain large values while the column is far from the deflection required by static equilibrium considerations. Thus,at a given instant of time a correct formulation of bending problem would be to assume the existence of a surplus moment increment, ΔM, which may be defined as the difference between the increments of internal and external moments developed solely due to bending during a certain increment of lateral deflection. ΔM may of course assume

zero value at certain isolated instants of time, but it has positive or negative values for the rest of the time. The concept of surplus moment increment will be discussed in greater detail in Chapter 7.

3.2 Numerical Evaluation of the Influence of Axial and Lateral Bending Inertia

The axial and lateral motion of Column B, shown in Fig. 1(b) is studied herein on the basis of the following assumptions:

1. The column has an elastic hinge which deforms in the manner depicted in Fig. 4;

2. The lateral position shown in Fig. 1(b) corresponds to a temporary lateral configuration at a certain instant of time simultaneous with the increase of axial load;

3. The initial state of the column at zero load level is given and subsequent motion of the column, simultaneous with loading up to the Euler load, is sought both in the axial and lateral directions; the axial load may be applied eccentrically, however, the direction of the axial load remains unchanged throughout the process of loading; and

4. The influence of the gravitational force on the motion of the column is taken into account.

In the axial direction, the motion of the column is governed by the following equations (see Appendix C, Sec. c):

$$Z = A_1 \sin kt + A_2 \cos kt + F_1 \tag{31}$$

and

$$\dot{Z} = A_1 k \cos kt - A_2 k \sin kt \tag{32}$$

in which Z= the axial deformation; $\dot{Z}$ = the axial deformation rate; and the terms F_1, k, A_1 and A_2 are defined in Appendix C by Eqs. (C 47), (C 48), (C 51) and (C 52) respectively.

The axial deformation, Z_s, according to the static theory is found from the following equation, see Eq. C(45) of Appendix C:

$$Z_s = \frac{P_e}{h} \tag{33}$$

in which P_e = the external axial load; and

$$h = \frac{AE}{d} \tag{34}$$

where A, E = the area respective modulus of elasticity of one hinge element; and d = half the depth of the elastic hinge, see Fig. 4.

In the lateral direction, the motion of the column is governed by the following equations (see Appendix C, Sec. b):

$$\alpha = C_1 \sin \omega t + C_2 \cos \omega t + F \tag{35}$$

and

$$\dot{\alpha} = C_1 \cdot \omega \cdot \cos \omega t - C_2 \cdot \omega \cdot \sin \omega t \tag{36}$$

in which α, $\dot{\alpha}$ = the deflection angle and angular velocity respectively; and the values F, ω, C_1 and C_2 are defined in Appendix C by Eqs. (C 30), (C 31), (C 36) and (C 37) respectively, provided that in Eq. (C 29) in Appendix C, the values of the deviation angle, θ, and the axially induced internal moment increment, ΔM_{ia}, are set equal to zero.

By equating the internal moment

$$M_i = C (\alpha_s - \alpha_o) \tag{37}$$

with the external moment

$$M_e = (P + \frac{M \cdot g}{2}) \cdot L\alpha_s + P \cdot X_o \tag{38}$$

in which

$$C = \frac{AbE}{\lambda}^{1}, \quad \lambda = \frac{d}{b} \tag{39}$$

α_s = the deflection angle according to the static theory; α_o = initial value of the deflection angle; and X_o = the initial eccentricity; the following equation would be found for the deflection angle, α_s:

$$\alpha_s = \frac{C \cdot \alpha_o + P \cdot X_o}{C - (P + \frac{M \cdot g}{2}) \cdot L} \tag{40}$$

The above mathematical analysis is used in a computer program (see Program 2, Appendix D) for evaluating the influence of the axial and lateral bending inertia on the motion of the simple column. The results for two different data sets are shown in Figs. 8 and 9A (first data set) and Fig. 9B (second data set). The first data set contains the following values:

A = 5 square centimeters; b = d = 5 centimeters; L = 2.5 meters; E = 10^9 Newtons per square meter; g = 10 meters per second square; M = 100 kg for the computations of Fig. 8 and Figs. 9A(c), (d) and (e) and M = 500 kg for Figs. 9A(a) and (b); c = loading rate = 2000 Newtons per second for Figs. 9A(b) and (d), c = 5000 Newtons per second for Fig. 9A (e), and c = 10000 Newtons per second for Fig. (8); Δt = the time step chosen for one computation cycle = 0.01 seconds; and X_o = the initial eccentricity = .1 centimeters.

---

1. See Eq. (C 15) of Appendix C.

Fig. 8 shows that the axial deformation behaviour of the column according to both static and dynamic theories closely follow each other such that within the scale of Fig. 8 the two load deformation curves almost perfectly coincide with each other.

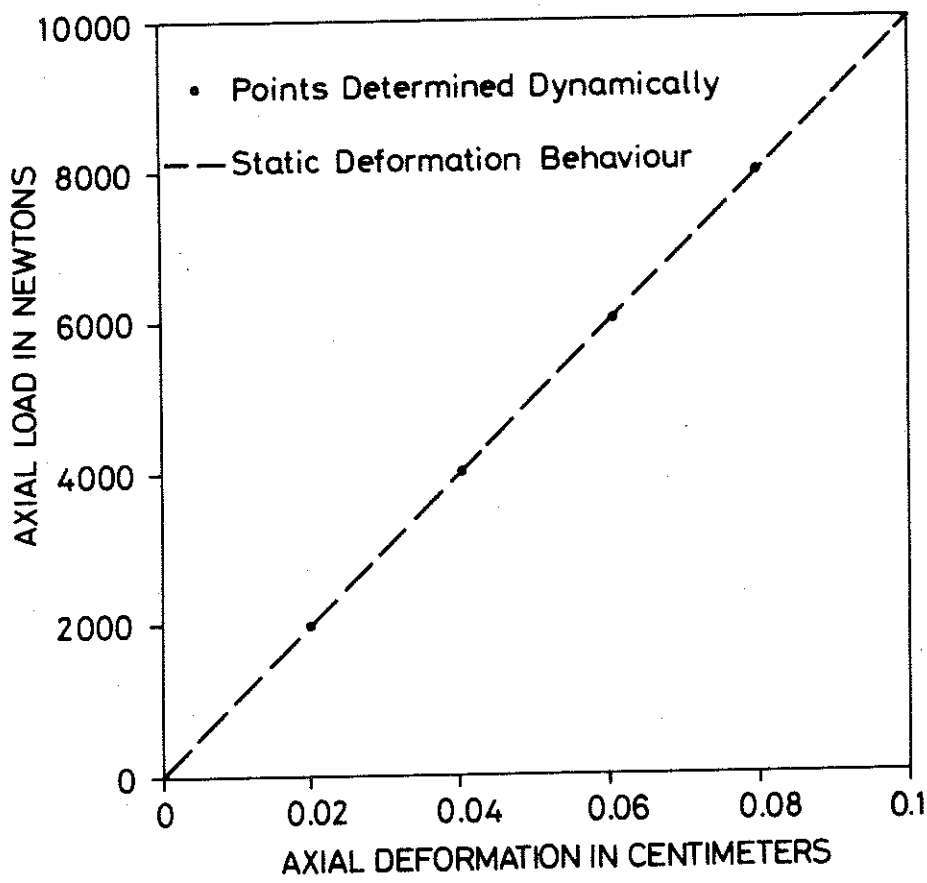

FIG. 8. STATIC AND DYNAMIC AXIAL DEFORMATION FOR LOADING RATE, c = 10000 NEWTONS PER SECOND

It is significant to note that the dynamic and static theories in Fig. 8 are in good agreement even for the loading rate, c = 10000 Newtons per second which will be the largest loading rate ever to be used in the present work. For smaller loading rates, the discrepancy between the static and dynamic theories would still be smaller.

Fig. 9A shows the load deflection behaviour of the column simultaneous with the increase of axial load according to both static and dynamic theories, for some parameter variations indicated in the diagram. The discrepancy between the static and dynamic theories at a number of load levels is shown by a flash which originates at the dynamically unstable position of the column and ends at the corresponding position of static equilibrium. The length of this flash is a measure of the instability of the column at the given load level. The discrepancy between the static and dynamic theories is shown to increase as the axial load approaches the Euler load.

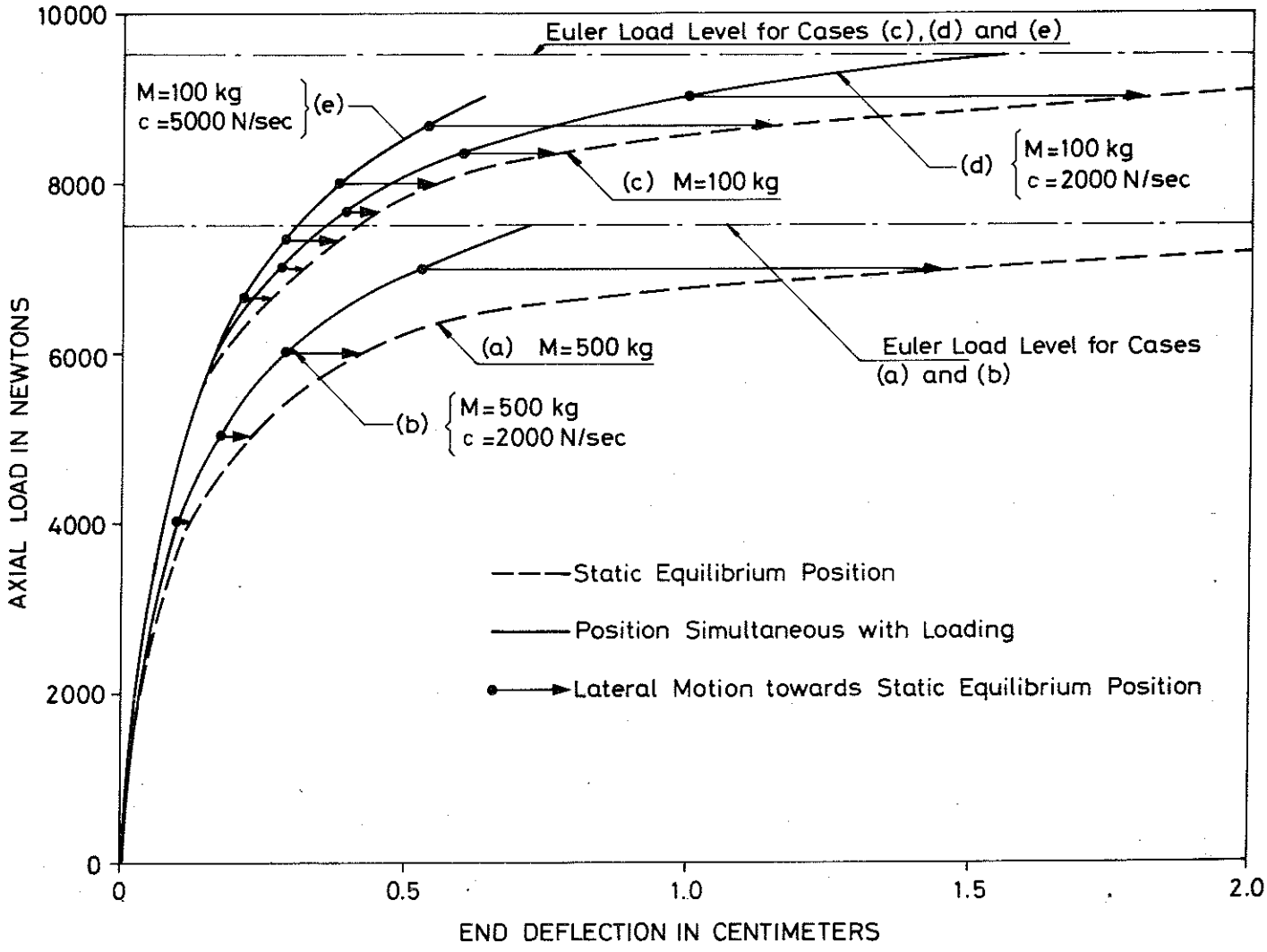

FIG. 9A. LOAD DEFLECTION BEHAVIOUR OF ECCENTRICALLY LOADED SIMPLE ELASTIC COLUMN FOR THE FIRST DATA SET.

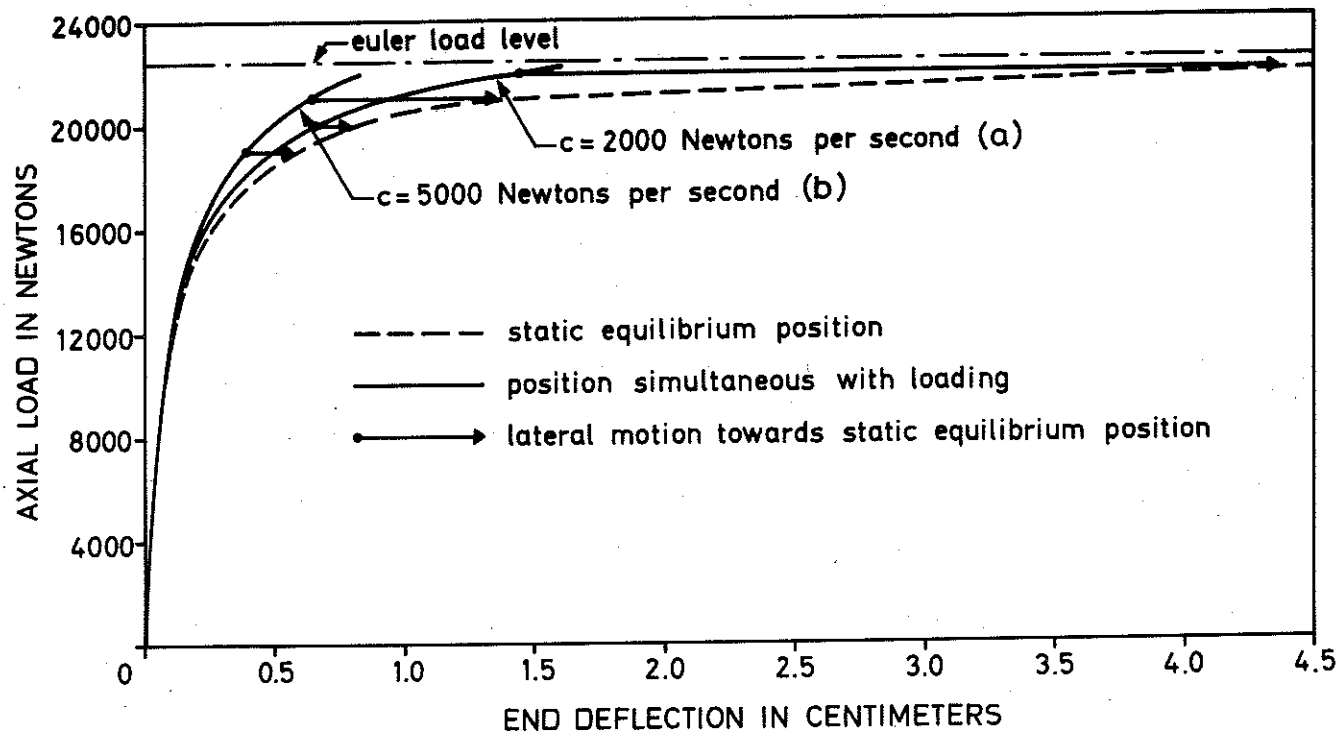

FIG. 9B. LOAD DEFLECTION BEHAVIOUR OF ECCENTRICALLY LOADED SIMPLE ELASTIC COLUMN FOR THE SECOND DATA SET.

The load deflection behaviour shown in Fig. 9B corresponds to the second data set with the following values (see the notations in the first data set):

$A = 5\ cm^2$; $b = 5$ cm; $d = 10$ cm; $L = 5$ m; $E = 10^{10}$ Newtons/m^2; $g = 10$ m/sec^2; $M = 500$ kg; $c = 2000$ Newtons/sec for Fig. 9B(a), and $c = 5000$ Newtons/sec for Fig. 9B(b); $\Delta t = 0.01$ sec; and $X_o = 0.1$ cm.

A comparison of the first and second data sets and the corresponding diagrams in Figs. 9A and 9B shows that, although the modulus of elasticity corresponding to Fig. 9B has increased ten times, the column with the new data in the second data set essentially shows the same load deflection behaviour as the column in the first data set. However, the extent of instability, i.e., the deviation of the time dependent dynamic positions from the corresponding static positions, in Fig. 9B has observably decreased in comparison with Fig. 9A.

It may be inferred from both Figs. 9A and 9B, that the static load deflection curve, shown by broken lines, asymptotically approaches the Euler load level as the lateral deflection attains infinitely large values. However, the curve obtained by studying the load deflection behaviour of a column simultaneous with loading, indicated by full-line, maintains finite lateral deflection even in the immediate vicinity of the Euler load. This curve may even intersect the corresponding critical level while the axial load continues to increase above the Euler load within a finite bending range. Nevertheless, as soon the axial load ceases to increase, the dynamically unstable column would move towards the static equilibrium configuration. If there are no energy losses and if the axial load lies below the Euler load, the unstable column would finally reach the static equilibrium configuration and begin to oscillate around that position. However, if the axial load is equal to or greater than the Euler load, the dynamically unstable column would indefinitely continue to move laterally.

It should be observed that both the buckling behaviour of the column simultaneous with loading above the Euler load according to large displacement theory, see Fig. 6(d), and the bending behaviour of the eccentrically loaded column simultaneous with loading below the Euler load, according to the small displacement theory, see Figs. 9A and 9B, may most conveniently

be described in terms of the following two distinct buckling or bending phases:

1. Phase 1 refers to the behaviour of the column simultaneous with the increase of axial load; and

2. Phase 2 refers to the column behaviour under the influence of a constant axial load; in other words, Phase 2 describes the transition from the dynamically unstable state of the column at the end of the loading period (end of Phase 1) to a dynamically stable state which implies the stable oscillations of the column around a position of equilibrium in the deflected configuration. For an elastic column with no energy losses during Phase 2, the dynamically stable oscillations of the column take place around the equilibrium position determined according to the static theory.

The concepts of buckling Phases 1 and 2 discussed above will extensively be used herein in the following chapters.

3.3 Concluding Remarks

The analysis of the elastic column has shown that the load deflection behaviour of the column simultaneous with the increase of axial load may not always conform to the pattern advocated by the static theory. However, it is important to note that regardless of the column behaviour simultaneous with loading, the final deflected equilibrium configurations in the case of the elastic column without energy losses would always coincide with the position determined according to the static theory. Thus, the two-phase buckling behaviour established in the course of the study herein may be of little practical significance for an elastic column since it affects neither the maximum column load nor the final deflected equilibrium configurations. Nevertheless, the two-phase buckling concept, defined and illustrated for the elastic column, may turn out useful for developing the concepts of inelastic buckling, where the time factor or more specifically, the deformation and strain reversal history may play a significant role in determining the maximum column load and in finding the buckling behaviour for loads below the maximum level.

PART II

BUCKLING BEHAVIOR OF PERFECT INELASTIC COLUMN

PART II. BUCKLING BEHAVIOUR OF PERFECT INELASTIC COLUMN

Introduction

The perfect inelastic column is defined herein as an initially straight centrally loaded inelastic column which would remain straight up to the tangent modulus load. Above that load level, the buckling behaviour of the perfect inelastic column with constant tangent modulus and prior to the occurrence of strain reversal, is shown in Sec. 4.1 to be dynamically equivalent to the behaviour of a perfect elastic column above the Euler load. The criterium for strain reversal is discussed in Sec. 4.2 and the possible general influences of the stress strain diagram and strain reversal phenomenon are pointed out in Secs. 4.3 and 4.4 respectively.

Although a realistic approach to the problem of column stability is the assumption of an imperfect column, i.e., a column with initial imperfections and/or disturbances which would bend simultaneously with loading from zero load level, the investigation of buckling of a perfect column is conceptually useful for clarification of some significant concepts of stability. It should be noted that classically, the perfect inelastic column has, in the past, been devoted much time and space. Thus, the study of the behaviour of perfect inelastic column herein has the twofold objective of serving as a pedagogical step towards understanding the complicated properties of an imperfect inelastic column; and clarifying the actual column behaviour as compared with the behaviour predicted by the classical static theory.

The numerical evaluation of the characteristics of the perfect inelastic column is accomplished through the analyses of two models. The analysis of Model 1 in Chapter 5 is devoted to the study of the load deflection behaviour of the perfect inelastic column with a constant tangent modulus above the tangent modulus load, subjected to the restriction that no strain reversal occurs simultaneously with loading; and that the load does not exceed the reduced modulus load. The analysis of Model 2 in Chapter 6 is devoted to the study of the complete buckling behaviour of a perfect inelastic column with bilinear stress strain diagram between the tangent modulus and the reduced modulus load, taking into account the possibility of strain reversal simultaneous with loading. In this latter model, the actual load deflection behaviour for various loading rates is compared with the corresponding load deflection behaviour predicted by Shanley Theory.

4. DISCUSSION OF GENERAL CONCEPTS

4.1 Dynamic Equivalence

A state of dynamic equivalence between elastic and inelastic columns can intuitively be asserted under the following two assumptions: 1) The tangent modulus in the inelastic range maintains a constant value, Fig. 10(a); and 2) the tangent modulus governs the deformation throughout the column. These two assumptions can be regarded as temporary restrictions and the cases when one or both of these restrictions are removed will subsequently be studied in the following discussion.

Evidently, if the above two conditions are satisfied, the dynamic properties, i.e., the time-deflection behaviour of elastic and inelastic columns with identical bending rigidities will be precisely equivalent. If the elastic and inelastic columns thus compared are assumed to have precisely the same dimensions, then the equality of their bending rigidities implies that the value of the tangent modulus, E_t, of the inelastic column must be equal with the modulus of elasticity, E, of the elastic column. An immediate consequence of this dynamic equivalence is that the inelastic column tends to become dynamically unstable at a certain critical load in the same way as the elastic column tends to dynamic instability at the Euler load. This critical load occurs at the tangent modulus load which is obtained from the Euler load by replacing the elastic modulus, E, with the tangent modulus, E_t.

The validity of the dynamic principle established above depends

entirely on the simultaneous validity of the two underlying assumptions. Thus, to begin with, it is significant to find out under what conditions those two assumptions are physically possible. The first assumption, that the tangent modulus has a constant value, simply means that the stress strain diagram of the column can be approximated by a bilinear form as shown in Fig. 10(a). Therefore, the physical possibility of the first assumption is a matter of material properties of the column. The second assumption, that the tangent modulus applies to the whole column, implies that deformation throughout the column takes place in the inelastic range and that no strain reversal occurs in any part of the column.

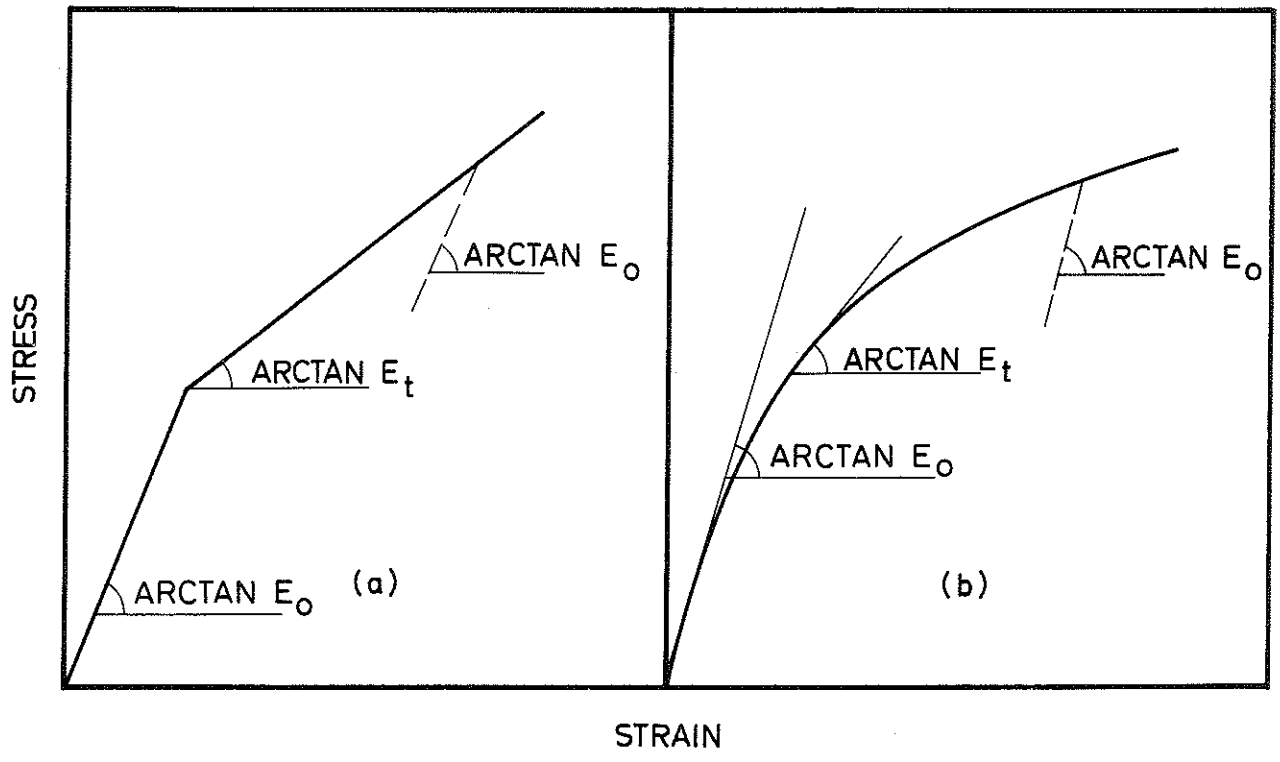

FIG. 10. STRESS STRAIN DIAGRAM, (a) BILINEAR CURVE; (b) ARBITRARY CURVE

4.2 Strain Reversal Criterium

No unloading can take place, if the column remains straight throughout loading, or, if the deformation rate due to the simultaneous increase of axial load exceeds the deformation rate due to bending within the whole column. This principle is illustrated in Fig. 11.

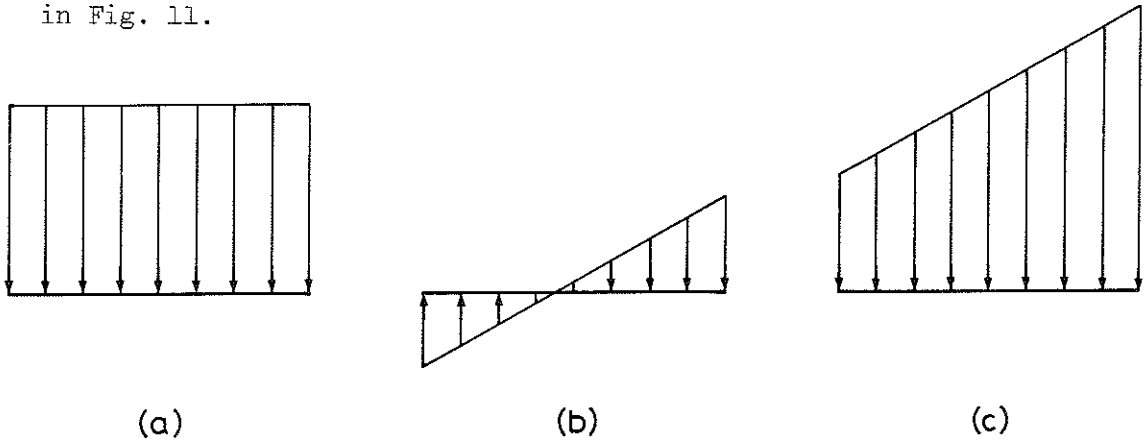

FIG. 11. DEFORMATION RATE ON A CROSS SECTION OF THE COLUMN: (a) DUE TO THE INCREASING AXIAL LOAD; (b) DUE TO SIMULTANEOUS BENDING; (c) DUE TO THE COMBINED EFFECT OF INCREASING AXIAL LOAD AND BENDING.

Fig. 11(a) shows the axial deformation rate over every cross section of the column due to the increase of axial load; Fig. 11(b) shows the simultaneous bending deformation rate over the cross section of maximum bending strain; and Fig. 11(c) depicts the resulting deformation rate. As long as the resulting strain rate does not reverse direction, no strain reversal can take place in the column.

If an initially straight column begins to bend simultaneously with loading at any loading level, including the tangent modulus load, then the strain rate caused due to lateral deflection may initially be small in comparison with the axial deformation rate, in which case

an immediate strain reversal may not occur before velocity of lateral motion becomes sufficiently large. This situation may naturally be altered if the column is subjected to a sufficiently violent velocity disturbance. In the absence of that, no strain reversal takes place immediately and the tangent modulus applies to the whole column; then from the previous discussion of principle of dynamic equivalence, it follows that the inelastic column becomes dynamically unstable as the column load increases above the tangent modulus load. Thus, the phenomenon of unstable bending and the principle of no initial strain reversal simultaneous with loading are mutually compatible and can occur simultaneously.

4.3 Influence of Stress Strain Diagram

Relaxing the assumption of a constant tangent modulus and attributing to the column an arbitrary stress strain diagram of the type shown in Fig. 10(b) cannot affect the unstable dynamic behaviour of the inelastic column at the immediate neighbourhood of the tangent modulus load. However, as the axial load continues to increase and the increment of load above the tangent modulus level attains finite values, the successive increments of lateral deflection develop continuously decreasing increments of internal moment due to the fact that the value of the tangent modulus decreases continuously with increasing deformation, see Fig. 10(b). This leads to the result that the unstable lateral motion of an inelastic column simultaneous with loading above the tangent modulus load would be more greatly accelerated if the stress strain diagram has an arbitrary shape with continuously decreasing tangent modulus as compared with the case of a bilinear stress strain diagram. This concept will be more precisely clarified in Sec. 7.2.

Thus, the shape of the stress strain diagram does not alter the fundamental result inferred from the principle of dynamic equivalence, that is to say, an inelastic column becomes dynamically unstable at the tangent modulus load and that the unstable lateral motion of the column continues with no strain reversal as long as the deformation rate due to bending is less than the deformation rate due to the increase of axial load. As shown in Fig. 10(b), it is assumed that the tangent modulus is continuously decreasing. In other words, the rather unusual case when the tangent modulus increases with increasing deformation is excluded from the above discussion. Even this latter unusual case may be taken into account by observing that,

in an interval of increasing tangent modulus, the bending rigidity increases and the unstable motion partially decelerates.

4.4 Influence of Strain Reversal

The results of the discussion so far indicate that the assumption of no strain reversal simultaneous with the increase of axial load may be valid at least at the early stage of bending of an initially straight inelastic column loaded above the tangent modulus load. However, strain reversal occurs in the following two situations:

1. As the axial load continues to increase above the tangent modulus load, the velocity of lateral motion of the unstable column eventually becomes large enough to cause some strain reversal to begin.

2. Regardless of bending deformation rate, if the axial load at any level ceases to increase, the axial deformation rate in Fig. 11(a) would tend to zero and consequently the resulting bending deformation over all cross sections of the column due to the ensuing lateral motion would be accompanied by maximum possible strain reversal throughout the back side of the column , i.e. the region of the column which is currently undergoing decreasing bending strain.

The occurrence of strain reversal simultaneous with loading may partly give rise to a nonuniform distribution of axial stresses with subsequent eccentric behaviour to be explained in Sec. 7.3, and partly develop a greater resistance to bending due to pure bending effect. The occurrence of strain reversal under the influence of a constant axial load implies no eccentric behaviour while the column is developing its maximum bending rigidity. These ideas will be more fully explored in Chapter 7. However, it may presently suffice with the intuitive understanding that a greater bending rigidity during phase 2 raises the load-bearing capacity of the column as compared

with the tangent modulus theory. The logical implication of this result is that the dynamic instability which is observed at the tangent modulus load is a temporary phenomenon and that there exists a maximum critical column load which definitely exceeds the value of the tangent modulus load. It must be emphasized that this statement is valid only for a perfect column which is assumed to remain straight up to the tangent modulus load. For an actual imperfect column - to be treated in the next chapter - although the question of strain reversal plays a central role, the size of the maximum load has no relationship to the tangent modulus load and may fall below that level. It should be noted that the existence of a maximum column load does not imply that this maximum load has a unique value. In fact, it will presently be shown and illustrated in subsequent chapters that, in general, dynamics of the inelastic column affects the value of its maximum critical load. The mere existence of a maximum column load signifies that for any constant load below that level, the initially perfect inelastic column is absolutely stable in the sense that positions of the column during lateral motion would at all times remain within finite bounds. The numerical evaluation of such lateral equilibrium configurations for the initially perfect inelastic column, would be accomplished herein in the course of development of two column models which immediately follow in the next two chapters.

5. ANALYSIS OF MODEL 1

Abstract

Model 1 analyzes the partial load-deflection behaviour of a perfect inelastic column (Column B introduced in Sec. 1.2) prior to strain reversal during buckling Phase 1, i.e., the load deflection behaviour simultaneous with loading. The axial load begins to increase at the tangent modulus load, while the column deforms in the inelastic range with a constant tangent modulus. The analysis is carried out both according to an exact mathematical method and according to the multi-cycle computation technique described in Appendix C. The latter method is compared with the exact mathematical approach by a study of the corresponding results. Partial load-deflection curves are traced for various parameter variations. The behaviour of the column during buckling Phase 2, i.e., under the influence of constant axial load, is not treated herein dynamically, however, the first temporary position of equalized external and internal moments is determined in closed form. Subsequently, a modified Shanley formula is derived for the equilibrium position of the column, taking into account a predetermined initial deflection introduced at the tangent modulus load. However, no numerical comparison with the classical theory is attempted in this model. This task is left to Model 2, where the complete buckling behaviour of the perfect inelastic column with constant tangent modulus is thoroughly determined.

5.1 Introduction

For the convenience of reference, Column B introduced in Sec. 1.2 and shown in Appendix C is depicted again in Fig. 12. Since all subsequenced numerical illustrations herein are based on the buckling behaviour of this simple column, Fig. 12 shall, hereafter, be referenced from appropriate places in the following chapters. Model 1, which is

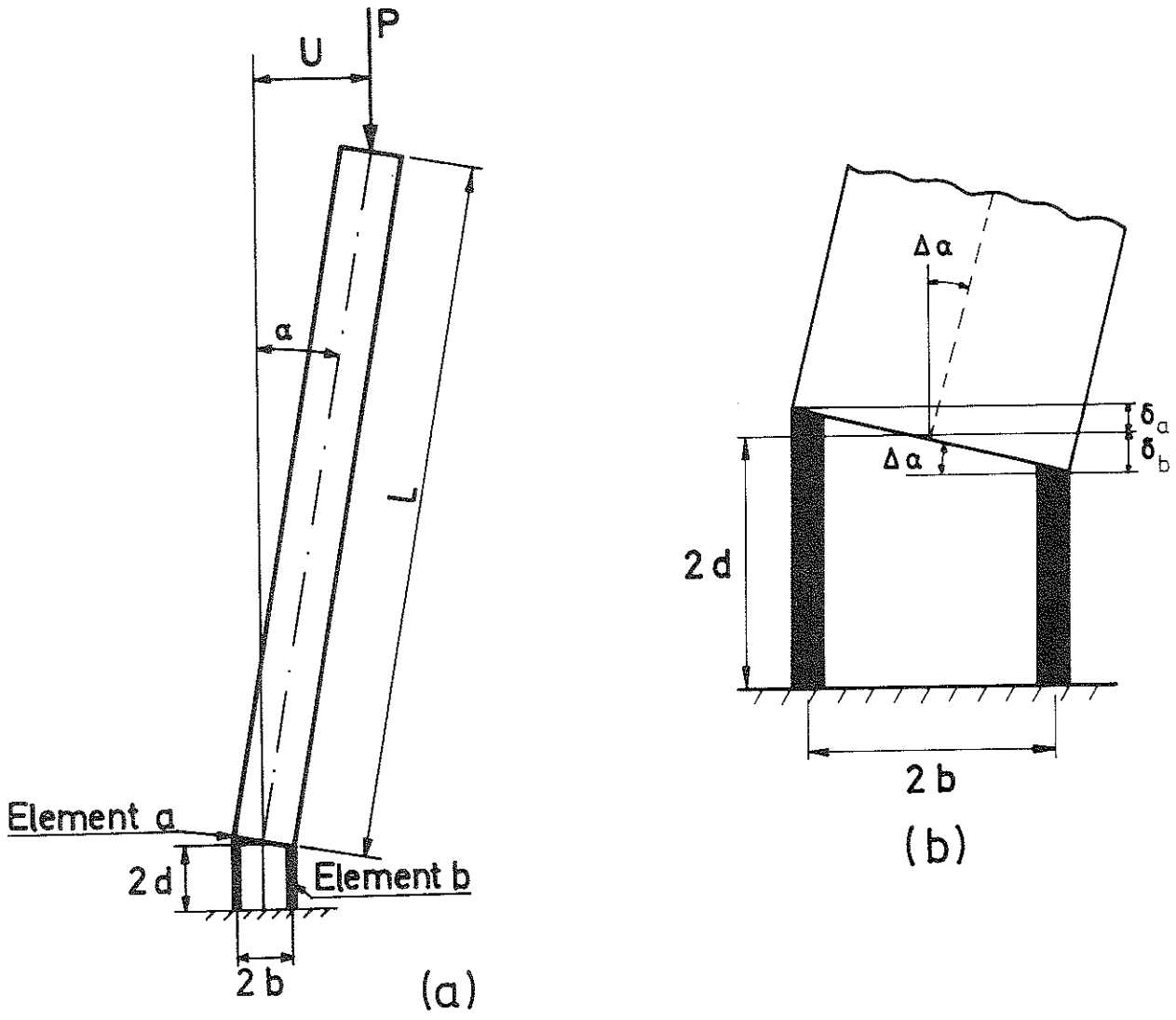

FIG. 12. THE SIMPLIFIED COLUMN: (a) THE DEFLECTED CONFIGURATION AT A CERTAIN INSTANT OF TIME DURING LATERAL MOTION; (b) THE DEFORMATION OF THE HINGE DUE TO AN INCREMENT OF LATERAL DEFLECTION

analyzed in this chapter, studies the load deflection behaviour of the simple column in Fig. 12 simultaneous with the increase of axial load above the tangent modulus load. The following specific assumptions are made:

1. Before the start of loading, the column is initially in a state of equilibrium at the tangent modulus load, and subsequent loading of the column takes place entirely in the inelastic range;

2. The inelastic hinge consists of a material with a bilinear stress strain diagram, see Fig. 10(a);

3. The column at the tangent modulus load is subjected to a small disturbance which may comprise an initial vanishingly small lateral deflection at the initial load and a possible initial velocity disturbance;

4. There is no excentricity in the application of the axial load, i.e., the column is centrally loaded;

5. The load deflection behaviour of the column simultaneous with loading is sought in a loading range where no strain reversal takes place in the column;

6. Since the gravitational force does not affect the motion of this perfect column above the tangent modulus load (see Appendix C, Sec. d), the behaviour of the column would be the same as if the gravitational acceleration, g, were equal to zero; thus, the own weight of the column is disregarded by setting g equal to zero in the applicable formulas; and

7. The axial load remains conservative throughout the process of loading, i.e., there is no deviation in the original direction of application of the external axial load.

5.2 Governing Equations

From the assumptions in Sec. 5.1, Eqs. (C 15), (C 55) and (C 57) of Appendix C reduce to the following forms:

$$C = \frac{AbE_b}{\lambda} \tag{41}$$

$$M_i = C_c \cdot \alpha_c \tag{42}$$

and

$$P_c = \frac{C_c}{L} \tag{43}$$

in which C = the bending rigidity; A = the area of one hinge element; E_b = tangent modulus corresponding to element b of the hinge in Fig. 12(b); λ = d/b where d,b = half the depth respective half the width of the hinge in Fig. 12(a); M_i = the internal moment at the tangent modulus load; C_c, α_c = the bending rigidity respective deflection angle at the tangent modulus load; P_c = the tangent modulus load; and L = the length of the column.

Using the notation, $P_t = P_c$, $C_t = C_c$, and observing that $C = C_c$, i.e., the bending rigidity is constant throughout the process of loading, then Eqs. (41) - (43) could be rewritten in the following forms:

$$C_t = \frac{AbE_t}{\lambda} \tag{44}$$

$$M_i = \frac{AbE_t}{\lambda} \cdot \alpha_c \tag{45}$$

and

$$P_t = \frac{AbE_t}{\lambda L} \tag{46}$$

in which $E_t = E_a = E_b$ where E_t = the constant tangent modulus and E_a and E_b correspond to the actual tangent moduli of hinge elements a and b respectively.

Noting that $C = C_c$ as described above and considering the fact that the increase of axial load, ΔP, takes place above the tangent modulus load, Eq. (C 58) of Appendix C leads to the following equation for the motion of the simple inelastic column above the tangent modulus load:

$$\ddot{\alpha} - \frac{\Delta P \cdot L}{I} \cdot \alpha = 0 \qquad (47)$$

Eq. (47) is exactly identical to Eq. (12) which describes the motion of the simple elastic column above the Euler load. This clearly verifies the assertion that, in the absence of strain reversal and with a constant tangent modulus in the inelastic range, an inelastic column loaded above the tangent modulus load behaves exactly the same as a corresponding elastic column loaded above the Euler load.

On the basis of the above observation, the analysis of the simple elastic column according to the small displacement theory in Sec. 2.4, corresponding to the increase of axial load above the Euler load is exactly applicable to the analysis of the present model. Thus, the deflection angle, α, and the angular velocity, $\dot{\alpha}$, corresponding to the solution of Eq. (47) is obtained from Eqs. (21) and (22) respectively. This solution is valid until strain reversal begins to occur in the column simultaneously with loading. The criterium for the occurrence of strain reversal is treated in Sec. 5.3.

The approximate numerical solution of the equations of motion of the present model is carried out by means of the multi-cycle computation technique introduced in Appendix C. However, for the sake of comparison, an exact mathematical solution is presented in Sec. 5.4.

5.3 Strain Reversal Criterium

The increase of axial load above the tangent modulus level causes a state of instability in the column with a certain initial imperfection. This instability results in a simultaneously increasing deflection and angular velocity. Strain reversal occurs in the axial element, a, of the column in Fig. 12(a) as soon as the rate of deformation due to bending exceeds the rate of deformation due to the increase of axial load.

The increment of axial load, ΔP, with a constant loading rate, is obtained from the equation

$$\Delta P = ct \tag{48}$$

where c is the loading rate in Newtons per second; and t is the time, starting at the tangent modulus load, in seconds.

From Eq. (48) and the definition of the axial strain increment, ε_{axial}, corresponding to ΔP it follows that

$$\varepsilon_{axial} = \frac{ct}{2AE_t} \tag{49 a}$$

For the accompanying bending strain increment, $\varepsilon_{bending}$, corresponding to ΔP, either of the two equations (C 18) or (C 19) would reduce to the form

$$\varepsilon_{bending} = \frac{\alpha}{2\lambda} \tag{49 b}$$

in which α specifically refers to the deflection angle increment corresponding to ΔP (the symbol Δ in front of $\Delta\alpha$ as well as in front of tha axial and bending strain increments is dropped for the sake of convenience).

Differentiation of Eqs. (49 b) and (49 a) with respect to time results in the following equations for the bending strain rate, $\dot{\varepsilon}_{bending}$, and the axial strain rate, $\dot{\varepsilon}_{axial}$:

$$\dot{\varepsilon}_{bending} = \frac{\dot{\alpha}}{2\lambda} \tag{50}$$

$$\dot{\varepsilon}_{axial} = \frac{c}{2AE_t} \tag{51}$$

where $\dot{\alpha}$ denotes the angular velocity of the column in radians per second.

For the loading range in which the value of the strain rate ratio, $\dot{\varepsilon}_{bending}/\dot{\varepsilon}_{axial}$ is smaller than unity, a reversal of strain in the column is physically impossible.

5.4 Exact Mathematical Solution

The reader, who prefers to quickly attain quantitative results by means of a simple physically comprehensible numerical procedure, may escape the present section without missing any substantial point. However, the reason for including this section, which is accompanied by a mathematical appendix, is twofold: Firstly, we wish to accquire an appreciation of the mathematical complexity of the problem if we were to seek closed-form solutions of the entire problem; secondly, we desire to test the numerical reliability of the approximate procedure - which is developed in Appendix C and utilized throughout the rest of this work - by comparing the exact and the approximate methods.

Using Eqs. (10) and (48), Eq. (47) may be rewritten in the form

$$\frac{d^2\alpha}{dt^2} - St\alpha = 0 \tag{52}$$

in which

$$S = \frac{3c}{ML} \tag{53}$$

The general solutions of α and its time derivative, $\dot{\alpha}$, are related to the solutions of the Stokes equation

$$\frac{d^2u}{dz^2} + zu = 0 \tag{54}$$

in the complex plane, z, according to the relations (see Appendix B):

$$\alpha = C_1\left[R(H2) + \sqrt{3}\, I(H2)\right] - C_2 I(H1) \tag{55}$$

$$\dot{\alpha} = 4C_1\gamma R(\dot{H}2) - C_2\gamma\left[I(\dot{H}1) + \sqrt{3}\, R(\dot{H}1)\right] \tag{56}$$

in which C_1, C_2 = arbitrary real constants; $\gamma = S^{1/3}/2$; Hi, $\dot{H}i$ (i = 1,2) = the particular solutions of the Stokes equation and the corresponding derivatives with respect to z on the ray arg $z = \pi/3$; and $R(Hi)$, $I(Hi)$, $R(\dot{H}i)$, $I(\dot{H}i)$ = the real and imaginary parts corresponding to the functions Hi and $\dot{H}i$ (see Appendix B).

The time elapsed after the start of loading at the tangent modulus load, during Phase 1, is found from the following equation (see Appendix B):

$$t_1 = \frac{2y}{\sqrt{3}\, S^{1/3}} \tag{57}$$

in which y = the imaginary coordinate of the complex variable, z.

The numerical values of the functions which appear in Eqs. (55) and (56) are given in Tables 1 and 2 for values of $y \leq 5.0$ and for equal intervals $\Delta y = 0.2$.

Substitution of the initial values of the functions in Tables 1 and 2 at zero time, corresponding to y = 0, into Eqs. (55) and (56) and subsequent solution of the equations lead to the following relations for C_1 and C_2 expressed in terms of the initial deflection angle, α_o, and the initial angular velocity, $\dot{\alpha}_o$:

$$C_1 = \frac{\dot{\alpha}_o}{\lambda(7\beta_1 + \sqrt{3}\,\beta_2)} + \frac{\alpha_o(\beta_2 + \sqrt{3}\,\beta_1)}{\beta_3(7\beta_1 + \sqrt{3}\,\beta_2)} \tag{58}$$

TABLE 1.-RESULTS OF COMPUTATION OF THE REAL AND IMAGINARY PARTS OF FUNCTION H1 AND THE CORRESPONDING DERIVATIVES FOR Z ON THE RAY arg $Z=\pi/3$

Y (1)	R(H1) (2)	I(H1) (3)	$R(\dot{H1})$ (4)	$I(\dot{H1})$ (5)
0.00	0.00000000	-1.07437570	.67829873	.39161595
.20	.00000000	-.89551680	.65625295	.37888781
.40	-.00000000	-.72734087	.60076906	.34685417
.60	-.00000001	-.57679033	.52624642	.30382850
.80	.00000000	-.44732999	.44426112	.25649428
1.00	.00000000	-.33975534	.36325337	.20972443
1.20	.00000000	-.25301230	.28871655	.16669058
1.40	.00000000	-.18492373	.22367346	.12913793
1.60	.00000000	-.13277054	.16926656	.09772609
1.80	-.00000000	-.09371424	.12534103	.07236568
2.00	-.00000000	-.06507340	.09094933	.05250962
2.20	-.00000000	-.04447982	.06474536	.03738075
2.40	.00000000	-.02994510	.04526502	.02613377
2.60	.00000000	-.01986598	.03110590	.01795901
2.80	-.00000000	-.01299319	.02102723	.01214008
3.00	.00000000	-.00838157	.01399183	.00807819
3.20	.00000000	-.00533466	.00917024	.00529444
3.40	-.00000000	-.00335131	.00592290	.00341959
3.60	.00000000	-.00207872	.00377181	.00217765
3.80	.00000000	-.00127345	.00236927	.00136790
4.00	.00000000	-.00077072	.00146861	.00084791
4.20	-.00000000	-.00046095	.00089864	.00051882
4.40	.00000000	-.00027251	.00054301	.00031350
4.60	.00000000	-.00015928	.00032411	.00018713
4.80	.00000000	-.00009207	.00019115	.00011036
5.00	-.00000000	-.00005264	.00011143	.00006433

TABLE 2.-RESULTS OF COMPUTATION OF THE REAL AND IMAGINARY PARTS OF FUNCTION H2 AND THE CORRESPONDING DERIVATIVES FOR Z ON THE RAY arg $Z=\pi/3$

Y (1)	R(H2) (2)	I(H2) (3)	$R(\dot{H}2)$ (4)	$I(\dot{H}2)$ (5)
0.00	0.00000000	1.07437570	.67829873	-.39161595
.20	.15680720	1.16711480	.70591701	-.37888782
.40	.31587131	1.27444600	.80056880	-.34685417
.60	.48306597	1.41348510	.98282630	-.30382851
.80	.66852500	1.60524920	1.28064910	-.25649429
1.00	.88746787	1.87689470	1.73531730	-.20972443
1.20	1.16184760	2.26539140	2.41004210	-.16669057
1.40	1.52326540	2.82329680	3.40295680	-.12913794
1.60	2.01783150	3.62775730	4.86736470	-.09772607
1.80	2.71407060	4.79462260	7.04403990	-.07236562
2.00	3.71568040	6.50082060	10.31360100	-.05250965
2.20	5.18216310	9.02024940	15.28250000	-.03738071
2.40	7.36240970	12.78201200	22.92562500	-.02613391
2.60	10.64984000	18.46592900	34.82513000	-.01795901
2.80	15.67379500	27.16080400	53.57404900	-.01213975
3.00	23.45247900	40.62926600	83.46461600	-.00807834
3.20	35.65137300	61.75532500	131.67289000	-.00529397
3.40	55.02408100	95.30785300	210.31592000	-.00342143
3.60	86.17148400	149.25547000	340.05629000	-.00217783
3.80	136.86145000	237.05226000	556.47505000	-.00136530
4.00	220.34440000	381.64846000	921.43914000	-.00085258
4.20	359.45378000	622.59268000	1543.55810000	-.00051498
4.40	593.93434000	1028.72460000	2615.32190000	-.00027466
4.60	993.65814000	1721.06650000	4481.11030000	-.00020599
4.80	1682.67440000	2914.47790000	7762.82190000	-.00008392
5.00	2883.36740000	4994.13870000	13593.93700000	-.00019836

$$C_2 = \frac{\alpha_o}{\beta_3} - C_1\sqrt{3} \tag{59}$$

in which $\beta_1 = 0.67829873$; $\beta_2 = 0.39161595$ and $\beta_3 = 1.0743758$.

5.5 Numerical Results

The exact and approximate methods developed above are used in a computer program (see Program 4, Appendix D) for determination of column behaviour simultaneous with loading above the tangent modulus load, prior to strain reversal. The results for two different data sets are presented in Figs. 13 and 14 A (first data set), and Fig. 14 B (second data set).

Fig. 13 shows a comparison of partial load-deflection pattern according to exact and approximate methods for a column of the type shown in Fig. 12 with the data appearing on the next page.

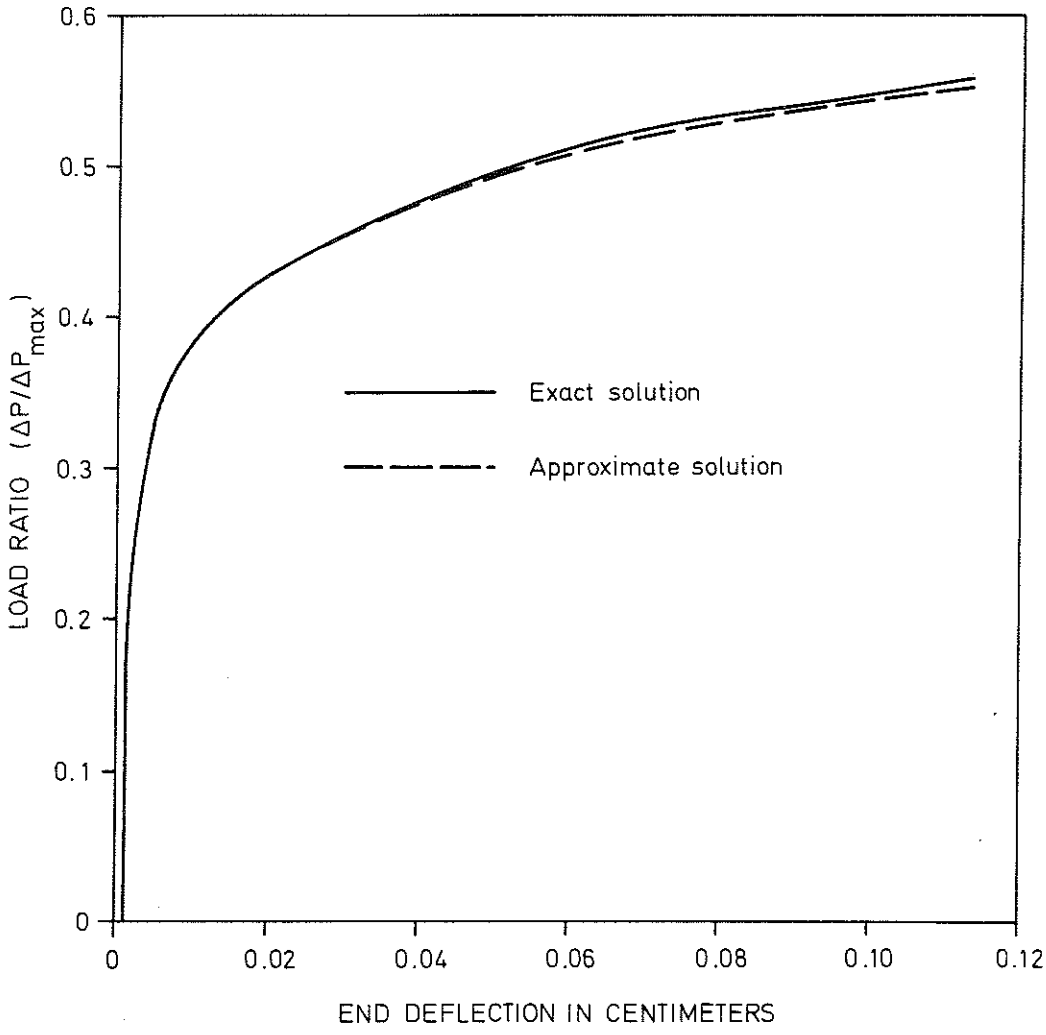

FIG. 13. COMPARISON OF EXACT AND APPROXIMATE METHODS

The reference column in the first data set, corresponding to Figs. 13 and 14 A, has the following numerical data:

L = 2.5 m; M = 100 kg; A = 5 cm^2; b = d = 5 cm; E_o = 2 x 10^9 Newtons/m^2; E_t = 10^9 Newtons/m^2; U_o = 0.001 cm; V_o = 0 cm/sec; and c = 1000 Newtons/sec.

Fig. 14 A shows the partial load-deflection curve of the above reference column as well as similar curves where one parameter of the reference column is varied at a time. The upper bound of buckling Phase 1 is confined in this model either to the double modulus load or a smaller load at which strain reversal begins to occur in the column. The latter case is marked, where applicable in Fig. 14 A, by a heavy point at the end of the load-deflection curve. The maximum load increment between the tangent modulus and reduced modulus loads, ΔP_{max}, which is used as a possible upper bound for the load increment, ΔP, above the tangent modulus load in the present calculations, is determined by the equation,

$$\Delta P_{max} = P_t \cdot \frac{K - 1}{K + 1} \tag{60}$$

in which P_t denotes the tangent modulus load; and

$$K = \frac{E_o}{E_t} \tag{61}$$

where E_o is the initial elastic modulus; and E_t is the constant tangent modulus in the inelastic range. Eq. (60) will be derived herein in the Section 5.6.

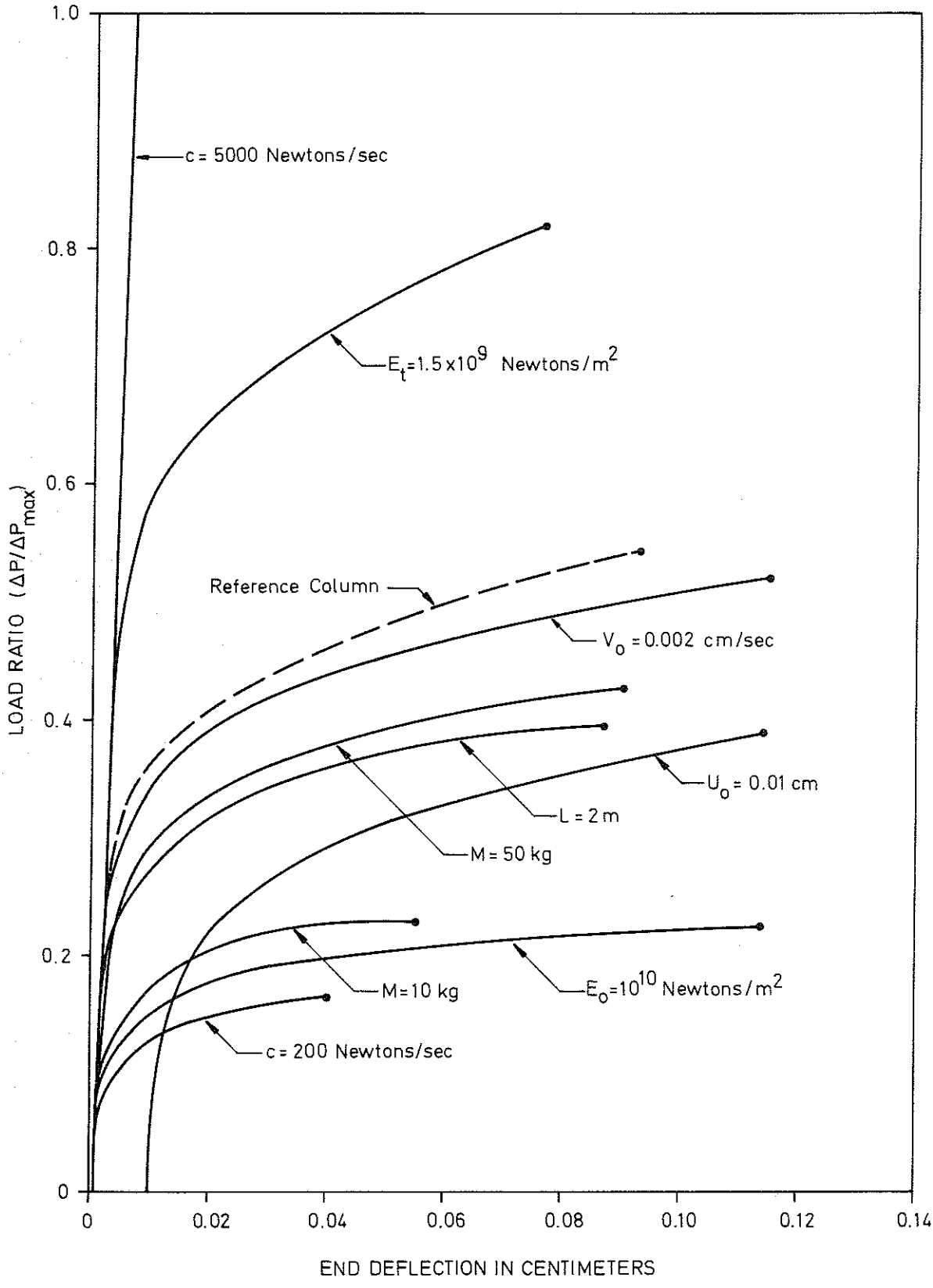

FIG. 14 A. PARTIAL LOAD-DEFLECTION CURVES FOR VARIOUS PARAMETER VARIATIONS CORRESPONDING TO THE FIRST DATA SET

Fig. 14 B shows an illustration similar to Fig. 14 A with a reference column whose data appears on the next page.

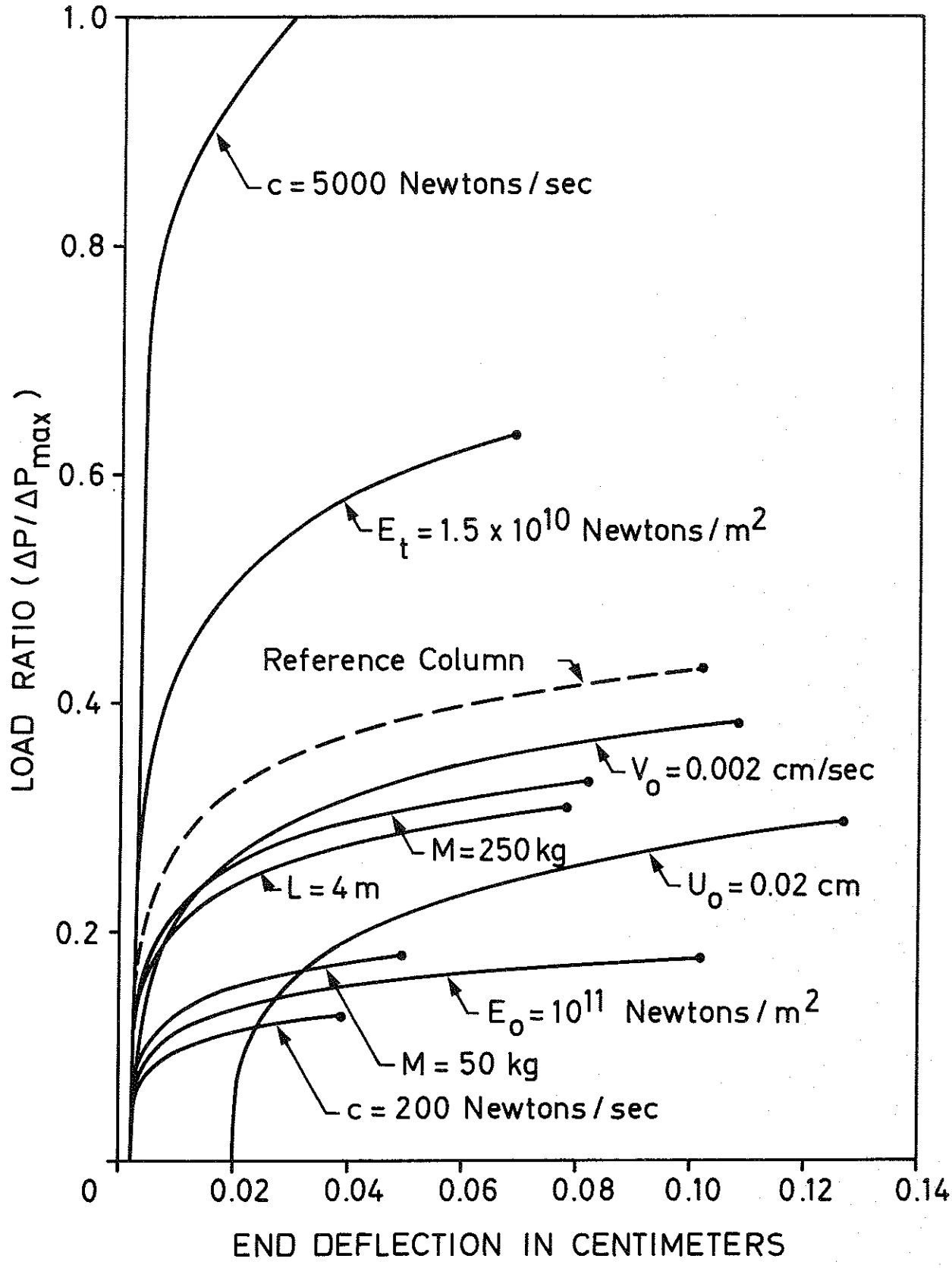

FIG. 14 B. PARTIAL LOAD DEFLECTION CURVES FOR VARIOUS PARAMETER VARIATIONS CORRESPONDING TO THE SECOND DATA SET

The reference column in the second data set, corresponding to Fig. 14 B, has the following numerical data:

$L = 5$ m; $M = 500$ kg; $A = 5$ cm^2; $b = 5$ cm; $d = 10$ cm; $E_o = 2 \times 10^{10}$ Newtons/m^2; $U_o = 0.001$ cm; $V_o = 0$ cm/sec; and $c = 1000$ Newtons/sec.

It should be noted that the illustrations shown in Figs. 14 A and 14 B are drawn on the basis of the computations performed according to the exact method. Furthermore, for the comparison of the exact and approximate methods in Fig. 13, the length of the time step, Δt, corresponding to one computation cycle according to the approximate method, is chosen equal to 0.01 seconds.

The loading range studied in Figs. 14 A and 14 B is given in the ratio form, $\Delta P/\Delta P_{max}$. However, the values of the tangent modulus, P_t, and the maximum load increment, ΔP_{max}, corresponding to the reference column in each of the two data sets are as follows: For the first reference column in Fig. 14 A, $P_t = 10000$ Newtons and $\Delta P_{max} = 3333$ Newtons; and for the second reference column in Fig. 14 B, $P_t = 25000$ Newtons and $\Delta P_{max} = 8333$ Newtons.

The present partial results show that there is good agreement between the exact mathematical method and the proposed approximate procedure; furthermore, parameter variations have considerable effect on the range of complete instability simultaneous with loading above the tangent modulus load.

5.6 The First Position of Moment Equalization

From the analysis so far, it has been observed that the behaviour of Model 1 is characterized by complete lateral instability during buckling Phase 1. However, during buckling Phase 2, the transverse motion of the column occurs under the influence of a constant axial load whereby the maximum bending rigidity of the column will be utilized. If the axial load is below its maximum level, the surplus moment increment would be positive during all deflection intervals in Phase 2, whereby the column would finally attain a state of stable oscillatory motion.[1]

The computations so far performed on Model 1 take into account the reduced modulus load as a possible upper limit. According to the analysis of Part I, the reduced modulus load is indeed the maximum column load for this model. This assertion is however mathematically proved in this section by the following technique: A closed-form solution for the position of the column is found, where the internal and external moments equalize for the first time. Subsequently, it is proved that this position remains finite as long as the axial load lies below the reduced modulus load. This is sufficient to assure the existence of stable configurations in the loading range below the reduced modulus load. This question would be further explained at the end of this section.

During Phase 1, $E_a = E_b = E_t$ and the column develops its minimum bending rigidity, C_{min}, whereupon, Eq. (44) may be rewritten in the form

$$C_{min} = \frac{AbE_t}{\lambda} \tag{62}$$

---

1. These concepts which were heuristically discussed in previous sections will be more fully developed in subsequent chapters herein.

During Phase 2, on the other hand, $E_b = E_t$ and $E_a = E$, see Fig. 10(a), whereby the column develops its maximum bending rigidity, C_{max}. Thus Eq. (C 15) of Appendix C results in the following equation:

$$C_{max} = \frac{2AbKE_t}{\lambda(K + 1)} \tag{63}$$

Equating the external moment, $M_e = P \cdot L \cdot \alpha$, with the internal moment $M_i = C_{max} \cdot \alpha$ and substituting Eq. (63) in the resulting equation leads to the following equation for the reduced modulus load, P_r:

$$P_r = \frac{C_{max}}{L} = \frac{2AbKE_t}{\lambda L(K + 1)} \tag{64}$$

Considering Eq. (C 16) of Appendix C and noting that the axially induced internal moment increment, ΔM_{ia}, is equal to zero for the present model during all loading intervals leads to the following equation for the total internal moment developed at the end of Phase 2:

$$M_i = M_o + C_{min}\Delta\alpha_1 + C_{max}\Delta\alpha_2 \tag{65}$$

in which $\Delta\alpha_1$, $\Delta\alpha_2$ = the increments of deflection angle corresponding to Phases 1 and 2 respectively as shown in Fig. 15(a); and

$$M_o = P_t L\alpha_o \tag{66}$$

denotes the initial moment in equilibrium with the external moment at the tangent modulus load.

From Fig. 15(a), the external moment, M_e, corresponding to the column load, $P_t + \Delta P$, can be written as

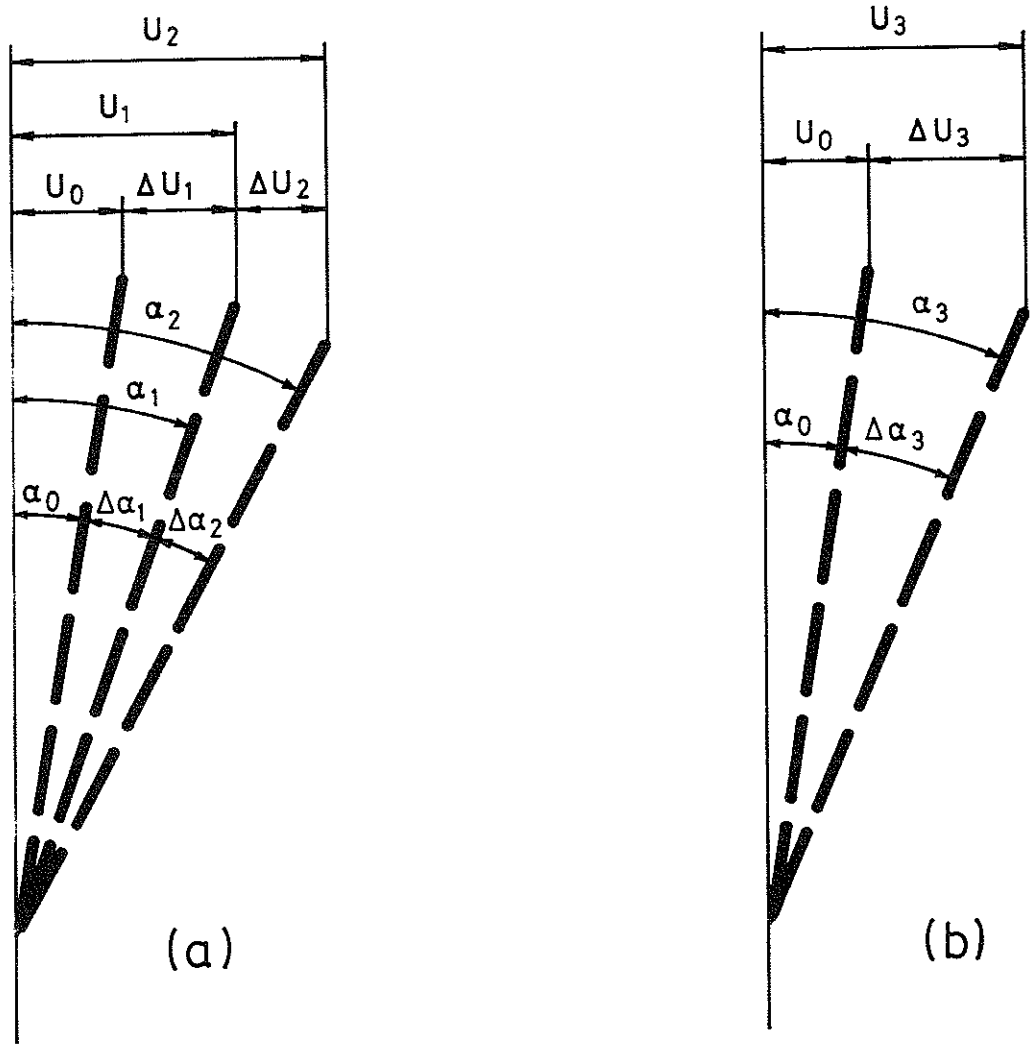

FIG. 15. VARIOUS POSITIONS OF THE LONGITUDINAL AXIS OF THE COLUMN: (a) ACCORDING TO THE PRESENT TWO-PHASE BUCKLING CONCEPT; (b) ACCORDING TO THE STATIC THEORY.

$$M_e = (P_t + \Delta P)(\alpha_1 + \Delta\alpha_2)L \tag{67}$$

in which

$$\alpha_1 = \alpha_o + \Delta\alpha_1 \tag{68}$$

The increment of load, ΔP, can be expressed as a fraction, f, of the tangent modulus load. Thus,

$$\Delta P = fP_t \tag{69}$$

From Eqs. (62) and (63) it follows that,

$$C_{max} = C_{min}\left(1 + \frac{K - 1}{K + 1}\right) \tag{70}$$

Equating the internal and the external moments from Eqs. (65) and (67) and subsequent substitutions of ΔP from Eq. (69), P_t from Eq. (46), C_{min} from Eq. (62), C_{max} from Eq. (63) and rearranging terms leads to

$$\Delta\alpha_2 = \frac{f\alpha_1}{\frac{K - 1}{K + 1} - f} \tag{71}$$

Noting that

$$\alpha_2 = \alpha_1 + \Delta\alpha_2 \tag{72}$$

Substitution of Eq. (71) into Eq. (72) results in

$$\alpha_2 = \frac{(K - 1)\alpha_1}{K - 1 - f(K + 1)} \tag{73}$$

For the critical value of f defined by the equation

$$f_c = \frac{K - 1}{K + 1} \tag{74}$$

the value of α_2 in Eq. (73) becomes infinitely large. It follows from Eqs. (46) and (64) that

$$\Delta P_{max} = P_r - P_t = P_t \frac{K - 1}{K + 1} \tag{75}$$

in which ΔP_{max} = ΔP at the reduced modulus load.

A comparison of Eqs. (69) and (75) leads to the conclusion that the value of f corresponding to the reduced modulus load coincides with the critical value, f_c, in Eq. (74).

On the other hand for loads below the reduced modulus level, i.e., for f values smaller than f_c, the value of α_2 in Eq. (73) would remain finite. This is a significant conclusion, since if the unstable column, at the end of buckling Phase 1, is capable of attaining a position of moment equalization during a finite deflection interval, the column would likewise be able to reach a position of motion reversal during an additional finite deflection interval. This follows from the fact that the bending rigidity of the column remains at the same constant value in moving from the position of moment equalization to the position of motion reversal.

Thus, the reduced modulus load coincides with the maximum load from Model 1; hence, for all loads below this maximum level, the lateral deflection remains finitely bounded, regardless of the size of the initial disturbances.

5.7 Derivation of Modified Shanley Formulas

The analysis of Model 1 herein has given rise to some fundamental equations describing the partial behaviour of the column during two distinct buckling phases. The development of the model may have raised the question how the present approach could be compared with the principles envisaged by Shanley in Refs. 5 and 6. The purpose of this section is to present some modified Shanley formulas for the numerical comparisons of the next chapter. For a discussion of Shanley Theory, see Appendix A.

In order to make numerical comparisons, Shanley formulas have to be derived for our column model in Fig. 12. However, in order to maintain a consistent model, a slight modification is made herein in Shanley's procedure by introducing a certain initial imperfection represented by the deflection angle, α_o, at the tangent modulus load. The original Shanley procedure could then be obtained by setting α_o equal to zero.

Analogous to Eq. (C 9) of Appendix C, the equation

$$\Delta\alpha_3 = \lambda(\varepsilon_a + \varepsilon_b) \tag{76}$$

expresses the relation between the total increment of the deflection angle, $\Delta\alpha_3$, shown in Fig. 15(b) and the corresponding total strain increments ε_a and ε_b corresponding to the elements a and b of the column in Fig. 12 respectively. For the sake of convenience, the symbol Δ in front of the total strain increments, $\Delta\varepsilon_a$ and $\Delta\varepsilon_b$, is omitted. The total increment here signifies the total value of the variable under conside-

ration minus its initial value.

Analogous to Eq. (C 10) of Appendix C, the total internal bending moment increment, ΔM_i, developed due to ε_a and ε_b is found from the equation

$$\Delta M_i = Ab(E_a \cdot \varepsilon_a + E_b \cdot \varepsilon_b) \tag{77}$$

Eq. (77) is obtained by omitting the index b and substituting ε_a and ε_b in place of $\Delta\varepsilon_{ba}$ respective $\Delta\varepsilon_{bb}$ in Eq. (C 10) of Appendix C. Since there is no division of the internal moment into axially induced and laterally induced increments in the present case, the omission of the index b does not cause any ambiguity.

The internal moment, M_i, can be obtained by summation of the contributions of the initial internal moment, M_o, in Eq. (66) and the internal moment developed due to the total strain increments ε_a and ε_b given by Eq. (77). Thus, it follows that

$$M_i = P_t L\alpha_o + Ab(E_a \cdot \varepsilon_a + E_b \cdot \varepsilon_b) \tag{78}$$

Taking moment of the axial load, P, about the center of the hinge in Fig. 15(b) and substitution of Eq. (76) into the resulting moment equation gives the following relation for the external moment, M_e:

$$M_e = P\left[L\alpha_o + \lambda L(\varepsilon_a + \varepsilon_b)\right] \tag{79}$$

The equality of the internal and external moments from Eqs. (78) and (79), proper use of Eq. (46) and the fact that $E_b = E_t$ and $E_a =$

$K \cdot E_t$ leads to the following expression for the axial load, P:

$$P = \frac{P_t(\varepsilon_b + K\varepsilon_a + \varepsilon_o)}{\varepsilon_a + \varepsilon_b + \varepsilon_o} \tag{80}$$

in which

$$\varepsilon_o = \frac{\alpha_o}{\lambda} \tag{81}$$

From Eq. (76) it follows that

$$\varepsilon_b = \frac{\Delta\alpha_3}{\lambda} - \varepsilon_a \tag{82}$$

Substitution of Eqs. (82) and (81) into Eq. (80) and subsequent rearrangement leads to

$$P = P_t\left[1 + \frac{\lambda}{\Delta\alpha_3 + \alpha_o}(K - 1)\varepsilon_a\right] \tag{83}$$

Since strain reversal is assumed to occur right from the start of bending, the increment of load, ΔP, above the tangent modulus load can be expressed by the following formula:

$$\Delta P = AE_t\varepsilon_b - AE_tK\varepsilon_a \tag{84}$$

The axial load, P can be written in the form

$$P = P_t + \Delta P \tag{85}$$

Substitution of Eq. (82) into Eq. (84), subsequent substitution of the resulting equation into Eq. (85) and rearrangement by the proper use of Eq. (46) leads to

$$P = P_t\left[1 + \frac{\Delta\alpha_3 L}{b} - \frac{\lambda L}{b}(1 + K)\varepsilon_a\right] \tag{86}$$

A comparison of Eqs. (83) and (86) results in the following expression for ε_a:

$$\varepsilon_a = \frac{\Delta\alpha_3 L(\Delta\alpha_3 + \alpha_o)}{\lambda b(K - 1) + \lambda L(\Delta\alpha_3 + \alpha_o)(1 + K)} \tag{87}$$

Substitution of Eq. (87) into Eq. (83) leads to

$$P = P_t\left[1 + \frac{L\Delta\alpha_3(K - 1)}{b(K - 1) + L(\Delta\alpha_3 + \alpha_o)(1 + K)}\right] \tag{88}$$

Substitution of Eq. (69) into Eq. (85) and subsequent comparison with Eq. (88) leads to

$$f = \frac{L\Delta\alpha_3(K - 1)}{b(K - 1) + L(\Delta\alpha_3 + \alpha_o)(1 + K)} \tag{89}$$

A solution of Eq. (89) for $\Delta\alpha_3$ gives:

$$\Delta\alpha_3 = \frac{fL\alpha_o(1 + K) + fb(K - 1)}{L[K - 1 - f(1 + K)]} \tag{90}$$

The total deflection angle, α_3, in Fig. 15(b) can be expressed as

$$\alpha_3 = \alpha_o + \Delta\alpha_3 \tag{91}$$

Substitution of Eq. (90) into Eq. (91) results in the following

equation for α_3:

$$\alpha_3 = \frac{fb(K - 1) + L\alpha_o(K - 1)}{L[K - 1 - f(1 + K)]} \tag{92}$$

A comparison of Eq. (92) with Eq. (73) shows that the equilibrium positions according to the two different equations become infinitely large for the same critical value of f expressed by Eq. (74). Thus, the equilibrium positions according to both theories asymptotically approach the reduced modulus level as upper bound.

It should be observed that the first position of moment equalization expressed by Eq. (73) has been obtained on an entirely different basis than the method of finding Shanley-type equilibrium position given by Eq. (92). Thus, although the two methods converge to the same upper bound due to the bilinear shape of the stress strain diagram, they may yield different equilibrium configurations for all the axial loads below the reduced modulus level. A numerical comparison would be attempted herein in the analysis of Model 2, in the next chapter.

6. ANALYSIS OF MODEL 2

Abstract

This model studies the complete buckling behaviour of the centrally loaded and initially straight simplified inelastic column with bilinear stress strain relationship. The column is assumed to remain perfect up to the tangent modulus load, whereafter it is subjected to disturbances simultaneous with loading in the form of initial deflection and/or initial velocity introduced at the tangent modulus load, and a possible velocity disturbance applied at any arbitrary loading level below the reduced modulus load. The possibility of strain reversal simultaneous with loading during buckling Phase 1 is taken into account. The only bound to axial loading is considered to be the maximum column load which in this model coincides with the reduced modulus load. During buckling Phase 2, the complete motion of the column is described and the properties of the resulting simple harmonic motion are determined. Flow diagrams for the entire solution of the problem are presented and numerical calculations are performed by a computer program.

6.1 Description of the Model and Identification of its State Variables

The simple inelastic column shown in Fig. 12 with a bilinear stress strain diagram governing the deformation of the two hinge elements, see Fig. 10(a), is chosen as the basic model. All the specific assumptions of Model 1 described in Sec. 5.1 herein are also applicable to Model 2 with the following three exceptions:

1. This model can take into consideration the possible occurrence of strain reversal simultaneous with loading;

2. the dynamic behaviour of the column during buckling Phase 2 is completely analyzed; and

3. In addition to the initial disturbances described for Model 1, an additional velocity disturbance simultaneous with loading may be applied at any loading level above the tangent modulus load.

It should be noted that although Model 1 did not treat the behaviour of the column during buckling Phase 2 dynamically, it was asserted that a first position of moment equalization would lead to infinitely large lateral deflection at the reduced modulus load. The fact that this is equally true for Model 2 shall be precisely explained herein in Sec. 7.4. However, for the purpose of the present analysis we may simply assume the reduced modulus load as the upper bound.

If we analyze the present model by the multi-cycle computation technique explained in Appendix C, then the state of the column consists of the set of all the variables whose initial values at the beginning of a time interval uniquely determine the current dynamic state without a knowledge of the past loading history of the given column. At the start of the current computation cycle, the set of variables con-

sisting of the axial load, P, the deflection angle, α, the angular velocity, $\dot{\alpha}$, and the stresses, σ_a and σ_b with respective deformation moduli[1], E_a and E_b, where the indices a and b refer to column elements a and b respectively, describes a group consisting of seven variables which are necessary for the determination of subsequent motion. However, the insufficiency of this group of variables may be visualized by a study of Fig. 16.

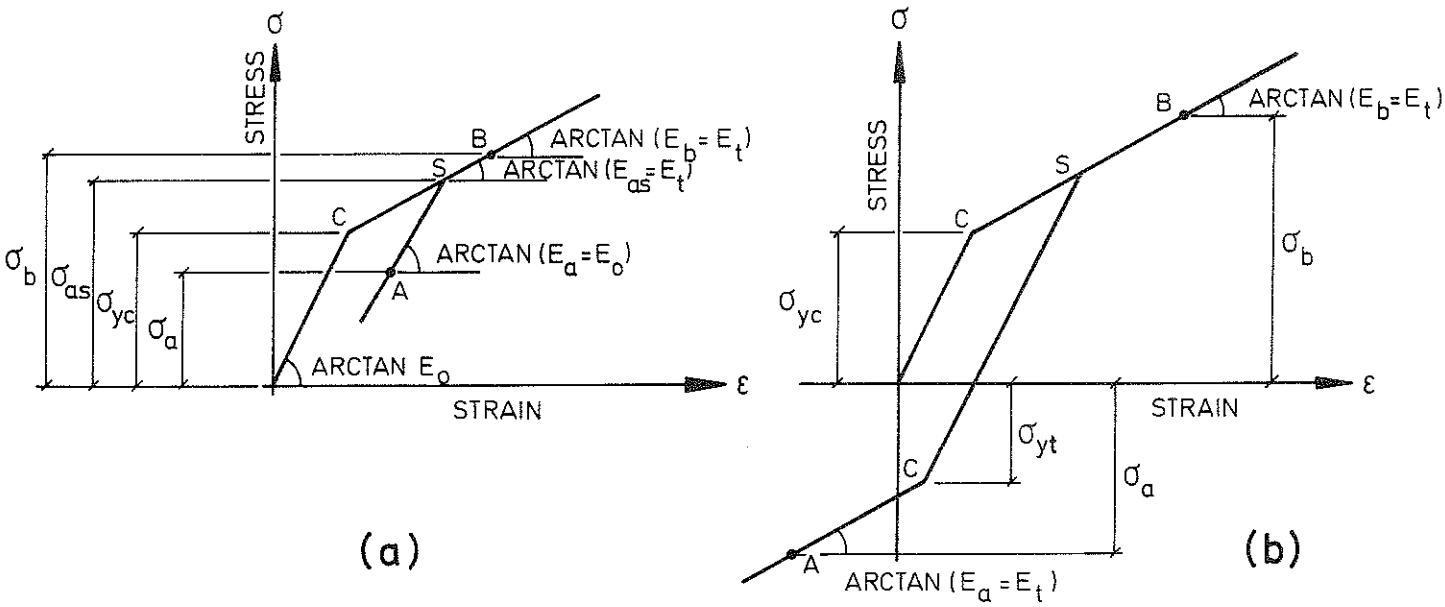

FIG. 16. TWO POSSIBLE STRESS STRAIN STATES CORRESPONDING TO THE TWO HINGE ELEMENTS OF THE SIMPLE INELASTIC COLUMN

In Fig. 16, the current position of the two column elements a and b on the bilinear stress strain diagram is marked by points A and B respectively. Point S in Fig. 16 marks the position at which strain reversal last occurred in element a at some instant of time in the

---

1. The word deformation modulus is used herein interchangeably with the modulus of elasticity or the tangent modulus as the case may be.

past. Fig. 16(a) shows that element a is currently deforming on an unloading line with a deformation modulus equal to the initial modulus of elasticity, E_o. However, upon further increase of axial load, the strain in element a may increase again to the extent that at some future instant of time, point A would move up to the position marked by point S on the original stress strain diagram. Any additional increase of strain above point S must be accompanied by a deformation modulus equal to the tangent modulus, E_t.

From the above discussion it follows that, if a column element, j, (j stands for either a or b) is currently deforming on an unloading line, the pair of values, σ_{js} and E_{js}, representing the stress respective deformation modulus at the latest position of strain reversal on the stress strain diagram must be known. This is a crucial information since as soon as the stress, σ_j, in element j, begins to exceed the stress level, σ_{js}, the current deformation modulus, E_j, corresponding to element j must be replaced by the value, E_{js}. Thus, the two pairs of values, (σ_{as}, E_{as}) and (σ_{bs}, E_{bs}), representing element a respective element b's stress and corresponding tangent modulus at the latest position of strain reversal on the stress strain diagram, must generally appear in the set of state variables.[1] However, from the four variables, σ_{as}

---

1. The state variables may also be referred to as the state space variables in accordance with the terminology of the modern control theory. In this sense, the column may be viewed as a controlled dynamic system with a set of control variables including loading rate, disturbances, stress strain diagram, etc.; a set of state variables as discussed above; and finally, a set of output variables comprising the maximum column load and the laterally stable deflected configurations. For column Model 2, the control variables do not affect the maximum load.

E_{as}, σ_{bs}, and E_{bs}, the pair, E_{as} and E_{bs} may uniquely be found from the other pair, σ_{as} and σ_{bs}, provided that the stress strain diagram is of the usual type, i.e., each stress level corresponding to only one strain. Nevertheless, both pairs are included in the set of state space variables for the sake of convenience and generality.

If a column element, j, is currently deforming on the original stress strain diagram, see point B in Fig. 16, then no information about σ_{js} and E_{js} is necessary, in which case the values σ_{js} and E_{js} may arbitrarily be assigned zero values. Thus, the state space variables, σ_{js} and E_{js} have positive values, when Element j is currently deforming on an unloading line, and they are arbitrarily assigned zero values when the element is deforming on the original stress strain diagram. Now, it may be shown that once σ_{js} and σ_j are specified, the deformation modulus, E_j, corresponding to element j is uniquely determined from a knowledge of the usual type $\sigma - \varepsilon$ curve. This is due to the fact that if $\sigma_{js} = 0$, then the element is deforming on the original stress strain diagram, in which case, the deformation modulus, E_j, can be determined from the stress strain diagram at the specified level, σ_j; however, if σ_{js} has a nonzero positive value, then the element is deforming on an unloading line, in which case, the deformation modulus, E_j, is equal to the initial modulus of elasticity, E_o.

When a column element begins to move on an unloading line with a continuously decreasing strain, a time may arrive at which the stress in the element may change from compression to tension. If this state of affairs continues, the stress may attain the new yield-point stress level, σ_{yt}, in tension, see Fig. 16(b). Thus, the element which was previously deformed in compression with a yield-point stress, σ_{yc}, has

now reached the yield-point stress, σ_{yt}, in tension.[1] Now, the following two cases may arise:

1. The tensile stress may begin to decrease with the possibility that the stress in the element may shift from tension to compression, in which case, the element may continue to move upwards on the unloading line towards the original position on the stress strain diagram; and

2. The tensile stress in the element continues to increase beyond the yield-point stress, σ_{yt}, in which case, we assume that no further strain reversal occurs in the column element under consideration.

It should be pointed out that Case 1 discussed above is an unlikely possibility, however, it is taken into account here due to the fact that the multi-cycle computation technique described in Appendix C and employed in the numerical analysis of this model, automatically takes care of this case if it occurs. It should be noted that neither of the above two cases warrant the inclusion of new variables as necessary information in the set of state space variables.

At the beginning of a computation cycle, the internal moment, M_i, of the column may be obtained from a knowledge of the corresponding stresses σ_a and σ_b, representing the stresses in the elements, a and b respectively. However, it is computationally convenient to include the internal moment, M_i, in the set of state space variables.

---

1. For actual materials, the value of σ_{yt} is smaller than σ_{yc} (Bauschinger effect), i.e., the new yield-point stress is lowered if a material specimen is unloaded from the inelastic range and subsequently loaded in the opposite direction up to the new yield-point stress.

Thus, from the above discussion we arrive at the following vector, SV, referred to herein as the System Vector containing the following 12 state space variables:

$$SV = (P, \alpha, \dot{\alpha}, \sigma_a, \sigma_b, \sigma_{as}, \sigma_{bs}, E_a, E_b, E_{as}, E_{bs}, M_i) \qquad (93)$$

in which the first seven variables are independent and are indispensable for a unique determination of the dynamic state of the column, whereas the last five variables are dependent[1] and are included merely for the sake of computational convenience.

The above state variables will now be more closely studied in the following sections.

---

1. This again assumes a usual-type stress strain diagram, i.e., each stress level corresponding to only one strain.

6.2 Determination of the State of the Column

The total magnitudes of the internal moment, M_i, and the stresses σ_a and σ_b, corresponding to element a respective element b at an instant of time during the current computation cycle, are found from the following equations, see Eqs. (C 21) - (C 23) of Appendix C:

$$M_i = M_{io} + \Delta M_i \tag{94}$$

$$\sigma_a = \sigma_{ao} + \Delta\sigma_{aa} - \Delta\sigma_{ba} \tag{95}$$

$$\sigma_b = \sigma_{bo} + \Delta\sigma_{ab} + \Delta\sigma_{bb} \tag{96}$$

in which M_{io}, σ_{ao}, σ_{bo} = the initial values of the variables at the beginning of the current computation cycle corresponding to the internal moment, stress in element a and stress in element b respectively; ΔM_i = the internal moment increment; $\Delta\sigma_{aa}$, $\Delta\sigma_{ab}$ = axial stress increments, i.e., the stress increments caused due to the increase of axial load in elements a and b respectively; and $\Delta\sigma_{ba}$, $\Delta\sigma_{bb}$ = the bending stress increments, i.e., the stress increments caused solely due to bending of the column in elements a and b correspondingly.

The incremental magnitudes just described are obtained from the following equations, see Eqs. (C 17), (C 6a), (C 6b), and (C 20) of Appendix C:

$$\Delta M_i = C \cdot \Delta\alpha - \frac{\Delta P \cdot b(K - 1)}{(K + 1)} \tag{97}$$

$$\Delta\sigma_{aa} = \frac{K \cdot \Delta P}{A(K + 1)} \tag{98}$$

$$\Delta\sigma_{ab} = \frac{\Delta P}{A(K + 1)} \tag{99}$$

and

$$\Delta\sigma_{ba} = \Delta\sigma_{bb} = \frac{K \cdot E_b \cdot \Delta\alpha}{\lambda(K + 1)} \tag{100}$$

in which C = the bending rigidity of the column; $\Delta\alpha$ = deflection angle increment; ΔP = the axial load increment added to the existing axial load at the beginning of the current computation cycle; λ = d/b where d,b = half the depth respective half the width of the hinge in Fig. 12(b); $K = E_a/E_b$, where E_a, E_b = the current deformation moduli corresponding to elements a and b respectively; and A = area of one hinge element. The bending rigidity, C, is defined by the following equation, see Eq. (C 15) of Appendix C:

$$C = \frac{2A \cdot b \cdot K \cdot E_b}{\lambda(K + 1)} \tag{101}$$

Disregarding the gravitational force, and considering the fact that for the present model both the excentricity, X_o, and the deviation, θ, of the axial load from its original direction, are equal to zero, Eq. (C 27) of Appendix C leads to the following differential equation describing the motion of the column Model 2:

$$\ddot{\alpha} + \frac{(C - P \cdot L)}{I} \cdot \alpha = \frac{-M_{io} - \Delta M_{ia} + C \cdot \alpha_o}{I} \tag{102}$$

in which $\ddot{\alpha}$ = the second derivative of the deflection angle with respect to time; P = the current axial load; L = length of the column; α = current deflection angle; I = mass moment of inertia of the column defined for a slender column by Eq. (10); α_o = the initial deflection angle at the beginning of the current interval; and ΔM_{ia} = the axially induced internal moment increment, due to the increase of axial load

at the beginning of the current computation cycle, obtained from the following equation, see Eq. (C 7) of Appendix C:

$$\Delta M_{ia} = (\Delta\sigma_{ab} - \Delta\sigma_{aa}) \cdot A \cdot b \tag{103}$$

in which $\Delta\sigma_{ab}$ and $\Delta\sigma_{aa}$ are defined by Eqs. (99) and (98) respectively.

Using the notations

$$\Delta M = C - P \cdot L \tag{104}$$

$$H = -M_{io} - \Delta M_{ia} + C\alpha_o \tag{105}$$

$$F = \frac{H}{\Delta M} \tag{106}$$

and

$$\omega = \sqrt{|\Delta M|/I} \tag{107}$$

in which $|\Delta M|$ represents the absolute value of ΔM, Eq. (102) leads to the following alternatives for the solution of the deflection angle, α, and the angular velocity, $\dot{\alpha}$:

1. if $\Delta M < 0$ then the solutions are

$$\alpha = C_1 \sinh \omega t + C_2 \cosh \omega t + F \tag{108}$$

and

$$\dot{\alpha} = C_1\omega \cosh \omega t + C_2\omega \sinh \omega t \tag{109}$$

2. if $\Delta M > 0$ then the solution of Eq. (102) leads to

$$\alpha = C_1 \sin \omega t + C_2 \cos \omega t + F \tag{110}$$

and

$$\dot{\alpha} = C_1 \omega \cos \omega t - C_2 \omega \sin \omega t \tag{111}$$

The constants, C_1 and C_2, in the above equations are found from the initial condition at time, $t = 0$, at the beginning of the computation cycle:

$$C_1 = \frac{\dot{\alpha}_o}{\omega} \tag{112}$$

and

$$C_2 = \alpha_o - F \tag{113}$$

The calculations for deflection angle, angular velocity and stresses corresponding to Model 2 are sequentially shown in Fig. 17. In this flow diagram an entry point A and an exit point B are marked in between which the desired calculation pattern is shown. The final values of α and $\dot{\alpha}$ at the end of the time interval, Δt, are found by setting, $t = \Delta t$, in the applicable equations of motion.

During a computation cycle, the axial and bending strain increments are obtained by the following equations, see Eqs. (C 5), (C 18), and (C 19) of Appendix C:

$$\Delta\varepsilon_{aa} = \Delta\varepsilon_{ab} = \frac{\Delta P}{AE_b(K + 1)} \tag{114}$$

$$\Delta\varepsilon_{ba} = \frac{\Delta\alpha}{\lambda(K + 1)} \tag{115}$$

and

$$\Delta\varepsilon_{bb} = \frac{K \cdot \Delta\alpha}{\lambda(K + 1)} \tag{116}$$

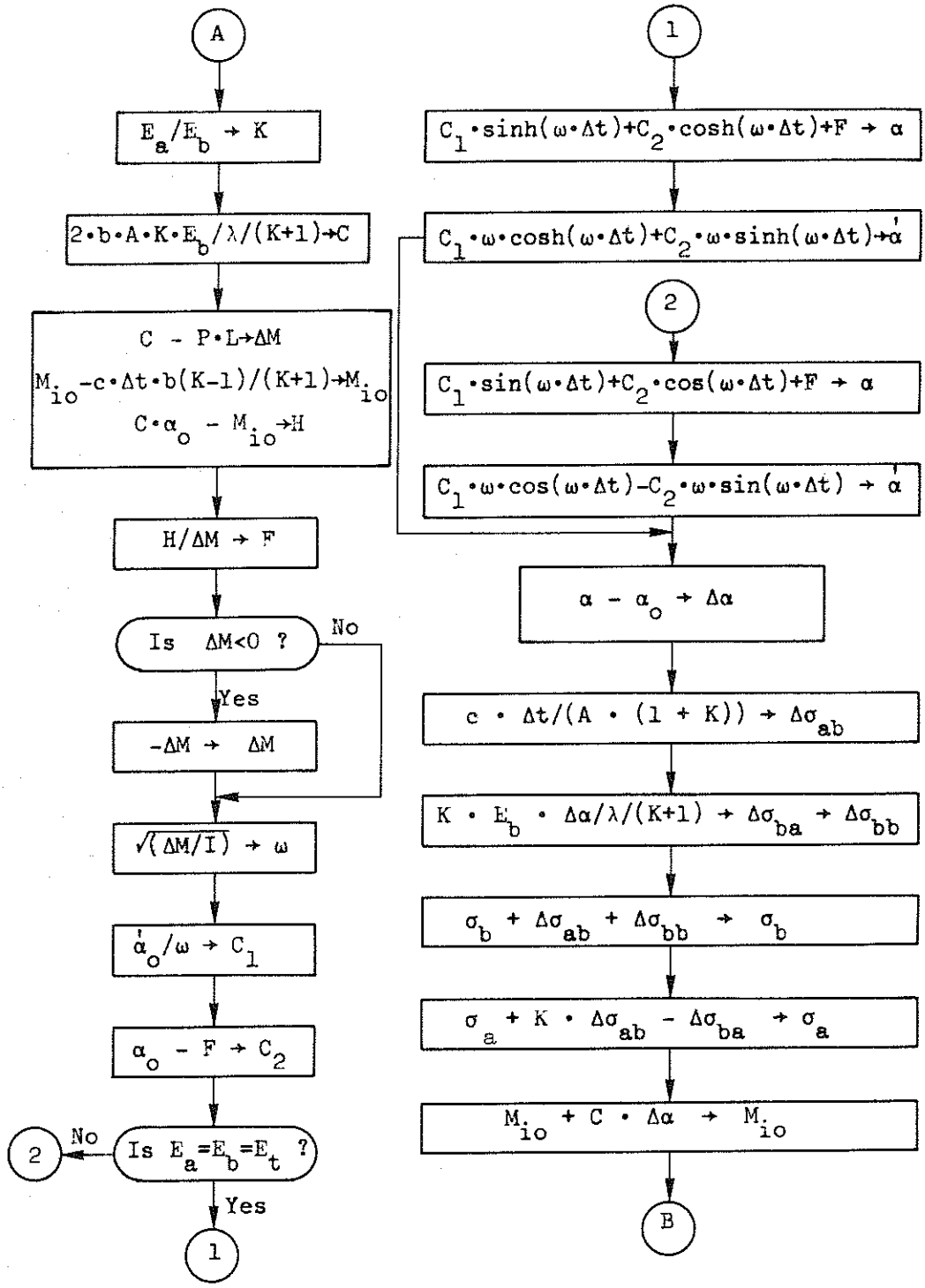

FIG. 17. CALCULATION OF DEFLECTION ANGLE, ANGULAR VELOCITY, STRESSES, AND MOMENT STATE OF MODEL 2

in which $\Delta\varepsilon_{aa}$, $\Delta\varepsilon_{ab}$ = the axial strain increments, i.e., the strain increments due to the axial deformation in elements a respective b simultaneous with loading at the beginning of the computation cycle; and $\Delta\varepsilon_{ba}$, $\Delta\varepsilon_{bb}$ = the bending strain increment, i.e., the strain increments in elements a respective b solely due to subsequent bending of the column. Since, $\Delta\varepsilon_{aa} = \Delta\varepsilon_{ab}$, we may rewrite Eq. (114) in the following form by using a single notation, $\Delta\varepsilon_{axial}$ for the axial strain increment:

$$\Delta\varepsilon_{axial} = \frac{\Delta P}{AE_b(K + 1)} \tag{117}$$

It should be noted that in the solution of Eq. (102) in this section the case $\Delta M = 0$ was not taken into account. This is due to the fact for a column with bilinear stress strain diagram, and for the loading range above the tangent modulus load and below the reduced modulus load, the column studied is either dynamically unstable if the tangent modulus applies to the deformation of both hinge elements, or the column is dynamically stable if the unloading modulus applies to at least one hinge element. The general argument that for a column with bilinear stress strain diagram, the maximum column load would coincide with the reduced modulus load, is treated in Sec. 7.8.

6.3 Strain Reversal Criteria in Forward and Backward Directions

When the rate of bending strain in forward or backward direction, due to the lateral motion of the column, exceeds the rate of axial strain due to the simultaneous increase of axial load, then strain reversal begins to occur in element a or b respectively. Since the current value of a column parameter during a given time interval is considered as the sum of a constant initial value at the beginning of the interval plus an increment which changes with time during that interval, then the rate of change of that column parameter is equivalent to the rate of change of the corresponding increment with respect to time. Making use of this concept and taking the derivatives of the strain increments in Eqs. (117), (115) and (116) with respect to time leads to the following equations for the axial strain rate, $\dot{\varepsilon}_a$; and the bending strain rates, $\dot{\varepsilon}_{ba}$ and $\dot{\varepsilon}_{bb}$, in elements a and b respectively:

$$\dot{\varepsilon}_{axial} = \frac{c}{AE_b(K + 1)} \tag{118}$$

$$\dot{\varepsilon}_{ba} = \frac{\dot{\alpha}}{\lambda(K + 1)} \tag{119}$$

and

$$\dot{\varepsilon}_{bb} = \frac{K\dot{\alpha}}{\lambda(K + 1)} \tag{120}$$

in which c = the loading rate considered as constant at least during each computation cycle; and $\dot{\alpha}$ = the angular velocity corresponding to the end of the current interval.

We now define two variables, saf (strain reversal identifier in element a during forward motion), and sbb (strain reversal identifier

in element b during backward motion), by the following equations:

$$saf = \frac{\dot{\varepsilon}_{ba}}{\dot{\varepsilon}_{axial}} = \frac{\dot{\alpha} AE_b}{\lambda c} \tag{121}$$

and

$$sbb = \frac{-\dot{\varepsilon}_{bb}}{\dot{\varepsilon}_{axial}} = -\frac{K\dot{\alpha} AE_b}{\lambda c} \tag{122}$$

During forward or backward motion, strain reversal begins to occur in element a or b as soon as the value of saf in Eq. (121) or the value of sbb in Eq. (122) exceeds unity. A minus sign appears on the right side of Eq. (122) because the value of the angular velocity, $\dot{\alpha}$, during backward motion is negative.

In order to generate information about the instant of time at which strain reversal begins or ends at an element of the column, we also determine the values of saf and sbb at the beginning of each interval and denote them by saf_o and sbb_o as follows:

$$saf_o = \frac{\dot{\alpha}_o AE_b}{\lambda c} \tag{123}$$

and

$$sbb_o = \frac{-K\dot{\alpha}_o AE_b}{\lambda c} \tag{124}$$

in which $\dot{\alpha}_o$ = the angular velocity at the beginning of the time interval.

Now, suppose that at the end of a computation cycle during forward motion, the value of saf is greater than or equal to unity while the value of saf_o is less than 1. This indicates that strain reversal in element a has just started. If, on the other hand, saf_o is greater than unity but saf is less than or equal to 1, then this shows that strain reversal in element a has ended during the current time interval. The

same argument applies to strain reversal in element b. Fig. 18 shows the flow diagram depicting the generation of the entire information regarding the possible occurrence of strain reversal in forward and backward directions.

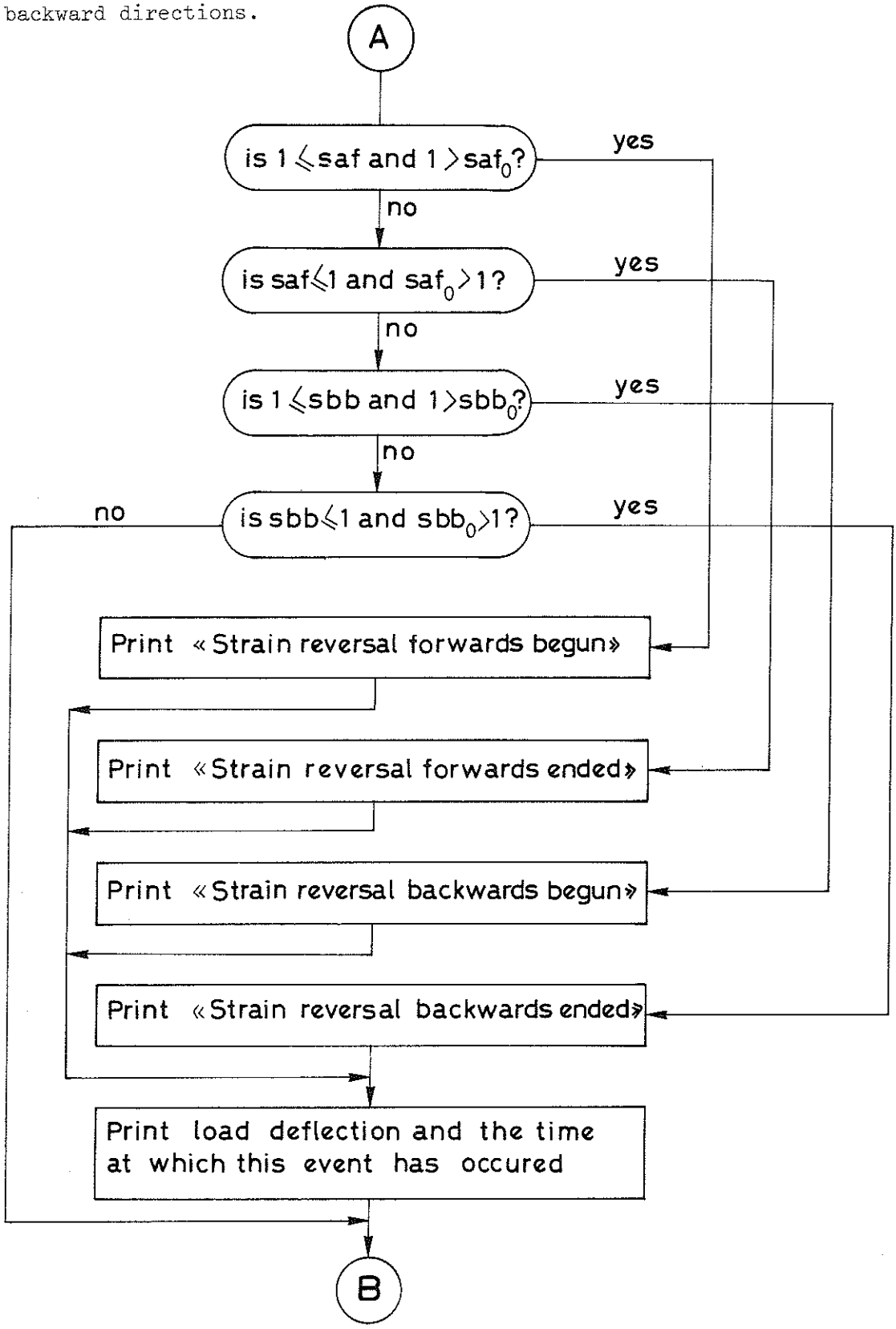

FIG. 18. PROCESS OF GENERATING INFORMATION ON THE OCCURRENCE OF STRAIN REVERSAL IN FORWARD AND BACKWARD DIRECTIONS.

6.4 Determination of State Variables Corresponding to Strain Reversal

When strain reversal occurs in an element of the column, the corresponding stress level and tangent modulus, would be preserved so that it can be possible to recover those values as soon as the element returns to the previous position on the stress strain diagram.

There are two situations when a column element may deform on an unloading line: 1) when strain reversal occurs during buckling Phase 1; and 2) when the loading rate becomes zero during buckling Phase 2, whereby maximum strain reversal occurs in the column while moving in a certain direction. Thus, for the simplified column, it would be possible for both elements, a and b to deform along an unloading line either during buckling Phase 1 or during buckling Phase 2. The state space variables, σ_{as}, E_{as} corresponding to element a and σ_{bs}, E_{bs} corresponding to element b, would be stored as long as the unloading modulus governs the deformation of the corresponding element, see Sec. 6.1.

The whole process of storing and restoring state space variables corresponding to strain reversal during both buckling phases is shown in Fig. 19. All the variables used in this flow diagram have already been defined. A study of this flow diagram shows that as soon as element a or b reaches the original stress strain diagram, from a position on an unloading line, the previously stored variable, σ_{as} or σ_{bs} attains zero value. This state of affairs is thereafter maintained until a new strain reversal begins to occur.

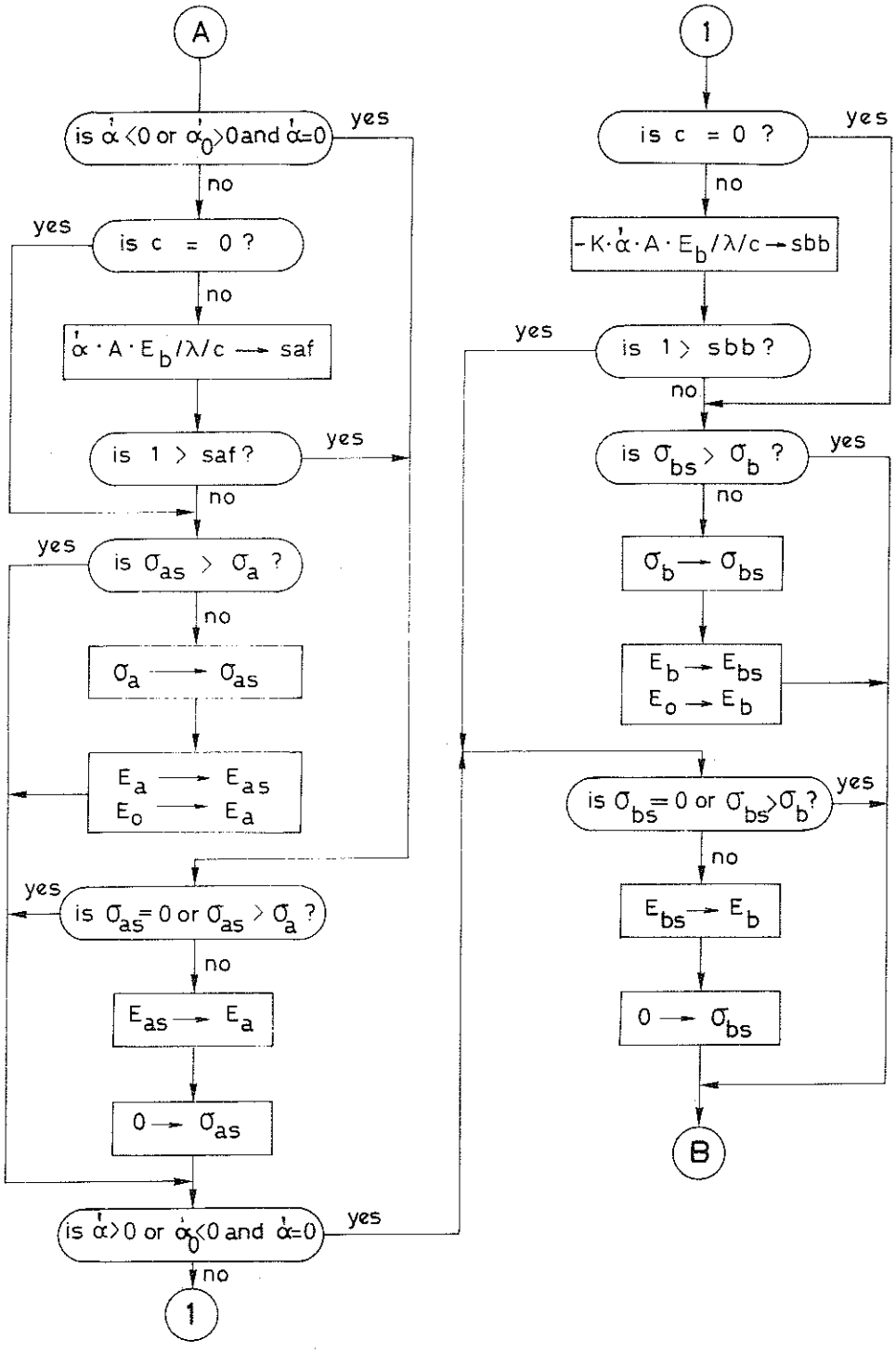

FIG. 19. TEST FOR STRAIN REVERSAL AND ASSIGNMENT AND TEMPORARY STORAGE OF PROPER DEFORMATION MODULI AND STRESS LEVELS.

6.5 Determination of Motion During Buckling Phase 2

Buckling Phase 2 starts as soon as the axial load ceases to increase. At this instant of time, the column may either be moving in forward or backward direction. In either case, the strain would increase on the front side of the column[1] possibly along the original stress strain diagram, while strain reversal occurs on the back side of the column[1] (front- and back sides are identified relative to the direction of motion). If the axial load lies below the maximum level, the column would reach a first position of motion reversal and begin to move in the opposite direction. A second position of motion reversal would soon be attained while the column begins to move towards a third end position, etc.

For the present simplified model, at least one element would be deforming along an unloading line before the first motion reversal, whereafter both column elements would initially deform along two different unloading lines. However, before the second motion reversal, the strain at the element on the front side of the column may increase up to the previous level on the original stress strain diagram, whereafter the tangent modulus would govern the deformation of that element until a second position of motion reversal is attained. While the column is moving towards a third position of motion reversal, both elements would be deforming along two different unloading lines throughout the

---

1. The front side in the case of this simple column refers to the column element at which the compressive stress due to bending is increasing at a certain instant of time; the back side refers to the other column element

motion. This is due to the fact that the maximum possible bending rigidity of the column is now developed and a third position of motion reversal is attained with a lateral deflection which would never exceed the range between the first two motion reversal positions. Thus, after the third motion reversal, the motion of the column is already a simple harmonic one.

An outline of the procedure for finding equilibrium configurations for Model 2 is depicted in Fig. 20 where the motion of the column is analyzed in a sequential flow diagram up to third position of motion reversal.The four variables α_{max}, t_{max}, α_{min}, t_{min} appearing in Fig. 20 indicate the deflection angles and related times corresponding to positions of motion reversal. The indices max and min indicate two successive maximum and minimum positions of motion reversal. The variables N_1 and N_2 are two integer variables. N_1 is used to preserve the values of state space variables stored at the end of buckling Phase 1, and the integer, N_2 in Fig. 20 is used to count the number of motion reversal positions. P_o represents an axial load greater than the tangent modulus load at which the load is kept constant and subsequent lateral motion is analyzed; P_o^* is the largest value of P_o for which lateral equilibrium configurations are studied. All other variables are already defined.

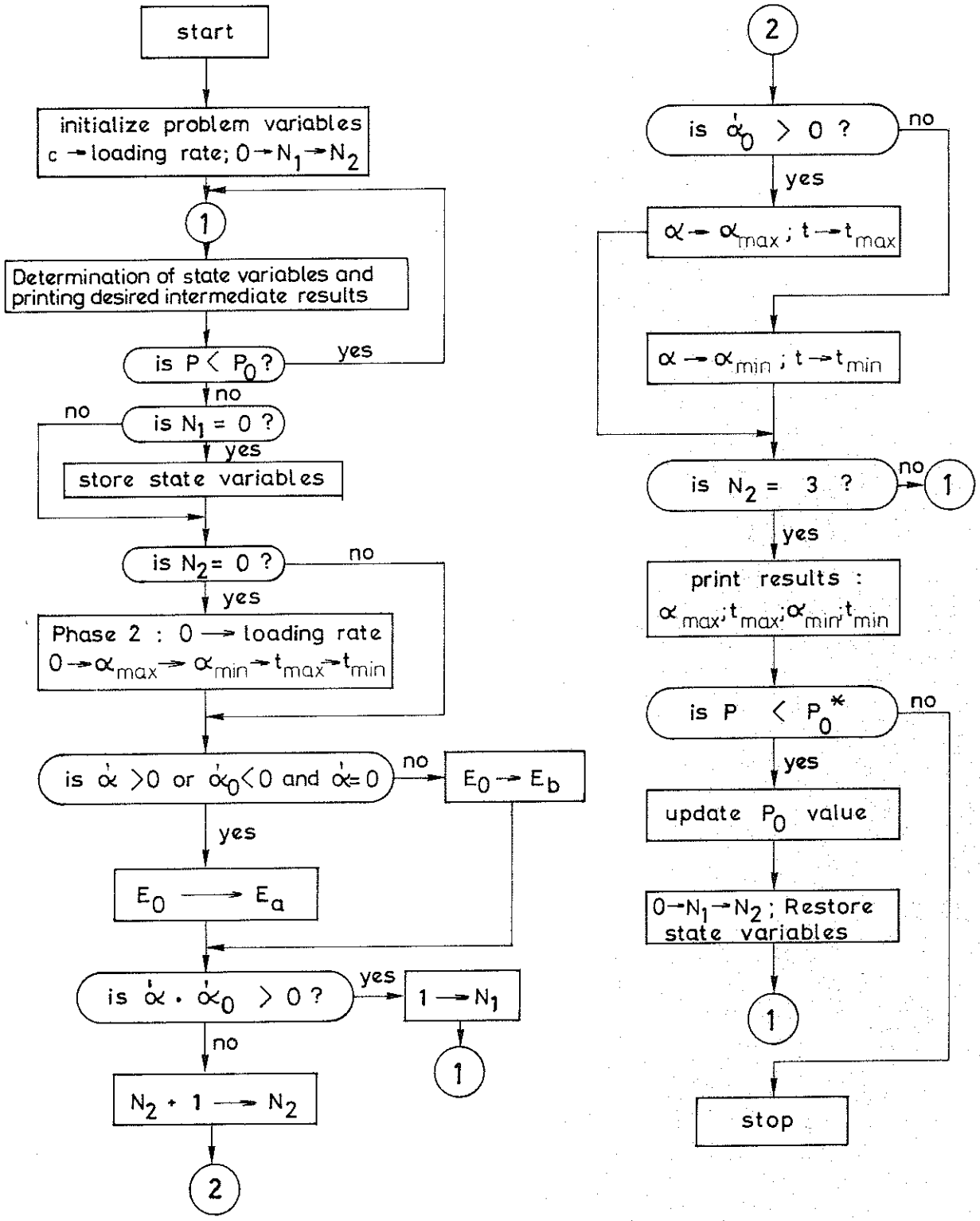

FIG. 20. FLOW DIAGRAM FOR THE PROCESS OF FINDING EQUILIBRIUM CONFIGURATIONS OF MODEL 2

6.6 Numerical Results for Buckling Behaviour According to Model 2

Since the reduced modulus load represents the upper bound for Model 2, the complete buckling behaviour of the column could be described by finding out the load-deflection pattern, from the initially straight configuration at the tangent modulus load, up to the dynamically stable lateral positions under the influence of a predetermined constant axial load, between the tangent modulus and the reduced modulus loads.

In order to determine the effect of parameter variations on the buckling behaviour, a reference column is analyzed in the first place, whereafter one parameter of the reference column is changed at a time and the buckling behaviour is determined all over again for the column with the new parameter combination. The column in Fig. 12 having a deformable hinge with bilinear stress strain diagram, see Fig. 10(a), is used as the reference column with the following numerical data:

$b = d = 5$ centimeters; $A = 5$ square centimeters; $L = 2.5$ m; $M = 100$ kg; $E_o = 2 \times 10^9$ Newtons per square meter; $E_t = 10^9$ Newtons per square meter; $c = 50$ Newtons per second; $U_o = 10^{-3}$ centimeters; $V_o = 0$ centimeters per second; $D = \Delta P_d / \Delta P_{max} = 1$, in which ΔP_d = the load increment above the tangent modulus load, at which a disturbance velocity, V_1, is introduced; and $V_1 = 0$ centimeters per second.

It should be noted that the parameter combination, $D = 1$ and $V_1 = 0$, implies that no disturbance velocity is introduced in the reference column for loads above the tangent modulus load.

The computations are performed by a computer program (see Program 6, Appendix D), and the results are summarized in Table 3. Each parameter combination in Table 3 is identified by a number which appears in the first column of the table; the second column gives information about the names and values of the parameters subjected to variation as compared with the reference column; the third and fourth columns indicate the end deflection, U_1, and the corresponding time, t_1, at the end of buckling Phase 1; the fifth and sixth columns show the lateral deflection, U_{m1}, and the corresponding time, t_{m1}, corresponding to the first motion reversal position; the seventh and eighth, as well as the ninth and tenth columns provide similar information about the end deflection and time corresponding to the second and third positions of motion reversal respectively; and the last column indicates the load increment ratio, $\Delta P/\Delta P_{max}$, in which ΔP = the current constant load increment and ΔP_{max} = the maximum load increment corresponding to the reduced modulus load.

Thus, each line in Table 3 provides the most significant information about the complete buckling behaviour, for each predetermined load increment ratio, during buckling Phase 1 and up to the third position of motion reversal during buckling Phase 2. The range of dynamically stable lateral motion of the column is thoroughly determined after the third motion reversal, see Section 6.5.

The results of computations for 12 different parameter combinations are presented in Table 3. The buckling behaviour for each parameter combination is determined for four different load increment ratios, .4, .6, .8, and .9 respectively.

It should be noted that Model 2 assumes that the deformation of the column up to the tangent modulus load, at least, is governed by the tangent modulus. Thus, the choice of the initial deflection at the tangent modulus load is restricted in this model to small values in order to be compatible with the assumption of the initially perfect column which would remain straight up to the tangent modulus load. Furthermore, it should be observed that the deformation of the column elements at high load increment ratios, $\Delta P/\Delta P_{max}$, may become so excessive that the stress in the element on the backside, i.e., the element with decreasing bending strain, may attain tensile stress in the inelastic range. If this happens, the column may permanently become dynamically unstable.

Thus, a column with a bilinear stress strain diagram may turn out laterally unstable even at loads below the reduced modulus load, provided that the possibility of tensile stresses in the inelastic range is taken into account. If for the present model we choose the yield point stress in compression, σ_{yc}, equal to the yield point stress in tension, σ_{yt}, such that $\sigma_{yc} = 0.8\ \sigma_t$ where σ_t refers to the average stress at the tangent modulus load, then the results recorded in Table 3 are obtained. Table 3 shows that in most cases the columns studied become laterally unstable at a load ratio equal to 0.9. This is indicated in Table 3 by the appearance of the word "unstable" at the proper location where this instability phenomenon occurs. The criterion used in the computer program to test the lateral stability in such cases will be given in Sec. 7.7.

Thus, whenever a column with bilinear stress strain diagram does

not become permanently unstable before attaining the reduced modulus load, it is implicitly understood that there exists no risk of instability due to suffering tensile stresses in the elastic range.

TABLE 3. - EFFECT OF PARAMETER VARIATIONS ON COMPLETE BUCKLING BEHAVIOUR OF INITIALLY PERFECT INELASTIC COLUMN AT VARIOUS LOAD LEVELS ABOVE THE TANGENT MODULUS LOAD

Column No.	Names and Values of Parameters Subjected to Variation	Position at the End of Phase 1		First Motion Reversal		Second Motion Reversal		Third Motion Reversal		Final Load Ratio $\Delta P/\Delta P_{max}$
		U_1 in cm	t_1 in sec	U_{m1} in cm	t_{m1} in sec	U_{m2} in cm	t_{m2} in sec	U_{m3} in cm	t_{m3} in sec	
1	Reference Column c = 50 N/sec U_o = .001 cm V_o = 0; M = 100 kg D = $\Delta P_d/\Delta P_{max}$ =1 V_1 = 0; E_t = 10^9 N/m^2; E_o = 2×10^9 N/m^2	.979	26.67	.994	27.01	.988	27.32	.994	27.63	.4
		2.304	40.0	2.340	40.39	2.327	40.71	2.340	41.03	.6
		6.267	53.34	6.485	53.92	6.447	54.25	6.485	54.59	.8
		unstable								.9
2	c = 100 Newtons per second	.884	13.34	.905	13.66	.895	13.96	.905	14.27	.4
		2.159	20.0	2.229	20.39	2.205	20.71	2.229	21.03	.6
		5.944	26.67	6.386	27.26	6.31	27.60	6.386	27.93	.8
		unstable								.9

TABLE 3 CONTINUED:

Column No.	Names and Values of Parameters Subjected to Variation	Position at the End of Phase 1		First Motion Reversal		Second Motion Reversal		Third Motion Reversal		Final Load Ratio
		U_1 in cm	t_1 in sec	U_{m1} in cm	t_{m1} in sec	U_{m2} in cm	t_{m2} in sec	U_{m3} in cm	t_{m3} in sec	$\Delta P/\Delta P_{max}$
3	c = 500 Newtons per second	.305	2.67	.453	3.00	.387	3.31	.453	3.62	.4
		1.243	4.00	1.61	4.44	1.506	4.76	1.610	5.08	.6
		3.78	5.34	5.59	6.05	5.35	6.38	5.586	6.72	.8
		7.301	6.00	unstable						.9
4	c = 1000 Newtons per second	.013	1.34	.035	1.81	.0290	2.12	.035	2.43	.4
		.222	2.0	.814	2.59	.698	2.91	.814	3.23	.6
		1.915	2.67	4.249	3.39	3.953	3.72	4.249	4.06	.8
		3.696	3.00	unstable						.9

TABLE 3 CONTINUED:

Column No.	Names and Values of Parameters Subjected to Variation	Position at the End of Phase 1		First Motion Reversal		Second Motion Reversal		Third Motion Reversal		Final Load Ratio
		U_1 in cm	t_1 in sec	U_{m1} in cm	t_{m1} in sec	U_{m2} in cm	t_{m2} in sec	U_{m3} in cm	t_{m3} in sec	$\Delta P/\Delta P_{max}$
5	c = 5000 Newtons per second	.0012	.27	.0030	.81	.0026	1.12	.0030	1.42	.4
		.0018	.40	.0075	1.06	.0064	1.38	.0075	1.70	.6
		.0032	.54	.0318	1.54	.0293	1.88	.0318	2.21	.8
		.0043	.60	.0853	2.03	.0813	2.37	.0852	2.72	.9
6	$U_o = 10^{-4}$ centimeters; c = 50 Newtons per second	.9192	26.67	.9310	27.0	.9256	27.31	.9310	27.61	.4
		2.212	40.0	2.250	40.40	2.237	40.72	2.250	41.04	.6
		6.089	53.34	6.299	53.91	6.262	54.25	6.299	54.58	.8
		unstable								.9

TABLE 3 CONTINUED:

Column No.	Names and Values of Parameters Subjected to Variation	Position at the End of Phase 1		First Motion Reversal		Second Motion Reversal		Third Motion Reversal		Final Load Ratio $\Delta P/\Delta P_{max}$
		U_1 in cm	t_1 in sec	U_{m1} in cm	t_{m1} in sec	U_{m2} in cm	t_{m2} in sec	U_{m3} in cm	t_{m3} in sec	
7	$U_o = 10^{-4}$ centimeters; c = 100 Newtons per second	.7906	13.34	.8106	13.66	.8009	13.96	.8106	14.27	.4
		2.020	20.0	2.087	20.39	2.064	20.71	2.087	21.03	.6
		5.665	26.67	6.092	27.27	6.021	27.60	6.092	27.94	.8
		unstable								.9
8	$U_o = 10^{-4}$ centimeters; c = 500 Newtons per second	.0396	2.67	.1071	3.14	.0882	3.45	.1071	3.75	.4
		.8901	4.0	1.086	4.43	1.0294	4.76	1.0863	5.08	.6
		3.192	5.34	4.653	6.01	4.448	6.34	4.653	6.68	.8
		6.178	6.0	unstable						.9

TABLE 3 CONTINUED:

Column No.	Names and Values of Parameters Subjected to Variation	Position at the End of Phase 1		First Motion Reversal		Second Motion Reversal		Third Motion Reversal		Final Load Ratio $\Delta P/\Delta P_{max}$
		U_1 in cm	t_1 in sec	U_{m1} in cm	t_{m1} in sec	U_{m2} in cm	t_{m2} in sec	U_{m3} in cm	t_{m3} in sec	
9	$U_o = 10^{-4}$ centimeters; c = 1000 Newtons per second	.0013	1.34	.0035	1.81	.0029	2.12	.0035	2.43	.4
		.0223	2.0	.0985	2.62	.0843	2.94	.0985	3.26	.6
		.5876	2.67	2.614	3.51	2.399	3.84	2.614	4.18	.8
		1.80	3.0	unstable						.9
10	$U_o = 10^{-4}$ centimeters; c = 5000 Newtons per second	.0001	.27	.0003	.81	.002	1.12	.0003	1.42	.4
		.0002	.4	.0007	1.06	.0006	1.38	.0007	1.70	.6
		.0003	.54	.0032	1.54	.0029	1.88	.0032	2.21	.8
		.0004	.60	.0085	2.03	.0081	2.37	.0085	2.72	.9

TABLE 3 CONTINUED:

Column No.	Names and Values of Parameters Subjected to Variation	Position at the End of Phase 1		First Motion Reversal		Second Motion Reversal		Third Motion Reversal		Final Load Ratio $\Delta P/\Delta P_{max}$
		U_1 in cm	t_1 in sec	U_{m1} in cm	t_{m1} in sec	U_{m2} in cm	t_{m2} in sec	U_{m3} in cm	t_{m3} in sec	
11	V_o = .1 centimeters per second	1.060	26.67	1.073	26.98	.067	27.28	1.073	27.59	.4
		2.420	40.0	2.459	40.40	2.447	40.73	2.459	41.05	.6
		6.505	53.34	6.732	53.91	6.692	54.25	6.732	54.58	.8
		unstable								.9
12	V_1 = .1 centimeters per second; $\Delta P_d/\Delta P_{max}$ =.5	.9790	26.67	.9942	27.00	.9876	27.32	.9942	27.63	.4
		2.305	40.0	2.316	40.35	2.312	40.67	2.316	41.0	.6
		6.241	53.34	6.499	53.96	6.458	54.29	6.499	54.63	.8
		unstable								.9

In the program for the present computation, the possibility of tensile stresses for both column elements is taken into account, however, the Bauschinger effect is disregarded by choosing the yield-point stress in tension, σ_{yt}, equal to the previous yield-point stress in compression, σ_{yc}, see Fig. 16. However, σ_{yt} can be given any desired value in the program in case sufficient material data on the Bauschinger effect is provided.

A complete typical buckling behaviour of the simple column during both buckling phases is illustrated in Fig. 21.

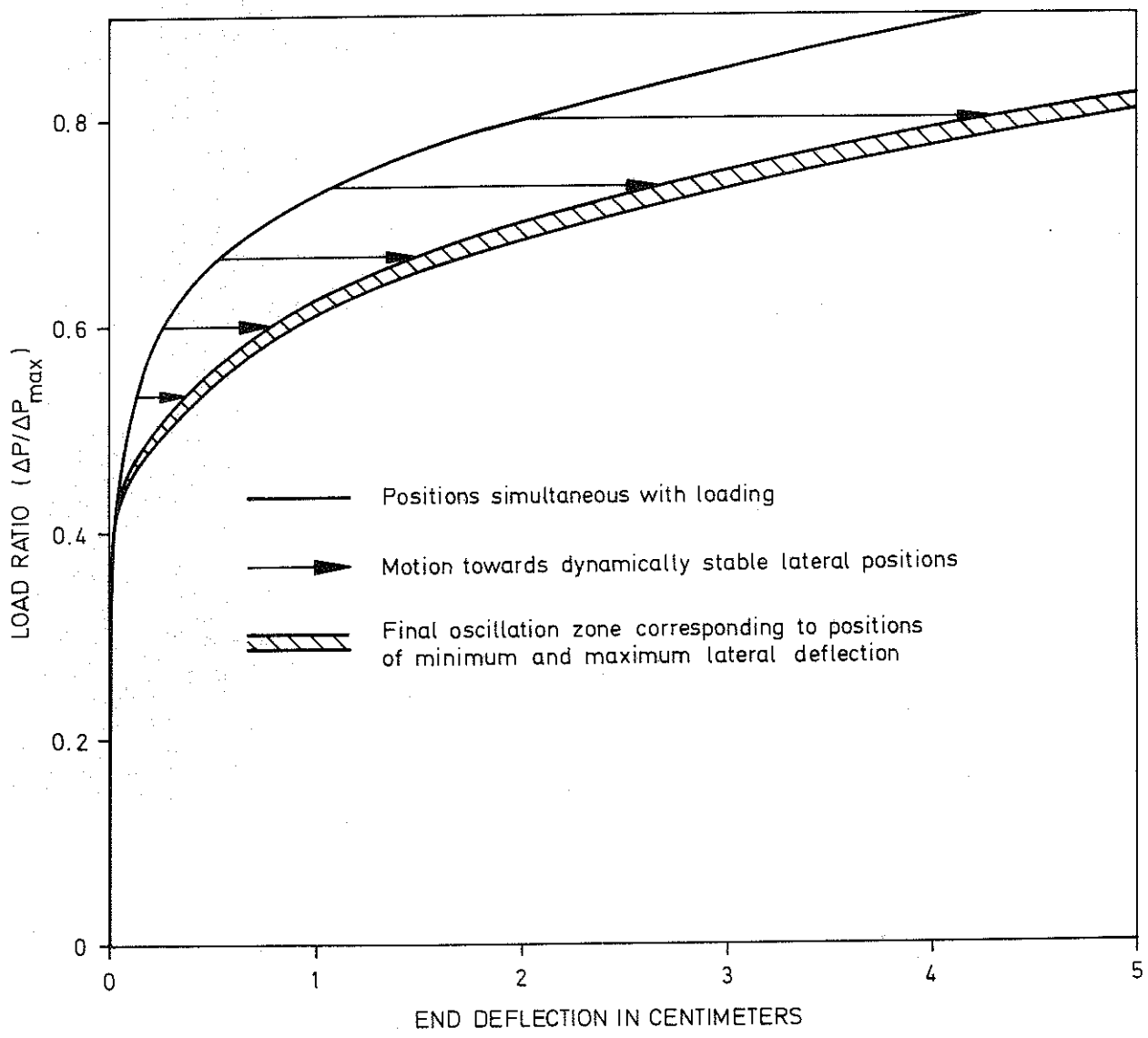

FIG. 21. LOAD DEFLECTION BEHAVIOUR OF COLUMN 4 IN TABLE 3 DURING BOTH BUCKLING PHASES

Fig. 21 shows that the final stable oscillations of the column, under constant axial load below the maximum level, occur in a narrow zone (shade area) between positions of minimum and maximum lateral deflection. If the lateral deflection zone thus obtained is drawn for a number of columns recorded in Table 3 with different loading rates, and if the corresponding load deflection relationship predicted by Shanley theory is marked for the sake of comparison, we arrive at the illustration shown in Fig. 22A.

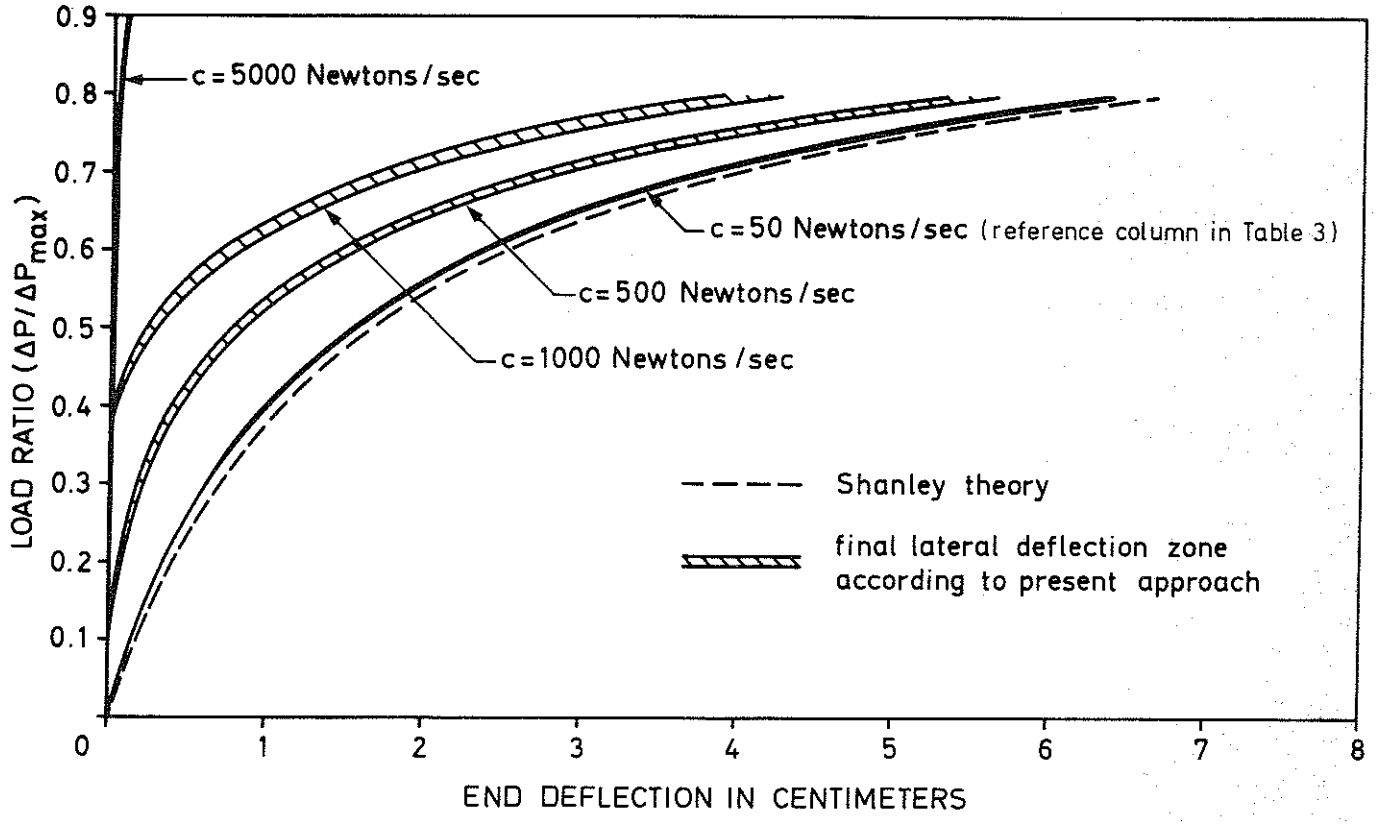

FIG. 22A. FINAL LATERAL DEFLECTION ZONE ACCORDING TO THE PRESENT APPROACH FOR VARIOUS LOADING RATES COMPARED WITH THE LATERAL EQUILIBRIUM POSITIONS ACCORDING TO SHANLEY THEORY

As another illustration of the load deflection behaviour, a new set of calculations is performed for the same simple column (see Fig. 12) with the following data:

b = 5 cm; d = 10 cm; L = 5 m; M = 500 kg; $E_o = 2 \cdot 10^{10}$ Newtons/m^2; $E_t = 10^{10}$ Newtons/m^2; c = 50 Newtons/sec; $U_o = 10^{-3}$ cm; and no velocity disturbance during lateral motion.

The results of the computations with a reference column having the above data is shown in Fig. 22 B.

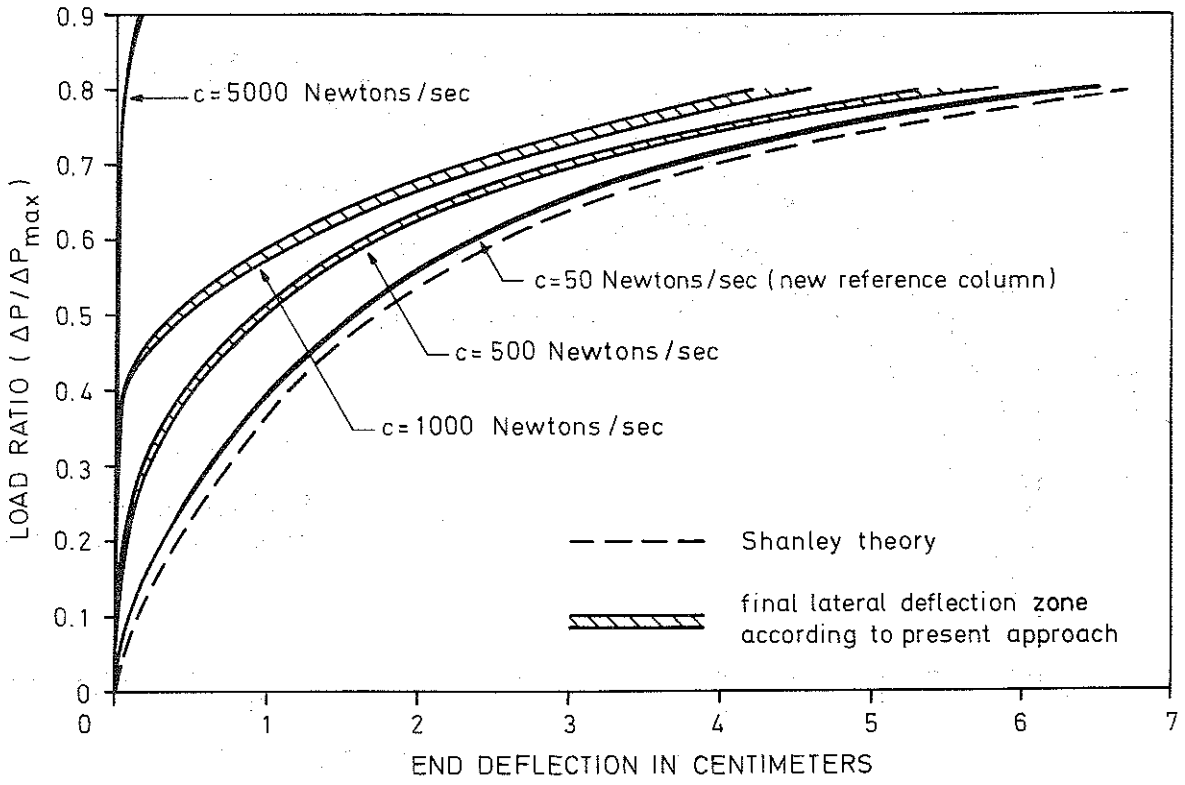

FIG. 22 B. FINAL LATERAL DEFLECTION ZONE ACCORDING TO THE PRESENT APPROACH FOR VARIOUS LOADING RATES COMPARED WITH THE LATERAL EQUILIBRIUM POSITIONS ACCORDING TO SHANLEY THEORY.

In the numerical illustrations of the present section, the length of the time step, Δt, corresponding to each computation cycle is chosen equal to .001 seconds. New computations with Δt = .001 seconds were performed for this model. However, no apprecial difference was observed. The possible influence of the time step on the buckling behaviour of the simple column with arbitrary stress strain diagram will be discussed in greater detail in Sec. 8.9.

It should be noted that the tangent modulus load, P_t, and the maximum load increment, ΔP_{max}, for the reference columns in Figs 22A and 22B have the following numerical values: For the reference column in Table 22A, P_t = 10000 Newtons, and ΔP_{max} = 3333 Newtons; for the reference column in Table 22B, P_t = 25000 Newtons, and ΔP_{max} = = 8333 Newtons.

Both Figs 22A and 22B show that by maintaining a fixed initial imperfection and varying the duration of loading, as the loading rate gets smaller values, the lateral deflection zone according to the present approach, gets narrower and nearer to the load deflection behaviour envisaged by Shanley. On a ceteris paribus basis, the discrepancy between the two approaches increases in the direction of the increasing loading rate.

PART III

BUCKLING BEHAVIOR OF IMPERFECT INELASTIC COLUMN

PART III. BUCKLING BEHAVIOUR OF IMPERFECT INELASTIC COLUMN

Introduction

The imperfect inelastic column is characterized as a column which would start bending simultaneously with loading right from zero load level; if the axial load does not change direction throughout the process of lateral deflection, it is identified as conservative and otherwise nonconservative. The chief objective of the present study is exploring the numerous properties of the maximum column load and disclosing the remarkable buckling phenomena describing the load deflection behaviour of the imperfect column subjected to various prescribed imperfections or disturbances.

Chapter 7 is devoted to the exploration of fundamental general concepts which are sequentially utilized to describe the complete imperfect column behaviour. These general concepts include the development of the concept of surplus moment increment in Sec. 7.1; influence of laterally induced bending moment in Sec. 7.2; influence of axially induced bending moment in Sec. 7.3; description of the moment state in Sec. 7.4; exploration of the conditions for motion reversal in Sec. 7.5; description of the concept of maximum column load in Sec. 7.6; illustration of motion reversal criteria for the simple column in Sec. 7.7; and determination of the maximum column load in Sec. 7.8.

The numerical evaluation of imperfect simple column behaviour is accomplished by the analysis of Model 3 in Chapter 8 in which the model is described and its state equations identified in Sec. 8.1; the stress state of the column is thoroughly determined and the corresponding tangent

moduli on the stress strain diagram assigned in Sec. 8.2; the concepts of two computer programs entitled "Multi-Cycle Search Method" and "Single-Cycle Search Method" are developed in Secs. 8.3 and 8.4 respectively; the dynamic state of the column at limiting stress levels, i.e., at the points between two adjacent subdivisions on the multilinear stress strain diagram, is determined in Sec. 8.5; the main program based on the concept of Single-Cycle Search Method, together with brief descriptions of the corresponding subroutines, is presented in Sec. 8.6; extensive numerical results related to the maximum column load for three different data sets is presented and tabulated in Sec. 8.7; the reliability of the numerical results is examined in Sec. 8.8 by recording the computations for the maximum column load of a certain column according to the two differently conceived programs developed in Sec. 8.3 and 8.4; and the influence of the choice of the computation time step is thoroughly discussed and illustrated in Sec. 8.9.

The various properties of the maximum column load are discussed and illustrated in Chapter 9, including a discussion of the decisive factors influencing the size of the maximum column load in Sec. 9.1; the influence of variations of velocity disturbances in Sec. 9.2; influence of variations of initial eccentricity or initial deflection in Sec. 9.3; and influence of variations of loading rate in Sec. 9.4.

Additional salient buckling phenomena are disclosed in Chapter 10 comprising the induced permanent deflection in reverse direction in Sec. 10.1; self-induced permanent deflection in reverse direction in Sec. 10.2; influence of gravitational force in Sec. 10.3; influence of nonconservative axial load simultaneous with loading and/or during buckling Phase 2 in Sec. 10.4; abnormal behaviour of backwards inclined columns in Sec. 10.5; and final stable equilibrium configurations in Sec. 10.6.

Numerical results for dynamically stable lateral configurations of Model 3 are included in Chapter 11; and summary and conclusions are presented in Chapter 12.

7. DISCUSSION OF GENERAL CONCEPTS

7.1 Development of the Concept of Surplus Moment Increment

The analysis of imperfect elastic column in Chapter 3 shows that the difference between the actual column behaviour simultaneous with loading and that predicted by the static theory may get accentuated as the axial load approaches the critical value. This characteristic is additionally illustrated in Fig. 23.

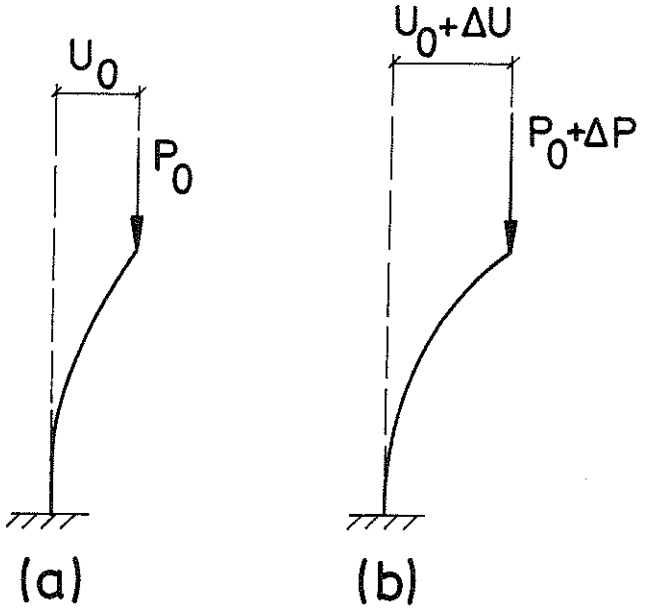

FIG. 23. CONFIGURATION OF THE COLUMN AT TWO INSTANTS OF TIME DURING LATERAL DEFLECTION: (a) JUST BEFORE AND (b) SOMETIME AFTER THE INCREASE OF AXIAL LOAD, ΔP

Fig. 23 conveys the information that an increment of lateral deflection, ΔU, gives rise to the following two significant external moment increments:

(a) The increment, $P_o \cdot \Delta U$, i.e., the increase caused due to the existing axial load, P_o, suffering an additional deflection, ΔU; and

(b) the increment, $\Delta P \cdot U$, i.e., the increase due to the current deflection, U, being imposed on the newly arriving load increment, ΔP.

Thus, at the fixed-end cross section, the external moment increment, ΔM_{e1}, where the index e refers to the external moment and the index 1 to buckling Phase 1, may be expressed as

$$\Delta M_{e1} = P_{o1} \cdot \Delta U + \Delta P \cdot U \qquad (125)$$

in which P_{o1}= the initial value of the axial load immediately before the increase of axial load at the start of buckling phase 1; U = the current end deflection; and ΔU, ΔP = the deflection respective axial load increments.

Using a multi-cycle computation technique, analogous to that of Appendix C, we may consider the axial load increment, ΔP, as a constant value applied at the beginning of the first computation cycle. In this case, the deflection increment, ΔU, would be a function of time. Additional increments of axial load may be added to the axial load at the start of subsequent computation cycles, each time considering the state of the column at the end of a sufficiently short time step as the initial state for the immediately following computation cycle.

Setting the axial load increment, ΔP, equal to zero in Eq. (125) for all subsequent computation cycles, would result in the following equation for the external moment increment, ΔM_{e2}, corresponding to buckling Phase 2:

$$\Delta M_{e2} = P_{o2} \cdot \Delta U \tag{126}$$

in which P_{o2} = the axial load at the start of buckling Phase 2.

Defining the surplus moment increment, ΔM, as the difference between the internal bending moment increment, ΔM_{ib}, developed solely due to pure bending effect, and the external moment increment, ΔM_e, corresponding to a certain deflection interval, the following relation is obtained:

$$\Delta M = \Delta M_{ib} - \Delta M_e \tag{127}$$

Substitution of Eqs. (125) and (126) into Eq. (127), one at a time, results in the following two equations for the surplus moment increments, ΔM_1 and ΔM_2, corresponding to buckling Phases 1 and 2 respectively:

$$\Delta M_1 = \Delta M_{ib} - P_{o1} \cdot \Delta U - \Delta P \cdot U \tag{128}$$

and

$$\Delta M_2 = \Delta M_{ib} - P_{o2} \cdot \Delta U \tag{129}$$

It should be noted that the terms P_{o1} and P_{o2} are used in this section to distinguish between the initial values of the axial load at the start of buckling Phases 1 and 2 respectively. However, the symbol P_o alone would refer to the axial load at the beginning of any computation cycle.

Now, if we assume that the column in Fig. 23(a) was initially in a state of equilibrium under a relatively large axial load, P_{o1}, such that $P_{o1} + \Delta P$ would still lie below the critical load level, then the difference, $\Delta M_{ib} - P_{o1} \cdot \Delta U$, may have a small psoitive value for small values of ΔU. Thus, large lateral deflection increments may be required

to counteract the influence of the term, $\Delta P \cdot U$, in Eq. (128) in moving towards a new equilibrium configuration. It should be observed that so far we have only discussed the influence of the size of the axial load on the ensuing lateral deflection. However, for an inelastic column the decrease of bending rigidity due to inelastic material properties is another factor which will be explained in greater detail in the following sections.

7.2 Influence of Laterally Induced Bending Moment

In addition to the proximity of the axial load to its critical level, the following two factors may turn out to be influential in determining the instability of the inelastic column:

1. The capacity of the column to generate bending moment may deteriorate as it proceeds to deform in the regions of the stress strain diagram with continuously decreasing tangent moduli; and

2. The uniform axial deformation of the column, simultaneous with the increase of axial load, may give rise to an axially induced bending moment increment which would partially counteract the internal moment caused due to pure bending effect, during a given time step.

Both the above factors tend to accentuate the process of lateral bowing. Consequently, in the following analysis we first treat the influence of material properties on the ability of the column to produce internal moment solely due to bending in this section; and in the next section the problem of axially induced internal moment is tackled.

It should be observed that the zone of decreasing bending strain over a cross section of an inelastic column may deform in a region of the stress strain diagram with higher tangent moduli than the corresponding zone of increasing bending strain. Furthermore, it should be remembered that the stress distribution caused solely due to bending effect does not give rise to any additional increment of axial load. Thus, assuming a linear strain distribution over a column cross section, it follows that the point, which suffers no additional bending strain during an incremental rotation of that cross section does not usually lie at

the middle of the cross section. This is illustrated in Fig. 24.

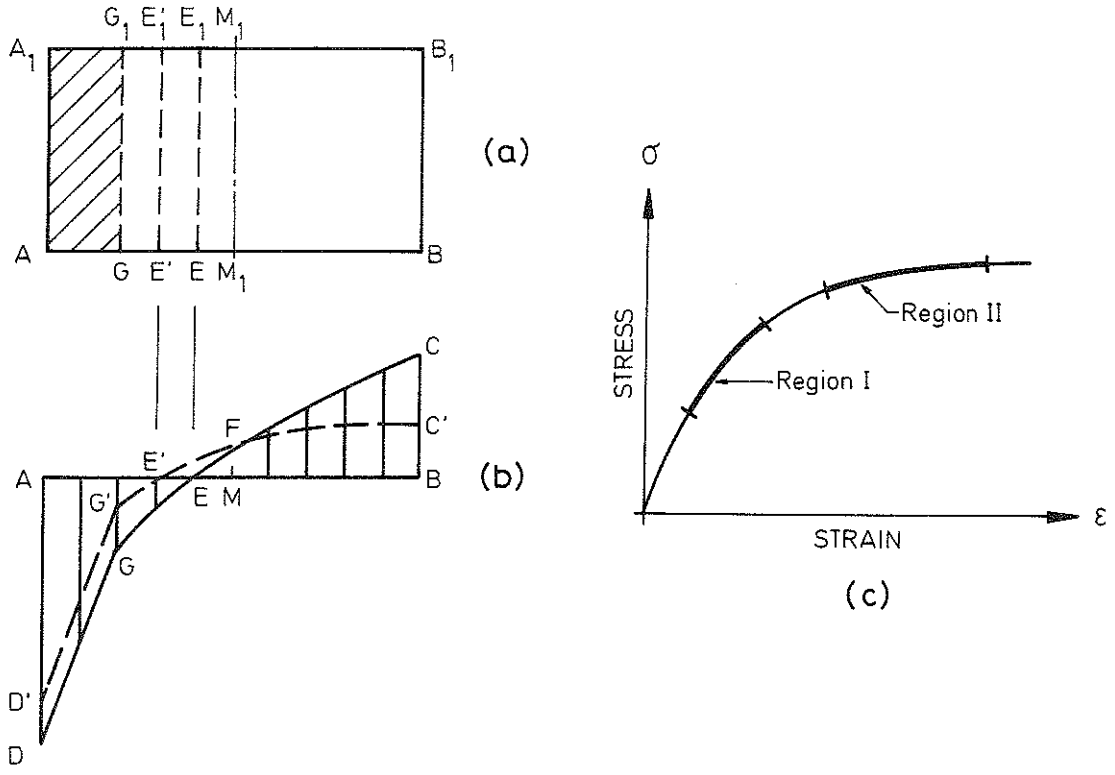

FIG. 24. ILLUSTRATION OF DECREASE IN BENDING RIGIDITY DUE TO LATERALLY INDUCED INFINITESIMAL STRESS DISTRIBUTION

Fig. 24(a) shows a rectangular cross section of the column in which strain reversal has already occured on the shaded part of the area enclosed by the boundary points, AA_1G_1G. Fig. 24(b) shows two superimposed incremental stress distributions corresponding to the same rotation, $\Delta\alpha$, of the cross section, AA_1B_1B, but deforming at different regions of the stress strain diagram, see Fig. 24(c). We temporarily assume that during the infinitesimal rotation, $\Delta\alpha$, of the cross section simultaneous with loading, the same varying unloading zone, AA_1G_1G, shown in Fig. 24(a), applies to both cases under consideration. This

partly implies that no appreciable difference is observed between the two cases regarding the propagation of the unloading zone simultaneous with loading. Thus, if E´ lies to the left of E, the area AD´G´E´ would wholly lie within the area ADGE in Fig. 24(b).

Since in Fig. 24(b) the area ADGE must be equal with the area EFCB and the area AD´G´E´ must be equal with the area E´FC´B, and observing that the area AD´G´E´ is smaller than the area ADGE, it follows that

$$A_{E´F\ C´B} < A_{EFCB} \tag{130}$$

in which A stands for the area and the alphabetic indices indicate the corresponding enclosing boundary points in Fig. 24(b).

The laterally induced internal bending moment increments, ΔM_{ib}^{I} and ΔM_{ib}^{II} corresponding to Cases I and II respectively are obtained from the equations

$$\Delta M_{ib}^{I} = \Delta M_{ADGE} + \Delta M_{EFCB} \tag{131}$$

and

$$\Delta M_{ib}^{II} = \Delta M_{AD´G´E´} + \Delta M_{E´FC´B} \tag{132}$$

in which ΔM stands for moment of the area with respect to the middle point of the cross section, M, in Fig. 24(b); and the alphabetic indices indicate the corresponding boundary points.

Since, from Inequality (130), the area E´FC´B is smaller than the area EFCB in Fig. 24(b) and since the common part of these two partial

areas consists of the area, EFC′B, it follows that the area E′FE is smaller than the area FCC′. Furthermore, the center of gravity of the area FCC′ lies further away from the point M than the center of gravity of the area, E′FE. This leads to

$$\Delta M_{E'FE} < \Delta M_{FCC'} \tag{133}$$

in which ΔM and the corresponding alphabetic indices have the same meaning as above.

From Inequalities (130) and (133) it follows that the moment of the area EFCB with respect to M is larger than that of the area E′FC′B. From this result together with Eqs. (131) and (132) and the geometry of Fig. 24(b), it may be inferred that

$$\Delta M_{ib}^{II} < \Delta M_{ib}^{I} \tag{134}$$

Inequality (134) shows that for the same rotation of a column cross section, the internal bending moment developed solely due to bending decreases as the column proceeds to deform an at higher region of the stress strain diagram with lower values of tangent moduli, provided that the zones of unloading over the cross section are identical during the deformation in the two different regions.

The information conveyed by Inequality (134) would be equally valid even if point E′in Fig. 24(b) happens to lie to the right of point E. In that case, the line of arguments used in the above analysis would be still applicable by interchanging the role of the areas AD′G′E′and ADGE in Fig. 24(b) with the corresponding areas E′FC′B and EFCB respectively. Further-

more, it should be observed that in Fig. 24(b), the unloading zone covers only a portion of the zone of decreasing bending strain. This situation can only occur simultaneous with the increase of axial load. When the axial load ceases to increase, the unloading zone covers the entire zone of decreasing bending strain. However, in this latter case, the extent of the unloading zone over a cross section, corresponding to two different regions of the stress strain diagram with varying tangent moduli, cannot be the same. This situation is additionally discussed in the remarks which follow.

Since,the propagation of the unloading zone simultaneous with the increase of axial load, during finite rotations of the cross section, cannot remain identical as a general rule for the two cases studied above, then the conclusion above may appear to be of limited use. However, we utilize the illustration in Fig. 24 in order to make the following general observations, which would equally be valid for infinitesimal as well as finite rotations of the cross section:

1. If a column cross section deforms with a greater total unloading zone in Region I than in Region II of Fig. 24(c), then for the same cross section rotation, the partial areas ADGE and EFCB in Fig. 24(b) would be additionally enlarged compared with the case of equal unloading zones depicted in Fig. 24. In this case Inequality (134) is definitely valid;

2. On the contrary, if the total unloading zone corresponding to Region II of Fig. 24(c) is greater, the partial areas AD´G´E´ and E´FC´B in Fig. 24(b) would be further magnified as compared with the case of equal unloading zones shown in Fig. 24. In this case no definite conclusion can be drawn on the validity of Inequality (134);

3. from the discussion of the second point above, it may be visualized that it is possible for a column which has reached higher regions on a stress strain diagram, Fig. 24(c), to develop larger laterally induced internal bending moment increments over the cross section of maximum bending strain than the same column deforming on lower regions of the stress strain diagram, provided that the extent of unloading zone in the former situation is sufficiently larger than that of the second one;

4. for a column in which no strain reversal has yet occurred, i.e., when the shaded area in Fig. 24(a) is equal to zero, the deformation in Region II of Fig. 24(c) develops lower laterally induced internal bending moment increments than the deformation in Region I of the same stress strain diagram; and

5. during buckling Phase 2, a column develops larger bending moment increment in Region I than in Region II of the stress strain diagram shown in Fig. 24(c). The unloading zone shaded in Fig. 24(c) cannot in this case be the same in the two different regions.

It should be noted that in the cases discussed above, an increase in the laterally induced internal moment may not necessarily imply an increase in the bending rigidity of the column simultaneous with loading. This uncertainty may arise due to the possible counteracting influence of the axially induced internal moment to be discussed herein in the next section. However, when the axial load ceases to increase, the laterally induced internal moment increment in the process of lateral deflection during Phase 2 is a direct measure of the bending rigidity of the column. This concept is further clarified in Secs. 7.3 and 7.4.

7.3 Influence of Axially Induced Bending Moment

The axially induced internal moment increment mentioned in the previous section will now be illustrated by means of Fig. 25.

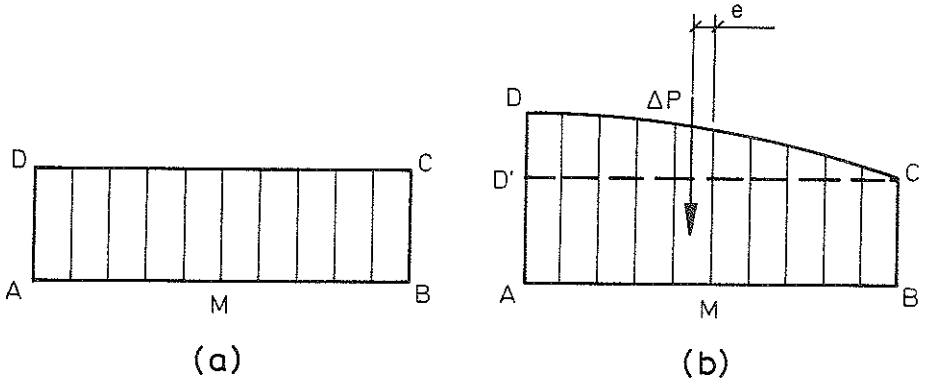

FIG. 25. ILLUSTRATION OF AXIALLY INDUCED INCREMENTAL STRAIN AND STRESS DISTRIBUTION

Fig. 25(a) shows the strain caused over a column cross section, due to an increase of axial load, ΔP, at the beginning of a computation cycle. Since we assume that the column axially responds immediately to an increase of axial load, this would give rise to a uniform incremental strain distribution as soon as the axial load increment is applied. It should be noted that the immediate axial response of the column to the increase of axial load has already been illustrated herein in Sec. 3.2.

Fig. 25(b) shows the incremental stress distribution induced due to the strain distribution of Fig. 25(a). This nonuniform stress distribution is caused due to the fact that the deformation of various points on a cross section of the column is not usually governed by a single tangent modulus. The zone of increasing bending strain which wholly or partly lies to the right of the middle point, M, in Fig. 25(b),

generally deforms with lower tangent moduli than the zone of decreasing bending strain to the left of Point M.

Thus, the internal axial load increment, ΔP, is excentrically applied as shown in Fig. 25(b). Since, ΔP, in Fig. 25(b) lies to the left of Point M, it definitely gives rise to an internal bending moment increment which acts in opposite direction to the laterally induced moment increment from Fig. 24(b). Thus, assuming the laterally induced bending moment increment, ΔM_{ib}, to be positive, the corresponding axially induced internal moment increment, ΔM_{ia}, is obtained from the equation

$$\Delta M_{ia} = -\Delta P \cdot e \qquad (135)$$

in which e is the excentricity of ΔP, shown in Fig. 25(b).

As an illustration of the influence of the axially induced internal moment, we may refer to Fig. 21 already presented in Sec. 6.6. The load deflection behaviour of the initially perfect centrally loaded simple inelastic column with a bilinear stress strain diagram reveals that up to a certain increase of axial load above the tangent modulus load, the deflection of the column simultaneous with loading as well as subsequent lateral motion under the influence of constant axial load remain within a relatively small deflection range. This behaviour corresponds to the lateral motion of the column before strain reversal begins to occur. In that situation a constant tangent modulus applies to both the column elements, in which case the magnitude of axially induced moment increment is equal to zero. However, as soon as strain reversal takes place, the axially induced moment increments begin to exert their detrimental influence. This is observed in Fig. 21 by a noticeable

bowing of the load deflection curve beyond certain loading range.

From Eq. (135) it may be inferred that as soon as the axial load ceases to increase, the axially induced internal moment increment altogether vanishes. Thus, the lateral deflection of the column during buckling Phase 2 is accompanied with the development of the maximum bending rigidity partly due to maximum strain reversal simultaneous with bending in the zone of decreasing bending strain; and partly due to the disappearance of the destabilizing axially induced internal moment increments.

With the aid of the knowledge obtained in the course of the last three sections herein, we now attempt to present a clear picture of the moment state of the inelastic column, in general.

7.4 Description of the Moment State of an Inelastic Column

From the exposition of the laterally and axially induced internal moment increments in the previous two sections, it may be clear that, on the basis of the multi-cycle computation technique developed herein for the solution of the column problem, the axially induced internal moment increment begins to act on the column right from the beginning of the computation cycle. This leads to the following equation for the total internal moment, M_{io}, at the start of the current time interval:

$$M_{io} = M_i \text{ (end of previous cycle)} - \Delta P \cdot e \qquad (136)$$

in which M_i stands for internal moment; and the term $-\Delta P \cdot e$ from Eq. (135) is the axially induced moment increment.

The laterally induced internal moment increment does not appear in Eq. (136), since that equation only expresses the initial internal moment at the beginning of the computation cycle.

The laterally induced internal moment increment, ΔM_{ib}, is, on the other hand, a variable which changes throughout the deflection interval. Thus, the internal moment, M_i, at the end of the computation cycle may be written in the following form:

$$M_i \text{ (end of current cycle)} = M_{io} + \Delta M_{ib} \qquad (137a)$$

The axially induced moment increment, ΔM_{ia}, indirectly appears in Eq. (137 a) through its presence in the initial term, M_{io}.

Thus, in the equation describing the motion of the column during a computation cycle, the only moment increment which would appear as a variable simultaneous with deflection is the laterally induced increment, ΔM_{ib}. This explains why in the definition of the surplus moment increment in Eq. (127), we included only the term, ΔM_{ib}, which is a variable throughout the process of bending. The other moment increment, ΔM_{ia}, affects the column as constant increments appearing only at the beginning of the computation cycles. The analysis of Model 2 has already shown herein that the variable, ΔM, defined by Eq. (104) significantly affects the type of solution of the equation of motion of the simple column. A closer look at Eq. (104) reveals that the term, ΔM, defined by that equation actually represents the surplus moment increment for a unit rotation of the central axis of the simple inelastic column.

Substitution of Eq. (136) into Eq. (137 a) gives a complete picture of the emergence of both internal moment increments during the course of one cycle:

$$M_i \text{ (end of current cycle)} = M_i \text{ (end of precious cycle)} - \\ - \Delta P \cdot e + \Delta M_{ib} \qquad (137b)$$

During buckling Phase 2, the axially induced internal moment increment vanishes, in which case the surplus moment increment defined by Eq. (127) represents the difference between the internal and external moment increments during the entire computation cycle. In addition to the surplus moment increment (SMI), we introduce the notion of the total internal moment surplus (TIMS) at a given column cross section defined herein according to the following equation:

$$TIMS = |M_i| - |M_e| \tag{138a}$$

in which $|M_i|$ = the absolute value of the total internal moment; and $|M_e|$ = the absolute value of the total external moment where the external moment, M_e, is defined by the equation

$$M_e = P \cdot U \tag{138b}$$

in which P, U = the current values of the axial load and the deflection at the actual cross section respectively.

The values of SMI, TIMS and the kinetic energy of the column at the start of Phase 2 are decisive factors which together with stress strain diagram determine the question of motion reversal to be explored in the next section.

7.5 Exploration of the Conditions for Motion Reversal

Motion reversal is a self-explanatory word which means changing the direction of motion. This is pictorially illustrated in Fig. 26.

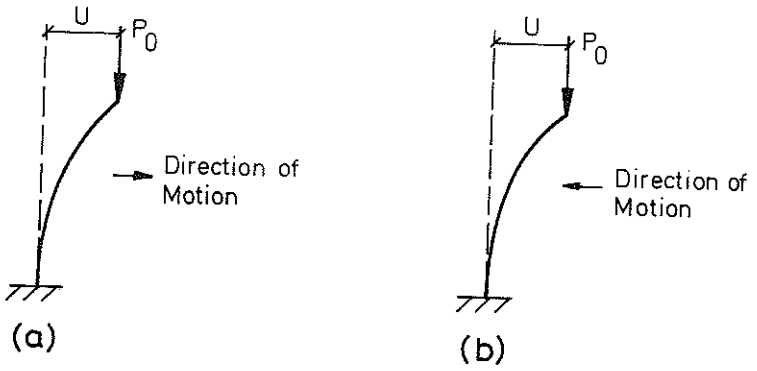

FIG. 26. LATERAL CONFIGURATION OF THE COLUMN UNDER CONSTANT AXIAL LOAD: (a) BEFORE MOTION REVERSAL; (b) AFTER MOTION REVERSAL

The concept of motion reversal depicted in Fig. 26 implies that the deflected form of the column is preserved subsequent to motion reversal. In other words, every point of the column attains the extremum position at the same time. This behaviour, which is true in the case of vibration of elastic structures (23), is assumed to be equally valid in the present analysis.

From the above discussion it follows that the reversal of motion at any arbitrary column cross section may imply the motion reversal

for the column as a whole. Thus, in the following sections, we may often desire to single out the cross section subjected to greatest bending strain for the analysis of motion reversal or the evaluation of maximum column load. This is due to the fact that the conditions at this cross section are most crucial for the determination of the stability of the column. When there is no explicit reference to any particular cross section, it is the cross section of maximum bending strain which is implied.

Motion reversal may occur during both buckling phases. The occurrence of this phenomenon during buckling Phase 1 may be explained as follows: Suppose that at a certain instant of time, t, during loading, the kinetic energy of the column has attained a finite value while the column is moving in forward direction. It is further assumed that during a future increase of axial load, ΔP, the axially induced internal moment increment is negligible while the corresponding surplus moment increment has a positive and relatively large value. The loading rate may additionally be supposed to be sufficiently small. Thus, the increment of time, Δt, corresponding to the increase of axial load, ΔP, may be so large that the kinetic energy of the column may be totally absorbed during this time period due to the continuous increase of the total internal moment surplus defined by Eq. (138a). Thus, motion reversal simultaneous with loading may occur in the given loading range.

The occurrence of motion reversal during buckling Phase 2 is the single criterium for the stability of the column under a given constant axial load. The following sufficient conditions may be formulated for either the existence or the lack of existence of a motion

reversal position during Phase 2:

1. If the surplus moment increment (SMI) is positive throughout the future increments of lateral deflection, a motion reversal position would be definitely attained regardless of the current values of TIMS and the kinetic energy of the column. This is due to the fact that the current value of TIMS would continuously increase until the kinetic energy is reduced to zero and motion reversal position is attained.

2. If the SMI and the TIMS are both negative, no motion reversal position would be reached provided that the value of SMI remains negative throughout the future increments of lateral deflection. In this case, the value of TIMS can never attain positive values as a consequence of further lateral deflection.

3. If the SMI is negative throughout subsequent lateral motion, but the current value of TIMS is positive, the column may or may not attain a motion reversal position depending on the current kinetic energy, the future range of the stress strain diagram, and the relative magnitudes of the current values of SMI and TIMS. The possibility of motion reversal with negative SMI will be more closely studied herein in Secs. 7.6 and 7.7.

7.6 Description of the Concept of Maximum Column Load

According to the static theory, the maximum column load is the smallest load above which no finite deflected configuration of the column could be found at which the external and internal moments are equalized over all cross sections of the column. According to the actual column behaviour, the inelastic column may become unstable under a constant axial load, even though it may pass through a position of moment equalization. It is the objective of this section to disclose this and other interesting phenomena.

According to the discussion of the previous section, the lateral motion of the column is sensitively dependent on the value of the surplus moment increment, ΔM, at the cross section subjected to greatest strain. There are two factors which contribute to the smallness of ΔM, defined by Eq. (127), viz., a high level of the axial load, and low values of the actual tangent moduli corresponding to the deformation of the column at the given cross section. Both these factors may be combined for an inelastic column to give rise to the possible deflection behaviour depicted in Fig. 27.

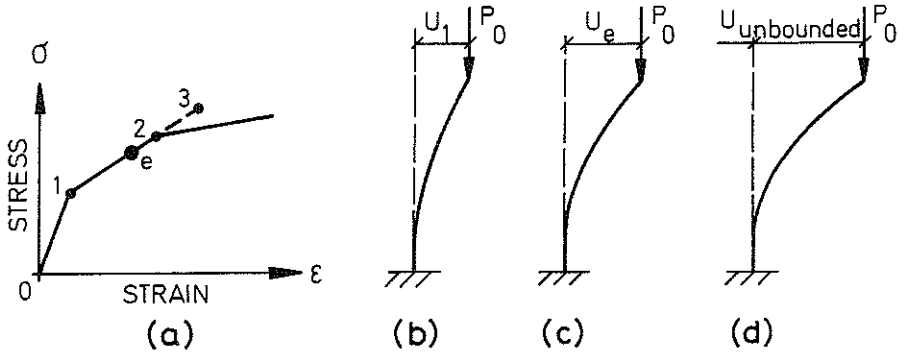

FIG. 27. (a) STRESS STRAIN DIAGRAM; (b), (c), and (d) POSSIBLE TEMPORARY POSITIONS CORRESPONDING TO END OF PHASE 1, POSITION OF MOMENT EQUALIZATION, AND SUBSEQUENT UNBOUNDED DEFLECTION RESPECTIVELY

Fig. 27(a) shows a trilinear stress strain diagram corresponding to the column shown in Fig. 27(b) - (d). The column in Fig. 27(b) with a constant axial load, P_o, depicts the assumed dynamically unstable position at the end of Phase 1, viz., at the instant of time when the axial load has just ceased to increase. It is assumed that at the axial load, P_o, the zone of increasing bending strain at the fixed-end cross section of the column in Fig. 27(b), is wholly deforming in the inelastic range between Points 1 and 2 in Fig. 27(a). Thus, for a small rotation of the fixed-end cross section, just before and after reaching the load level, P_o, the incremental stress distribution solely due to bending may look something like in Fig. 28:

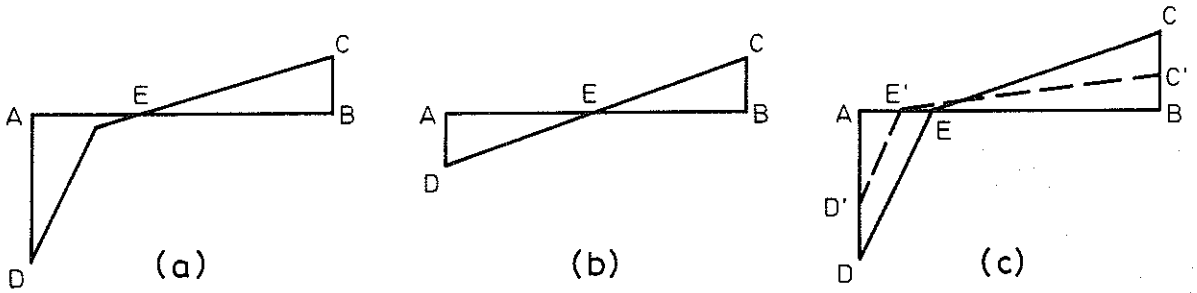

FIG. 28. INCREMENTAL STRESS DISTRIBUTIONS AT THE FIXED-END CROSS SECTION IN FIG. 27(b): (a) OR (b) IMMEDIATELY BEFORE; (c) JUST AFTER REACHING THE AXIAL LOAD P_o

Fig. 28(a) shows the incremental bending stresses over the fixed-end cross section, AB, with some strain reversal simultaneous with loading immediately before keeping the axial load at the constant level, P_o. Fig. 28(b) may depict the same situation as in Fig. 28(a) but with no strain reversal simultaneous with loading. Regardless of whether

Fig. 28(a) or (b) is applicable, the incremental stress distribution under the influence of constant axial load just after reaching the axial load, P_o, is shown by the area ADECB in Fig. 28(c). With the reduction in bending rigidity which occurs in the column at the stress level marked by Point 1 in Fig. 27(a) due to the fall in the value of the tangent modulus, the surplus moment increment under the influence of the axial load, P_o, may have already attained a small positive value at the configuration shown in Fig. 27(b). This is due to a decrease in the value of the laterally induced bending moment increment, according to the analysis of Sec. 7.2.

Fig. 27(c) shows the position of moment equalization at which the stress strain corresponding to Point B in Fig. 28(c) is represented by Point e in Fig. 27(a). However, due to the assumed low value of the surplus moment increment beyond the configuration shown in Fig. 27(b), the column may have attained a considerable kinetic energy at the position indicated in Fig. 27(c), to the extent that, if the tangent modulus were assumed to remain unchanged after Point 2 in Fig. 27(a), a position of motion reversal would have been attained by the column at Point 3 in Fig. 27(a), corresponding to the stress strain at the point of maximum strain in the column, i.e., Point B in Fig. 28. However, before reaching a motion reversal position, the bending rigidity of the column begins to decrease as soon as the stress at the point of maximum strain in the column exceeds the level indicated by Point 2 in Fig. 27(a). After some additional deflection beyond this stage, the zone of increasing bending strain at the fixed-end cross section may wholly deform in the inelastic range beyond Point 2 in Fig. 27(a).The incremental stress distribution corresponding to this case at the cross section of maximum strain is illustrated by the area AD´E´C´B, in Fig. 28(c).

The surplus moment increment, due to the combined influence of the axial load, P_o, and the new internal moment increment caused by the incremental stress distribution AD´E´C´B in Fig. 28(c), may have now attained a finite negative value. The question of possible motion reversal now entirely depends on the kinetic energy of the column plus the total internal moment surplus existing at this new state. This may be explained more closely as follows:

Beyond the position of moment equalization at the cross section AB, the total internal moment exceeds the corresponding external moment over that cross section as long the incremental stress distribution ADECB in Fig. 28(c) is applicable. This is inferred from the fact that a position of motion reversal is assumed for the column provided that the tangent modulus beyond Point 1 in Fig. 27(a) maintains a constant value throughout the subsequent deformation, recall the significance of Point 3 in Fig. 27(a).

Thus, with positive surplus moment increment beyond the position of moment equalization, the total internal moment over cross section AB continuously exceeds the corresponding external moment up to the state where the surplus moment increment becomes negative. In subsequent deflection beyond this stage, the total internal moment surplus must counteract the effect of the newly emerging negative surplus moment increment and simultaneously neutralize the existing kinetic energy of the column. If the total existing internal moment surplus at the new state is sufficiently small and the kinetic energy sufficiently large, the column may never attain a motion reversal position and the state of the column under the axial load, P_o, is unstable.

If on the other hand, the kinetic energy is sufficiently small and the total existing internal moment surplus is sufficiently large, at a given state, the column may reach a motion reversal position even in the presence of a negative surplus moment increment.

With the above fundamental insight into the nature of motion reversal in an inelastic column, we are now in a position to present a physically precise definition of the maximum column load as the smallest axial load at which the column under the influence of that constant load does not attain a position of motion reversal. The maximum column load could also be defined as the greatest axial load at which a dynamically stable lateral deflection zone could be attained for the fundamental deflection mode of the column under the influence of that constant axial load These two definitions of maximum column load differ only by a load increment corresponding to one computation cycle; the difference between the two maximum column loads according to the two definitions may become arbitrarily small by choosing a sufficiently small time step, Δt, corresponding to one computation cycle. Due to its computational convenience, the first definition of the maximum column load presented in this section would be adopted herein in the following sections.

The discussion in this section reveals the remarkable property that for an inelastic column, it is possible for the surplus moment increment to attain negative values without the column having reached the maximum axial load. This and other motion reversal phenomena will now be illustrated in the next section for the simple inelastic column shown in Fig. 12.

7.7 Illustration of Motion Reversal Criteria for the Simple Column

We assume that the simple column shown in Fig. 12 consists of a hinge whose elements correspond to any arbitrary stress strain diagram; however, for practical reasons we may assume that the stress strain diagram of the type shown in Fig. 10(b) is applicable. Furthermore, the column may be assumed to be imperfect from zero load level. Using the multi-cycle computation technique described in Appendix C, the motion of the column may sequentially be followed from zero load level up to any desired axial load.

During the current computation cycle, the motion of the column is governed by the following equation, see Eq. (C 27) of Appendix C:

$$\ddot{\alpha} + \frac{(C - P\cdot L - \frac{MgL}{2})}{I}\alpha = \frac{P\cdot X_o - M_{io} - \Delta M_{ia} + C\cdot\alpha_o - P\theta\cdot L}{I} \qquad (139)$$

in which M = the total mass of the column; g = the gravitational acceleration; X_o = the excentricity in the application of axial loading; θ = the deviation of the axial load from its original axial direction; and all other symbols are already defined in Sec. 6.2.

Using the notations, see Eqs. (C 28) - (C 31) of Appendix C,

$$\Delta M = C - P\cdot L - \frac{M\cdot g\cdot L}{2} \qquad (140)$$

$$H = P\cdot X_o - M_{io} - \Delta M_{ia} + C\cdot\alpha_o - P\cdot\theta\cdot L \qquad (141)$$

$$F = \frac{H}{\Delta M} \qquad (142)$$

and $$\omega = \sqrt{|\Delta M|/I} \tag{143}$$

in which $|\Delta M|$ = the absolute value of ΔM, then the deflection angle α and angular velocity, $\dot{\alpha}$, are found according to the following alternatives:

1. if $\Delta M < 0$ then the solutions are

$$\alpha = C_1 \sinh \omega t + C_2 \cosh \omega t + F \tag{144}$$

and $$\dot{\alpha} = C_1 \omega \cosh \omega t + C_2 \omega \sinh \omega t \tag{145}$$

2. if $\Delta M > 0$ then the solution of Eq. (139) leads to

$$\alpha = C_1 \sin \omega t + C_2 \cos \omega t + F \tag{146}$$

and $$\dot{\alpha} = C_1 \omega \cos \omega t - C_2 \omega \sin \omega t \tag{147}$$

The constants, C_1 and C_2, in the above equations are found from the initial condition at time, $t = 0$, at the beginning of the computation cycle:

$$C_1 = \frac{\dot{\alpha}_o}{\omega} \tag{148}$$

and $$C_2 = \alpha_o - F \tag{149}$$

3. if $\Delta M = 0$, then Eq. (139) leads to the solutions

$$\alpha = \frac{H}{2I} t^2 + \dot{\alpha}_o \cdot t + \alpha_o \tag{150}$$

$$\alpha' = \frac{H}{I} t + \alpha'_o \tag{151}$$

Computationally a simple criterium for the occurrence of motion reversal during each computation cycle is available according to the following relationship:

$$\alpha'_o \cdot \alpha' \leq 0 \tag{152}$$

in which α'_o, α' = the angular velocity at the beginning respective at the end of the computation cycle.

Eq. (152) expresses the fact that if the angular velocity at the beginning and at the end of the interval under consideration is of opposite sign, or if their product is equal to zero, then this indicates the occurrence of motion reversal during that computation cycle.

Eq. (152), although useful as a criterium for possible oscillations simultaneous with loading, is of limited use for determining the maximum column load under the influence of a constant axial load. This is due to the fact that Eq. (152) conveys no information about when the motion reversal cannot occur. Thus, using Eq. (152) in a computer program at a situation where no motion reversal is physically possible, one would have to wait before the lateral deflection and velocity of the column grow beyond the computer capacity, hence resulting in numerical overflow. We may, however, avoid this problem by establishing motion reversal criteria based on the dynamic state of the column in general. This may also serve as illustration of the general concepts proposed in Secs. 7.5 and 7.6.

To begin with, it should be observed that the notation, ΔM, defined by Eq. (140) expresses the difference between the internal and the external moments for a unit rotation, $\alpha = 1$, of the fixed end cross section of the column shown in Fig. 12. This is due to the fact that for a unit rotation of the given cross-section, the term, C, defined according to Eq. (101) represents the laterally induced internal moment and the remaining terms in Eq. (140) express the external moment. Thus, depending on the variable, ΔM, the following alternatives exist for the occurrence of motion reversal:

1. If $\Delta M > 0$, the angular velocity of the column is obtained from Eq. (147). Setting $\dot{\alpha}$ equal to zero in Eq. (147) and assuming that the variable terms appearing in that equation remain constant between now and a possible motion reversal position, then the motion reversal time, or return time, t_r, is found as follows:

$$t_r = \frac{\pi}{2\omega} \tag{153}$$

If $C_1 = 0$, the solution would be either $t_r = 0$ or

$$t_r = \frac{\pi}{\omega} \tag{154}$$

The solution $t_r = 0$ is however trivial, whereas Eq. (154) expresses the time interval between two successive motion reversal positions, provided that the assumption of no change in the column variables remains valid throughout the motion.

When both C_1 and C_2 are different from zero, the solution depends on the sign of the ratio C_1/C_2. If C_1/C_2 is negative the solution is

$$t_r = \frac{\pi - \text{Arctan}\left(-\frac{C_1}{C_2}\right)}{\omega} \tag{155}$$

and when C_1/C_2 is positive, the solution is obtained by the following equation:

$$t_r = \frac{\text{Arctan}\left(\frac{C_1}{C_2}\right)}{\omega} \tag{156}$$

Substitution of the proper return time, t_r, into Eq. (146) yields the corresponding deflection angle which would specify the motion reversal position. It should be noted that in the case when $\Delta M > 0$, a solution for the motion reversal time, t_r, always exists according to one of the above solutions.

2. If $\Delta M < 0$, then the assumption that the column variables appearing in Eq. (145) remain unchanged between now and the possible return time, t_r, and setting the value of the angular velocity, $\dot{\alpha}$, in that equation equal to zero, results in the following motion reversal time, t_r:

$$t_r = \frac{\ln\left(\sqrt{\frac{C_2 - C_1}{C_2 + C_1}}\right)}{\omega} \tag{157}$$

Eq. (157) has a solution if and only if the expression $(C_2 - C_1)/(C_2 + C_1)$ is greater than unity.

3. If the surplus moment increment happens to be equal to zero, the corresponding solutions for t_r, using Eq. (151) is

$$t_r = \frac{-\dot{\alpha}_o \cdot I}{H} \tag{158}$$

A positive and finite solution in this last case exists only if $\dot{\alpha}_o$ and

H are of opposite sign and the value of H is different from zero.

It is remarkable to observe that when the surplus moment increment is equal to or less than zero, a motion reversal position is physically possible subjected to certain restrictions which impose conditions on the current dynamic state of the column. On the contrary, a motion reversal position is always unconditionally attainable when the surplus moment increment is greater than zero.

On the basis of the motion reversal criteria discussed in Sec. 7.5 and illustrated in this section, a general procedure for determination of the maximum column load is presented in Sec. 7.8.

7.8 Determination of Maximum Column Load

Suppose that upon loading a column, the axial load ceases to increase at a certain level, P_o, at which it is desired to determine whether the current axial load lies above, below or possibly just at the maximum column load. In order to resolve this problem, it is necessary to carefully follow subsequent motion of the column during buckling Phase 2 in a sufficient number of deflection intervals in the following way: During each small deflection interval, additional internal stresses are induced in the column, see Fig. 29 below.

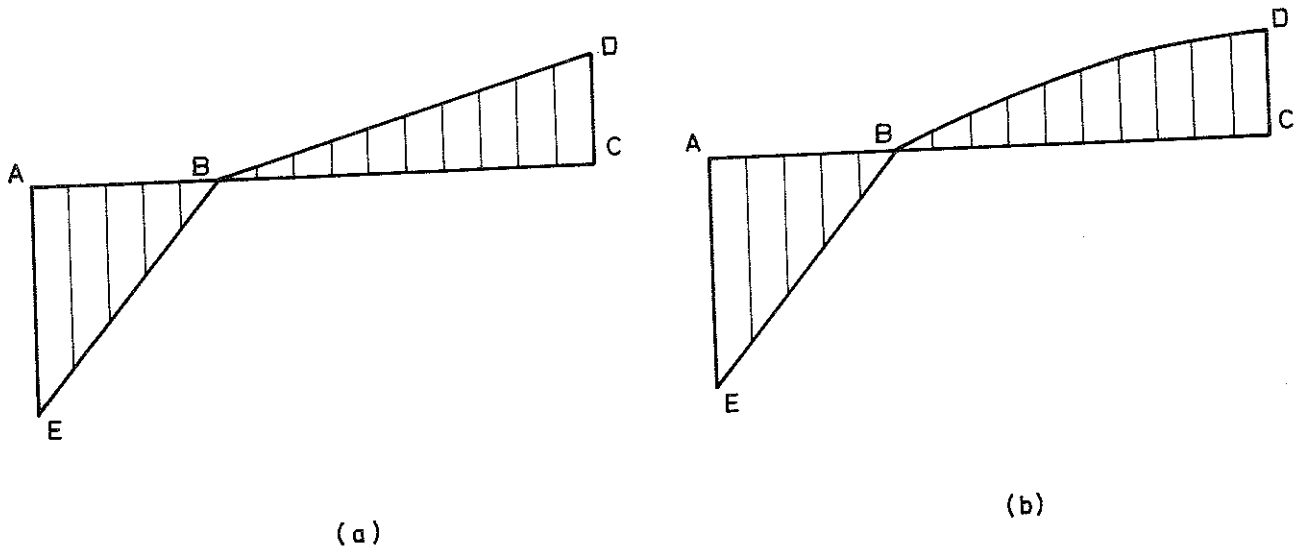

FIG. 29. INCREMENTAL PHASE 2 STRESS DISTRIBUTION OVER THE CROSS SECTION OF THE COLUMN SUBJECTED TO MAXIMUM STRAIN: (a) DUE TO A BILINEAR STRESS STRAIN DIAGRAM; (b) DUE TO AN ARBITRARY STRESS STRAIN DIAGRAM WITH CONTINUOUSLY DECREASING TANGENT MODULUS

Each such incremental stress distribution gives rise to an increment of internal moment, ΔM_i, with a corresponding increment of external

moment, ΔM_e, defined by the relation

$$\Delta M_e = P_o \cdot \Delta U \tag{159}$$

where ΔU represents the increment of lateral deflection. Then the surplus moment increment defined by Eq. (127) is determined during each deflection interval whereafter either of the following two alternatives may arise:

1. During all successive intervals of time, the value of the surplus moment increment, ΔM, remains positive all the way until the velocity in the direction of motion becomes zero, namely, the column attains a position of motion reversal, and thus the current axial load lies below the maximum level.

2. The value of ΔM in some deflection interval during buckling Phase 2 turns out to be nonpositive (zero or negative) before the velocity in the direction of motion tends to zero. This means that, depending on the shape of the stress strain diagram, Fig. 10, the future increments of lateral deflection would all produce nonpositive values of ΔM with either constant absolute value if Fig. 10(a) with the corresponding incremental stress distribution of Fig. 29(a) are applicable, or with increasing absolute values if Fig. 10(b) with the corresponding incremental stress distribution of Fig. 29(b) are valid. In either case, if the column does not attain a position of motion reversal, then the current value of the axial load either exceeds or is equal to the maximum column load. In this situation, it would be necessary to reduce the axial load by an increment, ΔP, that is to say, the column has to be loaded up to the level, $P_o - \Delta P$. The procedure just described is repeated. If the column at this new level, $P_o - \Delta P$, attains a position of motion reversal, then the previously

tested load level, P_o, is just equal to the maximum column load.

The procedure described above is pictorially illustrated in Fig. 30. The behaviour of an inelastic column during both buckling phases is examined for two consecutive constant axial load levels differing by an increment, ΔP.

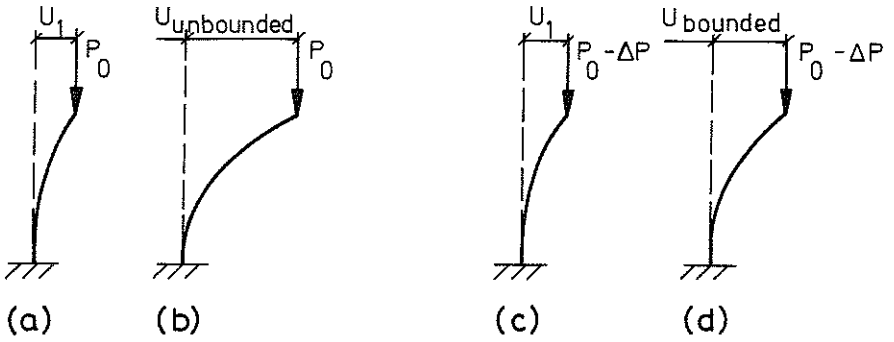

FIG. 30. TEST FOR ATTAINMENT OF THE MAXIMUM COLUMN LOAD: (a) AND (c) CONFIGURATIONS AT THE END OF BUCKLING PHASE 1; (b) AND (d) POSSIBLE BEHAVIOUR DURING BUCKLING PHASE 2

If the motion of the column during buckling Phase 2 turns out to be unbounded under the axial load, P_o, see Fig. 30(b), and bounded under the axial load, $P_o - \Delta P$, see Fig. 30(d), then the axial load, P_o, according to the definition given in Sec. 7.6, coincides with the maximum column load.

Fig. 30 illustrates the precise meaning of the maximum column load in the context of the present development of the column action described herein. Based on this concept, a computationally efficient way of determining the maximum column load would be to load the column up to an

axial load, P_o, which is surely considered to lie below the maximum level. All the pertinent information about the dynamic state of the column is now stored and subsequent behaviour of the column during buckling Phase 2 is investigated. If the column attains a motion reversal position, then the previously stored information about the state of the column at the load, P_o, is recovered and the loading of the column is continued from the axial load, P_o up to a new constant load level, $P_o + \Delta P$. Again, the information about the dynamic state of the column at this new load level is stored and subsequent motion during buckling Phase 2 is studied until the criterium for motion reversal shows the existence or the lack of existence of a motion reversal position.

If during the second trial described above, a motion reversal position during buckling Phase 2 is not found, then the current axial load coincides with the maximum load. However, if a motion reversal position is found, then the previously stored states of the column at the end of buckling Phase 1 under the axial load, $P_o + \Delta P$, is restored, and the axial load is increased, starting from $P_o + \Delta P$ level and up to a new level, etc. The procedure described is continued until at some axial load, no motion reversal position is found for the column during buckling Phase 2. The axial load corresponding to that situation would be equal to the maximum column load.

If the column does not attain a motion reversal position during buckling Phase 2 in the first trial described above, then the current axial load, P_o, may exceed the maximum column load. In that situation, a lower P_o-value must be tried, starting all over again from zero load level, since no information about the dynamic state of the column is

available for the axial load, $P_o - \Delta P$. This explains why it is computationally time saving if the first trial P_o-level lies reasonably below the maximum load.

It should be observed that the technique described above is only actual if the shape of the stress strain diagram is of the type shown in Fig. 10(b). Otherwise, if the stress strain diagram happens to be bilinear, Fig. 10(a), the parameter variations have no effect on the magnitude of the maximum column load. This could be proved in the following way:

When the tangent modulus remains constant throughout buckling Phase 2, then the value of the surplus moment increment, ΔM, remains unchanged during all subsequent equal deflection intervals, ΔU. This is due to the fact that the value of the laterally induced internal moment increment, ΔM_{ib}, is constant, see Fig. 29(a). Furthermore, since the axial load is constant and equal deflection increments, ΔU, is assumed, then the value of ΔM_e, according to Eq. (159) is constant, hence according to Eq. (129), the value of ΔM_2 also remains unchanged, from one interval to another. However, it should be recalled that if the tangent modulus remains constant in the inelastic range, the following two properties are valid at the constant axial load equal to the reduced modulus load:

1. The surplus moment increment is equal to zero; and
2. equality between internal and external moments is maintained for all possible lateral deflections.

The first property above follows from the fact that the reduced

modulus load is originally obtained by the equality between internal and external moments if the initially centrally loaded column is infinitesimally deflected. In other words, during the infinitesimal increment of lateral deflection from the straight to the bent position, the value of ΔM_2 from Eq. (129) must be equal to zero. However, since according to the above analysis, the value of ΔM_2 remains constant from one deflection interval to another, this constant value must necessarily remain equal to zero during all possible deflection intervals, since its value during the first deflection interval from the straight to the bent position is equal to zero.

The second property follows as a consequence of the first property due to the fact that if the internal and external moments are equal during the first deflection interval from the straight to the bent position, and if the surplus moment increment is zero during all subsequent defelction intervals, then the internal and external moments must necessarily be equal for all possible lateral deflections.

As an extension of the above argument, it follows that if the axial load is kept constant above the reduced modulus load, the surplus moment increment according to Eq. (129) must necessarily be negative for all possible lateral deflection increments; furthermore, the external moment defined according to Eq. 138(b) must exceed the corresponding internal moment, M_i, for all possible lateral deflections, in which case, the value of TIMS according to Eq. (138a) would also be negative for any assumed lateral deflection.

Since the value of SMI and TIMS according to the above analysis

are both negative for loads above the reduced modulus load, it follows from the analysis of Sec. 7.5 that no motion reversal position would be attained in the course of lateral deflection during buckling Phase 2.

The above discussion leads to the conclusion that the reduced modulus load can always be considered as the maximum load for a column with bilinear stress strain diagram, in which case the possibility of negative surplus moment in stability considerations of the problem is eliminated.

Thus, in the following analysis, it is assumed that the stress strain diagram is of the type shown in Fig. 10(b), in which case the effect of parameter variations may turn out to be significant. However, the functional dependence of maximum column load on variations of dynamic parameters is an extremely involved problem, since the influence of changes in one column parameter depends on the current values of all other parameters involved. In order to analytically penetrate into this fascinatingly complex research area, the general factors affecting the value of the maximum column load for a given stress strain diagram have to be disclosed. In the process of enumerating all possible factors, two general causes may be singled out as the most significant factors influencing the value of the maximum load, i.e. the dynamic state of the column at the end of Phase 1 and the shape of the stress strain diagram applicable to subsequent deformation of the column during buckling Phase 2.

Before exploring the properties of maximum column load in Chapter 9, the simple model shown in Fig. 12 is analyzed in Chapter 8, assuming an arbitrary stress strain diagram and taking into consideration column

imperfection right from zero load level. The analysis of Model 3 in Chapter 8 is intended to provide numerical illustration for the significant arguments to be put forth in Chapters 9 and 10.

8. ANALYSIS OF MODEL 3

Abstract

This model makes a complete quantitative analysis of the general buckling phenomena explored herein. The simple column of Models 1 and 2 is preserved; however, the column is assumed to be initially imperfect with disturbances introduced right from zero loading level. The allowable disturbances comprise excentricity, initial deflection and velocity disturbance applied at any time during the loading process. A velocity disturbance may also be imparted to the column at the beginning of buckling Phase 2. Furthermore, an additional disturbance in the form of changes in the original direction of the axial load may be assumed simultaneous with loading, in which case the axial load is either brought to its original direction before it maintains a constant value, or the axial load continues to change direction simultaneously with bending during buckling Phase 2. There is no restriction on the shape of the stress strain diagram which may have any arbitrary form; however, for practical purposes a general stress strain diagram with a continuously falling or a piecewise constant tangent modulus is assumed. The stress strain curve is approximated by a multilinear diagram. The effect of the gravitational force may also be taken into account. Two computer programs are developed both of which treat buckling Phase 1 on the basis of the multi-cycle computation technique described in Appendix C; however, the two programs (Programs 7 and 8 of Appendix D) differ in the treatment of buckling Phase 2. While Program 7 essentially deals with buckling Phase 2 in the same manner as buckling Phase 1 with zero loading rate, Program 8 analytically deter-

mines the dynamic state of the column at stress levels where the tangent moduli may change on the multilinear stress strain diagram. Program 8 is computationally more efficient; however, it cannot take into consideration the effect of possible disturbances introduced at arbitrary instants of time during buckling Phase 2 such as changes in the direction of the axial load simultaneous with bending in the process of buckling Phase 2. Program 7 is computationally more time consuming, but it can cope with all possible disturbances during both buckling phases. Each program is capable of checking the results of the other one. This is shown to be specially valuable since the structurally simpler program (Program 7) designed for dealing with particular situations can verify the results of the considerably more complicated program (Program 8) designed for achieving greater computational efficiency. The dependence of maximum column load on the variations of dynamic parameters as well as all the other significant buckling phenomena disclosed herein are numerically verified by the analysis of this model.

8.1 Description of the Model and Identification of State Equations

The simple column shown in Fig. 12 is assumed to be initially imperfect, subjected to an excentricity in the application of the axial load, X_o, an initial deflection, U_o, initial velocity disturbance, V_o, a velocity disturbance, V_1, applied at any arbitrary load, P_d, a velocity disturbance, V_2, imparted at the start of buckling Phase 2, and a deviation angle, θ, of the axial load from its original direction, which may either assume zero value before the end of Phase 1, or continue to grow during Phase 2. These disturbances are treated as parameter variables some or all of which may assume zero values in a particular situation. The time dependent axial loading is assumed to start from zero load level. The effect of gravitational force may optionally be taken into consideration. The model is capable of handling a loading rate which may be an arbitrary function of time, however, for the sake of simplicity, a constant loading rate is assumed in each numerical simulation which may, of course, vary from one case to the other. The chosen stress strain diagram used in the calculations has a continuously decreasing or piecewise constant tangent modulus as the stress level increases. However, the model can deal with a stress strain diagram of any arbitrary shape in which the tangent modulus may even be a piecewise increasing function of time.

The objective of the present analysis is finding out, for various parameter combinations, the value of the maximum column load and determining the special properties of the dynamically stable states for loads below the maximum level. The problem is treated on the basis of the approximate multi-cycle computation technique described in Appendix C. Thus, with the known initial state of the column at zero load, the system vector defined by Eq. (93) is determined at the end of an

arbitrarily chosen short interval of time. The system vector thus obtained is considered as the initial vector for the second interval; the calculated system vector at the end of the second interval is taken to be the initial vector at the beginning of the third interval, etc. The calculations are performed with a time interval, $\Delta t = 0.01$ seconds, which is of an order of magnitude that yielded reliable results in Model 1 as compared with the exact numerical solution. The choice of time step, Δt, will additionally be discussed and illustrated in connection with the numerical results of this model.

The equation of motion of the column is already given by Eq. (139) in Sec. 7.7. Depending on whether the surplus moment increment defined by Eq. (140) assumes negative, or positive, or zero value, the corresponding solutions for the deflection angle, α, and the angular velocity, $\dot{\alpha}$, are obtained by either of the following three pairs of equations: Eqs. (144) and (145) for ΔM smaller than zero, or Eqs. (146) and (147) for ΔM greater than zero, or Eqs. (150) and (151) for ΔM equal to zero. The various alternative solutions of Eq. (139) and the method of calculating internal moment is shown in Fig. 31. All the variables in this flow diagram are already defined, in Sec. 7.7 and Sec. 6.2.

From the general treatment of the problem in Appendix C, it follows that the stress strain and internal moment states of Model 2, presented in Sec. 6.2, are equally applicable to the present model, nevertheless, the arbitrary shape of the stress strain diagram in the current analysis makes it necessary to develop a procedure for assigning new values of deformation moduli as the stresses in the column elements change during both buckling phases. This task is accomplished in the following section.

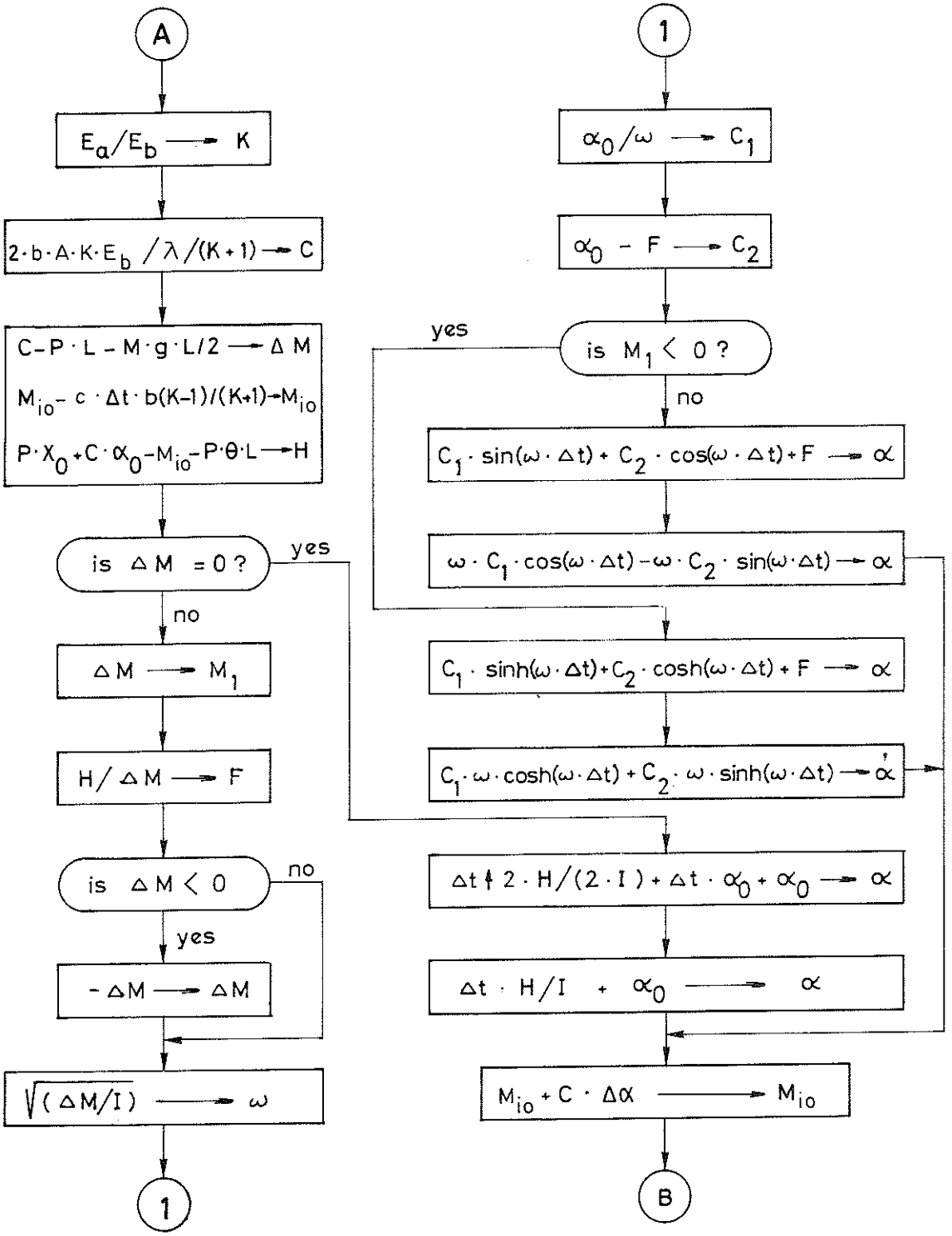

FIG. 31. CALCULATION OF DEFLECTION ANGLE, ANGULAR VELOCITY AND INTERNAL MOMENT IN THE COURSE OF ONE CYCLE

8.2 Assignment of Stress Levels and Deformation Moduli on the Stress Strain Diagram

In order to determine the proper value of the deformation modulus corresponding to each column element at each time interval during the motion of the column, the current stress at each element must be determined at the end of the interval. The value of this stress is then compared with the corresponding value on the actual stress strain diagram in order to pick the appropriate value of the deformation modulus to be applied to the element in question during the next time interval. During each computation cycle lasting the chosen time interval, Δt, the value of the deformation modulus corresponding to each column element is assumed to remain constant.

For the current model, both elements may undergo tensile stresses with the following restriction: Although the tensile stress in both elements may increase beyond the proportionality limit[1], no subsequent strain reversal is supposed to take place in the inelastic range in tension. By allowing tension in the material, subsequent to compression, the proportionality limit of the material is lowered (Bauschinger effect). Although this phenomenon could easily be incorporated in the computer program for the analysis of the current model, Bauschinger effect is neglected because of the infrequency of tensile stresses in the column elements and due to the fact that no precise material data is available regarding the Bauschinger effect. Thus, if tensile stresses occur in column elements after complete unloading, the original stress strain diagram is assumed to be valid in tension as well as it is applicable in compression.

This assignment of deformation moduli to column elements is accomplished

1. For evaluation of numerical results, see Sec. 8.7.

according to the following procedure: The stress strain diagram is divided into a convenient number of consecutive limiting stress levels as shown in Fig. 32.

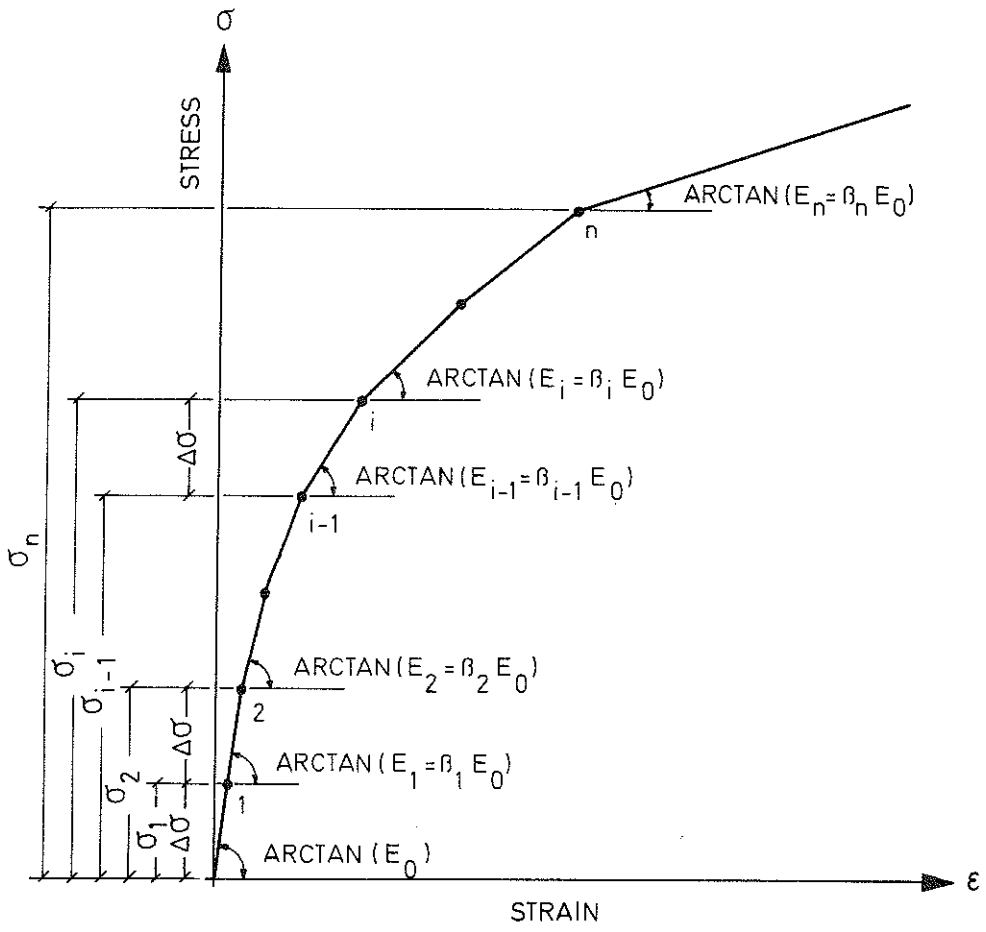

FIG. 32. REPRESENTATION OF A GENERAL STRESS STRAIN DIAGRAM CORRESPONDING TO MODEL 3 BY A MULTILINEAR CURVE

Each consecutive limiting stress level, which may also be referenced herein as limiting stress level, or simply abbreviated as LSL, defines a stress level in Fig. 32, uniquely determined by the intersection of two short line segments which approximately represent the tangent lines to the stress strain diagram at two consecutive stress intervals. The stress axis in Fig. 32 is divided into N equal stress

increments, $\Delta\sigma$, in such a way that each arbitrary LSL consists of i times the constant stress increment $\Delta\sigma$ (i = an integer):

$$\sigma_i = i\ \Delta\sigma \tag{160}$$

For determination of the state variables E_a and E_b which are included in the system vector in Eq. (93), the current stresses σ_a and σ_b are first calculated from Eqs. (95) and (96) respectively. These stresses are then compared with Eq. (160) for the current value of the integer, i. If the absolute value of the stress in an element just exceeds or is equal to the value from Eq. (160), then the deformation modulus, E_i, is applied to the element under consideration and the corresponding integer, i, is incremented by 1.

The procedure just described is shown in Fig. 33. The symbols A_1, A_2, A_3 and B_o in this flow diagram are integer variables, which are substitutes for integer variable, i, in Eq. (160), corresponding to positive values of σ_a, σ_b and negative values of σ_a and σ_b respectively. The integer variable, N, in Fig. 33 is the maximum number of limiting stress levels beyond which the tangent modulus remains constant. The one dimensional array, A(...), indicated in Fig. 33, corresponds to the entire set of actual β-values, principally defined in Fig. 32.

With all the fundamental background acquired so far, we now develop two computer programs for the twofold purpose of finding maximum column load and determining the dynamically stable behaviour of the column for axial loads below the maximum level.

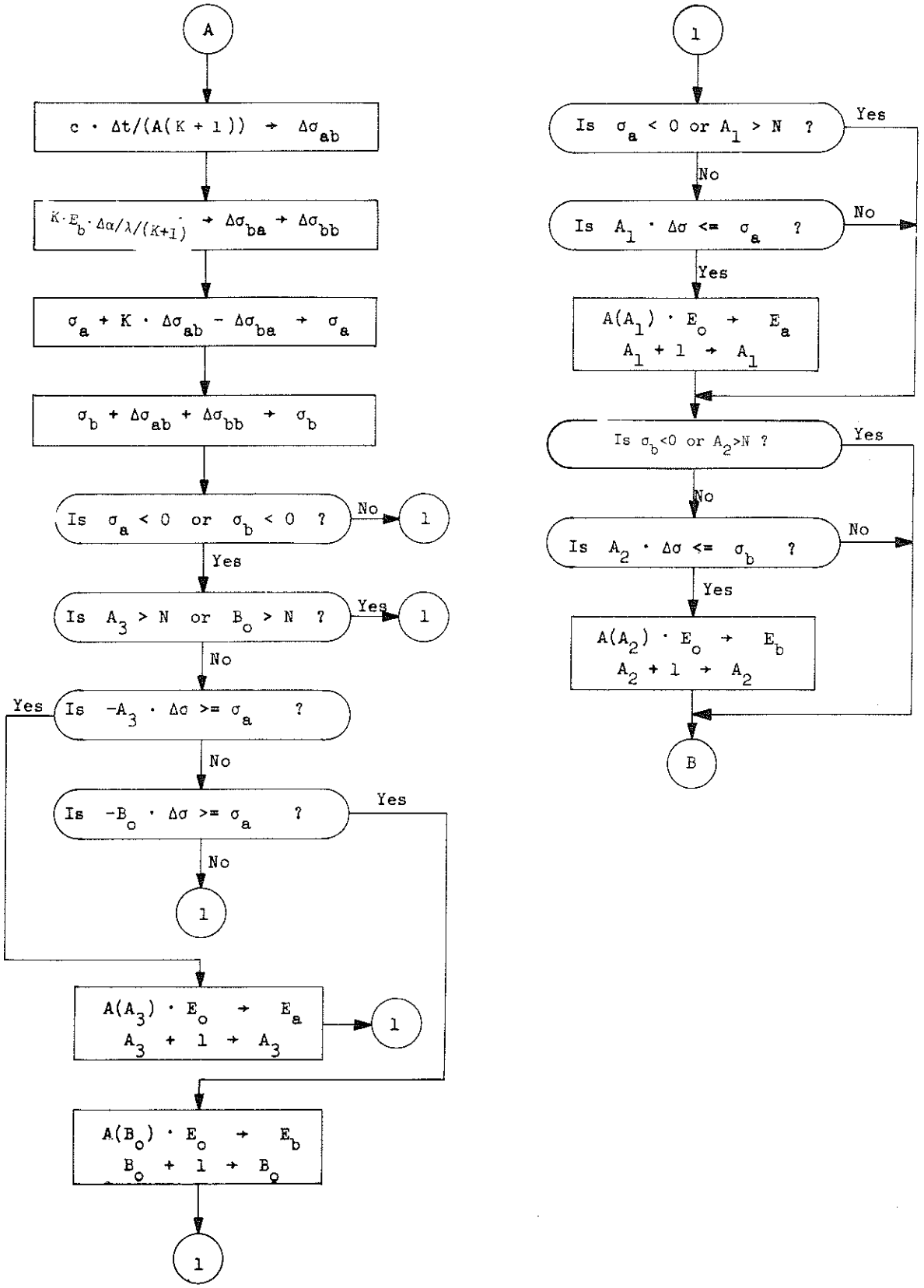

FIG. 33. DETERMINATION OF STRESS LEVELS AND ASSIGNMENT OF CORRESPONDING TANGENT MODULI ON THE STRESS STRAIN DIAGRAM.

8.3 Multi-Cycle Search Method

In the devlopment of the ideas of this paper, the concept Multi-Cycle Search method was originally conceived as a way of finding the maximum column load and determining dynamically stable lateral configurations of the column for axial loads below the maximum level. The name Multi-Cycle Search method is intended to imply the many calculation cycles required during each trial for determination of the maximum column load. The search for maximum load according to this procedure can be described as follows:

The axial load is allowed to increase up to a level P_o, which is believed to lie in the neighbourhood and below the maximum column load. This is accomplished by successively increasing the axial load up to the desired level during an appropriate number of time intervals, Δt. The system vector defined by Eq. (93) is repeatedly recalculated during each time interval so that the state space variables are fully determined when the axial load reaches P_o-level(end of buckling Phase 1). At this instant of time, the axial load is kept constant and the current values of state space variables are stored. The motion of the colum during buckling Phase 2 is followed by simply setting the value of the loading rate equal to zero. By doing this, the state equations used during buckling Phase 1 may equally be utilized during buckling Phase 2.

When the calculation cycle is repeated with zero loading rate, the assignment of appropriate deformation moduli is accomplished by the procedure shown in Fig. 19. This flow diagram which is used in both buckling phases, takes care of buckling Phase 2 by simply escaping the lines which calculate the variables saf and sbb described in

Section 6.3 . The values of these two variables are undefined during buckling Phase 2.

Since the axial load during buckling Phase 2 maintains a constant value, no approximation would be involved in the choice of the time interval, Δt, as long as deflection and velocity equations are concerned. Thus, in order to quickly decide whether the column attains a position of motion reversal, one may be tempted to increase the time step, Δt, during Phase 2. This however, may give rise to serious errors for the following reason:

When the column is moving towards a position of possible motion reversal during buckling Phase 2, the stresses at the elements on the front side are continuously increasing. For, the present simple model, this implies that the stress in either of the two elements a or b is increasing simultaneously as the motion proceeds. Now, if the time step, Δt, is chosen too large, the stresses in column elements during one calculation cycle may rise too high. Consequently, some actual tangent moduli may be wrongly assigned in the process. Since, the surplus moment increment is constant during one calculation cycle, by using a large time step, we may be unrealistically assuming too large bending rigidity throughout that cycle. Thus, because of the possibility of disregarding actually smaller tangent moduli, the column may apparently reach a position of motion reversal, whereas in reality no such position could have been attained if time intervals were chosen sufficiently short.

Thus, the time interval, Δt, which was considered appropriate for Phase 1, would be kept unchanged during buckling Phase 2. This process,

however, may involve performing many calculation cycles before attaining a possible position of motion reversal. This is how the name Multi-Cycle Search method was originally born. Now, the number of motion reversal positions required, to assure that the current axial load, P_o, lies below the maximum load, depends on the current direction of motion, see Fig. 34.

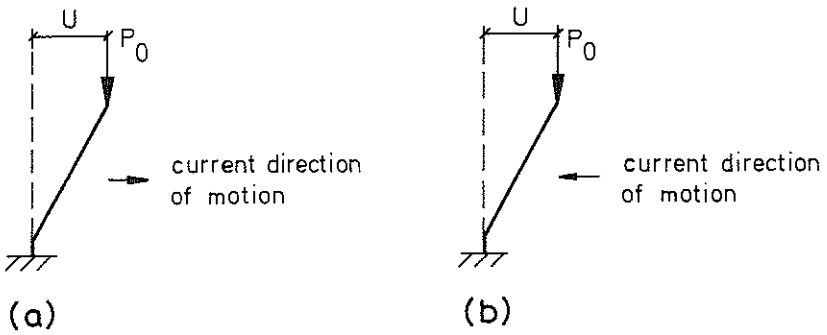

FIG. 34. TWO ALTERNATIVE MOTION STATES OF THE SIMPLE COLUMN AT THE BEGINNING OF BUCKLING PHASE 2

If the motion of the column is currently increasing the existing deflection of the column - which would most likely be the case - the attainment of one motion reversal position is sufficient, see Fig. 34(a). However, if the motion of the column happens to be currently decreasing the existing deflection of the column, see Fig. 34(b), two motion reversal positions must be tried.

In order to continue the search for maximum load, the axial load is updated and the state space variables stored at the end of buckling Phase 1 are restored. At the end of the next Phase 1, the search for P_{max} continues again as described above. The procedure is repeated until P_{max} is attained.

It should be noted that if no position of motion reversal is attained during the first trial, the axial load either lies above or is equal to the maximum load . Thus, it is important that the first trial value safely lies below the maximum level. Although a low, first trial value of P_o may cost computer time, additional costs would be incurred if it happens to lie above the maximum load.

For finding equilibrium configurations for axial loads below the maximum level, the column load is first increased up to the desired level, P_o, whereafter the loading rate is set equal to zero and subsequent motion of the column during buckling Phase 2 is followed up to the third motion reversal position, see Sec. 6.5. If lateral stable configurations for several load levels are desired, the state space variables at the end of buckling Phase 1 corresponding to each load level are stored before proceeding to buckling Phase 2. After determining the lateral configurations in the manner described above, the state space variables are restored and the column load is then increased up to the new desired load level, whereafter the above procedure is repeated during the next Phase 2.

An outline of Multi-Cycle Search method is shown in Fig. 35 which sequentially follows the procedure just described. If upon entering the program the parameter, J, is set equal to 1, the program follows the procedure for finding P_{max}. If otherwise, J = 0, the steps mentioned above for determination of stable lateral positions are carried out. An integer variable, N, is set equal to 1 upon entering Phase 1 for the first time. Integer N is incremented by 1 at Label 4, that is to say, each time the column reaches a motion reversal position during the process of finding lateral stable positions. If the trial for P_{max}

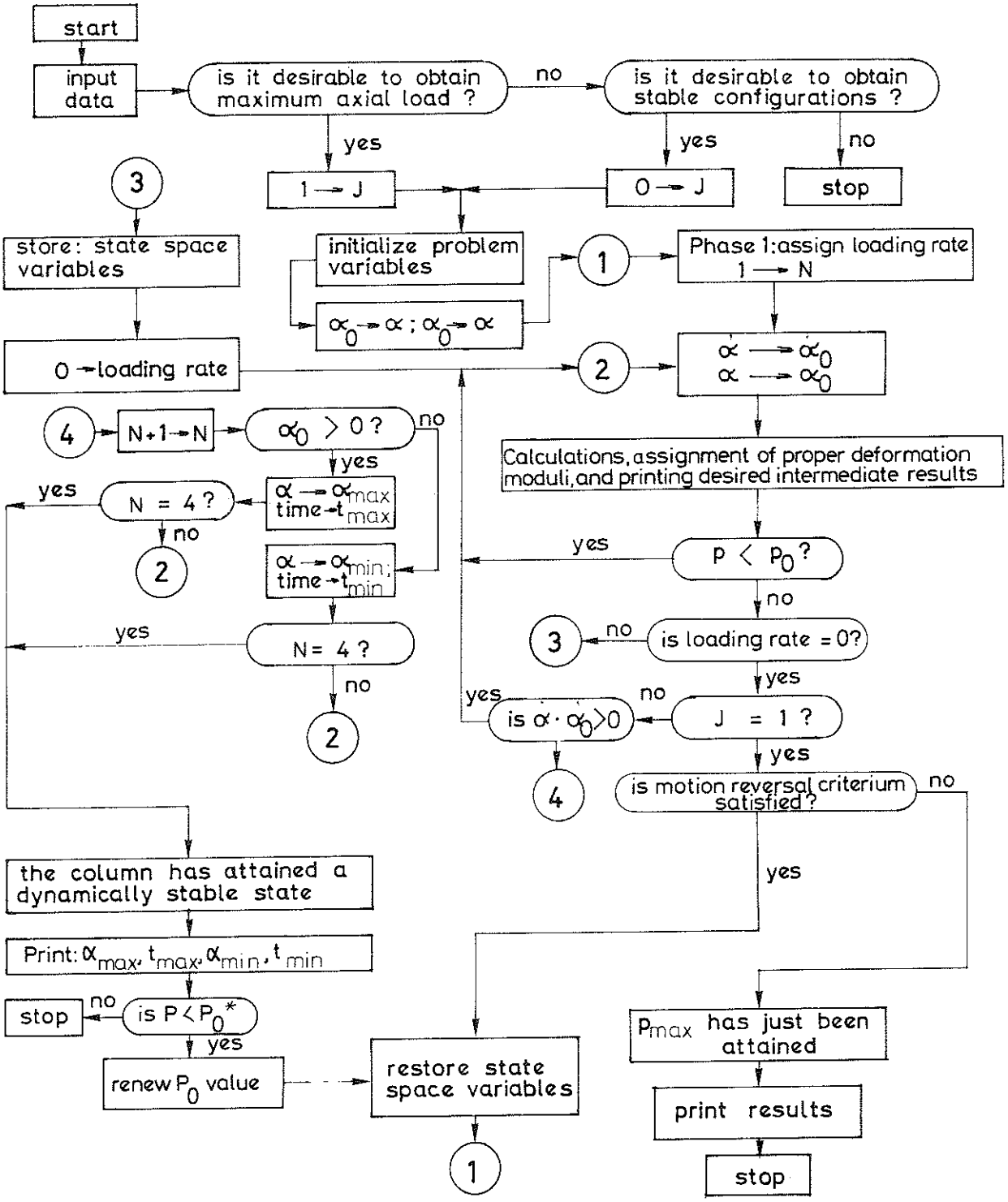

FIG. 35. PROCESS OF FINDING MAXIMUM AXIAL LOAD AND STABLE LATERAL CONFIGURATIONS ACCORDING TO MULTI-CYCLE SEARCH METHOD

fails or if the lateral stable positions for new load level are desired, the state space variables are restored and control is transferred to Label 1 where the integer variable N is set equal to 1 again.

Multi-Cycle Search method, is particularly efficient for the second objective of the program, i.e., finding stable lateral positions. This is due to the fact that for this purpose, the program requires no trials, besides, because of maintaining a sufficiently short time step, Δt, throughout the calculations, necessary information about the state of the column may be printed out whenever desired during Phase 2 as well as during Phase 1. However, the first objective of the program, i.e., finding maximum load, may take too long computer time, particularly if the first trial axial load happens to lie considerably below the maximum level. Thus, our present aim is to find a method of increasing the time step, Δt, without committing the possible errors mentioned in the above discussion. This task is accomplished by the concept of Single-Cycle Search method developed in the next section. Nevertheless, it should be noted that if disturbances such as changes in the direction of the axial load or velocity disturbances are introduced simultaneous with bending during buckling Phase 2, then the Multi-Cycle Search method described in this section is the only alternative which can cope with these particular situations. Thus, Program 7 of Appendix D, which is based on the concept of Multi-Cycle Search method developed herein, can treat the problem of a nonconservative axial load during buckling Phase 2. Even the possible occurrence of a velocity disturbance at the beginning of Phase 2 is included in Program 7.

8.4 Single-Cycle Search Method

In the course of actual computer testing of the Multi-Cycle Search method developed in the previous section, it was found out that the process of determining maximum column load according to that program is too time consuming to be accepted as the basis for future extensions to more conventional column models. Thus, an effort was made to develop a program which could increase the time step, Δt, during Phase 2 without wrongly assigning the actual values of the tangent moduli. In the course of accomplishing this objective, a number of complicated problems were successively faced which took considerable time to resolve. The concept of Single-Cycle Search method has consequently evolved to meet our present objective. The main concept may be explained as follows.

As far as buckling Phase 1 is concerned, there is no difference between the approach to be described now and the Multi-Cycle Search method explained in the previous section. Differences arise as soon as the axial load reaches the first trial level, P_o. For the present approach the following course of action is successively followed: At the beginning of buckling Phase 2 the state space variables are stored and, the direction of motion of the column is observed. With respect to the direction of motion, the element on the back side is assigned the value of the unloading modulus, E_o. On the front side, the strain is currently increasing. The action to be taken now depends on whether or not the element with increasing strain is currently moving on an unloading line. Thus one of the following two actions is taken depending on which alternative is true:

a. If the element on the front side is currently deforming on an unloading line, it would be then necessary to determine whether the column first attains a position of motion reversal, or whether the element on the front side would first attain a sufficiently high stress level to begin to deform on the original stress strain diagram. If the former event occurs, the position of motion reversal is calculated, but if the second event occurs, the problem would be similar to the case treated in the following alternative:

b. If the element on the forward side is currently deforming on the original stress strain diagram, or if it is moving on an unloading line but motion reversal does not occur before the stress in the element reaches the original stress strain diagram, then the angle, α_c, and the time, t_c, corresponding to the next LSL (consecutive limiting stress level) in element j on the front side (either element a or b), are calculated. If element j is currently deforming on an unloading line, the next LSL is the state variable, σ_{js}, and the next tangent modulus to be assigned is the state variable, E_{js}. However, if the element is currently deforming on the original stress strain diagram between stress levels, σ_{i-1} and σ_i, see Fig. 32, then the next LSL is σ_i and the next tangent modulus to be assigned is E_i.

If in the above alternative, element j on the front side is currently deforming on the original stress strain diagram, the calculated critical time, t_c, corresponding to the next LSL, must be compared with the <u>return time</u>, t_r, corresponding to the next motion reversal. If t_r happens to be smaller than or equal to t_c, the position of motion reversal is determined as described below. However, if t_r is found to be greater than t_c, the new state of the column, whose front side element, j, is currently deforming between the stress levels, σ_{i-1}

and σ_i, would be determined such that the following relations hold:

$$\alpha = \alpha_c \tag{161}$$

$$\sigma_j = \sigma_i \tag{162}$$

and

$$E_j = E_i \tag{163}$$

in which α_c = the deflection angle defined as above; index j corresponds to the element on the front side which for the present model may be either element a or b; and the index i corresponds to the LSL lying immediately above element j's current stress on the stress strain diagram, before the new state of the column defined by Eqs. (161) - (163) is established.

The surplus moment increment, ΔM, corresponding to the new state of the column is now determined. If ΔM happens to be smaller than or equal to zero and the corresponding motion reversal criterium, derived in Sec. 7.7, is not satisfied, then the current axial load lies above or is equal to the maximum column load. However, if ΔM is found to be positive, the current limiting stress level, σ_i, is moved to the next higher limiting stress level, σ_{i+1}, and the whole process described in alternative b above up to the present point is repeated. Thus a loop is established which successively finds new states of the column corresponding to new limiting stress levels.

A jump out of the above loop occurs if one of the following three events takes place during a certain execution of the loop:

1. The surplus moment increment may turn out to be negative or equal to zero and the corresponding motion reversal criterium violated, in which case, the current axial load is either greater or equal to the maximum load; consequently the computations are terminated;

2. t_r may happen to be less than or equal to t_c as described above in which case the loop is terminated and the motion reversal position is determined; and

3. the next limiting stress level may lie above the last limiting stress level, σ_n, see Fig. 32, in which case the loop is again terminated and the next motion reversal position is determined as described below.

If the stress level, σ_c, corresponding to the next LSL in either of the two alternatives a or b above, corresponds to a time, t_c, which is greater than the return time, t_r, corresponding to the next motion reversal, then the state of the column corresponding to the next motion reversal position is determined as described in Sec. 7.7.

The number of motion reversal positions required, to assure that the current axial load lies below the maximum load, depends on the current direction of motion, see Fig. 34. If the motion of the column is currently increasing the existing column deflection, see Fig. 34(a), then one motion reversal position, and otherwise, see Fig. 34(b), two motion reversal positions must be tried.

If the current axial load is found to lie below the maximum level, then the axial load is increased by an amount, ΔP, the state space variables are restored, and the new system vector at the end of the new buckling Phase 1 is found and stored, whereafter the whole procedure described above is repeated. The computations would continue in the manner described until the maximum column load is found.

For determination of equilibrium configurations below the maximum level, the behaviour of the column up to three successive motion reversal positions is found, in the manner described in Sec. 6.5. For the purpose of determining equilibrium positions below the maximum level, we may desire to receive information on the state of the column at any arbitrary time during Phase 2. This is not possible with Single-Cycle Search method, since the states of the column during buckling Phase 2 according to this approach are related to the limiting stress levels, as a consequence of which no information can be printed out during intermediate states of the column. Thus, for this purpose, the Multi-Cycle Search method is more flexible. However, if only the state of the column corresponding to the limiting stress level, or the motion reversal configurations is desired, this program is equally useful.

An outline of Single-Cycle Search method is presented in Fig. 36 which shows the most important branching points and the block structure of the program. At point A, the program either branches to Left Block (LB) or to Right Block (RB) depending on whether the column is currently moving in backward or in forward direction. These two blocks together perform the functions of alternative a above. At points B or C, the control is either transferred to Middle Block (MB) corresponding to alternative b above, or the program moves to Motion Reversal Block where the next motion reversal position is determined.

The Middle Block in Fig. 36, is terminated either when P_{max} is attained or if the control is transferred to Motion Reversal Block. At point D either the program branches back to Left Block or Right Block if more than one motion reversal position is desired, or it moves to point E whereafter either the trial for P_{max} is renewed, or if the

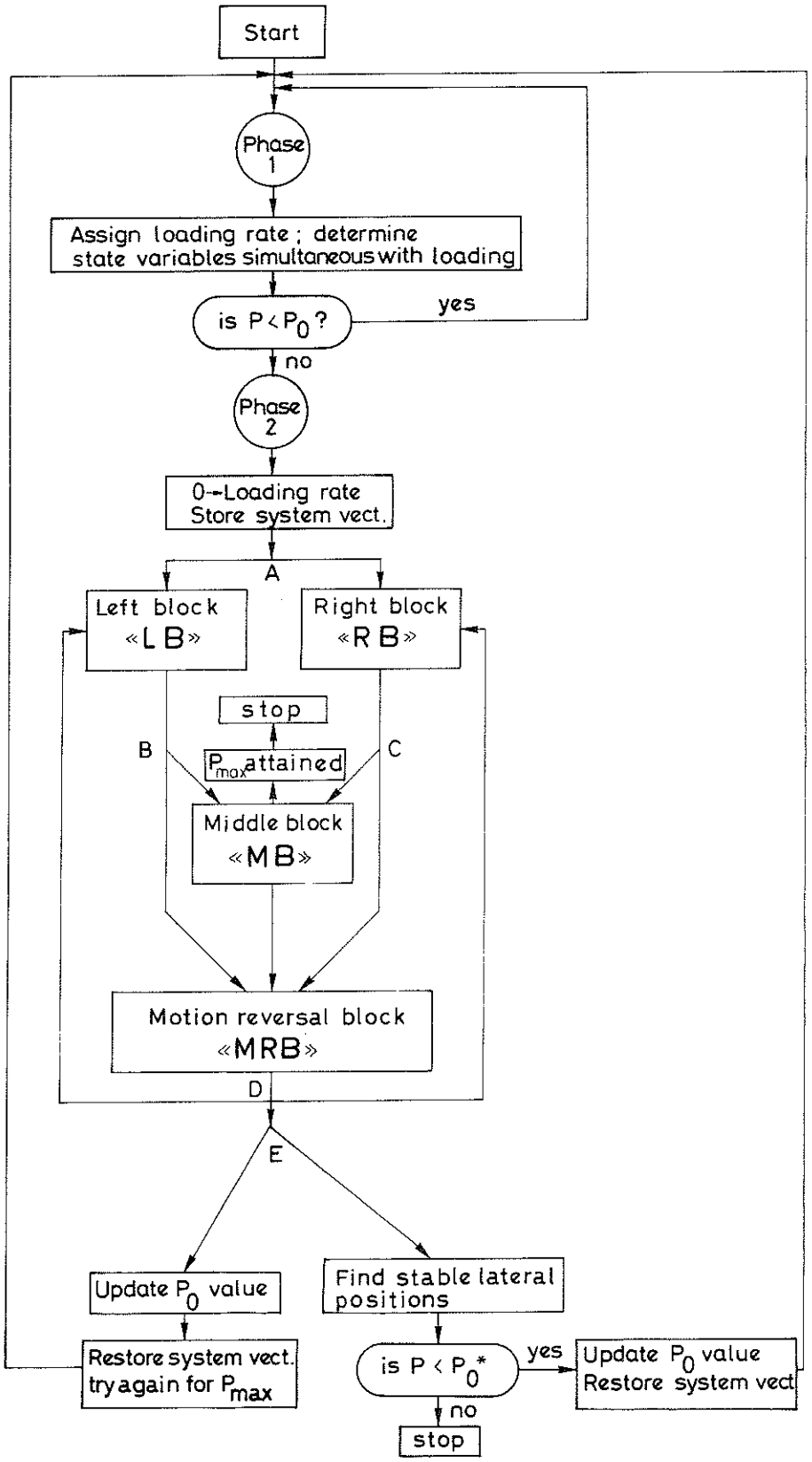

FIG. 36. OUTLINE OF SINGLE-CYCLE SEARCH METHOD

objective is to find equilibrium configurations, new desired load level is specified and the control is transferred to the buckling Phase 1.

It should be noted that so far, the general concept of Single-Cycle Search method has been presented in this section. The method of determining the time, t_c, corresponding to the next LSL and a description of the main program with its subroutines will be presented in the following sections.

8.5 Determination of Column State at Limiting Stress Levels

According to the discussion in Sec. 8.4, the variables α_c, t_c and σ_c denote the respective values of deflection angle, time and stress corresponding to the state of the column at a consecutive limiting stress level (LSL). For element j situated on the front side with respect to the direction of motion, the LSL was identified in Sec. 8.4 to be either the state variable, σ_{js}, if the element is currently deforming on an unloading line, or the limiting stress level, σ_i, if the column is currently deforming on the original stress strain diagram between stress levels, σ_{i-1} and σ_i, see Fig. 32. In either case, the two variables, σ_c and α_c may be defined by the equations

$$\alpha_c = \alpha + \Delta\alpha_c \tag{164}$$

and

$$\sigma_c = \sigma_j + \Delta\sigma_c \tag{165}$$

in which α = the current deflection angle; σ_j = the current value of stress at the element on the front side; $\Delta\alpha_c$ = the difference between the present deflection angle and the value corresponding to the next LSL; and $\Delta\sigma_c$ = the difference between the present stress in element j and the value corresponding to the next LSL.

The stresses in column elements during buckling Phase 2 change solely due to the bending effect, in which case Eq. (100) gives a certain stress increment due to a corresponding increment of lateral deflection. Thus, replacing $\Delta\alpha$ in Eq. (100) by $\Delta\alpha_c$ and $\Delta\sigma_{ba}$ by $\Delta\sigma_c$ and solving the resulting equation for $\Delta\alpha_c$ leads to

$$\Delta\alpha_c = \frac{\Delta\sigma_c \lambda (K + 1)}{KE_b} \tag{166}$$

The next problem to be resolved is how to find the time, t_c, corresponding to the deflection angle, α_c, once α_c is given by Eq. (164) in which $\Delta\alpha_c$ is determined from Eq. (166). The determination of t_c is found to be necessary for finding out the column state at various limiting stress levels.

Before attaining the maximum column load during buckling Phase 2, the surplus moment increment, ΔM, may be either positive, zero, or negative. Thus, the following three alternatives for determination of the state of the column at the next LSL must be examined:

1. Case $\Delta M > 0$. - Then setting α in Eq. (146) equal to α_c leads to the following equation for the determination of the corresponding time, t_c:

$$C_1 \sin \omega t_c + C_2 \cos \omega t_c = \alpha_c - F \tag{167}$$

If $C_1 = 0$, Eq. (167) would lead to the solution

$$t_c = \frac{2 \operatorname{Arctan} \left(\sqrt{\dfrac{C_2 - \alpha_c + F}{C_2 + \alpha_c - F}} \right)}{\omega} \tag{168}$$

When $C_2 + \alpha_c - F = 0$, Eq. (168) results in

$$t_c = \frac{\pi}{\omega} \tag{169}$$

If C_1 is different from zero, then by using the notations

$$\frac{C_2}{C_1} = C_3 \tag{170}$$

and

$$\frac{\alpha_c - F}{C_1} = D_3 \tag{171}$$

Eq. (167) could be expressed in the form

$$(C_3 + D_3) \tan^2 \frac{\omega t_c}{2} - 2 \tan \frac{\omega t_c}{2} - (C_3 - D_3) = 0 \tag{172}$$

If $C_3 + D_3 = 0$ and $D_3 > 0$, Eq. (172) gives

$$t_c = \frac{2 \text{ Arctan } (D_3)}{\omega} \tag{173}$$

If $C_3 + D_3 = 0$ and $D_3 \leq 0$, Eq. (172) results in

$$t_c = \frac{2\left[\pi - \text{Arctan}(-D_3)\right]}{\omega} \tag{174}$$

If the expression $C_3 + D_3$ is different from zero, Eq. (172) leads to the general solution

$$t_c = \frac{2 \text{ Arctan } \left(\frac{1}{C_3 + D_3} \pm \sqrt{\frac{1}{(C_3 + D_3)^2} + \frac{C_3 - D_3}{C_3 + D_3}} \right)}{\omega} \tag{175}$$

The proper sign in front of the square root in Eq. (175) can be determined according to the following three alternatives:

a. If $1/(C_3 + D_3) < 0$ and $(C_3 - D_3)/(C_3 + D_3) \leq 0$, the solution is

$$t_c = \frac{\left[2\P - 2 \text{ Arctan } \left(\frac{-1}{C_3 + D_3} - \sqrt{\frac{1}{(C_3 + D_3)^2} + \frac{C_3 - D_3}{C_3 + D_3}} \right)\right]}{\omega} \tag{176}$$

b. If $1/(C_3 + D_3) > 0$ and $(C_3 - D_3)/(C_3 + D_3) \leq 0$, the solution would be

$$t_c = \frac{2 \text{ Arctan } \left(\frac{1}{C_3 + D_3} - \sqrt{\frac{1}{(C_3 + D_3)^2} + \frac{C_3 - D_3}{C_3 + D_3}} \right)}{\omega} \tag{177}$$

c. In all other cases the solution is

$$t_c = \frac{2 \text{ Arctan } \left(\frac{1}{C_3 + D_3} + \sqrt{\frac{1}{(C_3 + D_3)^2} + \frac{C_3 - D_3}{C_3 + D_3}} \right)}{\omega} \tag{178}$$

2. Case $\Delta M = 0$. - If the surplus moment increment happens to be equal to zero, the corresponding solution for t_c, using Eq. (150) is

$$t_c = \left(R_3 \pm \sqrt{R_3^2 - R_4} \right) \cdot I \tag{179}$$

in which

$$R_3 = \frac{-\dot{\alpha}_o}{H} \tag{180}$$

and

$$R_4 = \frac{2(\alpha_o - \alpha_c)}{HI} \tag{181}$$

If $R_3^2 - R_4$ is smaller than zero or R_4 is greater than zero and R_3 is smaller than zero, then there is no positive solution for t_c. If R_4 and R_3 both are greater than zero then the minus sign and otherwise the plus sign in Eq. (179) holds.

3. Case $\Delta M < 0$. - The time, t_c, corresponding to the position of the column at the next LSL may be obtained by replacing α and t in Eq. (144) by the corresponding quantities, t_c and α_c:

$$C_1 \sinh \omega t_c + C_2 \cosh \omega t_c = \alpha_c - F \tag{182}$$

Using the notations

$$\alpha_c - F = R \tag{183}$$

$$\frac{R}{C_2 + C_1} = R_1 \tag{184}$$

and

$$\frac{C_2 - C_1}{C_2 + C_1} = R_2 \tag{185}$$

Eq. (182) leads to the following solution for t_c:

$$t_c = \frac{\ln\left(R_1 \pm \sqrt{R_1^2 - R_2}\right)}{\omega} \tag{186}$$

Since R_2 must be greater than unity for the existence of a motion reversal position, the following conditions must be satisfied for the existence of a meaningful solution for t_c[1]:

1. the expression $R_1^2 - R_2$ must be positive; and
2. the term R_1 must also be positive.

If, in addition, the expression $R_1 - \sqrt{R_1^2 - R_2}$ is greater than unity then the minus sign and otherwise the plus sign should be used in Eq. (186).

---

[1] A solution may exist for t_c even when R_2 is less than unity and perhaps less than zero; however, in that case, since no motion reversal position is possible, the solution is no longer useful.

8.6 Description of the Main Program Based on the Concept of Single-Cycle Search Method

The determination of the return time, t_r, in Sec. 7.7 and the time, t_c, corresponding to the next consecutive limiting stress level, in Sec. 8.5, comprise the main analytical tools for the construction of a program based on the concept of Single-Cycle Search method. The main ideas are described in Sec. 8.4 upon which a computer program is developed, see Program 8 in Appendix D. The entire flow diagram for the main program with its subroutines is included in Appendix E. However, the flow diagram for the main program, together with a short description of its subroutines is presented below in order to enhance the overall understanding of the general discussion in Sec. 8.4.

The program to be presented below consists of a main part together with 26 subroutines. The flow diagram of the main program is shown in Fig. 37. However, to begin with, the essential contents of the subroutines are shortly described below in order to understand their functions as they are encountered in the main program. The symbols used in the following description have already been defined and have occured at different places throughout this paper.

Subroutine 1: This subroutine calculates the variables, K, C, M_{io} at the beginning of the computation cycle, ΔM, H, F, ω, C_1 and C_2.

Subroutine 2: This subroutine determines the time, t_c, for positive values of the surplus moment increment, ΔM, according to the different alternatives explained in Sec. 8.5, whereafter it calls Subroutine 4.

Subroutine 3: For positive values of the surplus moment increment, this subroutine assigns deflection and velocity states of the column corresponding to a position where the column element on the front side of motion has exactly attained a stress equal to a limiting stress level on the stress strain diagram, whereafter Subroutine 6 is called.

Subroutine 4: This subroutine determines the return time, t_r, according to the various alternatives presented in Sec. 7.7 for positive values of surplus moment increment, ΔM. For negative or zero values of ΔM, the control is transferred to Subroutine 20 or 23 respectively.

Subroutine 5: This subroutine evaluates the deflection and velocity states of the column in the general case whenever, the surplus moment increment, ΔM, is positive. For negative or zero values of ΔM, the control is transferred to Subroutines 17 and 18, or, Subroutine 24 respectively.

Subroutine 6: This subroutine determines the internal moment and the stress state of the column at the end of the computation cycle and assigns the appropriate values of tangent moduli on the original stress strain diagram to the column elements.

Subroutine 7: This subroutine optionally takes into account the influence of a nonconservative axial load.

Subroutine 8: This subroutine prints the current values of the 8 variables: Load, end deflection, time, angular velocity, and the four values of E_a, E_b, σ_a and σ_b indicating deformation moduli respective stresses corresponding to elements a and b respectively. Two consecutive lines

are printed with four variables on each line in the order mentioned above.

Subroutine 9: This subroutine in coordination with Subroutine 26 optionally determine the influence of the gravitational force.

Subroutine 10: This subroutine calculates the current values of time and axial load, and determines the initial values of deflection and angular velocity. During Phase 1, this subroutine also determines the initial values of strain reversal parameters, saf_o and sbb_o.

Subroutine 11: This subroutine calculates the stress, σ_c, corresponding to the next consecutive limiting stress level, as defined in Sec. 8.5, whereafter it calls either of the three Subroutines 2, 22, or 19 depending on whether the surplus moment increment is positive, zero, or negative respectively.

Subroutine 12: This subroutine assigns the time, t_c, to the time step parameter, Δt, whereafter either of the three Subroutines 3, 25, or 21 are called depending on whether ΔM is positive, zero, or negative respectively.

Subroutine 13: This subroutine controls the assignment of the proper values of deformation moduli corresponding to the deformation of a column element on an unloading line during buckling Phase 2, as well as in connection with strain reversal during buckling Phase 1. It also determines the state space variables σ_{as}, E_{as}, σ_{bs}, and E_{bs}.

Subroutine 14: This subroutine generates information about the occurrence

of strain reversal in a certain column element and then calls Subroutine 8 for printing additional information on the state of the column at the time of strain reversal.

Subroutine 15: This subroutine prints information concerning the attainment of P_{max} in either forward or backward direction. If P_{max} is attained, then Subroutine 8 is called for printing information about the current state of the column; subsequently the number of trials at the time of attainment of the maximum column load is printed.

Subroutine 16: This subroutine restores the state space variables stored at the end of buckling Phase 1.

Subroutine 17: This subroutine calculates the values of the functions $\sinh(\omega\Delta t)$ and $\cosh(\omega\Delta t)$.

Subroutine 18: This subroutine determines the deflection and angular velocity when the surplus moment increment is negative.

Subroutine 19: This subroutine determines the time, t_c, when the surplus moment increment is negative.

Subroutine 20: This subroutine finds out the return time, t_r, for negative values of the surplus moment increment.

Subroutine 21: For negative values of the surplus moment increment, this subroutine assigns deflection and velocity states of the column corresponding to a position where the column element on the front side of motion has exactly attained a stress equal to a limiting stress level

on the stress strain diagram, whereafter Subroutine 6 is called.

Subroutine 22: This subroutine determines the time, t_c, when the surplus moment increment is zero.

Subroutine 23: This subroutine determines the return time, t_r, for $\Delta M = 0$.

Subroutine 24: This subroutine calculates deflection and angular velocity when $\Delta M = 0$.

Subroutine 25: For zero values of the surplus moment increment, this subroutine assigns deflection and velocity states of the column corresponding to a position where the column element on the front side of motion has exactly attained a stress equal to a limiting stress level on the stress strain diagram, whereafter Subroutine 6 is called.

Subroutine 26: This subroutine in coordination with Subroutine 9 optionally determine the influence of the gravitational force.

In the flow diagram which follows in Fig. 37, all except the six symbols, N_1, N_3, J, Q_8, Y_1 and R_5 amy already be familiar from previous sections. These additional symbols are all integer variables used in the following situations:

N_1 counts the number of motion reversal positions in connection with the determination of equilibrium configurations for loads below the maximum level; N_3 is set equal to 1 when the column is moving backwards at the

beginning of buckling Phase 2, and set equal to zero otherwise; J is set equal to 1 when finding maximum column load, and set equal to zero when finding stable lateral configurations; Q_8 is set equal to zero whenever the column attains a motion reversal position during buckling Phase 2, and set equal to 1 otherwise; Y_1 is given the value -1 whenever there is no solution to the time , t_c, corresponding to the next limiting stress level, and given the value 1 otherwise; and R_5 is given the value 1 whenever the criterion for motion reversal under the influence of a constant axial load is not satisfied, and set equal to zero otherwise.

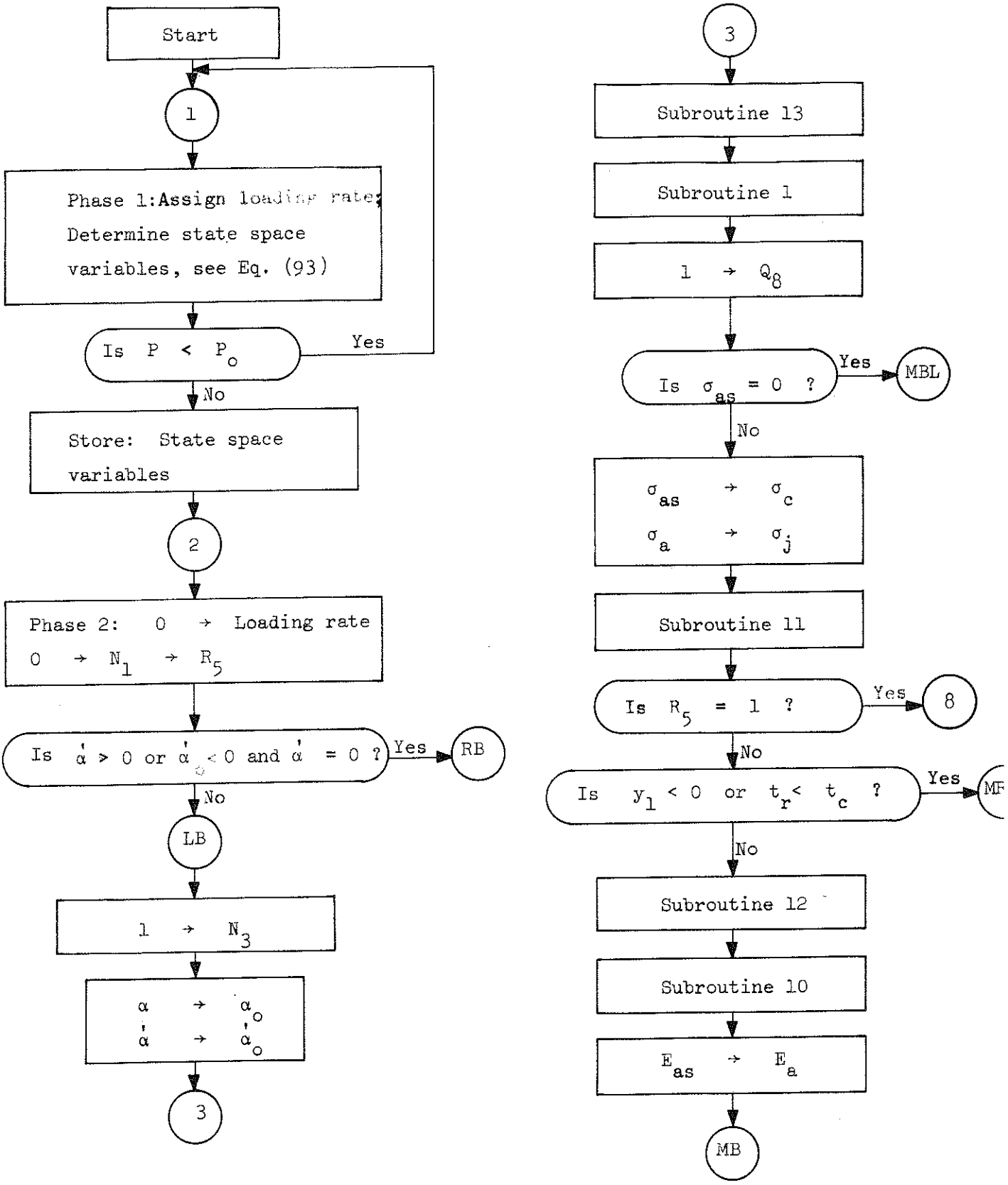

FIG. 37. MAIN PROGRAM DESCRIBING THE PROCESS OF FINDING MAXIMUM COLUMN LOAD AND STABLE LATERAL CONFIGURATIONS ACCORDING TO SINGLE-CYCLE SEARCH METHOD

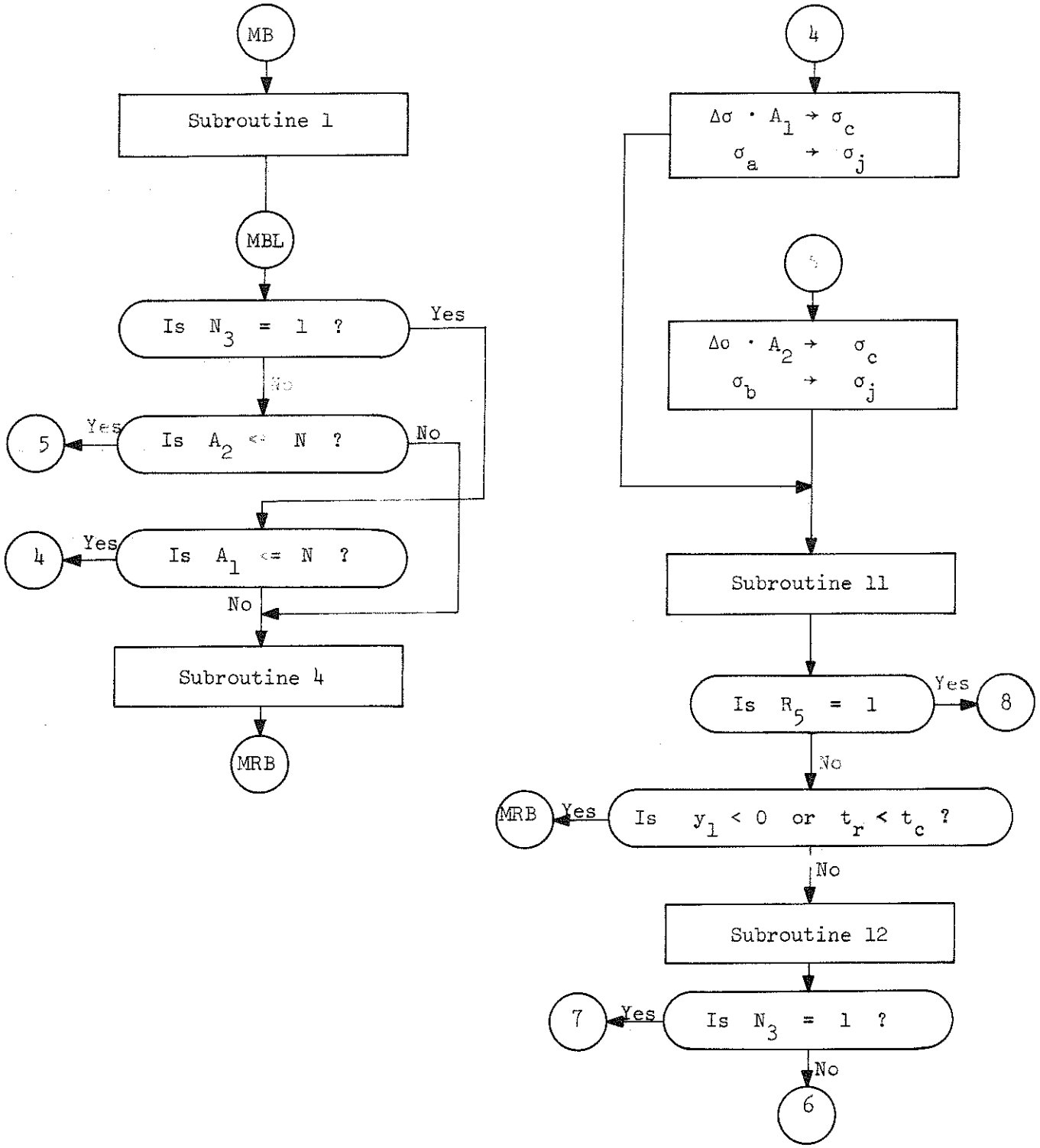
MB
Subroutine 1
MBL
Is N_3 = 1 ?
Yes
No
5
Yes
Is A_2 <= N ?
No
4
Yes
Is A_1 <= N ?
No
Subroutine 4
MRB
4
$\Delta\sigma \cdot A_1 \rightarrow \sigma_c$
$\sigma_a \rightarrow \sigma_j$
5
$\Delta\sigma \cdot A_2 \rightarrow \sigma_c$
$\sigma_b \rightarrow \sigma_j$
Subroutine 11
Is R_5 = 1
Yes
8
No
MRB
Yes
Is $y_1 < 0$ or $t_r < t_c$?
No
Subroutine 12
7
Yes
Is N_3 = 1 ?
No
6

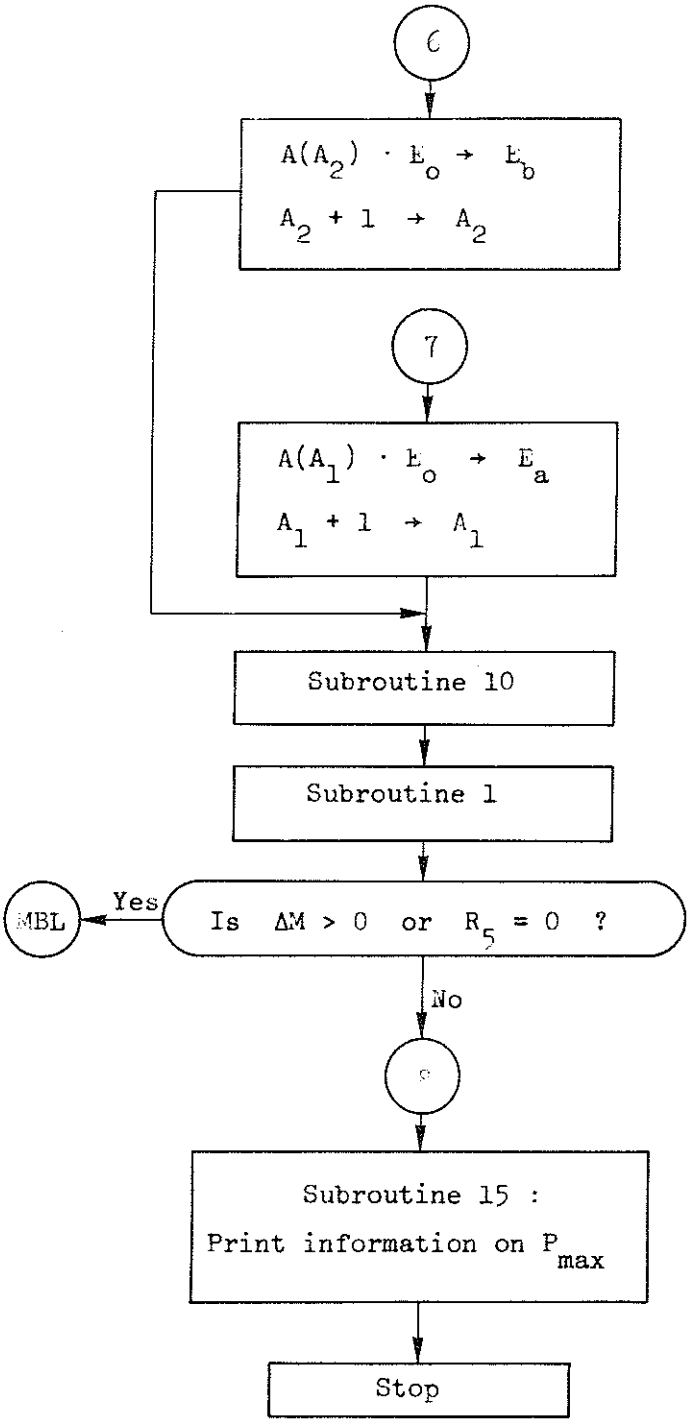
6
A(A2) · Eo → Eb
A2 + 1 → A2
7
A(A1) · Eo → Ea
A1 + 1 → A1
Subroutine 10
Subroutine 1
MBL
Yes
Is ΔM > 0 or R5 = 0 ?
No
8
Subroutine 15 :
Print information on Pmax
Stop

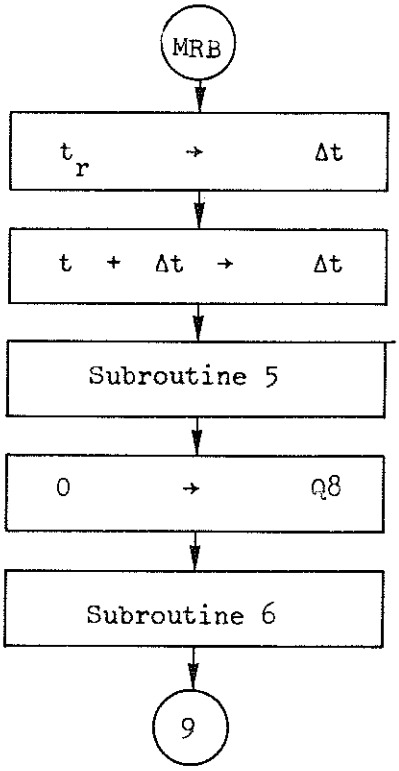
MRB
tr → Δt
t + Δt → Δt
Subroutine 5
0 → Q8
Subroutine 6
9

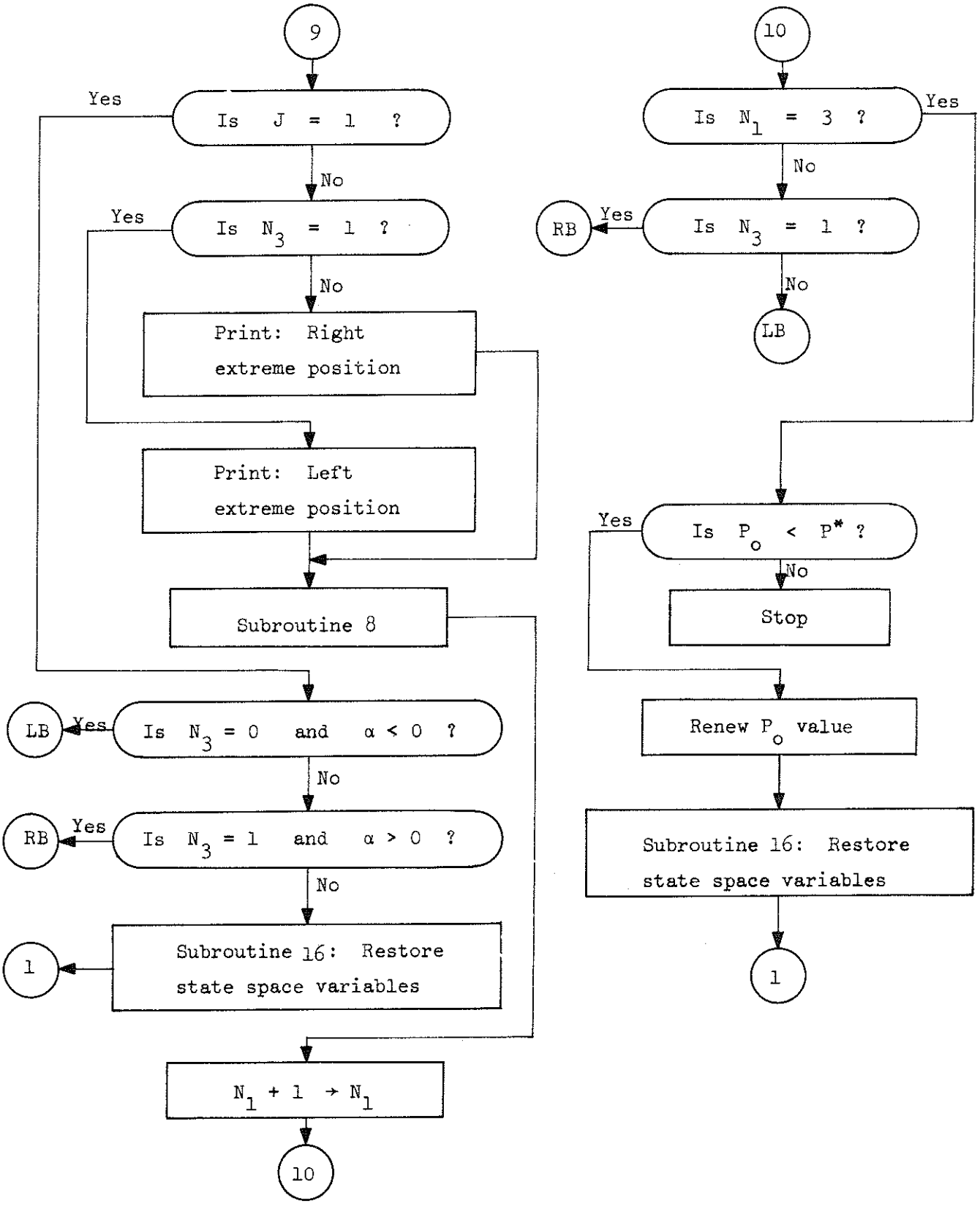
9
Yes
Is J = 1 ?
No
Yes
Is N_3 = 1 ?
No
Print: Right extreme position
Print: Left extreme position
Subroutine 8
LB
Yes
Is N_3 = 0 and α < 0 ?
No
RB
Yes
Is N_3 = 1 and α > 0 ?
No
1
Subroutine 16: Restore state space variables
N_1 + 1 → N_1
10
10
Is N_1 = 3 ?
Yes
No
RB
Yes
Is N_3 = 1 ?
No
LB
Yes
Is P_o < P^* ?
No
Stop
Renew P_o value
Subroutine 16: Restore state space variables
1

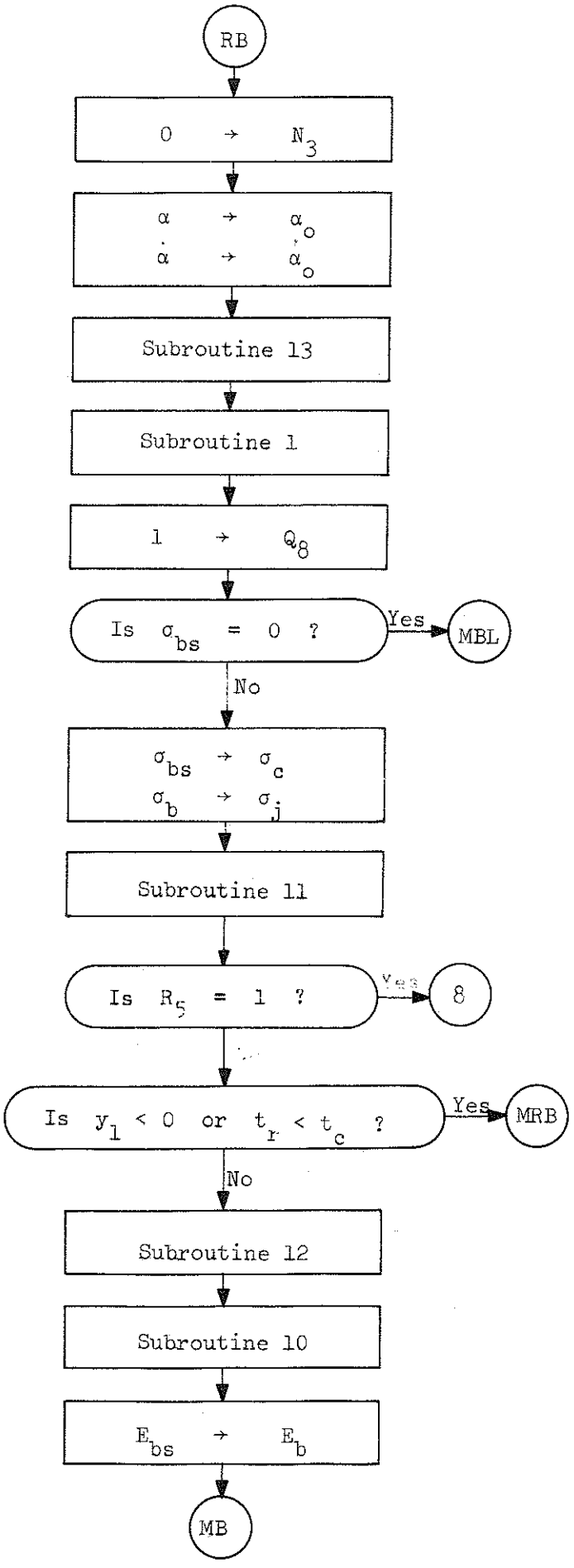
RB
0 → N_3
α → α_o
$\dot{\alpha}$ → $\dot{\alpha}_o$
Subroutine 13
Subroutine 1
1 → Q_8
Is σ_{bs} = 0 ?
Yes
MBL
No
σ_{bs} → σ_c
σ_b → σ_j
Subroutine 11
Is R_5 = 1 ?
Yes
8
Is y_1 < 0 or t_r < t_c ?
Yes
MRB
No
Subroutine 12
Subroutine 10
E_{bs} → E_b
MB

8.7 Numerical Results for Maximum Column Load

The determination of maximum column load herein precedes the calculations for the dynamically stable lateral positions, due to the fact that a demarcation of the boundary line between regions of stability and instability requires a precise knowledge of the maximum column load. If, for a particular parameter combination, the maximum column load is determined, then we may definitely assert that for all possible axial loads below that level, there exists dynamically stable lateral configurations which could be found for each predetermined axial load.

The concept of Single-Cycle Search method developed in the previous chapter is utilized in constructing a computer program, see Program 8 of Appendix D, with the aid of the analytical tools acquired in the analysis of Model 3. The initially imperfect simple column in Fig. 12 is assumed to have a deformable hinge with any arbitrary stress strain relationship. For the purpose of the present computations, the stress strain diagram is assumed to have 79 limiting stress levels, see Fig. 32, with the following array of β-values:

Array of β-Values

1, 1, 1, 1, .667, .572, .5, .445, .4, .308

.268, .236, .23, .222, .218, .208, .2, .193, .185, .178

.17, .167, .167, .167, .167, .165, .164, .163, .162, .154

.148, .143, .138, .134, .111, .111, .111, .111, .111, .111

.11, .11, .11, .109, .1, .1, .1, .1, .1, .1

.1, .1, .1, .1, .1, .1, .1, .1, .1

.084, .077, .063, .061, .057, .053, .05, .048, .046, .044

.04, .033, .028, .026, .024, .017, .015, .013, .011, .01

The above β-values are ratios of the tangent moduli at the limiting stress levels to the initial elastic modulus. The multilinearization of the stress strain diagram is performed according to the procedure depicted in Fig. 32. The value of $\Delta\sigma$ defined in that principal figure is separately chosen in each of the three data sets below, such that the reduced modulus load in each case would occur at the sixtieth limiting stress level with the corresponding tangent modulus determined according to the array of β-values given above. The relative shape of the stress strain diagram, determined by the numerical ratios given in the above array of β-values is depicted in Fig. 38. The relative shape here implies that at each limiting stress level, the consecutive tangent moduli retain their corresponding ratios regardless of the possible changes in the value of the initial elastic modulus.

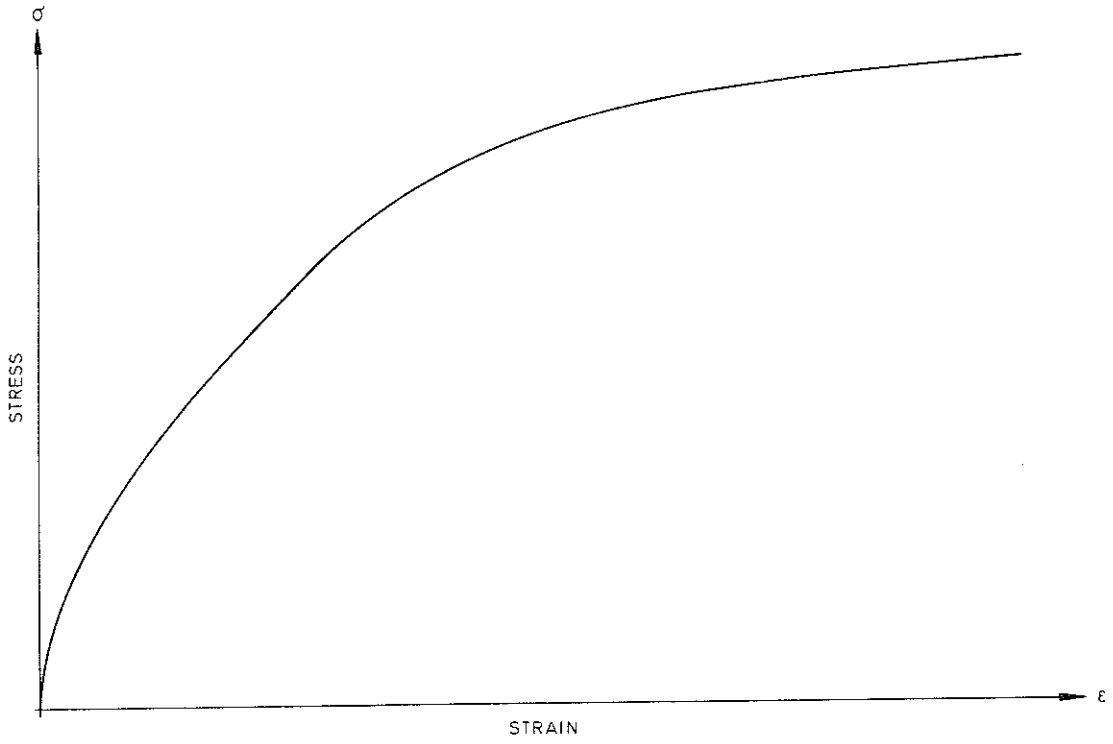

FIG. 38. RELATIVE SHAPE OF THE STRESS STRAIN DIAGRAM USED IN THE COMPUTATIONS OF MODEL 3.

With the proper choice of $\Delta\sigma$ and the initial modulus of elasticity, E_o, the stress strain diagram, whose relative shape is shown in Fig. 38, would be uniquely determined. A study of the array of β-values in this section shows that the stress strain diagram is chosen such that it includes both regions of constant and continuously decreasing tangent modulus.

Three sets of calculations are performed and recorded in Tables 4 A - 4 C corresponding to three different data sets. In the first set, recorded in Table 4 A, the parameters which are maintained at constant values are: b = d = 5 cm; A = 5 cm^2; L = 2.5 m; M = 100 kg; and $E_o = 10^{10}$ Newtons per square meter. On the other hand, the parameters subjected to variations in Table 4 A are: initial deflection, U_o, initial velocity disturbance, V_o, initial eccentricity, X_o, loading rate, c, and a velocity disturbance, V_1, introduced at any arbitrary loading level, P_d, during buckling Phase 1. The effect of variations of a velocity disturbance introduced at the beginning of buckling Phase 2 on the maximum column load is presented in diagrammatic form in Sec. 9.2. This fact, however, is not recorded in Table 4 A. Furthermore, the influence of gravitational force and the effect of changes in the direction of application of the external load are postponed to be separately treated herein in Secs. 10.3 and 10.4. With the above numerical values corresponding to the first data set, the values of the tangent modulus and the reduced modulus loads are found to be equal to 11 100 and 18 180 Newtons respectively.

In the second set of calculations, recorded in Table 4 B, the parameters kept at constant values are: b = d = 10 cm; A = 5 cm^2; L = 5 m, M = 500 kg; and $E_o = 10^{10}$ Newtons per square meter; whereas the initial deflection, U_o, and loading rate, c, are subjected to variations. The

objective of this set of calculations is mainly to evaluate the influence of an increase in the mass and length of the column. Compared with the first set, the value of the hinge element area, A, is kept the same while the hinge width and depth, 2 b respective 2 d, are increased in the same proportional ratio as the length, L, in order to maintain the same tangent modulus and reduced modulus loads described above for the first data set.

For the third set of calculations recorded in Table 4 C, the parameters maintained at constant values are: b = 5 cm; d = 10 cm; A = 5 cm^2; L = 5 m; M = 500 kg; and $E_o = 10^{11}$ Newtons per square meter. The parameters subjected to variations in this case are initial deflection, U_o, and loading rate, c, as in Table 4 B. The objective of this set of calculations is mainly to observe the influence of an increase in the value of the initial tangent modulus, E_o. Compared with the first data set, the values of the hinge element area, A, and the hinge width, 2 b, are kept at the same values while the hinge depth, 2 d, is increased by the same ratio as the column length, L. This is done in order to prevent the maximum column load from attaining a high value with due regard to the total computer time required. The values of the tangent modulus and the reduced modulus loads for this set of calculations are found to be 27 750 and 45 450 Newtons respectively.

It should be noted that while the column length, L, in both Tables 4 B and 4 C is increased two times compared with Table 4 A, the initial deflection, U_o, corresponding to each loading rate, c, is also increased two times in order to maintain the same U_o/L ratio in all the three tables. It should further be noted that the last column of Tables 4 A - 4 C

indicates the direction of failure in either forward or backward direction at the time of attaining the maximum column load. This remarkable possibility which has not hitherto been discussed, will be treated herein in Secs. 10.1 and 10.2.

It may be worthwhile to note that at the time of attaining the maximum column load, the stress in the column element, subjected to strain reversal, may attain the inelastic range in tension after complete unloading. However, among all the columns recorded in Tables 4A - 4C, this phenomenon was observed only in the last six entries in Table 4C (Columns No. 31 - 36 of Table 4C with initial end deflection, U_o = 2 cm). Since, according to the Single-Cycle Search method, the control and assignment of deformation moduli during buckling Phase 2, corresponding to tensile stresses in the inelastic range for a column element, takes place each time the other column element reaches a limiting stress level in compression, it follows that the Multi-Cycle Search method with shorter control intervals may lead to more accurate results in such situations. Nevertheless, a recalculation of Columns No. 31 - 36 of Table 4C according to Multi-Cycle Search method resulted in identical maximum column loads.

It should be observed that throughout the calculations corresponding to Tables 4A - 4C, the length of the time step, Δt, corresponding to one computation cycle is chosen equal to 0.01 seconds. Reducing the time step may in some instances affect the results, particulary for columns with small initial imperfections and large loading rates. However, the influence of the time step on the size of the maximum column load deserves particular attention, whereby it is separately treated in Sec. 8.9.

The numerical results tabulated in this section will sequentially be utilized in subsequent analysis herein in order to illustrate the disclosure of various buckling phenomena.

TABLE 4A. - INFLUENCE OF PARAMETER VARIATIONS ON THE VALUE OF THE MAXIMUM COLUMN LOAD CORRESPONDING TO THE FIRST DATA SET

Column No.	c Loading Rate in Newtons per second	U_o Initial End Deflection in cm	V_o Initial End Velocity in cm/sec	P_d Disturbance Load Level in Newtons	V_1 Disturbance End Velocity in cm/sec	X_o Initial Eccentricity in cm	P_{max} Maximum Column Load in Newtons	Direction of Failure
1	100	.0001	0	20000	0	0	13482	Forward
2	500	.0001	0	20000	0	0	13785	Forward
3	1000	.0001	0	20000	0	0	14060	Reverse
4	2000	.0001	0	20000	0	0	14360	Forward
5	5000	.0001	0	20000	0	0	15350	Forward
6	10000	.0001	0	20000	0	0	16600	Forward
7	100	.001	0	20000	0	0	13356	Forward

TABLE 4A CONTINUED:

Column No.	c Loading Rate in Newtons per second	U_o Initial End Deflection in cm	V_o Initial End Velocity in cm/sec	P_d Disturbance Load Level in Newtons	V_1 Disturbance End Velocity in cm/sec	X_o Initial Eccentricity in cm	P_{max} Maximum Column Load in Newtons	Direction of Failure
8	500	.001	0	20000	0	0	13430	Forward
9	1000	.001	0	20000	0	0	13590	Forward
10	2000	.001	0	20000	0	0	13900	Forward
11	5000	.001	0	20000	0	0	14850	Forward
12	10000	.001	0	20000	0	0	16100	Forward
13	100	.01	0	20000	0	0	13184	Forward
14	500	.01	0	20000	0	0	13205	Forward

TABLE 4A CONTINUED:

Column No.	c Loading Rate in Newtons per second	U_o Initial End Deflection in cm	V_o Initial End Velocity in cm/sec	P_d Disturbance Load Level in Newtons	V_1 Disturbance End Velocity in cm/sec	X_o Initial Eccentricity in cm	P_{max} Maximum Column Load in Newtons	Direction of Failure
15	1000	.01	0	20000	0	0	13230	Forward
16	2000	.01	0	20000	0	0	13400	Forward
17	5000	.01	0	20000	0	0	13850	Forward
18	10000	.01	0	20000	0	0	14900	Forward
19	100	.1	0	20000	0	0	12666	Forward
20	500	.1	0	20000	0	0	12670	Forward
21	1000	.1	0	20000	0	0	12670	Forward

TABLE 4A CONTINUED:

Column No.	c Loading Rate in Newtons per second	U_o Initial End Deflection in cm	V_o Initial End Velocity in cm/sec	P_d Disturbance Load Level in Newtons	V_1 Disturbance End Velocity in cm/sec	X_o Initial Eccentricity in cm	P_{max} Maximum Column Load in Newtons	Direction of Failure
22	2000	.1	0	20000	0	0	12700	Forward
23	5000	.1	0	20000	0	0	12650	Forward
24	10000	.1	0	20000	0	0	12900	Forward
25	100	.5	0	20000	0	0	11461	Forward
26	500	.5	0	20000	0	0	11460	Forward
27	1000	.5	0	20000	0	0	11460	Forward
28	2000	.5	0	20000	0	0	11460	Forward

TABLE 4A CONTINUED:

Column No.	c Loading Rate in Newtons per second	U_o Initial End Deflection in cm	V_o Initial End Velocity in cm/sec	P_d Disturbance Load Level in Newtons	V_1 Disturbance End Velocity in cm/sec	X_o Initial Eccentricity in cm	P_{max} Maximum Column Load in Newtons	Direction of Failure
29	5000	.5	0	20000	0	0	11400	Forward
30	10000	.5	0	20000	0	0	12500	Forward
31	100	1	0	20000	0	0	10524	Forward
32	500	1	0	20000	0	0	10520	Forward
33	1000	1	0	20000	0	0	10520	Forward
34	2000	1	0	20000	0	0	10500	Forward
35	5000	1	0	20000	0	0	10500	Forward

TABLE 4A CONTINUED:

Column No.	c Loading Rate in Newtons per second	U_o Initial End Deflection in cm	V_o Initial End Velocity in cm/sec	P_d Disturbance Load Level in Newtons	V_1 Disturbance End Velocity in cm/sec	X_o Initial Eccentricity in cm	P_{max} Maximum Column Load in Newtons	Direction of Failure
36	10000	1	0	20000	0	0	10400	Forward
37	5000	.001	.2	20000	0	0	14900	Reverse
38	5000	.0015	.2	20000	0	0	15100	Reverse
39	5000	.0020	.2	20000	0	0	15200	Reverse
40	5000	.0025	.2	20000	0	0	16200	Reverse
41	5000	.0026	.2	20000	0	0	16300	Reverse
42	5000	.0027	.2	20000	0	0	16750	Forward

TABLE 4A CONTINUED:

Column No.	c Loading Rate in Newtons per second	U_o Initial End Deflection in cm	V_o Initial End Velocity in cm/sec	P_d Disturbance Load Level in Newtons	V_1 Disturbance End Velocity in cm/sec	X_o Initial Eccentricity in cm	P_{max} Maximum Column Load in Newtons	Direction of Failure
43	5000	.003	.2	20000	0	0	16150	Forward
44	5000	.001	.5	20000	0	0	14150	Reverse
45	5000	.001	1	20000	0	0	15450	Reverse
46	5000	.001	.01	20000	0	0	15050	Forward
47	5000	.001	0	5000	.2	0	15400	Forward
48	5000	.001	0	7500	.2	0	14600	Forward
49	5000	.001	0	10000	.2	0	14100	Forward

TABLE 4A CONTINUED:

Column No.	c Loading Rate in Newtons per second	U_o Initial End Deflection in cm	V_o Initial End Velocity in cm/sec	P_d Disturbance Load Level in Newtons	V_1 Disturbance End Velocity in cm/sec	X_o Initial Eccentricity in cm	P_{max} Maximum Column Load in Newtons	Direction of Failure
50	5000	.001	0	20000	0	.001	14350	Forward
51	5000	.001	0	20000	0	.01	13750	Forward

TABLE 4B. - INFLUENCE OF PARAMETER VARIATIONS ON THE VALUE OF THE MAXIMUM COLUMN LOAD CORRESPONDING TO THE SECOND DATA SET

Column No.	c Loading Rate in Newtons per second	U_o Initial End Deflection in cm	V_o Initial End Velocity in cm/sec	P_d Disturbance Load Level in Newtons	V_1 Disturbance End Velocity in cm/sec	X_o Initial Eccentricity in cm	P_{max} Maximum Column Load in Newtons	Direction of Failure
1	100	.0002	0	20000	0	0	13592	Forward
2	500	.0002	0	20000	0	0	14452	Forward
3	1000	.0002	0	20000	0	0	14920	Forward
4	2000	.0002	0	20000	0	0	16200	Forward
5	5000	.0002	0	20000	0	0	17450	Forward
6	10000	.0002	0	20000	0	0	17800	Forward
7	100	.002	0	20000	0	0	13372	Forward

TABLE 4B CONTINUED:

Column No.	c Loading Rate in Newtons per second	U_o Initial End Deflection in cm	V_o Initial End Velocity in cm/sec	P_d Disturbance Load Level in Newtons	V_1 Disturbance End Velocity in cm/sec	X_o Initial Eccentricity in cm	P_{max} Maximum Column Load in Newtons	Direction of Failure
8	500	.002	0	20000	0	0	13770	Forward
9	1000	.002	0	20000	0	0	14150	Forward
10	2000	.002	0	20000	0	0	15540	Forward
11	5000	.002	0	20000	0	0	17000	Forward
12	10000	.002	0	20000	0	0	17600	Forward
13	100	.02	0	20000	0	0	13197	Forward
14	500	.02	0	20000	0	0	13345	Forward

TABLE 4B CONTINUED:

Column No.	c Loading Rate in Newtons per second	U_o Initial End Deflection in cm	V_o Initial End Velocity in cm/sec	P_d Disturbance Load Level in Newtons	V_1 Disturbance End Velocity in cm/sec	X_o Initial Eccentricity in cm	P_{max} Maximum Column Load in Newtons	Direction of Failure
15	1000	.02	0	20000	0	0	13500	Forward
16	2000	.02	0	20000	0	0	14180	Forward
17	5000	.02	0	20000	0	0	15650	Forward
18	10000	.02	0	20000	0	0	16500	Forward
19	100	.2	0	20000	0	0	12667	Forward
20	500	.2	0	20000	0	0	12665	Forward
21	1000	.2	0	20000	0	0	12660	Forward

TABLE 4B CONTINUED:

Column No.	c Loading Rate in Newtons per second	U_o Initial End Deflection in cm	V_o Initial End Velocity in cm/sec	P_d Disturbance Load Level in Newtons	V_1 Disturbance End Velocity in cm/sec	X_o Initial Eccentricity in cm	P_{max} Maximum Column Load in Newtons	Direction of Failure
22	2000	.2	0	20000	0	0	12660	Forward
23	5000	.2	0	20000	0	0	13400	Forward
24	10000	.2	0	20000	0	0	14600	Forward
25	100	1.0	0	20000	0	0	11456	Forward
26	500	1.0	0	20000	0	0	11450	Forward
27	1000	1.0	0	20000	0	0	11410	Forward
28	2000	1.0	0	20000	0	0	11360	Forward

TABLE 4B CONTINUED:

Column No.	c Loading Rate in Newtons per second	U_o Initial End Deflection in cm	V_o Initial End Velocity in cm/sec	P_d Disturbance Load Level in Newtons	V_1 Disturbance End Velocity in cm/sec	X_o Initial Eccentricity in cm	P_{max} Maximum Column Load in Newtons	Direction of Failure
29	5000	1.0	0	20000	0	0	11400	Forward
30	10000	1.0	0	20000	0	0	11600	Forward
31	100	2	0	20000	0	0	10520	Forward
32	500	2	0	20000	0	0	10505	Forward
33	1000	2	0	20000	0	0	10470	Forward
34	2000	2	0	20000	0	0	10400	Forward
35	5000	2	0	20000	0	0	10300	Forward

TABLE 4B CONTINUED:

Column No.	c Loading Rate in Newtons per second	U_o Initial End Deflection in cm	V_o Initial End Velocity in cm/sec	P_d Disturbance Load Level in Newtons	V_1 Disturbance End Velocity in cm/sec	X_o Initial Eccentricity in cm	P_{max} Maximum Column Load in Newtons	Direction of Failure
36	10000	2.0	0	20000	0	0	10400	Forward

TABLE 4C. - INFLUENCE OF PARAMETER VARIATIONS ON THE VALUE OF THE MAXIMUM COLUMN LOAD CORRESPONDING TO THE THIRD DATA SET

Column No.	c Loading Rate in Newtons per second	U_o Initial End Deflection in cm	V_o Initial End Velocity in cm/sec	P_d Disturbance Load Level in Newtons	V_1 Disturbance End Velocity in cm/sec	X_o Initial Eccentricity in cm	P_{max} Maximum Column Load in Newtons	Direction of Failure
1	100	.0002	0	50000	0	0	33566	Forward
2	500	.0002	0	50000	0	0	34050	Forward
3	1000	.0002	0	50000	0	0	34950	Forward
4	2000	.0002	0	50000	0	0	34960	Forward
5	5000	.0002	0	50000	0	0	37850	Forward
6	10000	.0002	0	50000	0	0	40800	Forward
7	100	.002	0	50000	0	0	33211	Forward

TABLE 4C CONTINUED:

Column No.	c Loading Rate in Newtons per second	U_o Initial End Deflection in cm	V_o Initial End Velocity in cm/sec	P_d Disturbance Load Level in Newtons	V_1 Disturbance End Velocity in cm/sec	X_o Initial Eccentricity in cm	P_{max} Maximum Column Load in Newtons	Direction of Failure
8	500	.002	0	50000	0	0	33305	Forward
9	1000	.002	0	50000	0	0	33620	Forward
10	2000	.002	0	50000	0	0	34180	Forward
11	5000	.002	0	50000	0	0	35850	Forward
12	10000	.002	0	50000	0	0	38300	Forward
13	100	.02	0	50000	0	0	32761	Forward
14	500	.02	0	50000	0	0	32785	Forward

TABLE 4C CONTINUED:

Column No.	c Loading Rate in Newtons per second	U_o Initial End Deflection in cm	V_o Initial End Velocity in cm/sec	P_d Disturbance Load Level in Newtons	V_1 Disturbance End Velocity in cm/sec	X_o Initial Eccentricity in cm	P_{max} Maximum Column Load in Newtons	Direction of Failure
15	1000	.02	0	50000	0	0	32840	Forward
16	2000	.02	0	50000	0	0	32960	Forward
17	5000	.02	0	50000	0	0	33250	Forward
18	10000	.02	0	50000	0	0	35000	Forward
19	100	.2	0	50000	0	0	30744	Forward
20	500	.2	0	50000	0	0	30735	Forward
21	1000	.2	0	50000	0	0	30730	Forward

TABLE 4C CONTINUED:

Column No.	c Loading Rate in Newtons per second	U_o Initial End Deflection in cm	V_o Initial End Velocity in cm/sec	P_d Disturbance Load Level in Newtons	V_1 Disturbance End Velocity in cm/sec	X_o Initial Eccentricity in cm	P_{max} Maximum Column Load in Newtons	Direction of Failure
22	2000	.2	0	50000	0	0	30720	Forward
23	5000	.2	0	50000	0	0	30650	Forward
24	10000	.2	0	50000	0	0	30600	Forward
25	100	1.0	0	50000	0	0	26313	Forward
26	500	1.0	0	50000	0	0	26300	Forward
27	1000	1.0	0	50000	0	0	26300	Forward
28	2000	1.0	0	50000	0	0	26280	Forward

TABLE 4C CONTINUED:

Column No.	c Loading Rate in Newtons per second	U_o Initial End Deflection in cm	V_o Initial End Velocity in cm/sec	P_d Disturbance Load Level in Newtons	V_1 Disturbance End Velocity in cm/sec	X_o Initial Eccentricity in cm	P_{max} Maximum Column Load in Newtons	Direction of Failure
29	5000	1.0	0	50000	0	0	26150	Forward
30	10000	1.0	0	50000	0	0	25900	Forward
31	100	2	0	50000	0	0	23324	Forward
32	500	2	0	50000	0	0	23285	Forward
33	1000	2	0	50000	0	0	23270	Forward
34	2000	2	0	50000	0	0	23260	Forward
35	5000	2	0	50000	0	0	23150	Forward

TABLE 4C CONTINUED:

Column No.	c Loading Rate in Newtons per second	U_o Initial End Deflection in cm	V_o Initial End Velocity in cm/sec	P_d Disturbance Load Level in Newtons	V_1 Disturbance End Velocity in cm/sec	X_o Initial Eccentricity in cm	P_{max} Maximum Column Load in Newtons	Direction of Failure
36	10000	2	0	50000	0	0	22900	Forward

8.8. Reliability of Numerical Results

In a quantitative evaluation of the yet unexplored areas in the field of column stability, significant results on the properties of the maximum column load are presented in this chapter. Since this may have some impact on future research in this area, it must be made sure that the presented numerical results are reliably valid. A study of Program 8 in Appendix D may provide the answer. However, due to the complex logical structure of this program which has many possible pitfalls, the verification of numerical results may not be so straightforward even in the judgement of an experienced programmer. Fortunately, we possess a simple valuable device which can efficiently perform this job. The explanation follows from the fact that the two differently conceived programs developed in this chapter can control each other's results. This control process may be illustrated by the following 5 case studies. Each case study consists of examining the computations for the maximum load of a given column according to both Multi-Cycle and Single-Cycle Search methods.

For easy comparison, each corresponding pair of computations performed on Univac 1100, is placed on the same page with the results according to the Multi-Cycle Search method at the top, and those corresponding to the Single-Cycle Search method appearing at the bottom of the page.

The information printed in each partial case consists of four lines, the first two of which show the results corresponding to the dynamic state of the column, to be specified below, as soon as axial load ceases to increase (end of buckling Phase 1); the last two lines

indicate the results corresponding to similar information about the dynamic state of the column at the time of attaining maximum column load under the influence of constant axial load (during buckling Phase 2).

The two-line information about the dynamic state of the column printed each time consists of the values of the following eight quantities: the first line consists of the current axial load, P, in Newtons; current end deflection, U, in centimeters; the total loading time, t, in seconds; and the angular velocity, $\dot{\alpha}$, in radions per second. The second line gives information about the current deformation moduli, E_a and E_b as well as the current stresses σ_a and σ_b all expressed in Newtons/m^2 and corresponding to elements a and b respectively.

Case 1 studies Column 37 of Table 4A. This column indicates a salient feature, namely the indicated column failure in reverse direction despite the fact that the initial disturbance velocity is applied in the direction of the original deflection[1]. Both methods exactly lead to the same value of P_{max} equal to 14900 Newtons.

It should be noted that in all the five cases which follow, the first trial P_o level described in Secs. 8.3 and 8.4, is chosen the same according to both methods. Since, the Multi-Cycle and Single-Cycle Search methods both treat the buckling Phase 1 identically, the results appearing in the first two lines of each partial case (just at the time the search for maximum column load begins) are identical according to both methods. However, since the two procedures treat buckling Phase 2 in a completely different manner (explained in Secs. 8.3 and 8.4), it

---

1. This fact is treated in greater detail in Chapter 10.

is significant to observe that with some difference in the dynamic state of the column at the time of attaining the maximum column load, the two methods lead to maximum loads which are either identical or negligibly different from each other.

It should be noted that the observation of the computer time recorded below each partial case, reveals the comparable efficiency of the Single-Cycle Search method. This efficiency increases in cases where the number of trials above the first P_o level is considerably large, specially in the process of finding maximum column load for small loading rates, see Case 5 (computing times are expressed in seconds).

CASE 1. COLUMN NO. 37 OF TABLE 4A

a. Computations According to Multi-Cycle Search Method

MULTI-CYCLE SEARCH BEGUN :

* * * * *			
14800	-.25777679	2.959998	-.00742784
1E+09	1E+09	15317371	14282626.

P MAX IN REVERSE DIRECTION

* * * * *			
14900	-1.2406028	3.2949939	-.00808087
6.3E+08	1E+10	18791074.	11008910.

NO. OF TRIALS ABOVE THE FIRST P0 LEVEL = 3

TIME : 2.270

b. Computations According to Single-Cycle Search Method

SINGLE-CYCLE SEARCH BEGUN :

* * * * *			
14800	-.25777679	2.959998	-.00742784
1E+09	1E+09	15317371	14282626.

P MAX IN REVERSE DIRECTION

* * * * *			
14900	-1.23985	3.2935408	-.00812064
6.3E+08	1E+10	18787878	11012118.

NO. OF TRIALS ABOVE THE FIRST P0 LEVEL = 3

TIME : 1.245

CASE 2. COLUMN NO. 15 OF TABLE 4A

a. Computations According to Multi-Cycle Search Method

```
                    MULTI-CYCLE SEARCH BEGUN :
* * * * *
 13000          1.5738268       12.999988       .00434292
 1E+10          1E+09           8940037         17059921

                    PMAX IN FORWARD DIRECTION
* * * * *
 13240          2.0739985       13.381978       .00457159
 1E+10          6.3E+08         7691142.4       18788796.

NO. OF TRIALS ABOVE THE FIRST P0 LEVEL =      25

 TIME :  10.080
```

b. Computations According to Single-Cycle Search Method

```
                    SINGLE-CYCLE SEARCH BEGUN :
* * * * *
 13000          1.5738268       12.999988       .00434292
 1E+10          1E+09           8940037         17059921

                    P MAX IN FORWARD DIRECTION
* * * * *
 13230          2.2020851       13.572051       .00183642
 1E+10          6.1E+08         7369041.6       19090909.

NO. OF TRIALS ABOVE THE FIRST P0 LEVEL =      24

TIME :  2.672
```

CASE 3. COLUMN NO. 16 OF TABLE 4B

a. Computations According to Multi-Cycle Search Method

MULTI-CYCLE SEARCH BEGUN :

* * * * *			
14000	.82123782	6.9999941	.00334828
1.1E+09	1E+09	13178895	14821090.

PMAX IN FORWARD DIRECTION

* * * * *			
14180	3.0539064	7.8429843	.00444443
1E+10	6.3E+08	9571460.6	18788498.

NO. OF TRIALS ABOVE THE FIRST PO LEVEL = 10

TIME : 17.531

b. Computations According to Single-Cycle Search Method

SINGLE-CYCLE SEARCH BEGUN :

* * * * *			
14000	.82123782	6.9999941	.00334828
1.1E+09	1E+09	13178895	14821090.

P MAX IN FORWARD DIRECTION

* * * * *			
14180	3.0538009	7.8418962	.00444696
1E+10	6.3E+08	9572105	18787878.

NO. OF TRIALS ABOVE THE FIRST PO LEVEL = 10

TIME : 2.114

CASE 4. COLUMN NO. 30 OF TABLE 4C

a. Computations According to Multi-Cycle Search Method

MULTI-CYCLE SEARCH BEGUN :

* * * * *

25500	3.2742014	2.5499983	.00788192
1E+11	1E+10	9537842.4	41462108.

PMAX IN FORWARD DIRECTION

* * * * *

25900	4.7832714	2.9749934	.0049334
1E+11	4.6E+09	281044.14	51518816

NO. OF TRIALS ABOVE THE FIRST P0 LEVEL = 5

TIME : 4.310

b. Computations According to Single-Cycle Search Method

SINGLE-CYCLE SEARCH BEGUN :

* * * * *

25500	3.2742014	2.5499983	.00788192
1E+11	1E+10	9537842.4	41462108.

P MAX IN FORWARD DIRECTION

* * * * *

25900	4.7841836	2.9735805	.00496521
1E+11	4.6E+09	284793.58	51515151.

NO. OF TRIALS ABOVE THE FIRST P0 LEVEL = 5

TIME : 1.271

CASE 5. COLUMN NO. 31 OF TABLE 4C

a. Computations According to Multi-Cycle Search Method

```
                    MULTI-CYCLE SEARCH BEGUN :
* * * * *
 23000          5.0990191       229.97742       .0001889
 1E+11          7.7E+09         -442316.47      46436996

                    PMAX IN FORWARD DIRECTION
* * * * *
 23322          5.8783591       234.47618       .00027564
 6.67E+10       4.7999999E+09   -4119951.2      50758158

NO. OF TRIALS ABOVE THE FIRST P0 LEVEL =        323

 TIME : 279.772
```

b. Computations According to Single-Cycle Search Method

```
                    SINGLE-CYCLE SEARCH BEGUN :
* * * * *
 23000          5.0990191       229.97742       .0001889
 1E+11          7.7E+09         -442316.47      46436996

                    P MAX IN FORWARD DIRECTION
* * * * *
 23324          5.8764825       234.36481       .00034188
 6.67E+10       4.7999999E+09   -4115071.5      50757575.

NO. OF TRIALS ABOVE THE FIRST P0 LEVEL =        325

 TIME :  31.126
```

8.9 Choice of Time Step

The decision to choose the length of the calculation time step depends on a simultaneous consideration of two opposing factors, i.e., required degree of accuracy of numerical results and the demand for computer time. The length of the time step can affect the degree of precision of calculations in the following situations:

1. The approximate method, introduced herein in the analysis of Model 1 and additionally developed in the analyses of Models 2 and 3, assumes that the time step is sufficiently short to allow each continuously applied increment of axial load to be introduced at the beginning of the corresponding time interval.

2. If oscillations simultaneous with loading are violent, such buckling phenomena as strain reversal in one direction, motion reversal and subsequent strain reversal in the opposite direction may occur in a short period of time. If this time period is not sufficiently larger than the calculation time step, errors may arise in the output results.

3. In addition to the above two cases, which are valid for all column models, the length of the calculation time step may play a significant role in the case of a column with arbitrary stress strain diagram (Model 3). By choosing a large time step, in going from one column state to another, some of the actual tangent moduli on the stress strain diagram may wrongly be disregarded during the course of the given time step.

The possibility of disregarding some actual tangent moduli mentioned in Point 3 above may arise for appreciably large time steps. However, the choice of a time step which is not sufficiently small may lead

to a loss of accuracy even in cases where no actual tangent moduli are disregarded. The following discussion is intended to clarify this point. Furthermore, in the illustrations which follow, the procedure for testing the sufficiency of the time step is pointed out:

If a column possesses a sufficiently small initial imperfection, the stresses at various points of a given column cross section may follow each other with small differences even at relatively high axial loads. Thus, during the increase of axial load, in the course of a computation cycle, some zone of the given column cross section may attain stress levels slightly higher than a certain limiting stress level (LSL) on the stress strain diagram, whereas the stresses over the rest of the same cross section may slightly fall below that LSL. Due to this phenomenon, the increase of axial load, ΔP, in the course of the computation cycle would give rise to an axially induced internal moment increment, the magnitude of which depends on the size of ΔP.

Now, the bending of the column may be so small that, during the immediately following time step, the stresses all over the given cross section may rise above the current LSL. In other words, the duration of the stress distribution partly below and partly above a certain LSL may last only during the course of a single computation cycle. If this state of affairs remains unchanged even by reducing the magnitude of ΔP, i.e., if the single cycle duration of the stress distribution over a given cross section partially below and partially above a certain LSL is valid even after reducing the time step, this would imply that the original time step may cause an axially induced internal moment increment too large to be tolerated within a prescribed frame of accurary.

The error caused due to unwarranted excessive values of the axially induced internal moment increment would become significant provided that the output result, i.e., the value of the maximum column load is appreciably influenced by the choice of the time step. Since the axially induced internal moment increment accelerates the lateral instability of the column, see Sec. 7.3, the choice of an undesirably large time step may normally lead to a decrease of the maximum column load (this result may not conform to backwards-inclined columns which may behave abnormally, see Sec. 10.5).

In order to complete the above discussion, attention should be drawn to the following three significant points:

1. In the transition from below to above a certain LSL, it is assumed in the above argument that the duration of the stress distribution over a given cross section partly below and partly above that LSL lasts only during a single computation cycle; however, this process may last during several computation cycles the number of which may be different for two different time steps;

2. from the first point above, it may be concluded that the accumulated value of the axially induced internal moment increments in the transition from below to above a certain LSL corresponding to a larger time step may not necessarily be greater than that of a smaller time step; and

3. for the choice of a certain time step, the possible error in the maximum column load brought about at a certain LSL may not have the same direction as the error caused at other limiting stress levels; thus, the overall effect on the maximum column load would depend on the degree of proximity of the various limiting stress levels and the size of the loading rate.

The present analysis leads to the following procedure for testing the sufficiency of a given time step uniformly applied to the determination of maximum load for columns with different initial imperfections each of which corresponds to the same set of different loading rates:

First a column with small initial imperfection is chosen and for the largest given loading rate, the maximum column load is obtained for two different time steps, Δt_1 and Δt_2. If the two maximum column loads, $P_{max\ 1}$ and $P_{max\ 2}$, corresponding to Δt_1 and Δt_2 respectively do not appreciably differ from each other, the larger time step, Δt_1, is satisfactory for initial imperfections equal to or greater than the current value, as a consequence of which the test is resumed on a column with a smaller initial imperfection; however, if $P_{max\ 1}$ and $P_{max\ 2}$ considerably differ from each other, the next largest loading rate is tried, etc., until all the loading rates are exhausted, in which case a column with larger initial imperfection is tried. Now, the following situations may arise:

1. If for the largest initial imperfection and the smallest given loading rate, appreciable difference in $P_{max\ 1}$ and $P_{max\ 2}$ is observed, then the larger time step, Δt_1, is not appropriate and a smaller value must be tried;

2. if, on the other extreme side, for the smallest initial imperfection and largest loading rate, $P_{max\ 1}$ and $P_{max\ 2}$ are found not to appreciably differ from each other, then the larger time step, Δt_1, is good for all the given columns and a larger value may be tried if desired; and

3. if during the trial process outlined above, $P_{max\ 1}$ and $P_{max\ 2}$ are found to appreciably differ from each other for the first time

corresponding to a certain initial imperfection and a certain loading rate, then the larger time step, Δt_1, is good for all the columns with larger initial imperfections; however, for the same initial imperfection, the time step, Δt_1, may not be satisfactory unless at a smaller loading rate the difference between $P_{max\ 1}$ and $P_{max\ 2}$ becomes negligible again.

In order to illustrate the above analysis, Column No. 12 in Table 4A with the small initial deflection, $U_o = 10^{-3}$ centimeters and the largest of the loading rates, c = 10000 Newtons per second is chosen for the first trial. With a time step, Δt_1 = .01 seconds, the maximum column load, $P_{max\ 1}$, for this column recorded in Table 4A is 16 100 Newtons. Choosing a time step, Δt_2 = .001 seconds to be also applied in subsequent tests below, the maximum column load, $P_{max\ 2}$, is found to be 16 100 Newtons again. Thus, with no observed difference between $P_{max\ 1}$ and $P_{max\ 2}$, the test according to the above analysis is resumed on a column with smaller initial imperfection, i.e., Column No. 6 in Table 4 with $U_o = 10^{-4}$ centimeters and c = 10 000 Newtons per second. For this case the recorded value of $P_{max\ 1}$ in Table 4 is 16 600 Newtons and $P_{max\ 2}$ is found to be 17 250 Newtons, which indicates that the larger time step, Δt_1 = .01 seconds leads to considerable error for the actual column, or for columns with the same loading rate and smaller initial deflections.

For columns with the same initial imperfection as Column No. 6 of Table 4A but with smaller loading rates, the test has to continue. For Column No. 5, with c = 5 000 Newtons per second, the values of $P_{max\ 1}$ and $P_{max\ 2}$ are 15 350 and 16 045 Newtons respectively. Since the difference is still appreciable, the test is applied to Column No. 4 with c = 2 000 Newtons per second leading to $P_{max\ 1}$ = 14 360 Newtons and $P_{max\ 2}$ = 14 316 Newtons. Similarly, Column No. 3 of Table 4A with c =

1 000 Newtons per second leads to $P_{max\ 1}$ = 14 060 and $P_{max\ 2}$ = 14 040 Newtons. In the case of the last two columns, the observed error lies within the acceptable bounds.

In the above numerical investigation, we actually started with Column No. 12 of Table 4A with $U_o = 10^{-3}$ centimeters and the largest value of the loading rates. Since no error in P_{max} was observed, the test was transferred to Column No. 6 with smaller initial deflection without actually trying other loading rates before shifting to a lower initial deflection. This was done in accordance with the above analysis. In order to numerically verify this procedure, we maintain the same initial deflection as Column No. 12 ($U_o = 10^{-3}$ centimeters) and try smaller loading rates with the same values of Δt_1 and Δt_2. Thus, Column No. 11 of Table 4A with c = 5 000 Newtons per second results in $P_{max\ 1}$ = 14 850 Newtons and $P_{max\ 2}$ = 14 835 Newtons; Column No. 10 with c = 2 000 Newtons per second leads to $P_{max\ 1}$ = 13 900 Newtons and $P_{max\ 2}$ = 13 898 Newtons; and Column No. 9 results in $P_{max\ 1}$ = 13 590 Newtons and $P_{max\ 2}$ = 13 596 Newtons. It should be noted that the observed difference between $P_{max\ 1}$ and $P_{max\ 2}$ corresponding to Columns 9 - 11 of Table 4A is less than the loading increment, ΔP, corresponding to a single time step, Δt_1, in each particular case.

Thus, the numerical results obtained indicate that the choice of Δt = .01 seconds for the first 36 columns recorded in Table 4A is good in all cases except for Columns 5 and 6 in which case the time step, Δt, must be decreased. For columns with the tendency to fail in the reverse direction as indicated in Table 4A, the choice of the time step may have significant influence on the buckling behaviour. This fact is, however, further explained in Chapter 10.

It should be noted that the discussion in this section was limited to the results in Table 4A. However, similar observations are made for the results corresponding to Tables 4B and 4C. Thus, in presenting the results in diagrammatic form in subsequent chapters, attention is paid to the possible influence of the computation time step, Δt, by using $\Delta t = .001$ seconds, in cases where such a low value of Δt is warranted. Additional gains in accuracy in some few cases may be obtained by further decreasing the time step, Δt, below .001 seconds, or by incorporating additional subroutines in the program to eliminate the secondary effects brought about by the interrelationship of the limiting stress levels and the size of the load increment corresponding to one computation cycle. However, numerical results indicate that possible marginal gains attained in the numerical results presented herein, in cases for which the maximum column load has not yet converged to the true value, would be in the direction of increasing maximum column load. It should be noted that this last conclusion applies only to normally behaving columns which do not fail in reverse direction.

9. VARIATIONS OF MAXIMUM COLUMN LOAD

9.1 Decisive Factors Influencing the Size of the Maximum Column Load

The magnitude of the maximum column load for a column of given dimensions is entirely dependent on the shape of the stress strain diagram, and the dynamic state of the column at the beginning of buckling Phase 2. This dynamic state summarizes tha accumulated influences of initial imperfection, disturbances, eccentricity and of the dynamic charateristics of buckling Phase 1. It should be reminded that the dynamic state implies the magnitudes of the state space variables described in Sec. 6.1. As soon as the axial load ceases to increase at the end of buckling Phase 1, maximum strain reversal would be developed in the column simultaneously with a complete disappearance of the axially induced internal moment increments. This state of affairs which is illustrated in Fig. 39, would be maintained throughout buckling Phase 2.

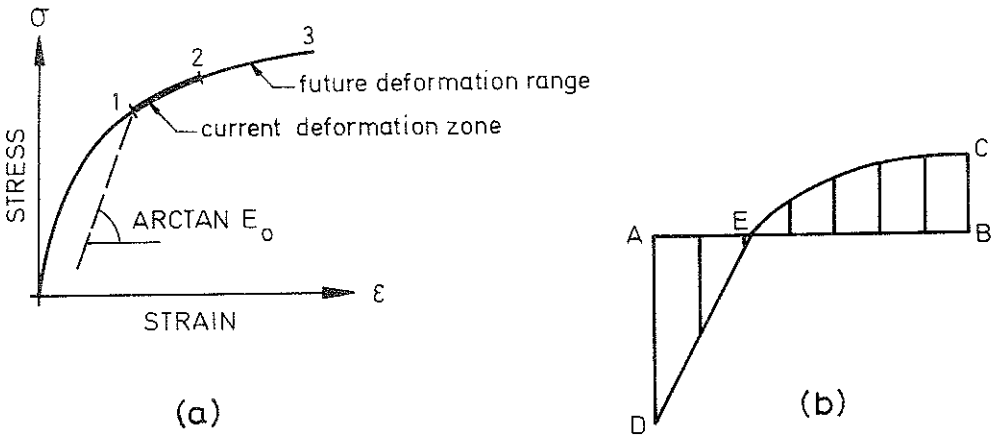

FIG. 39. STRESS STRAIN STATE OF THE COLUMN AT THE BEGINNING OF BUCKLING PHASE 2: (a) STRESS STRAIN DIAGRAM; (b) INCREMENTAL STRESS DISTRIBUTION AT THE CROSS SECTION OF MAXIMUM STRAIN

Figs. 39(a) and (b) show the stress strain diagram and an assumed incremental stress distribution at the cross section of maximum strain at the beginning of buckling Phase 2 correspondingly. The heavily marked zone 1 2 in Fig. 39(a) corresponds to the current deformation of the region of increasing bending strain indicated by EB in Fig. 39(b). Thus, points 1 and 2 in Fig. 39(a) show the current stress levels at points E and B of Fig. 39(b) respectively. At the region of decreasing bending strain shown by AE in Fig. 39(b), the deformation takes place along various unloading lines with a common modulus of elasticity, E_o.

Now, the question of the maximum column load could only be settled, if we could determine how far the deformation of the cross section AB in Fig. 39(b) would advance on the future deformation range of the stress strain diagram shown by the portion 2 3 in Fig. 39(a) which is a continuation of the stress strain diagram beyond the current deformation zone. In addition to the shape of the stress strain diagram, this question is in turn dependent on the existing kinetic energy of the column as well as on the existing value of TIMS (total internal moment surplus) which was defined in Sec. 7.4 as the value of the expression, $|M_i| - |M_e|$, i.e., the difference between the absolute values of the total internal and external moments. On a ceteris paribus basis, the larger the existing kinetic energy or the smaller the value of the TIMS, the greater would be the subsequent advance along the future deformation range in Fig. 39(a).

The shape of the stress strain diagram determines the SMI (surplus moment increment) values generated during subsequent motion of the column during buckling Phase 2. Since no axially induced internal moment

increment is acting during Phase 2 due to the constancy of the axial load, the maximum strain reversal which occurs, Fig. 39(b), becomes fully effective in developing the maximum bending rigidity of the column. The question of a possible motion reversal position, now, depends on whether this increase in bending rigidity under constant axial load, is capable of neutralizing the effects of the kinetic energy and a possible negative value of TIMS at the start of Phase 2.

From the above discussion, it follows that the question of stability of the column during Phase 2 is crucially dependent on the magnitude of TIMS and the kinetic energy at the end of Phase 1. These two factors are, in turn, determined by the whole loading history during buckling Phase 1. In addition to the initial imperfections and possible velocity disturbances, the loading rate may significantly affect the buckling behaviour and consequently the values of TIMS and kinetic energy simultaneously with loading. On a ceteris paribus assumption, an increase in loading rate for the same rotation of a column cross section may result in a greater value of the axially induced moment increment. This in turn may lead to a larger decrease of the internal moment and subsequent reduction in the value of TIMS simultaneous with the increase of axial load.

The possible occurrence of strain reversal during buckling Phase 1 and oscillations simultaneous with loading are two significant phenomena which might considerably affect the buckling behaviour, explained as follows:

1. The occurrence of strain reversal simultaneous with loading alone without oscillations, may have two opposing influences. Firstly, it develops a larger laterally induced internal moment increment during

the course of lateral deflection, in which case the value of SMI is increased; secondly, the phenomenon of strain reversal may increase the axially induced bending moment due to a larger discrepancy between the governing tangent moduli on the given cross section of the column. Thus, the occurrence of strain reversal during a computation cycle increases both the value of the surplus moment increment, SMI, and that of the axially induced internal moment increment, ΔM_{ia}. In other words, strain reversal may either increase or decrease the bending rigidity of the column. The net effect depends on which of the two quantities, SMI, and, ΔM_{ia}, is more greatly affected.

2. The influence of oscillations simultaneous with loading without strain reversal is illustrated in Fig. 40.

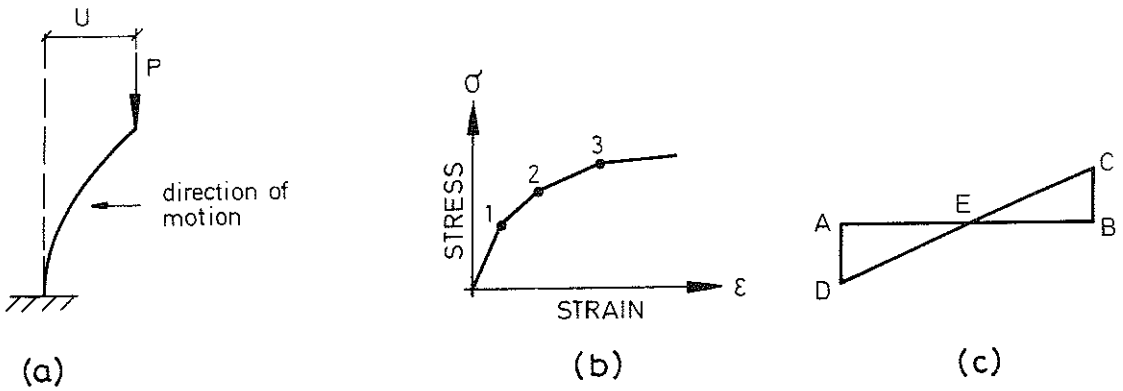

FIG. 40. ILLUSTRATION OF OSCILLATORY EFFECT: (a) COLUMN RETURNING FROM A MOTION REVERSAL POSITION; (b) MULTILINEAR STRESS STRAIN DIAGRAM; (c) INCREMENTAL STRESS DISTRIBUTION ON THE CROSS SECTION OF MAXIMUM STRAIN ON A LINE OF CONSTANT TANGENT MODULUS WITHOUT STRAIN REVERSAL

Fig. 40(a) shows a column which is moving in reverse direction

subsequent to a motion reversal in the original direction. We now make the following assumptions:

a. At the time the column switches from the original to the reverse direction, the stress at Point B in Fig. 40(c) would attain the LSL (limiting stress level) denoted by Point 1 in Fig. 40(b); and

b. before the column reaches the next motion reversal position in reverse direction, the zone of currently decreasing bending strain, EB, (note that the column is currently moving backwards) in Fig. 40(c) would wholly deform on the stresses strain interval, 1 2, in Fig. 40(b), regardless of whether or not the column has passed the position of zero deflection (U = 0).

If the above two assumptions are simultaneously satisfied, it would contribute to decreasing the ensuing lateral deflection simultaneous with loading in the original direction. This would also contribute to diminishing the advance of the zone of increasing bending strain during forward motion on the given stress strain diagram. Thus, due to the higher values of tangent moduli on the lower portions of the stress strain diagram, the value of the surplus moment increment simultaneous with the increase of axial load may increase, while the axially induced internal moment may decrease. Both these effects tend to increase the magnitude of the total internal moment on a ceteris paribus basis. This argument stated for a column having a stress strain diagram with continuously decreasing or piecewise constant tangent modulus would be as follows: If during the process of oscillations simultaneous with loading and without strain reversal, the backward motion of the column during a given cycle coincides with a region of the stress strain diagram in which the tangent moduli change more sharply than in the immediately preceding and in the immediately succeding region corresponding to forward motion, then this coincidence would contribute to diminishing the advance of the zone of increasing bending strain on the stress strain diagram during subsequent forward motion.

If analogous oscillatory behaviour is observed in other stress strain intervals, see Fig. 40(b), the total net effect would be an increase of the TIMS value at the end of buckling Phase 1. It should be noted that if the backward deflection of the column simultaneous with loading passes the position of zero deflection under favourable conditions, to be discussed herein in Secs. 10.1 and 10.2, the column may permanently deflect in reverse direction.

It should be observed that an increase of TIMS or a possible decrease of the kinetic energy of the column at the end of Phase 1 would result in a decreasing lateral deflection of the column during Phase 2 before attaining a possible motion reversal position. Thus, for a stress strain diagram with continuously decreasing or piecewise constant tangent modulus, an increase of TIMS or a decrease of the kinetic energy at start of Phase 2 may lead to an increase of the maximum column load and vice versa.

From the above discussion, it may be inferred that under favourable conditions, the oscillatory behaviour simultaneous with loading may increase the maximum column load; however, opposite result would be obtained if the backward motion of the column in the above analysis is substituted for the forward motion and vice versa. Thus, the oscillatory behaviour simultaneous with loading and without strain reversal may either increase or decrease the maximum column load. The same conclusion is also valid in the case of the occurrence of strain reversal simultaneous with loading as already discussed in this section. However, it should be pointed out that due to vanishing of the axially induced internal moment during buckling Phase 2, the occurrence of strain reversal under constant axial load activates the maximum internal bending moment capability of the column.

The analysis of the endogeneous decisive factors influencing the maximum column load in this section constitutes a partial basis for the exploration of the effect of exogeneous variables including the velocity disturbances, initial imperfection and loading rate presented in the next three sections. It should be mentioned that the exogeneous variables, which have been effective during the past loading history, indirectly affect the question of final stability of the column through their direct influence on the creation of the current dynamic state.

9.2 Influence of Variations of Velocity Disturbances

A velocity disturbance could be imparted to a column in form of impact velocity either as initial disturbance (at the tangent modulus load for a perfect column and at zero load level for an imperfect column), or as a disturbance applied at any arbitrary loading level.

Denoting the maximum column load by P_{max}, initial velocity by V_o, and a velocity disturbance corresponding to any load level by V_1, then the signs of the partial derivatives, $\partial P_{max}/\partial V_o$, and $\partial P_{max}/\partial V_1$, are not uniquely defined, i.e., they may be either positive or negative depending on the sizes of V_o and V_1, the shape of the stress strain diagram and the sizes of all other dynamic parameters. This may be shown by the following argument:

The tendency of the column to oscillate simultaneous with loading may get accentuated by introducing velocity disturbances. Furthermore, the occurrence, the corresponding load level, and the extent of propagation of a possible strain reversal in the column may be affected due to a velocity disturbance. Since, according to the analysis of the previous section, the influence of oscillations and strain reversal simultaneous with loading on the size of the maximum column load can either be positive or negative, it follows that the effect of a velocity disturbance may tend either to decrease or increase the maximum column load. This conclusion is, however, inferred from the assumption that oscillations and/or strain reversal occur in the column subsequent to the action of a velocity disturbance. Nevertheless, if no oscillations or strain reversal are observed during buckling Phase 1 either with or

without a velocity disturbance, then a velocity disturbance applied in the direction of motion would increase the kinetic energy without any oscillatory phenomenon. In that case the lateral deflection of the column would increase and the value of the maximum column load for a stress strain diagram with a continuously decreasing or piecewise constant tangent modulus may fall.

If the velocity disturbance is applied in the original direction of motion during buckling Phase 2, the kinetic energy of the column is increased, in which case, the maximum column load, according to the analysis of the previous section, would decrease.

The effect of velocity disturbances on the maximum column load of Model 3 during both buckling phases is numerically illustrated in Fig. 41, in which Column No. 11 of Table 4A is chosen as the starting point and subsequent variation of maximum load for this column is determined as a function of varying end velocity disturbance. This illustration shows that a velocity disturbance imparted at the beginning of buckling Phase 2 always reduces the maximum column load (dashed line) whereas the same velocity disturbance imparted at the start of Phase 1 turns out to exert a stronger influence which may either decrease or increase the maximum column load (full line). For larger velocity disturbances at the start of Phase 1, the maximum column load happens to appreciably decrease. In order to clearly visualize the effect of small velocity disturbances, the variation of the maximum column load as a function of velocity disturbance, in the range of zero to .01 centimeters per second, is additionally shown in Fig. 41 to the left of the diagram with a horizontal scale which is 40 times magnified in comparison with the horizontal scale to the right.

9.2 Influence of Variations of Velocity Disturbances

A velocity disturbance could be imparted to a column in form of impact velocity either as initial disturbance (at the tangent modulus load for a perfect column and at zero load level for an imperfect column), or as a disturbance applied at any arbitrary loading level.

Denoting the maximum column load by P_{max}, initial velocity by V_o, and a velocity disturbance corresponding to any load level by V_1, then the signs of the partial derivatives, $\partial P_{max}/\partial V_o$, and $\partial P_{max}/\partial V_1$, are not uniquely defined, i.e., they may be either positive or negative depending on the sizes of V_o and V_1, the shape of the stress strain diagram and the sizes of all other dynamic parameters. This may be shown by the following argument:

The tendency of the column to oscillate simultaneous with loading may get accentuated by introducing velocity disturbances. Furthermore, the occurrence, the corresponding load level, and the extent of propagation of a possible strain reversal in the column may be affected due to a velocity disturbance. Since, according to the analysis of the previous section, the influence of oscillations and strain reversal simultaneous with loading on the size of the maximum column load can either be positive or negative, it follows that the effect of a velocity disturbance may tend either to decrease or increase the maximum column load. This conclusion is, however, inferred from the assumption that oscillations and/or strain reversal occur in the column subsequent to the action of a velocity disturbance. Nevertheless, if no oscillations or strain reversal are observed during buckling Phase 1 either with or

without a velocity disturbance, then a velocity disturbance applied in the direction of motion would increase the kinetic energy without any oscillatory phenomenon. In that case the lateral deflection of the column would increase and the value of the maximum column load for a stress strain diagram with a continuously decreasing or piecewise constant tangent modulus may fall.

If the velocity disturbance is applied in the original direction of motion during buckling Phase 2, the kinetic energy of the column is increased, in which case, the maximum column load, according to the analysis of the previous section, would decrease.

The effect of velocity disturbances on the maximum column load of Model 3 during both buckling phases is numerically illustrated in Fig. 41, in which Column No. 11 of Table 4A is chosen as the starting point and subsequent variation of maximum load for this column is determined as a function of varying end velocity disturbance. This illustration shows that a velocity disturbance imparted at the beginning of buckling Phase 2 always reduces the maximum column load (dashed line) whereas the same velocity disturbance imparted at the start of Phase 1 turns out to exert a stronger influence which may either decrease or increase the maximum column load (full line). For larger velocity disturbances at the start of Phase 1, the maximum column load happens to appreciably decrease. In order to clearly visualize the effect of small velocity disturbances, the variation of the maximum column load as a function of velocity disturbance, in the range of zero to .01 centimeters per second, is additionally shown in Fig. 41 to the left of the diagram with a horizontal scale which is 40 times magnified in comparison with the horizontal scale to the right.

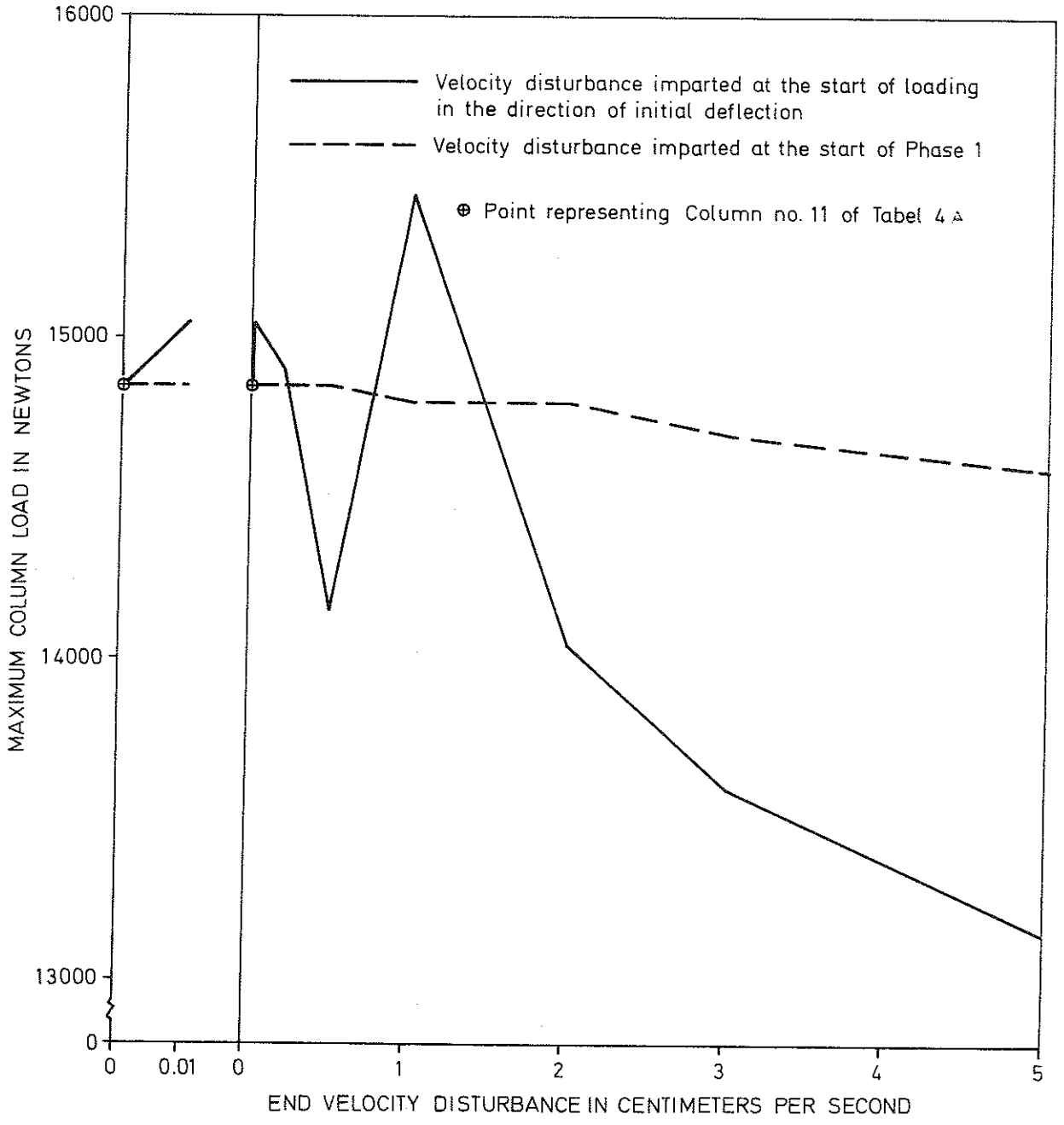

FIG. 41. EXAMPLE OF VARIATION OF MAXIMUM COLUMN LOAD AS A FUNCTION OF VELOCITY DISTURBANCES AT THE BEGINNING OF EITHER OF THE TWO BUCKLING PHASES FOR COLUMN NO. 11 OF TABLE 4 A.

9.3 Influence of Variations of Initial Eccentricity or Initial Deflection

Denoting the initial eccentricity by X_o, the initial deflection by U_o, then in the absence of a disturbance velocity and with the exception of a possible anomaly for a column with a tendency to bow permanently backwards - to be discussed in Secs. 10.1 and 10.2 - the two partial derivates, $\partial P_{max}/\partial X_o$ and $\partial P_{max}/\partial U_o$, may turn out to be positive under the circumstances described below.

If two columns A and B are different in initial end deflection, U_{oa} respective U_{ob}, and identical in every other respect, and if U_{oa} is assumed to be greater than U_{ob}, then the maximum column load, determined according to the procedure described in Sec. 7.8, would usually be less for column A than column B. This could be shown by the following argument:

During buckling Phase 1, Column B's deflection, U_b, would be less than Column A's deflection, U_a, at all loading levels. This is due to the fact that the initial value of deflection is less for Column B than Column A and all other things are identical. Besides, assuming that there is no disturbance velocity to induce interfering oscillations, then, at the same axial load at the end of buckling Phase 1, Column A has a greater deflection which leads to the result that the zone of increasing bending strain in Column A has attained higher stress levels with lower tangent moduli. Consequently, during buckling Phase 2, the surplus moment increment, ΔM, would be less for Column A during all consecutive deflection intervals. Thus, Column A may attain maximum load at a lower value than Column B. This proves the assertion. This argument, of course

assumes the existence of a stress strain diagram with continuously decreasing or piecewise constant tangent modulus. Furthermore, it should be noted that the effect of eccentricity on the size of the maximum column load is analogous to the influence of the initial end deflection.

If, however, the difference in initial imperfection gives rise to a completely different oscillation and strain reversal pattern, then the effect on the maximum column load could either be positive or negative. Thus, according to the present interpretation, if the oscillation and/or strain reversal pattern in the two columns mentioned above appreciably differ from each other, their influence on the maximum column load leads to a result different from that predicted above.

The effect of initial imperfection on the size of maximum column load of Model 3 is numerically illustrated in Figs. 42 A, 42 B and 42 C corresponding to the three data sets whose results were recorded in Tables 4 A, 4 B, and 4 C respectively. For a clear pictorial representation, the variation of maximum column load as a function of the initial deflection in the range of zero to .001 centimeters in Fig. 42 A, and in the range zero to .002 centimeters in Figs. 42 B and 42 C is shown to the left of each diagram with a horizontal scale which is 200 times magnified in comparison with that to the right.

The three different data sets, originally given in Sec. 8.7, contain the following numerical values corresponding to the simple column in Fig. 12:

The first data set contains the following basic data:

$L = 2.5$ m; $b = d = 5$ cm; $A = 5$ cm^2; $M = 100$ kg; and $E_o = 10^{10}$ N/m^2.

The second data set has the following basic data:

$L = 5$ m; $b = d = 10$ cm; $A = 5$ cm^2; $M = 500$ kg; and $E_o = 10^{10}$ N/m^2.

The third data set consists of the following basic data:

$L = 5$ m; $b = 5$ cm; $d = 10$ cm; $A = 5$ cm^2; $M = 500$ kg; and $E_o = 10^{11}$ N/m^2.

Figs. 42 A, 42 B and 42 C corresponding to the above three data sets show that the maximum column load for all loading rates continuously decreases as the initial end deflection increases. This is the normal column behaviour which may be violated by the abnormally behaving backwards-inclined columns (see Sec. 10.5). For a discussion of the influence of the loading rate on the size of the maximum column load, see Sec. 9.4.

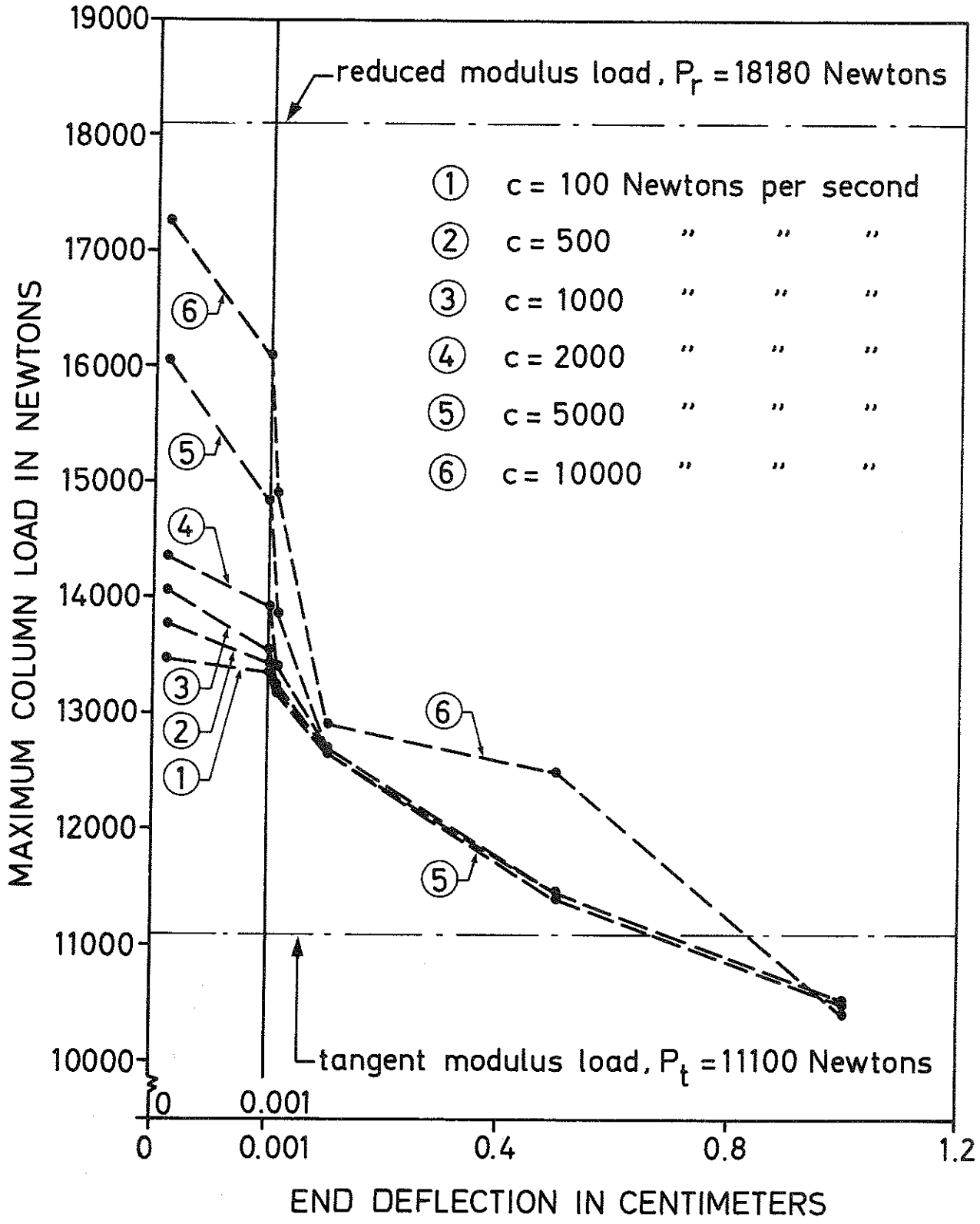

FIG. 42 A. VARIATION OF MAXIMUM COLUMN LOAD AS A FUNCTION OF THE INITIAL DEFLECTION CORRESPONDING TO THE FIRST DATA SET.

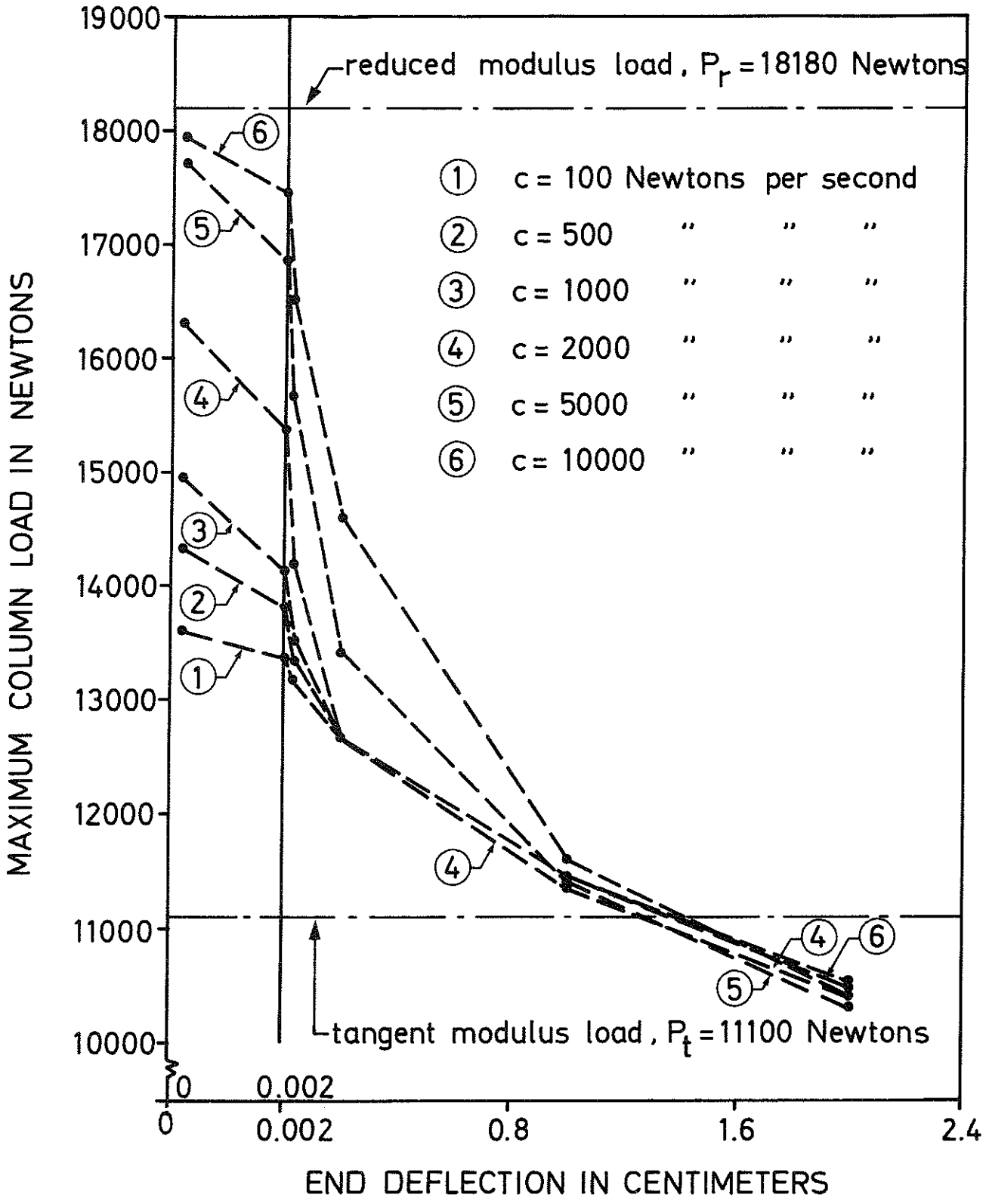

FIG. 42 B. VARIATION OF MAXIMUM COLUMN LOAD AS A FUNCTION OF THE INITIAL DEFLECTION CORRESPONDING TO THE SECOND DATA SET.

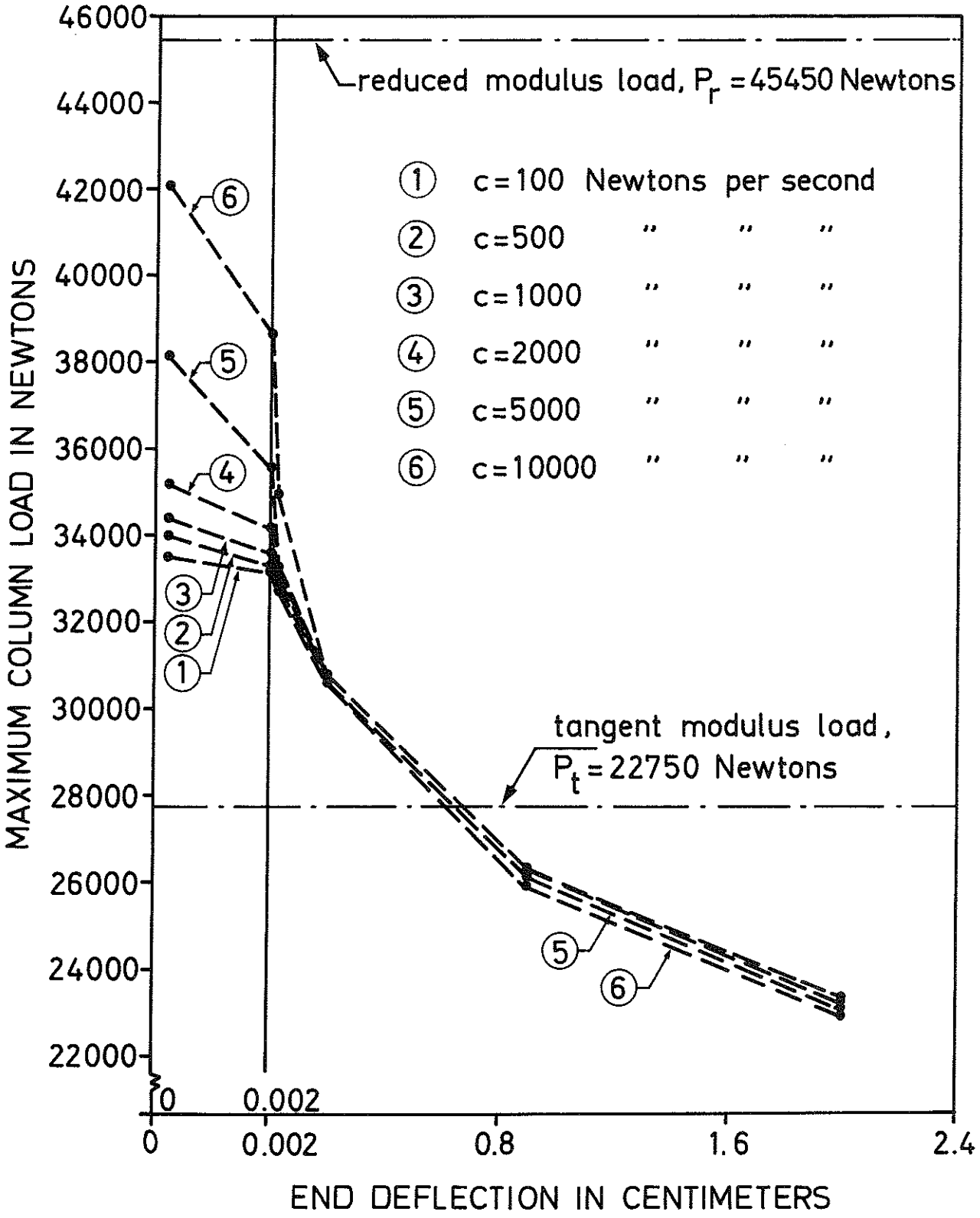

FIG. 42 C. VARIATION OF MAXIMUM COLUMN LOAD AS A FUNCTION OF THE INITIAL DEFLECTION CORRESPONDING TO THE THIRD DATA SET.

9.4 Influence of Variations of Loading Rate

Denoting the loading rate by c, the partial derivative, $\partial P_{max}/\partial c$, can be either positive or negative, even in the absence of a velocity disturbance. This nonuniqueness of the sign of the partial derivative arises due to the following reasons:

1. For sufficiently slow loading rates, oscillations may be induced in the column during buckling Phase 1, as predicted in Sec. 7.5, with the possibility of strain reversal simultaneous with loading. The effect of these phenomena on the size of the maximum column load, however, can either be positive or negative according to the analysis of Sec. 9.1.

2. For a certain increase of axial load, ΔP, during a computation cycle, a decrease in loading rate may give the column more time to bow laterally, in which case the value of the corresponding deflection increment would increase. Due to greater deflection, there would be a further advance of the zone of increasing bending strain, at the cross section of maximum strain, on the stress strain diagram with possibly lower tangent moduli. Now, if the decrease in bending rigidity due to lower values of tangent moduli does not offset the increase in laterally induced internal moment, ΔM_{ib}, due to possible strain reversal, then the effect of a decrease in loading rate may increase ΔM_{ib} during the respective deflection interval. However, the corresponding axially induced bending moment increment, ΔM_{ia}, may also increase due to a possibly greater variation of the values of the tangent moduli on the actual cross section, recall the analysis of Sec. 7.3. This possible increase in ΔM_{ia} may offset the possible increase in the corresponding ΔM_{ib}. Thus, the net effect on the current value of the internal moment can change in either direction.

3. A decrease in loading rate may result in a larger lateral deflection at the start of buckling Phase 2 with correspondingly smaller internal moment capacity during this phase provided that the stress strain diagram has continuously decreasing or piecewise constant tangent modulus. Thus, the behaviour of the column during buckling Phase 2 may lead to a decrease in the maximum column load due to a decrease in the loading rate during Phase 1.

The effect of the loading rate on the maximum column load for various initial imperfection of Model 3 is numerically illustrated in Figs. 43 A, 43 B and 43 C corresponding to the three different data sets with results according to Tables 4 A, 4 B and 4 C respectively. The basic data corresponding to these three data sets were given again in the previous section. The results show that the largest variation of the maximum column load as a function of the loading rate occurs for small initial imperfections. Furthermore, the illustrations in Figs. 43 A, 43 B and 43 C show that for nearly all initial deflections, the maximum column load increases as the loading rate increases; however, in a few cases where the initial deflection is large, an increase of axial load has resulted in a slight decrease of the maximum column load.

A comparison of Figs. 43 A and 43 B shows, that for the same initial modulus of elasticity, the influence of the loading rate on the size of the maximum column load is greater for a longer column with greater mass (second data set). A comparison of Figs. 43 B and 43 C shows that the influence of the loading rate on the size of the maximum column load decreases as the initial modulus of elasticity increases. It should be noted that the same observations could be made by a study of Figs. 42 A, 42 B and 42 C.

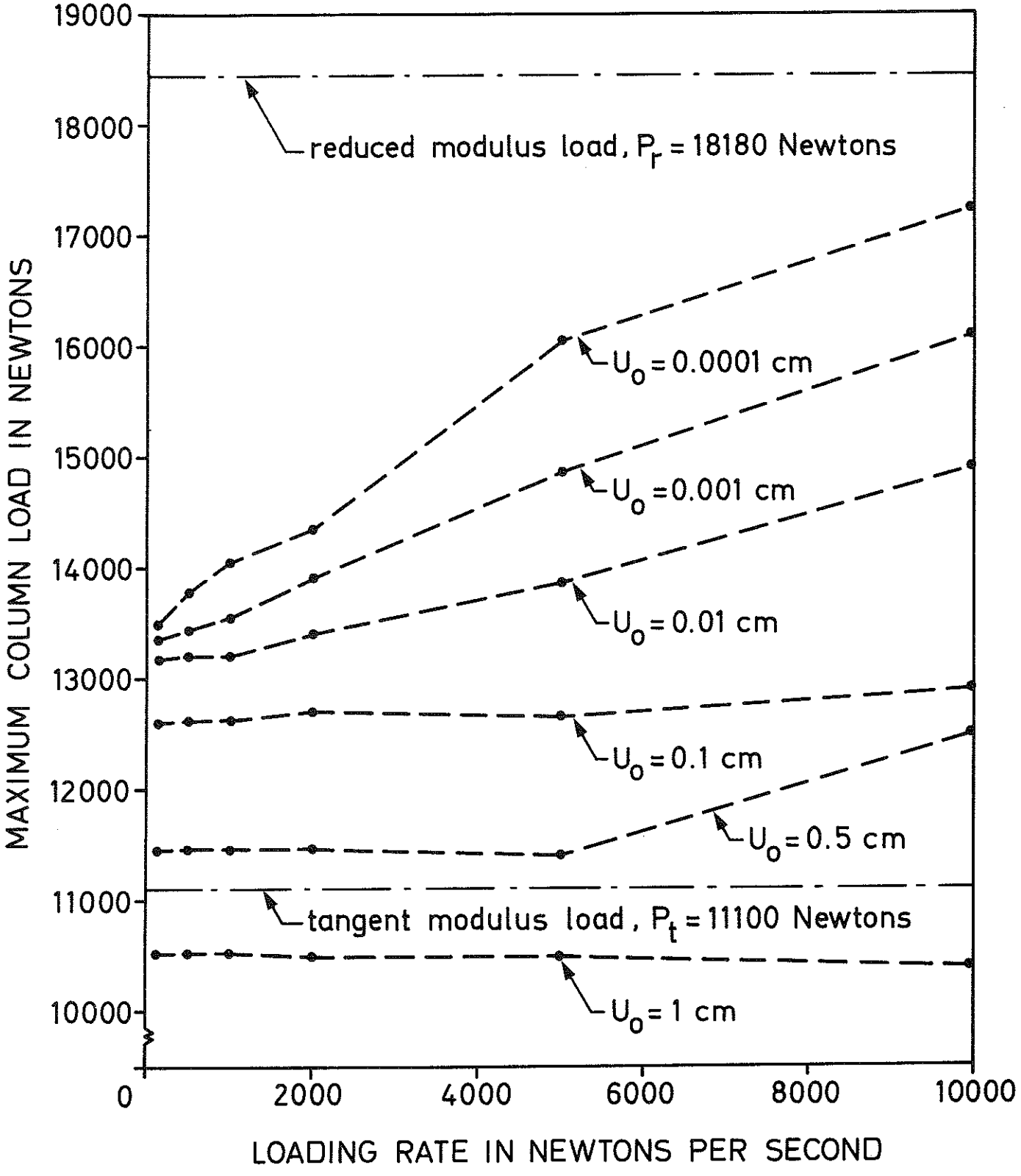

FIG. 43 A. VARIATION OF THE MAXIMUM COLUMN LOAD AS A FUNCTION OF THE LOADING RATE CORRESPONDING TO THE FIRST DATA SET.

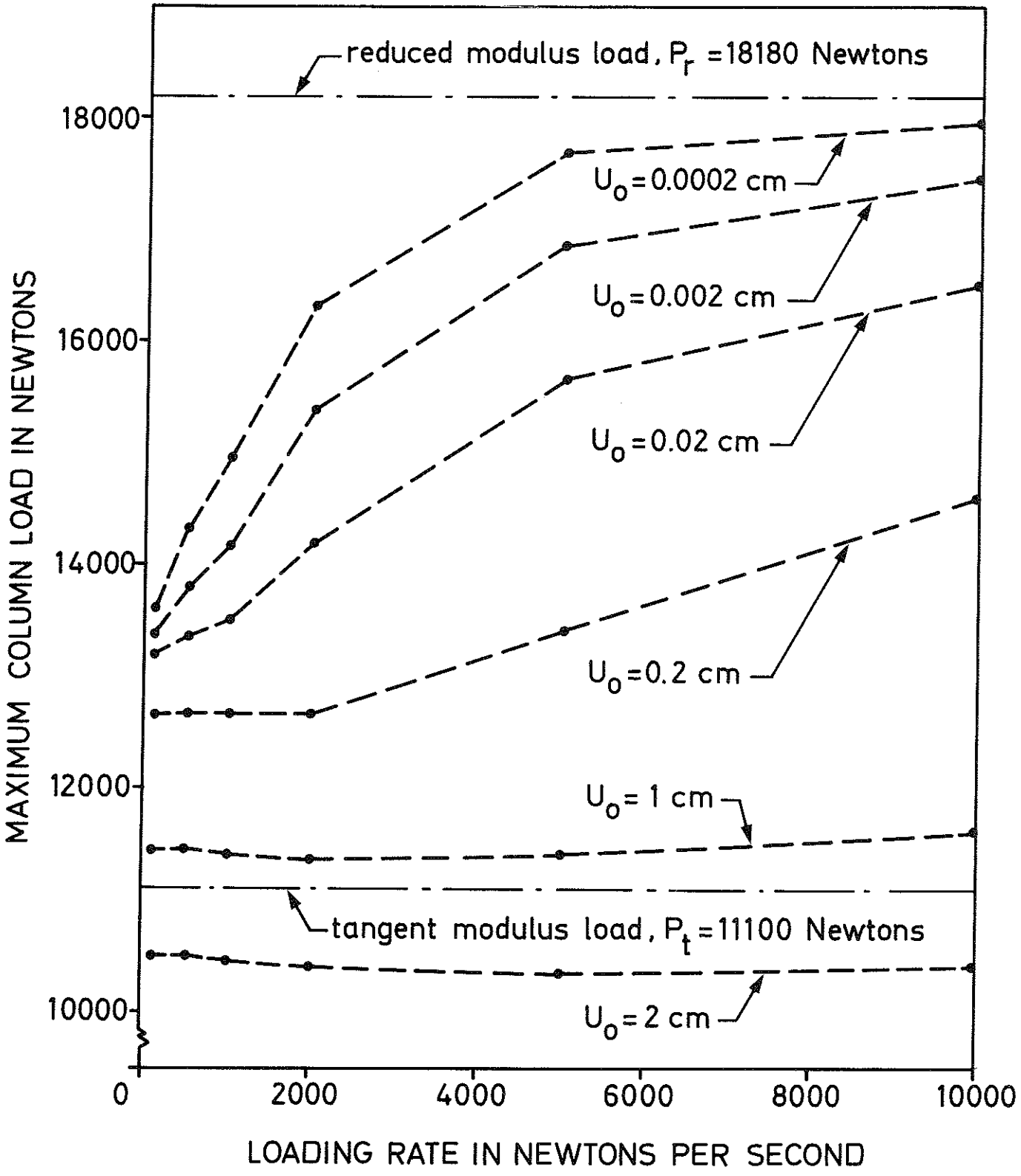

FIG. 43 B. VARIATION OF THE MAXIMUM COLUMN LOAD AS A FUNCTION OF THE LOADING RATE CORRESPONDING TO THE SECOND DATA SET.

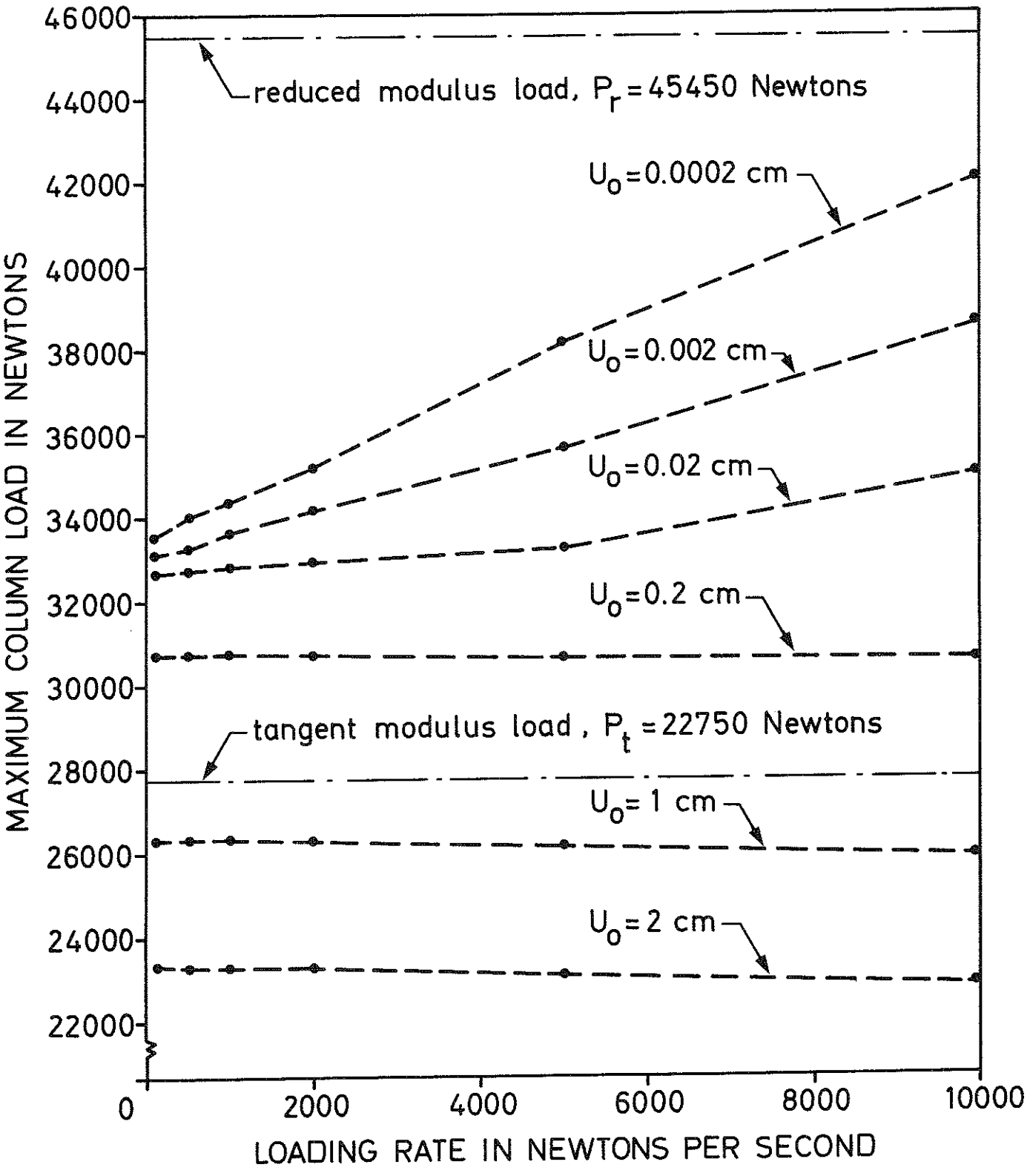

FIG. 43 C. VARIATION OF THE MAXIMUM COLUMN LOAD AS A FUNCTION OF THE LOADING RATE CORRESPONDING TO THE THIRD DATA SET.

10. ADDITIONAL SALIENT BUCKLING PHENOMENA

Introductory Remarks

This chapter is devoted to gaining additional insight in the buckling properties of an inelastic column with arbitrary stress strain diagram. Particularly in the first two following sections, a buckling concept is developed which predicts that under certain circumstances, it is possible for a column initially deflected in a certain direction to permanently bow or fail in the reverse direction. A column with such behaviour is identified herein as "backwards-inclined". Sec. 10.1 explains the fact that this phenomenon may be induced due to a certain velocity disturbance in combination with a favourable combination of dynamic parameters. Sec. 10.2 develops the idea that this phenomenon may be self-induced in the absence of velocity disturbances and with a well-disposed parameter combination.

However, it should be noted that according to the analysis of Secs. 10.1 and 10.2 a backwards inclined-column, regardless of whether its behaviour is induced or self generated, requires a small initial deflection. Particularly, in the case of a self-induced backwards-inclined column, the initial state may be charaterized by a nearly perfect inelastic column. Thus, it is evident that under these conditions, the slightest deviation of one column parameter from the desired combination may adversely affect the buckling behaviour in such a way that the expected phenomenon may no longer occur.

The above argument may explain the possible pitfall encountered in the numerical simulation of a backwards inclined column. This arises due

to the fact that a specified load-time relationship constitutes a parameter and a necessary ingredient for the observation of the phenomenon. An approximation of a continuous data system by a discrete data process causes a deviation which might turn out detrimental for the simulation of the physical event. Thus, by using the discrete data system developed in Appendix C, it is possible to generate a backwards-inclined column behaviour for the approximate method by choosing a certain calculation time step, Δt, without expecting to observe the phenomenon for different choices of Δt.

In reality, the multi-cycle computation technique treated in Appendix C gives the freedom of choice of an infinite number of load-time relationships each associated with a certain time step, Δt, corresponding to one computation cycle. Thus, on a ceteris paribus basis, the calculation time step, Δt, constitutes a parameter which cannot be chosen freely for the simulation of a backwards-inclined column. In other words, in the numerical simulations which follow in Secs. 10.1 and 10.2, the desired phenomenon is actually simultated for the approximate load-time relationship determined by the actual value of the time step, Δt. The possibility of the occurrence of the phenomenon for a continuous loading process would then follow from the principle that if a certain event could take place for a given load-time relationship, it may also occur for another loading process, but not necessarily with the same parameter combination.

In subsequent parts of this chapter, the effect of gravitational force and influence of possible changes in the direction of application of the axial load simultaneous with lateral deflection of the column during either one or both of the buckling phases are illustrated in

Sec. 10.3 and 10.4 respectively; an abnormal behaviour related to backwards-inclined columns is discussed in Sec. 10.5; and the lateral deflection properties of an inelastic column for axial loads below the maximum load is discussed in Sec. 10.6.

10.1 Induced Permanent Deflection in Reverse Direction

In Sec. 9.1, it was mentioned without further elaboration that a column initially deflected in one direction, may permanently bow or possibly fail in the reverse direction, due to some favourable velocity disturbance which may actually be introduced in forward direction, i.e., in the original bending direction. Our immediate aim is now to elaborate this question.

As a matter of illustration, we first show an extreme case where a column might fail in reverse direction during buckling Phase 2 when the stress strain diagram shown in Fig. 44 is applicable.

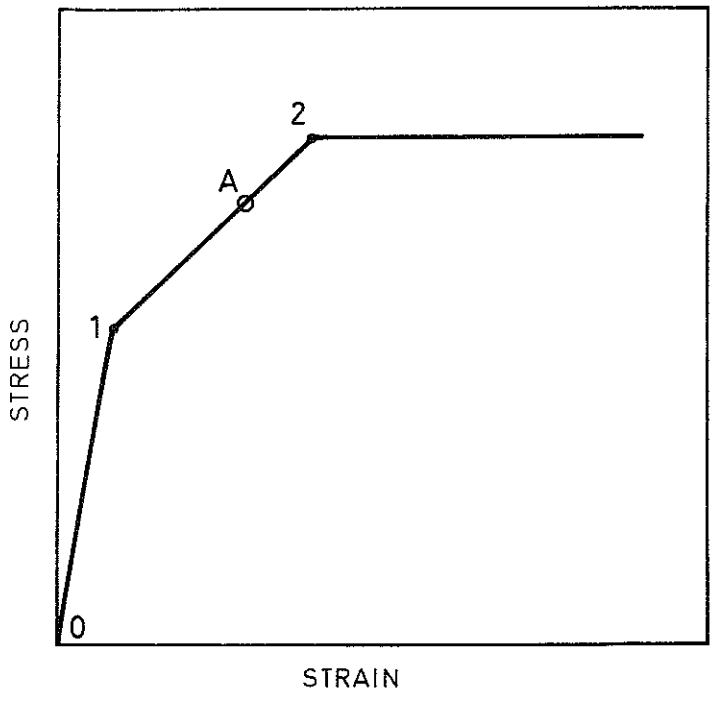

FIG. 44. A TRILINEAR STRESS STRAIN DIAGRAM

Suppose that a column with small initial deflection and with a trilinear stress strain diagram depicted in Fig.44 is subjected to a velocity disturbance at a stress level in the vicinity of point A. This disturbance is supposed to be sufficiently violent to start oscillatory cycles simultaneous with loading. Suppose further that just at the time when the most stressed part of the column attains limiting stress level 2, the column is in a position to reverse motion and starts travelling backwards. However, the tangent modulus at this load level is zero. Under these circumstances, the axial load may further increase and the stress levels in other parts of the column under increasing strain may reach level 2, in which case the bending rigidity of the column would soon approach zero. If at this instant the column has passed the point of zero deflection and the external moment at the cross section of maximum strain happens to be greater than the corresponding internal moment[1], then it could certainly be asserted that the column would indefinitely move in backward direction, according to the small displacement theory which is assumed to be valid throughout this work.

The above example illustrates the idea. We can now formalize the argument in more abstract manner. If, due to a disturbance velocity, oscillating cycles are induced in a column with relatively small deflection and excentricity and if the reverse motion of the column during some initial cycle coincides with a relatively sharp decrease in the tangent modulus, then due to a correspondingly sharp decrease in the bending rigidity, the column may undergo relatively large deflection before motion reversal takes place.

The above coincidence can incite in the column a tendency to deflect backwards more and more in subsequent oscillating cycles provided

---

1. This statement assumes absolute values of the moment magnitudes.

that the shape of the stress strain diagram during future oscillations is favourable to this phenomenon.

The above salient phenomenon reveals that, it may be possible for a column to become backwards-inclined. Thus, despite its initial deflection or eccentricity in one direction, a backwards inclined column may end up with a permanent deflection in reverse direction. The column may even attain its maximum axial load while moving in reverse direction during buckling Phase 2.

The property discussed above may be illustrated in Fig. 45 by studying the load deflection behaviour of Column No. 37 from Table 4A.

Fig. 45 shows the buckling behaviour of the given column during Phase 1 (full line) and lateral motion during Phase 2 (dashed line) at axial load levels corresponding to 10 000 and 14 850 Newtons. The last load level studied is just one computation cycle below the maximum column load. It may be observed that the initial velocity of .2 centimeters per second, imparted to the column at zero level, incites oscillatory cycles simultaneous with loading which gradually cause permanent bowing in reverse direction. During each buckling Phase 2, at the constant load levels mentioned above, the motion of the simple column is followed up to three successive motion reversal positions indicated in Fig.45 by points 1, 2 and 3 respectively. This is a sufficient number of trials before the column attains the state of a simple harmonic motion, recall the analysis of Sec. 6.5.

Columns are normally forwards-inclined. They could become backwards-inclined due to some velocity disturbance under favourable con-

ditions, or due to a well-disposed parameter combination in the absence of velocity disturbances as discussed in Sec. 10.2.

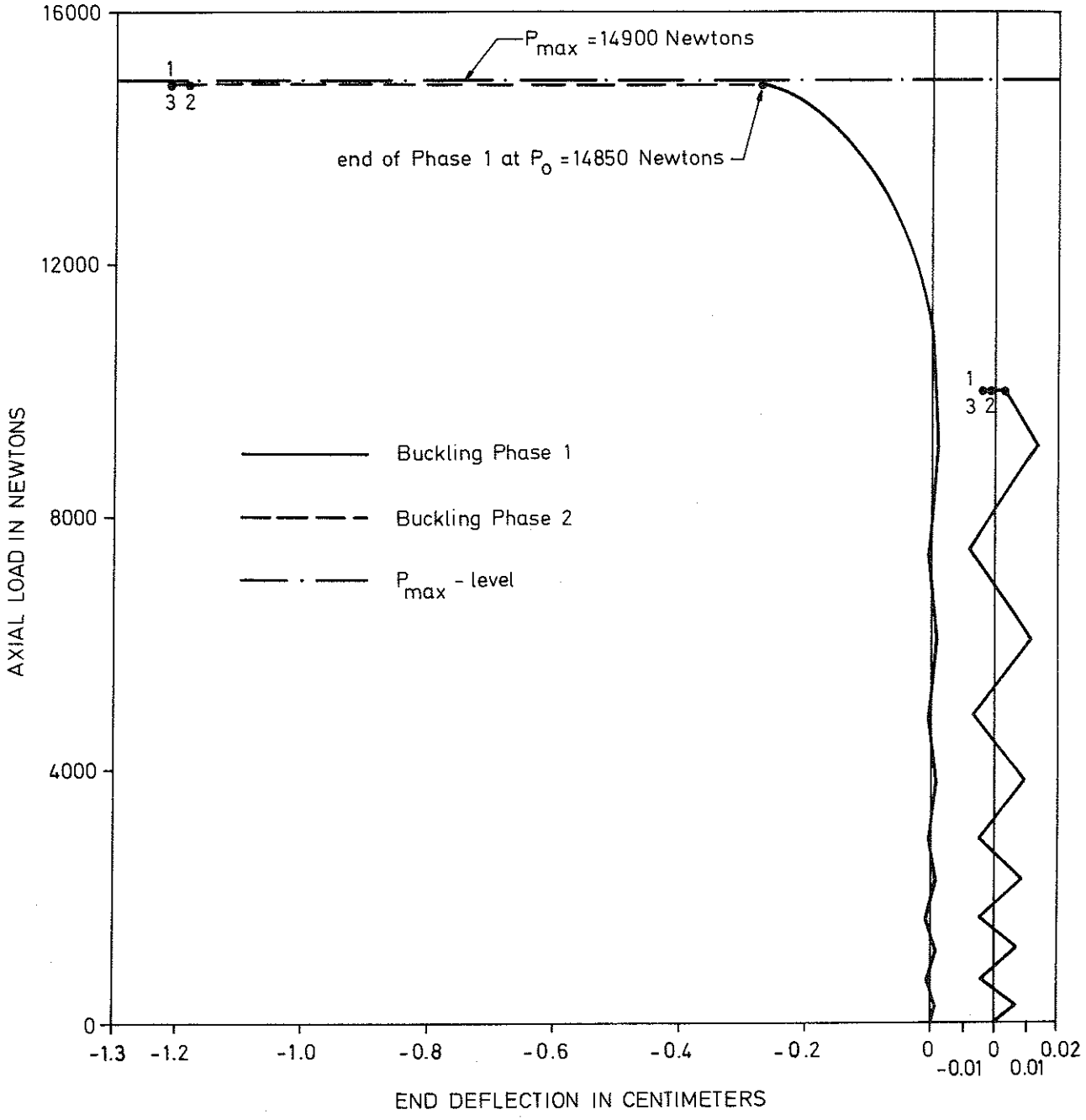

FIG. 45. BUCKLING BEHAVIOUR OF INDUCED BACKWARDS-INCLINED COLUMN NO. 37 OF TABLE 4 A.

The oscillatory behaviour of the column in Fig. 45 up to 10 000 Newtons load level is shown more clearly by the illustration on the right side of the diagram with a horizontal scale five times larger than the corresponding scale on the left side.

In order to test the sensitivity of the buckling phenomenon discussed in this section to changes in the value of the calculation time step, Δt, the following two numerical tests are performed:

1. If the time step for this column (Column 37 of Table 4 A) is reduced from 0.01 seconds to 0.001 seconds, the column remains backwards-inclined while the maximum column load changes from 14 900 Newtons to 15 175 Newtons; and

2. If for additional observation, the time step for the same column is further reduced to 0.0001 seconds, the column still remains backwards-inclined while the maximum column load changes from 15 175 Newtons to 15 099 Newtons.

Thus, the induced backwards-inclined behaviour numerically tested for the above column, is not so sensitive to changes in the value of the computation time step, Δt. Furthermore, numerical results show that this phenomenon may occur frequently. A study of Table 4 A shows that out of the ten columns, subjected to a velocity disturbance, V_o, at the start of loading, 7 columns failed in the reverse direction.

However, the size of the maximum column load for backwards-inclined columns may be sensitive to the choice of the time step, Δt. Due to their behaviour to permanently deflect backwards, these columns pass the position of zero deflection ($U = 0$) at high axial loads. Thus, it is expected that backwards-inclined columns may behave like nearly perfect columns at large axial load levels. Thus, the moment state of backwards-inclined columns, analogous to that of the nearly perfect columns, may be sensitive to small disturbances such as the secondary effects brought about by the size of the load increment corresponding to one computation cycle, see further Sec. 8.9. Thus, if accurate results for the maximum

column load is desired, in some situations such as the present one, a particularly small time step, Δt, must be used.

Numerical results in the next section reveal that if the phenomenon of permanent deflection in reverse direction is self-generated, then the size of the load increment corresponding to one computation cycle plays a decisive role on the observation of the phenomenon.

10.2 Self-Induced Permanent Deflection in Reverse Direction

The argument set forth in the previous section, to show the possibility of permanent lateral deflection in reverse direction, assumes that this phenomenon may be induced subsequent to introducing some favourable velocity disturbance. However, in the course of the discussion in Sec. 10.1, the notion of velocity disturbance is utilized to assure the occurrence of favourable oscillatory cycles simultaneous with loading. Since, oscillations simultaneous with loading can also take place in the absence of velocity disturbances, this raises the question whether the phenomenon of permanent deflection in reverse direction could also be self-induced. The following discussion is intended to answer this question:

Suppose that a column has so small initial deflection and excentricity that the resulting deflection during Phase 1 remains small before the column begins to deform in the inelastic range. Furthermore, suppose that up to a relatively large axial load in the inelastic range the axially induced internal moment remains inactive assuming that the bending deformation rate in the actual deformation range is sufficiently small not to give rise to the strain reversal phenomenon. The possibility of this state of affairs is illustrated in Fig. 46 in which the multi-cycle computation concept, described herein in the previous sections, is utilized.

Fig. 46(a) shows a multilinear stress strain diagram on which the limiting stress levels are indicated by points 1, 2, 3, 4, etc. The symbols $\Delta\sigma_{\max\ 1}$, $\Delta\sigma_{\max\ 2}$, $\Delta\sigma_{\max\ 3}$, $\Delta\sigma_{\max\ 4}$, etc. shown in 46(a) just one computation cycle below the respective stress levels 1, 2, 3, 4, etc.

are substitutes for $\Delta\sigma_{max}$ which, in turn, is defined as the maximum stress difference, i.e., the difference between the total stresses on the extreme sides of the cross section of maximum bending strain in the column. Fig. 46(b) shows the total stress distribution on the cross section of maximum strain, AB, on which the maximum stress difference corresponding to any position on the stress strain diagram, is marked. Fig. 46(c) shows the incremental stress distribution over the same cross section solely due to the increase of axial load, ΔP, at the beginning of one computation cycle. Between two consecutive limiting stress levels, and in the absence of strain reversal, the incremental axially induced stress, $\Delta\sigma_a$, is uniformly distributed over the cross section. We now demonstrate that it is possible for $\Delta\sigma_a$ to be uniformly distributed even when the stress over the cross section just passes beyond a limiting stress level.

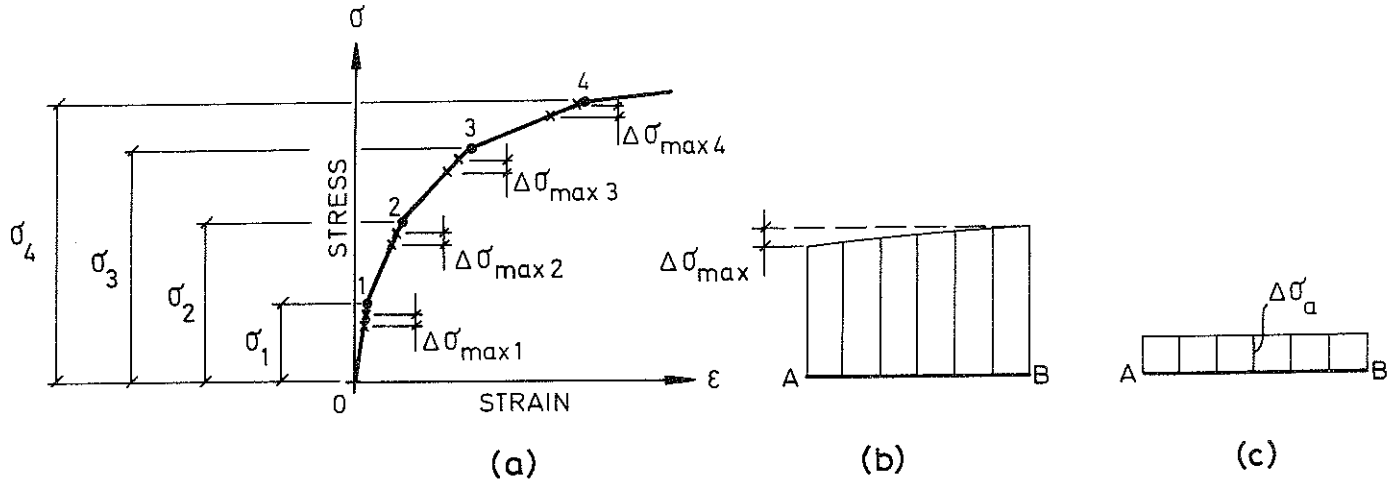

FIG. 46. SUCCESSIVE STATES OF STRESS IN A SELF-INDUCED BACKWARDS-INCLINED COLUMN.

The validity of the above assertion may be shown by a close study of Fig. 46(a). Just one computation cycle below some limiting stress level i, the value of $\Delta\sigma_{maxi}$ is assumed to be smaller than $\Delta\sigma_a$, so that we can write

$$\Delta\sigma_{maxi} < \Delta\sigma_a \tag{187}$$

We may assume a constant loading rate, so that $\Delta\sigma_a$ remains constant as long as the same tangent modulus applies to the whole cross section during loading.

Inequality (187) is definitely possible for a favourable combination of column parameters, since $\Delta\sigma_a$ depends only on the loading rate, whereas $\Delta\sigma_{maxi}$ depends on the initial imperfection, loading rate and the shape of the stress strain diagram up to the current state. For a given column, and a certain stress strain diagram with a given loading rate, it would be sufficient to vary the initial imperfection alone in order to arrive at Inequality (187).

Inequality (187) may not necessarily be true at all limiting stress levels; we may assume that it is true at the limiting stress levels 1 and 2, so that the following inequalities hold:

$$\Delta\sigma_{max\ 1} < \Delta\sigma_a \tag{188}$$

and

$$\Delta\sigma_{max\ 2} < \Delta\sigma_a \tag{189}$$

which express the fact that the first two maximum stress differences indicated in Fig. 46(a) are smaller than $\Delta\sigma_a$ in Fig. 46(c).

It should be noted that in Fig. 46(a), each maximum stress difference is marked by two crosses, the upper cross indicating the current

total stress at Point B and the lower cross showing the corresponding total stress at Point A of the given cross section in Fig. 46(b). Now considering Inequalities (188) and (189), we can even assume that the limiting stress levels 1 and 2 are so located that the following inequalities hold:

$$\sigma_1 - \sigma_{A1} < \Delta\sigma_a \tag{190}$$

and

$$\sigma_2 - \sigma_{A2} < \Delta\sigma_a \tag{191}$$

in which σ_1, σ_2 = the limiting stress levels in Fig. 46(a) corresponding to points 1 and 2 respectively; σ_{A1}, σ_{A2} = the stress at point A of the cross section in Fig. 46(b) one computation cycle below the stress levels 1 and 2 of Fig. 46(a) correspondingly; and $\Delta\sigma_a$ = the axially induced stress increment defined in Fig. 46(c).

Inequalities (190) and (191) may be rewritten in the form

$$\sigma_1 < \sigma_{A1} + \Delta\sigma_a \tag{192}$$

and

$$\sigma_2 < \sigma_{A2} + \Delta\sigma_a \tag{193}$$

Inequalities (192) and (193) express the fact at the beginning of the immediately following corresponding computation cycles, the stress at point A and thus surely the stress at point B both exceed the limiting stress levels 1 and 2 in Fig. 46(a).

The above analysis shows that it is possible for the stress in the column to exceed beyond some limiting stress levels without experiencing different tangent moduli at different points of the cross

section. However, at some higher stress level, the situation may turn out to be different. As a matter of illustration, the following inequalities may hold at point 3 in Fig. 46(a):

$$\sigma_3 - \sigma_{A3} > \Delta\sigma_a \tag{194}$$

and

$$\sigma_3 - \sigma_{B3} < \Delta\sigma_a \tag{195}$$

in which σ_{A3}, σ_{B3} = the stress at point A respective point B of the cross section in Fig. 46(b) just one computation cycle below point 3 in Fig. 46(a); σ_3 = the stress at point 3 in Fig. 46(a); and $\Delta\sigma_a$ = the axially induced stress increment defined in Fig. 46(c).[1]

Inequalities (194) and (195) may be rewritten in the form

$$\sigma_3 > \sigma_{A3} + \Delta\sigma_a \tag{196}$$

and

$$\sigma_3 < \sigma_{B3} + \Delta\sigma_a \tag{197}$$

Inequalities (196) and (197) show that at the start of the immediately following computation cycle, the stress at point B may reach the stress interval 34, whereas the stress at point A remains in the stress interval 23, at least during one computation cycle. This leads to a difference in the tangent moduli governing the deformation of the cross section AB in Fig. 46(b). Thus, the axially induced internal moment increment, ΔM_{ia}, gets activated during one or a few computation cycles until the stress at all points over the cross section reaches the stress interval 34 in Fig. 46(a), after which the value of ΔM_{ia} drops to zero again. Now, the state of the column just described may

---

1. Inequalities (194) and (195) do not have to hold simultaneously with Inequalities (188) and (189).

sufficiently explain the possibility of self-induced backwards-inclination as follows:

After experiencing the axially induced internal moment increment during the course of a few computation cycles, the column may temporarily find itself in a state of complete instability, i.e., the value of TIMS (total internal moment surplus) may attain negative values. In other words, the total external moment may temporarily exceed the total internal moment. At the axial loads corresponding to the stress interval, 34, in Fig. 46(a), the surplus moment increment may still have relatively large positive values. Thus, the unstable column may initially accelerate forwards in the stress interval, 34, up to a position at which the value of TIMS becomes equal to zero, whereafter the motion of the column continues until a motion reversal position is attained simultaneous with loading. This situation can only occur if the axially induced internal moment increments are different from zero only during a few computation cycles. This condition requires for instance, that if during forward motion, just before attaining a motion reversal position, the stress in the column increases beyond point 4 in Fig. 46(a), no additional axially induced moment increments are caused. In other words, at point 4, relations analogous to Inequalities (192) and (193) should hold. Furthermore, the surplus moment increment is assumed to remain positive throughout the motion before attaining the motion reversal position.

During backward motion, the stress over the cross section, AB, in Fig. 46(b) may pass higher limiting stress levels without experiencing the axially induced internal moment increments in the manner explained above until the column passes the position of zero deflection,

after which the stress at point A in Fig. 46(b) would exceed the stress at point B. If now the column passes higher limiting stress levels with stress relationship analogous to Inequalities (196) and (197) the column may begin to get backwards-inclined. The surplus moment increment may now successively attain smaller values in such a way that the backwards motion of the column simultaneous with the increase of axial load cannot be retarded. The occurrence of strain reversal under these circumstances may increase the tendency of the column to bow additionally backwards. Thus, the column may permanently bow in the reverse direction.

The remarkable phenomenon explained above may now be illustrated by studying the complete buckling behaviour of the self-induced backwards inclined column identified as Column No. 3 in Table 4A.This is illustrated in Fig. 47 in which the scale for positive deflection is chosen 500 times the scale for negative deflection. This duality in the choice of the scale is for the sake of obtaining a vivid picture of the behaviour of the column in the positive deflection range where the most interesting buckling phenomena described above take place.

Fig. 47 shows that the column almost remains straight up to 10 000 Newtons load level, at which the axially induced internal moment increments exert their influence in a small loading range, as a consequence of which the column sharply bows until a motion reversal position is attained. Subsequently, the column moves backwards and as the load continuously increases, the column continues to move backwards with no sign of another motion reversal position simultaneous with loading. If the axial load is kept at a constant value of 14 050 Newtons, i.e., one computation cycle below the maximum load, subsequent motion of the column

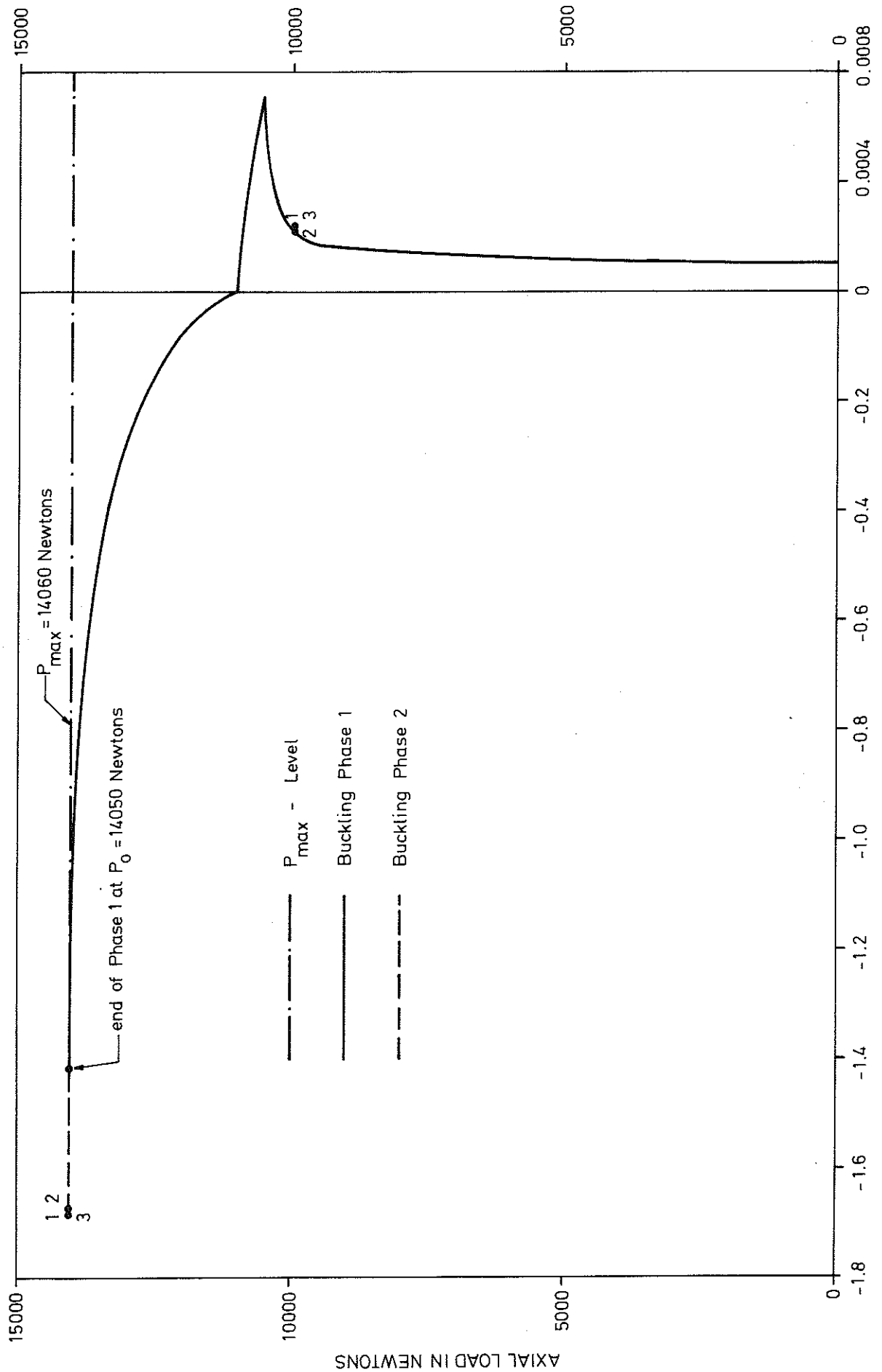

FIG. 47. BUCKLING BEHAVIOUR OF SELF-INDUCED BACKWARDS-INCLINED COLUMN No. 3 OF TABLE 4A

during buckling Phase 2 up to three consequtive motion reversal positions is indicated by points 1, 2 and 3 correspondingly. The final simple harmonic motion of the column takes place in the narrow interval between positions 2 and 3.

It should be noted that just before the sharp bending of the column during forward motion, the positions of the column at a constant axial load of 10 000 Newtons during buckling Phase 2 almost coincide with the position attained simultaneous with loading. This shows that the column is nearly in a straight configuration before the sharp forward bowing of the column initiates. Thus, it is worthwhile to note that the phenomenon of self-induced backwards inclination may occur more often for a nearly perfect column. In fact numerical simulations, not entered in Tables 4 A - 4 C, show that for still smaller values of initial imperfection, the phenomenon described in this section occurs more frequently.

From the arguments in the present section it may be deduced that the occurrence of self-induced permanent deflection in reverse direction is extremely sensitive to the loading process, i.e., the magnitude of the load increments applied at the start of the computation cycles. Thus, the choice of the time step on a ceteris paribus basis may be crucial for the observation of the phenomenon, see preliminary remarks at the beginning of this chapter. In fact, if the time step for Column 3 of Table 4 A is reduced from .01 seconds to .001 seconds, the column turns into a forward inclined column while the maximum column load changes from 14 060 Newtons to 14 040 Newtons. For lower values of Δt, not tested herein, the column may again become backwards-inclined. For a continuous loading process, the parameter combination required for backwards-inclined column behaviour may be nearly the same as the

the present column, but it does not coincide with it. Thus, because of both the infrequency and the crucial sensitivity of the phenomenon, self-induced permanent deflection in reverse direction is of little practical significance. However, the analysis in the present section may be conceptually significant, since it shows that the most striking and otherwise unexpected phenomena may be predicted and explained in terms of the powerful analytical tools developed herein. This aspect of the problem becomes more pronounced by pointing out that this and similar phenomena were actually predicted in the course of the present study using the general line of arguments developed herein before any numerical observation.

Although self-induced backwards-inclined column behaviour discussed in this section may be observed only for isolated values of Δt, the phenomenon of induced backwards-inclined column behaviour is not equally sensitive to the choice of the calculation time step, Δt, see Sec. 10.1.

Furthermore, it should be noted that the size of the maximum column load for the column studied in this section is not so sensitive to the choice of the time step parameter, Δt. This follows from the fact that, notwithstanding the value of the loading rate, $c = 5000$ Newtons/sec, for the column studied in Sec. 10.1, the value of the loading rate in the present example is considerably smaller ($c = 1000$ Newtons/sec). It should be recalled from the study in Sec. 8.9, that it is only the parameter combination, small initial deflection (nearly perfect column) and sufficiently large loading rate which may require the choice of a particularly small calculation time step, Δt.

10.3 Illustration of the Effect of Gravitational Force

It is shown in Appendix C, that for a perfect column, the gravitational force has no effect on the subsequent lateral motion of the column at a given load increment below or above the critical load provided that the initial deflection and velocity state of the column at the given load increment below or above the critical load is the same with or without taking into consideration the gravitational force. For a perfect column this is a legitimate assumption since the column is assumed to remain straight up to the critical load, as a consequence of which it is correct, for example, to consider that the initial deflection and velocity state of the column at the critical load itself is arbitrarily chosen to be the same regardless of whether or not the gravitational force enters into the calculation of the critical load. It should be noted however, that the gravitational force always reduces the size of the critical load, see Eq. C(57) of Appendix C.

For an imperfect column which is subjected to an initial imperfection from zero load level, the initial state of the column at the onset of loading cannot be chosen freely, since it depends on the magnitude of the gravitational force. In order to uniquely determine the initial state of the column under the influence of its own weight, it is necessary to precisely describe the past history of a column which is presently in a state of equilibrium in the deflected configuration solely under its own weight. Thus, the following assumptions are made:

1. The direction of the length axis of the column coincides with the direction of the gravitational force (vertical column);

2. The column is manufactured in the horizontal position so that it does not undergo any possible plastic deformation due to its own

weight prior to its erection; and

3 The column is held upright at the time of its erection such that the axial deformations of the column, due to the gravitational force, take place before subsequent lateral deflection due to an assumed initial imperfection.

The procedure just described may be illustrated by means of Fig. 48 for the simple two-element column in Fig. 12. Fig. 48 shows the valid multilinear stress strain diagram on which the initial uniform axial deformation of the column elements due to its weight at the time of erection is specified by the deformation at point A. For the sake of a general treatment, it is assumed that point A lies in the inelastic range.

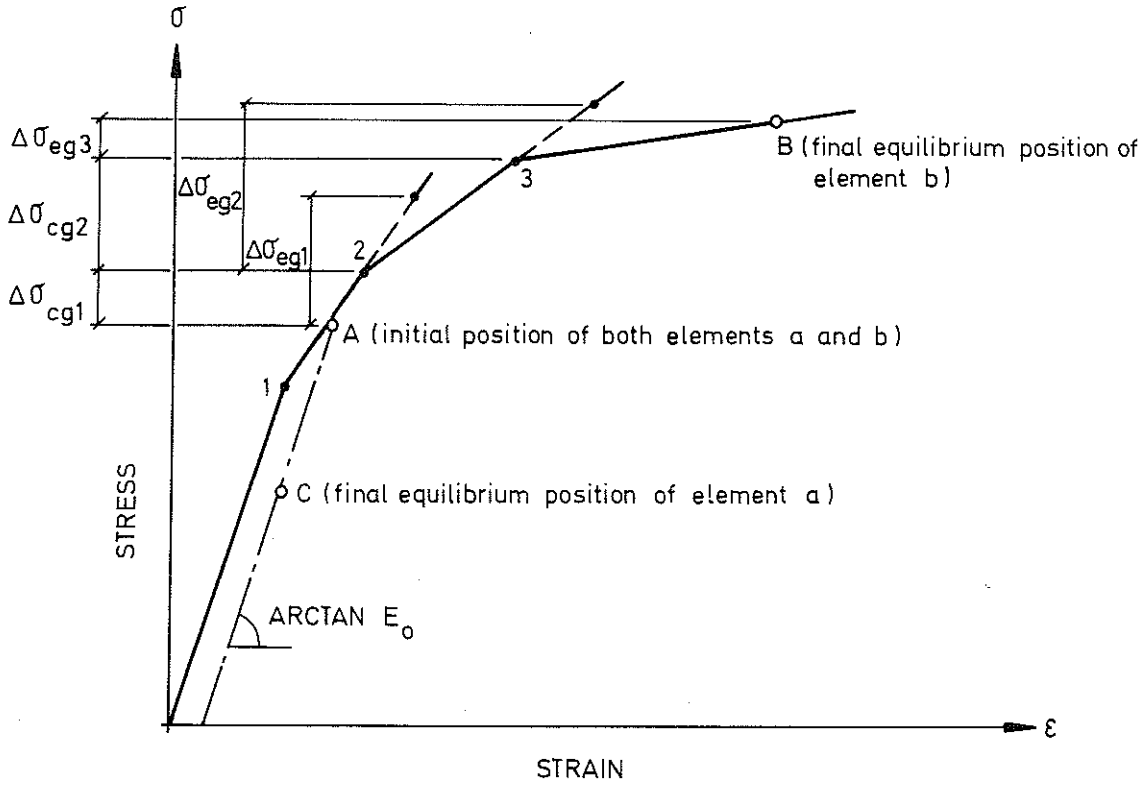

FIG. 48. ILLUSTRATION OF STRESS STRAIN HISTORY CORRESPONDING TO LATERAL DEFLECTION OF THE IMPERFECT COLUMN UNDER THE SOLE INFLUENCE OF THE GRAVITATIONAL FORCE.

After allowing the column to deflect under its own weight the stress in element B increases along the original stress strain diagram whereas the stress in element A decreases on the unloading line originating from point A. The final equilibrium positions of elements a and b are indicated in Fig. 48 by points C and B respectively. These final positions are found according to the following procedure:

Starting at point A and assuming the tangent modulus valid in the stress interval, 12, in Fig. 48 to be applicable hereafter throughout the lateral deflection, the stress increment in both elements corresponding to the presumed equilibrium position of the column is calculated. If the first calculated equilibrium stress increment, $\Delta\sigma_{eg\,1}$, for element b is less than the increment, $\Delta\sigma_{cg\,1}$, corresponding to the first LSL (limiting stress level) after point A, then the presumed equilibrium position is correct. However, if the calculated $\Delta\sigma_{eg\,1}$ is greater than $\Delta\sigma_{cg\,1}$, see Fig. 48, then the position of the column corresponding to the next LSL is calculated, whereafter the procedure described above is continued by successively comparing $\Delta\sigma_{eg2}$ with $\Delta\sigma_{cg2}$ and $\Delta\sigma_{eg3}$ with $\Delta\sigma_{cg3}$, etc., until finally at a certain stress interval, after i trials, the value of $\Delta\sigma_{eg\,i}$ falls below the value of $\Delta\sigma_{cg\,i}$ corresponding to the immediately following LSL (this has occurred after 3 trials in Fig. 48).

Subroutines 5 and 6 of Program 7 as well as Subroutines 9 and 26 of Program 8 are developed herein for determining the initial state of the column under the influence of its own weight in the manner explained above.

The effect of gravitational force may be illustrated by means of Fig. 49 which describes the complete two-phase buckling behaviour of Column 23 of Table 4 A with or without taking into account the gravita-

tional force. This illustration shows that the maximum load drops from a value of 12650 Newtons in the case of gravitational acceleration, $g = 0$, to a value of 11900 Newtons in the case of $g = 10$ m/sec^2. The difference between the two values is somewhat greater than the difference, $M \cdot g/2$, which is observed in the case of perfect columns, see Eq. (C 57) of Appendix C. This slight discrepancy with the perfect column is expected, since the initial deflection state of the column increases due to the gravitational force. For heavier columns greater discrepancies may result.

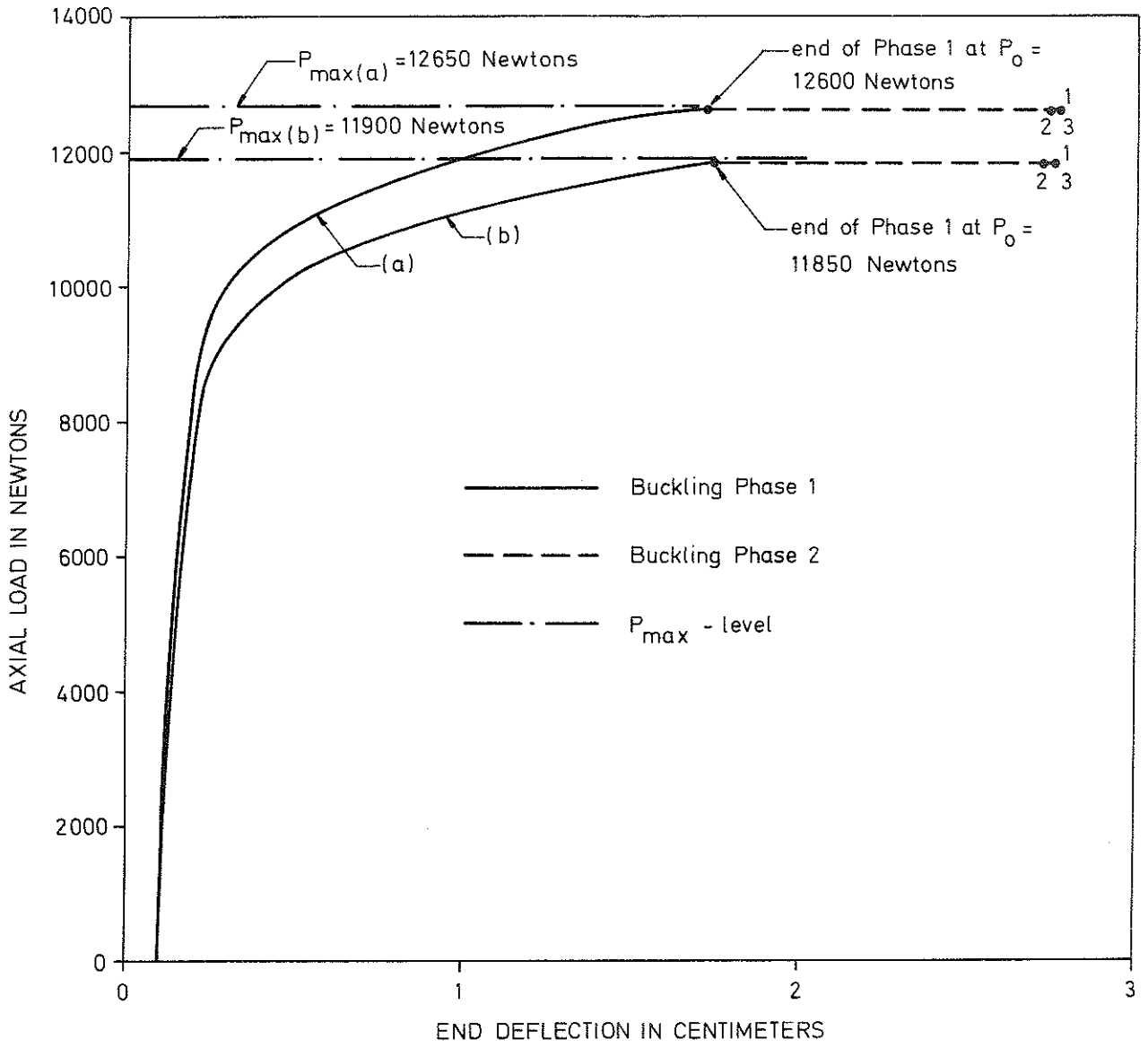

FIG. 49. COMPARISON OF BUCKLING BEHAVIOUR: (a) COLUMN 23 OF TABLE 4A WITH $g = 0$; (b) IDENTICAL COLUMN WITH $g = 10$ METERS PER SECOND SQUARE

Additional numerical examples for the influence of gravitational force on the buckling behaviour of the column is presented in Columns 16-18 of Table 6 in Chapter 11.

10.4 Effect of Nonconservative Axial Load

When the axial load changes direction during the process of lateral deflection of a built-in column, the work done by the force component, H, perpendicular to the original direction of application of the axial load, P, must be taken into account (Fig. 50).

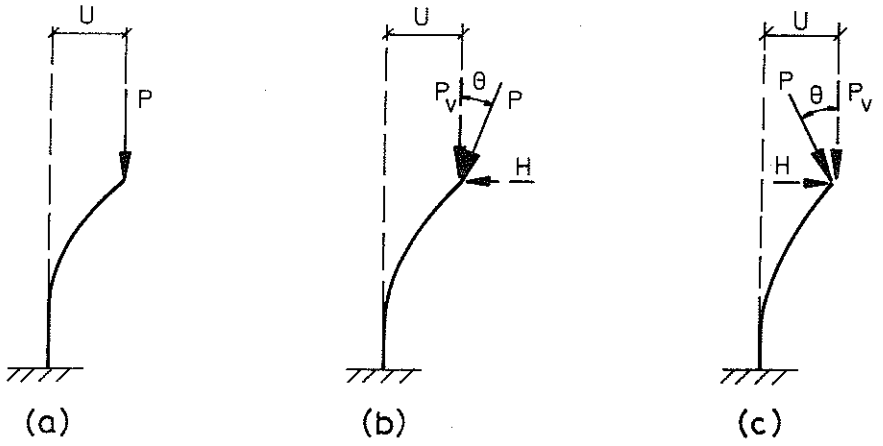

FIG. 50. DEFLECTED CONFIGURATION AT AN INSTANT OF TIME DURING LATERAL BUCKLING: (a) CONSERVATIVE AXIAL LOAD; (b) NONCONSERVATIVE AXIAL LOAD WITH POSITIVE DEVIATION ANGLE; AND (c) NONCONSERVATIVE AXIAL LOAD WITH NEGATIVE DEVIATION ANGLE

The problem of nonconservative axial load in the case of an elastic column is already resolved (21). The pioneering work appearing in Ref. 21 explores a number of interesting phenomena related to the buckling of an elastic column subjected to a constant nonconservative axial load with a deviation angle, θ, proportional to the angle between the end tangent to the deflection curve and the original straight axis of the column.

It should be noted that in the case of an elastic column, a direction change of the axial load simultaneous with loading in the manner depicted in Fig. 50(b), does not affect the critical load level provided that the nonconservative force recovers its original axial direction before reaching the Euler load. The net effect of a nonconservative axial force which changes direction simultaneous with the increase of axial load according to Fig. 50(b), but retains its original direction before reaching the Euler load is to disturb the column laterally without affecting either the final deflected equilibrium position or the magnitude of the critical load. The situation is different for an inelastic column for which a change of direction of the axial load during either buckling phase may affect all the output results. It is the objective of this section to further examine this problem.

From the manner the axial load of an inelastic column changes direction it may be possible to foresee the qualitative effect on the maximum column load. Fig. 50(b) shows a positive deviation angle, i.e., the axial load changes in the same direction as the end tangent to the deflection curve. Fig. 50(c) shows a negative deviation angle, i.e., the axial load changes in the opposite direction as the end tangent to the deflection curve. If the axial load changes direction positively, Fig. 50(b), then the horizontal component, H, of the inclined force, P, opposes the effect of the vertical component, P_v. Thus, the effect of a positive deviation angle is a decrease of the external moment throughout the lateral deflection and a subsequent increase in the critical load level as compared with conservative axial load in Fig. 50(a). The situation is the reverse for a negative deviation angle, Fig. 50(c), in which case the maximum load level may decrease.

Applying the multi-cycle computation technique utilized throughout this work, the effect of a nonconservative axial load is studied herein on the basis of the idea illustrated in Fig. 51. Using the notion of a proportional deviation angle proposed in Ref. 21, the variation of deviation angle is assumed to take place according to the following scheme:

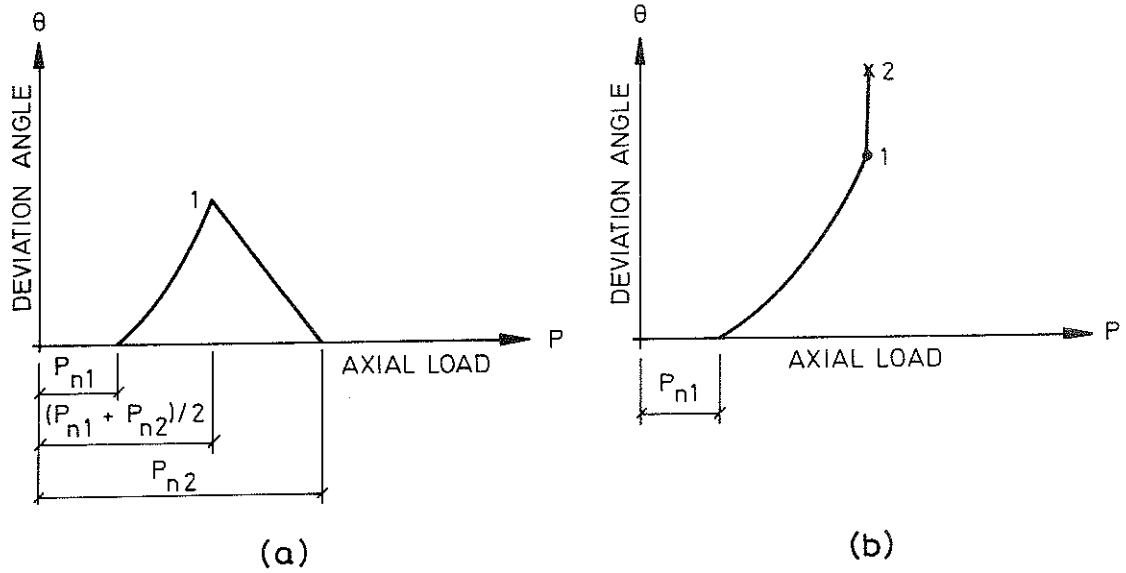

FIG. 51. VARIATION OF DEVIATION ANGLE: (a) DURING PART OF PHASE 1; AND (b) DURING PART OF PHASE 1 AND THROUGHOUT PHASE 2

Fig. 51(a) shows the variation of deviation angle, θ, between two axial load levels, P_{n1} and P_{n2}. The axial load begins to become nonconservative at P_{n1} beyond which the deviation angle of the simple column corresponding to Model 3 continues to increase during $\underline{n}$ computation cycles up to point 1 in Fig. 51(a) according to the following relationship:

$$\Delta\theta = m \cdot \Delta\alpha \tag{198}$$

in which $\Delta\theta$, $\Delta\alpha$ = the deviation angle increment respective deflection

angle increment corresponding to one computation cycle; and m = an arbitrary proportionality constant, positive for Fig. 50(b) and negative for Fig. 50(c).

The total deviation angle, θ, at the end of each computation cycle is obtained from the equation

$$\theta = \theta_o + \Delta\theta \tag{199}$$

in which θ_o = the initial value of the deflection angle at the start of the computation cycle; and $\Delta\theta$ is defined by Eq. (198)

Beyond point 1 in Fig. 51(a), the deviation angle may be assumed to decrease linearly, during another n computation cycles according to the following equation:

$$\theta = \theta_o - \frac{\theta_{max}}{n} \tag{200}$$

in which θ_o, θ = the deviation angle at the beginning respective at the end of a computation cycle; and θ_{max} = the maximum deviatition angle corresponding to point 1 in Fig. 51(a).

Thus, the axial load is altogether nonconservative during 2n computation cycles simultaneous with loading. It should be noted that according to this alternative, the axial load retains its original direction before the start of buckling Phase 2.

Fig. 51(b) shows a second alternative for which the nonconservative axial load extends into buckling Phase 2; in other words, the upper load limit, P_{n2}, shown in Fig. 51(a) is nonexistent in this alternative. It

should be observed that a computer solution of the nonconservative axial load throughout buckling Phase 2 can only be treated with the aid of Program 7 entitled "Multi-Cycle Search Method". This is due to the fact that Program 7 follows the motion of the column continuously during many computation cycles, in which case the deviation angle could continuously be increased at the end of each computation cycle. Program 8, on the other hand can only treat the alternative shown in Fig. 51(a).

Subroutine 7 of Program 8 and Subroutine 4 of Program 7 are developed herein to take care of the influence of nonconservative axial load in the manner described above. These subroutines can handle both positive and negative deviation angles.

The procedure explained above is numerically illustrated in Fig. 52 in which the complete buckling behaviour of Column 23 of Table 4A is traced and compared with the corresponding buckling behaviour according to the above two alternatives, having positive deviation angle, with the following numerical data:

$m = .9$, see Eq. (198); $P_{n1} = 10000$ Newtons; and $P_{n2} = 12500$ Newtons

In Fig. 52, the motion of the column is followed up to three successive motion reversal positions indicated by points 1, 2 and 3 respectively.

It may be noted that the effect of a nonconservative axial load with positive deviation angle is to increase the maximum column load and decrease the lateral bowing for loads below the maximum level. The effect of deviation angle on the buckling behaviour is more pronounced when the axial load is allowed to be nonconservative throughout buck-

ling Phase 2.

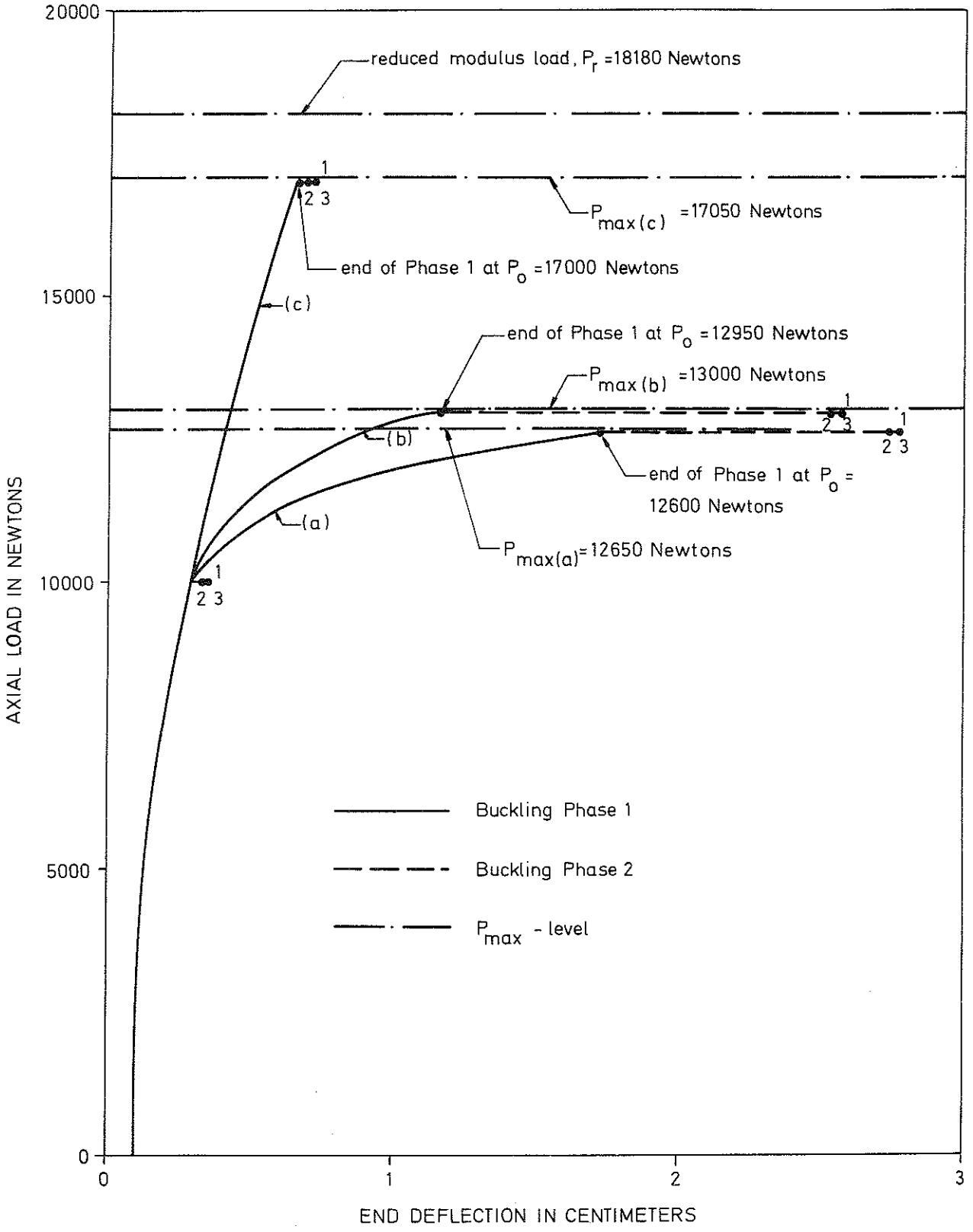

FIG. 52. COMPARISON OF CONSERVATIVE AND NONCONSERVATIVE BUCKLING BEHAVIOUR: (a) COLUMN 23 OF TABLE 4A; (b) IDENTICAL COLUMN WITH NONCONSERVATIVE AXIAL LOAD DURING PART OF PHASE 1; (c) IDENTICAL COLUMN WITH NONCONSERVATIVE AXIAL LOAD DURING PART OF PHASE 1 AND THROUGHOUT PHASE 2

Additional examples on the effect of nonconservative axial load are presented in Columns 19-22 of Table 5.

10.5 Abnormal Behaviour of Backwards Inclined Columns

Columns which tend to become backwards-inclined, according to the description in Sec. 10.1, may behave abnormally in the sense that parameter variations may give rise to opposite effects as compared with the forwards-inclined columns. The purpose of this section is to illustrate and explain these remarkable phenomena.

An increase in initial deflection and/or excentricity, on a ceteris paribus basis, may normally result in a decrease of the maximum column load and an increase of lateral deflection for loads below the maximum load. However, for a backwards-inclined column, this may lead to a tendency to bow more in forward direction and less in backward direction. This may give rise to an increase of bending rigidity in backward direction. Thus, in contrast to a forwards-inclined column, the maximum column load may rise and lateral deflection for loads below the maximum level may decrease. This argument certainly assumes that the increase in initial deflection and/or excentricity is confined within the range in which the column does not lose its original tendency to fail in the reverse direction.

The abnormal behaviour of backwards-inclined columns may be illustrated by Fig. 53 in which the variation of the maximum column load due to changing the initial end deflection is shown for a column which is originally backwards-inclined (Column No. 37 of Table 4A). Fig. 53 shows that up to a certain increase of initial end deflection the maximum column abnormally increases as the initial end deflection increases while the column remains backwards-inclined. However, as the initial end deflection increases beyond a certain value, on a ceteris paribus basis, the backwards-inclined column becomes forwards-inclined. In the

transition zone between backwards- and forwards-inclined zones, the final deflection pattern of the column is extremely sensitive to changes in the value of the initial deflection. The wavy line in Fig. 53 shows this transition zone.

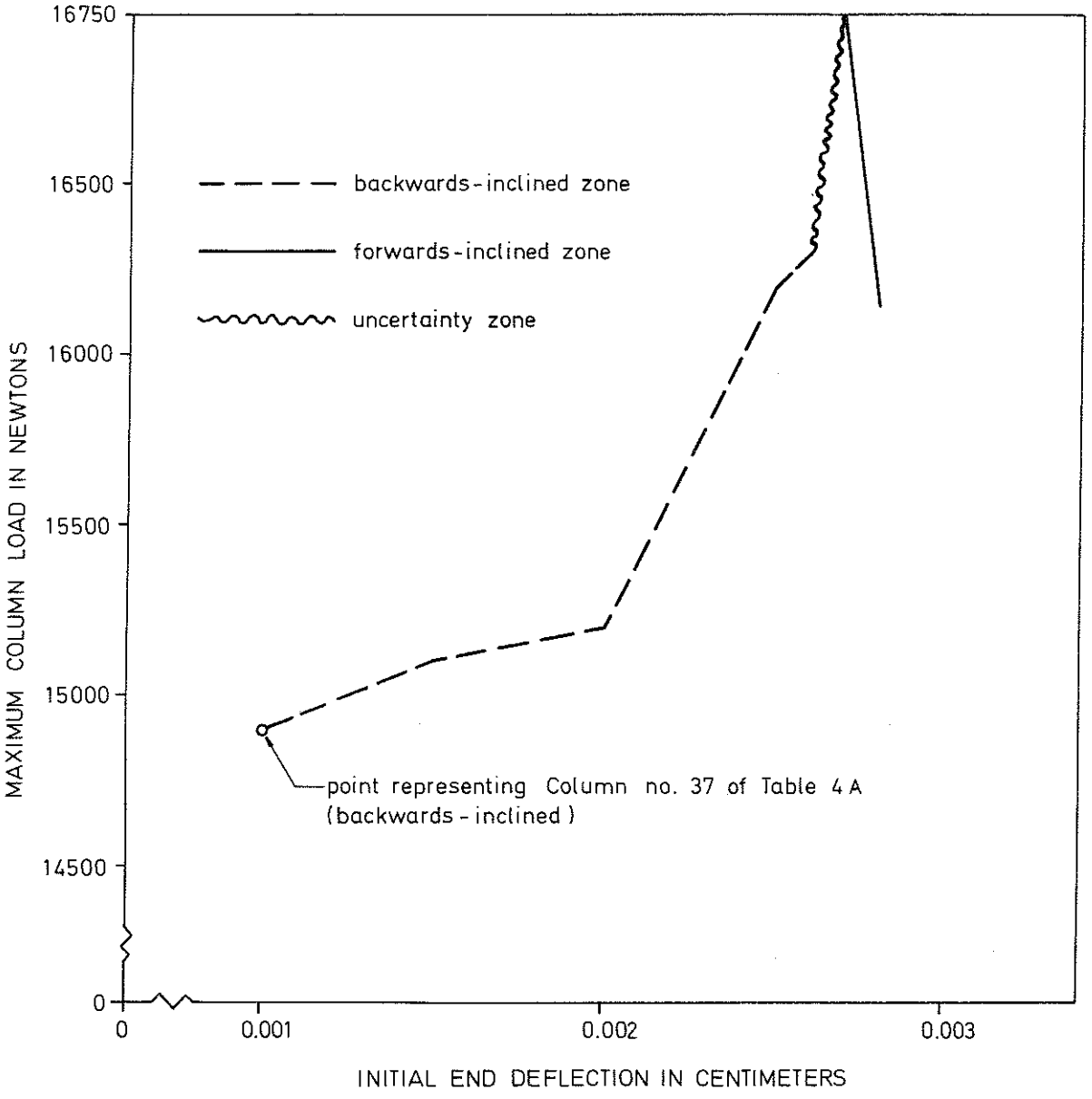

FIG. 53. ILLUSTRATION OF THE ABNORMAL BEHAVIOUR OF BACKWARDS-INCLINED COLUMNS

Because of the extreme sensitivity of the column behaviour in the transition zone between backwards- and forwards-inclined regions, the

transition zone is called herein the uncertainty zone. It is interesting to observe that just beyond the uncertainty zone in Fig. 53, the largest of the maximum column loads corresponds to a forwards-inclined column with an initial end deflection of 0.0027 centimeters. Any additional increase of the initial deflection of the column above 0.0027 centimeters results in a decrease of the maximum column load which is normally expected in the case of forwards-inclined columns.

10.6 Final Stable Equilibrium Configurations

At the maximum load, the column can never attain a position of motion reversal while moving in one direction during buckling Phase 2. In other words, amplitude of motion attains infinitely large values just at the maximum load. Observing this behaviour, one may be tempted to jump to the conclusion that for axial loads in the neighbourhood of maximum value, the ensuing oscillations attain large amplitudes. This is actually not the case. The explanation is as follows:

For an axial load just below the maximum value, the column may undergo a certain deflection before the first motion reversal during buckling Phase 2. This first bowing interval may not be necessarily large, specially, if the tangent moduli on the stress strain diagram change by discrete values at limiting stress levels, in which case the maximum load may occur just at one such limiting level. In this case, the surplus moment increment for the column in Fig.54(a) may, even before the first motion reversal, be sufficiently great to avoid excessive deflection.

The behaviour of the column during return motion is depicted in Fig.54(b) in which the zone, previously in a state of increasing strain, would partially undergo strain reversal and the zone previously in a state of strain reversal would now be undergoing increasing strain. In a part of this latter zone, the unloading modulus would still be applicable, at least in the initial stage of bending subsequent to the first motion reversal. Thus, the overall bending rigidity during this reverse motion would considerably be greater and the column would soon reach a second end position with a much

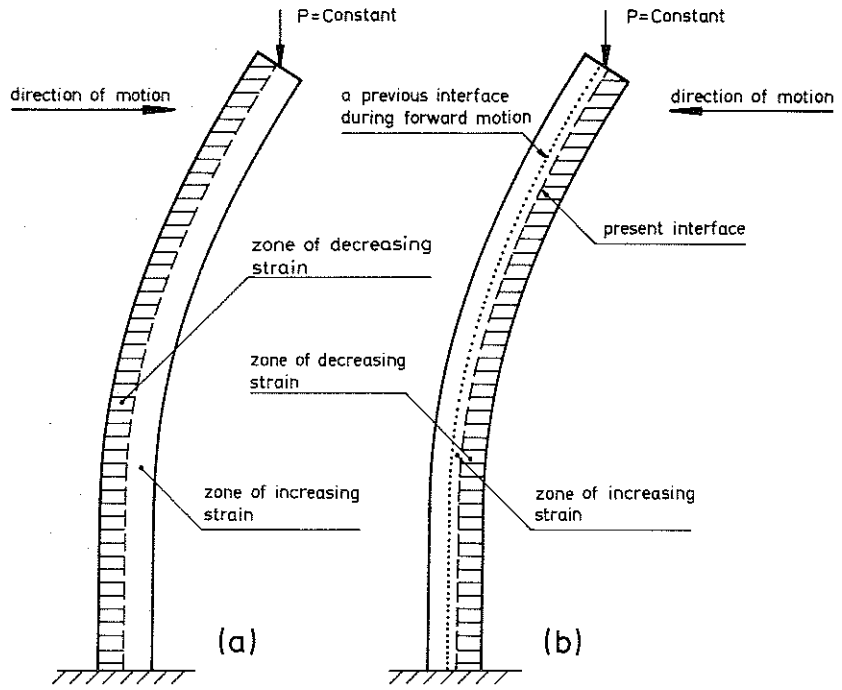

FIG. 54. BENDING OF THE INELASTIC COLUMN AT TWO DIFFERENT INSTANTS OF TIME DURING PHASE 2: (a) BEFORE MOTION REVERSAL; (b) AFTER MOTION REVERSAL

shorter amplitude. During subsequent oscillations, increasingly greater portions of the column would undergo strain reversal, while the motion becomes almost simple harmonic with small amplitudes.

The above situation is depicted in Fig. 55 in which the load-deflection of the column during buckling Phase 1 is shown up to maximum column load at point A. At a slightly less stress level at point B, the dotted horizontal line shows the behaviour of the column during Phase 2. At point 1, the motion reverses direction for the first time

and the other points show subsequent end positions in the order in which they occur. Final oscillations take place in the open interval between points 3 and 4 with small amplitudes.

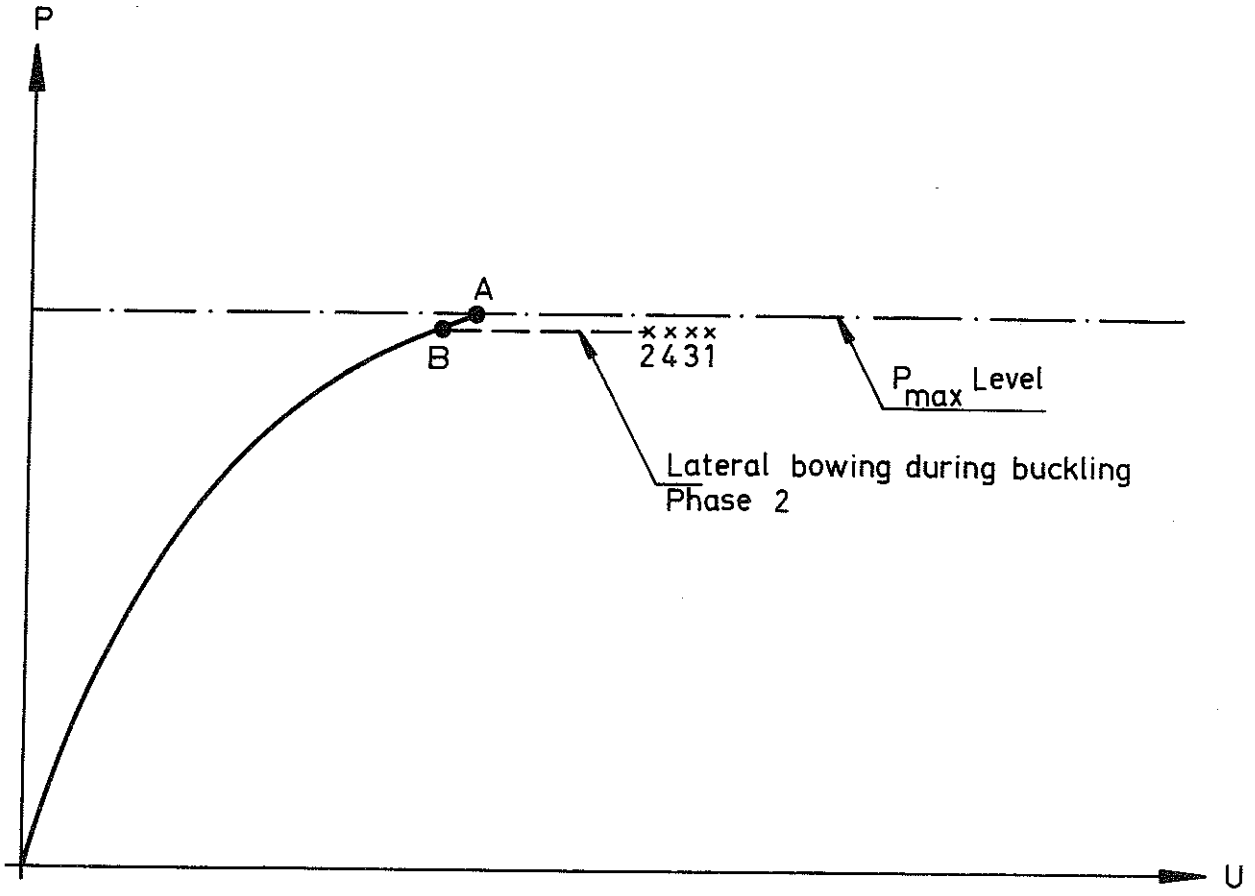

FIG. 55. TYPICAL COLUMN BEHAVIOUR DURING BUCKLING PHASES 1 AND 2

It should be observed that after the second motion reversal, the greatest strain reversal, which has ever occured on the front side of the column during Phase 2, has only been effective in the relatively short deflection interval between points 1 and 2 in Fig. 55. This is a significant observation, because it shows that although the final amplitude of oscillation is small and the surplus moment increment is great, the stability in this situation has no depth. The explanation

is that a small increase of axial load, for instance, would be sufficient to nullify the effect of strain reversal previously occured in the short deflection interval between points 1 and 2. The front side of the column would soon attain the previous tangent moduli and the column would reach a state of permanent instability.

It should be noted that in the case of Model 3 analyzed in Chapter 8, numerous examples of the buckling behaviour of the column during both phases have already been presented herein as illustrations of the properties discussed in this chapter as well as in Chapter 9. Additional illustrations will be presented in the next chapter.

11. NUMERICAL RESULTS FOR DYNAMICALLY STABLE LATERAL CONFIGURATIONS OF MODEL 3

Below the maximum column load, the buckling behaviour could be determined by loading the column up to any desired load level, whereafter the ensuing lateral motion is followed up to three consecutive motion reversal positions. After attaining the third motion reversal position, the range of lateral motion of the present column model is, similar to Model 2, thoroughly determined, see Sec. 6.5.

The purpose of this section is to determine the influence of parameter variations on the buckling behaviour of the column during both buckling phases. The reference column used in the present computations is the simple column shown in Fig. 12 with the following numerical data:

$b = d = 5$ centimeters; $A = 5$ square centimeters; $L = 2.5$ m; $M = 100$ kg; $E_o = 10^{10}$ Newtons per square meter; $c = 100$ Newtons per second; $U_o = .001$ centimeters; $V_o = 0$ centimeters per second; $P_d/P_a = 1$, where P_d denotes the axial load at which a velocity disturbance, V_1, is introduced and P_a = an arbitrary axial load equal to or greater than the maximum column load; $V_1 = 0$ centimeters per second; and $X_o = 0$ centimeters, where X_o is the eccentricity in the application of loading. The same stress strain diagram used for determination of the maximum column load is assumed for the present computations, see Fig. 38 and the corresponding array of β-values in Sec. 8.7.

It should be noted that the parameter combination, $P_d/P_a = 1$ and $V_1 = 0$, implies that no disturbance velocity is introduced in the

Reference Column for loads above zero load level.

The computations are performed by the program, Single-Cycle Search method (see Program 8, Appendix D) and the results are summarized in Table 5 for 22 parameter combinations, including the Reference Column. Each new parameter combination in Table 5, is obtained by changing one or maximum two parameters of the Reference Column at a time. Each line in Table 5 consists of 12 columns, the first ten of which are exactly identical to Table 3 described in Sec. 6.6. The eleventh column in Table 5 indicates the constant axial load, P_o, corresponding to the end of buckling Phase 1 and the beginning of buckling Phase 2; the twelfth column shows the value of the maximum column load corresponding to each parameter combination entered in Table 5.

Each parameter combination in Table 5 consists of four lines corresponding to P_o-load levels, 5000, 7500, 10000 and a fourth load level which is equal to the maximum column load minus a load increment corresponding to the increase of axial load in a single time step during buckling Phase 1. The choice of this last load level arises out of the desire to study the buckling behaviour of the column as near the maximum column load as the computations allow.

In the first 15 entries in Table 5, the axial load is considered to be conservative and the effect of gravitational force is disregarded. In entries 16 - 18, a gravitational acceleration g = = 10 meters per second square, is taken into account. In entries 19 - 22, the effect of a nonconservative axial load on the buckling is numerically evaluated.

TABLE 5. - INFLUENCE OF PARAMETER VARIATIONS ON THE COMPLETE BUCKLING BEHAVIOUR OF INITIALLY IMPERFECT INELASTIC COLUMNS LOADED UP TO VARIOUS AXIAL LOAD LEVELS

Column No.	Names and Values of Parameters Subjected to Variation	Position at the End of Phase 1		First Motion Reversal		Second Motion Reversal		Third Motion Reversal		P_o Final Constant Load in Newtons	Maximum Column Load in Newtons
		U_1 in cm	t_1 in sec	U_{m1} in cm	t_{m1} in sec	U_{m2} in cm	t_{m2} in sec	U_{m3} in cm	t_{m3} in sec		
1	Reference Column U_o = .001 centimeters; c = 100 Newtons/sec; M = 100 kg; $E_o = 10^{10}$ Newtons/m^2; $X_o = V_o = V_1 = g = 0$; $P_d/P_a = 1$; conservative axial load	.00126	50.0	.00132	50.123	0.00129	50.217	.00131	50.31	5000	13356
		.00183	75.0	.00187	75.073	.00182	75.239	.00183	75.333	7500	
		.00373	100.0	.00374	100.033	.00357	100.265	.00360	100.361	10000	
		1.901	133.544	2.071	134.480	2.071	134.577	2.071	134.675	13355	
2	c = 500 Newtons per second	.00147	10.0	.00135	10.104	.00141	10.206	.00137	10.299	5000	13430
		.00176	15.0	.00195	15.174	.00191	15.268	.00195	15.362	7500	
		.0040	20.0	.0041	20.080	.00396	20.277	.00398	20.373	10000	
		1.800	26.850	2.004	27.375	2.001	27.473	2.004	27.569	13425	

TABLE 5 CONTINUED:

Column No.	Names and Values of Parameters Subjected to Variation	Position at the End of Phase 1		First Motion Reversal		Second Motion Reversal		Third Motion Reversal		P_o Final Constant Load in Newtons	Maximum Column Load in Newtons
		U_1 in cm	t_1 in sec	U_{m1} in cm	t_{m1} in sec	U_{m2} in cm	t_{m2} in sec	U_{m3} in cm	t_{m3} in sec		
3	c = 1000 Newtons per second	.00135	5.0	.00130	5.042	.00152	5.205	.00146	5.298	5000	13590
		.00235	7.5	.00209	7.659	.00216	7.751	.00209	7.845	7500	
		.00391	10.0	.00422	10.124	.00412	10.228	.00419	10.324	10000	
		1.646	13.580	2.013	14.070	2.009	14.167	2.013	14.265	13580	
4	c = 2000 Newtons per second	.00122	2.50	.00129	2.588	.00124	2.705	.00127	2.798	5000	13900
		.00182	3.75	.00188	3.822	.00177	3.992	.00180	4.087	7500	
		.00284	5.0	.00335	5.131	.00321	5.230	.00332	5.326	10000	
		1.420	6.940	1.824	7.259	1.810	7.357	1.824	7.455	13800	

TABLE 5 CONTINUED:

Column No.	Names and Values of Parameters Subjected to Variation	Position at the End of Phase 1		First Motion Reversal		Second Motion Reversal		Third Motion Reversal		P_o Final Constant Load in Newtons	Maximum Column Load in Newtons
		U_1 in cm	t_1 in sec	U_{m1} in cm	t_{m1} in sec	U_{m2} in cm	t_{m2} in sec	U_{m3} in cm	t_{m3} in sec		
5	c = 5000 Newtons per second	.00116	1.0	.00117	1.070	.00116	1.211	.00116	1.304	5000	14850
		.00145	1.5	.00149	1.594	.00146	1.724	.00148	1.878	7500	
		.00209	2.0	.00288	2.172	.00273	2.268	.00288	2.363	10000	
		.300	2.96	1.340	3.413	1.317	3.512	1.340	3.610	14800	
6	c = 10000 Newtons per second	.00115	.50	.00119	.588	.00116	.705	.00118	.798	5000	16100
		.00141	.75	.00152	.859	.00147	.967	.00150	1.062	7500	
		.0020	1.0	.00343	1.193	.00318	1.288	.00343	1.384	10000	
		.0949	1.60	.657	2.115	.643	2.214	.657	2.312	16000	

TABLE 5 CONTINUED:

Column No.	Names and Values of Parameters Subjected to Variation	Position at the End of Phase 1		First Motion Reversal		Second Motion Reversal		Third Motion Reversal		P_o Final Constant Load in Newtons	Maximum Column Load in Newtons
		U_1 in cm	t_1 in sec	U_{m1} in cm	t_{m1} in sec	U_{m2} in cm	t_{m2} in sec	U_{m3} in cm	t_{m3} in sec		
7	U_o = .5 centimeters	.658	50.0	.659	50.087	.658	50.206	.659	50.30	5000	11461
		.908	75.0	.908	75.085	.908	75.227	.908	75.322	7500	
		1.820	100.0	1.824	100.147	1.823	100.243	1.824	100.338	10000	
		3.203	114.6	3.427	115.760	3.426	115.856	3.427	115.953	11460	
8	U_o = .5 centimeters; c = 500 Newtons per second	.658	10.0	.659	10.088	.659	10.207	.659	10.30	5000	11460
		.907	15.0	.911	15.102	.909	15.219	.910	15.314	7500	
		1.819	20.0	1.846	20.135	1.839	20.230	1.846	20.326	10000	
		3.096	22.91	3.466	23.647	3.463	23.743	3.466	23.840	11455	

TABLE 5 CONTINUED:

Column No.	Names and Values of Parameters Subjected to Variation	Position at the End of Phase 1		First Motion Reversal		Second Motion Reversal		Third Motion Reversal		P_o Final Constant Load in Newtons	Maximum Column Load in Newtons
		U_1 in cm	t_1 in sec	U_{m1} in cm	t_{m1} in sec	U_{m2} in cm	t_{m2} in sec	U_{m3} in cm	t_{m3} in sec		
9	U_o = .5 centimeters; c = 1000 Newtons per second	.657	5.0	.662	5.097	.659	5.206	.660	5.30	5000	11460
		.907	7.5	.914	7.602	.910	7.720	.912	7.814	7500	
		1.796	10.0	1.868	10.172	1.857	10.268	1.868	10.364	10000	
		3.063	11.45	3.545	12.155	3.542	12.252	3.545	12.348	11450	
10	U_o = .5 centimeters; c = 2000 Newtons per second	.659	2.5	.667	2.583	.661	2.708	.663	2.801	5000	11460
		.909	3.75	.922	3.847	.914	3.972	.917	4.066	7500	
		1.775	5.0	1.883	5.169	1.865	5.265	1.883	5.360	10000	
		3.001	5.72	3.539	6.242	3.532	6.338	3.539	6.434	11440	

TABLE 5 CONTINUED:

Column No.	Names and Values of Parameters Subjected to Variation	Position at the End of Phase 1		First Motion Reversal		Second Motion Reversal		Third Motion Reversal		P_o Final Constant Load in Newtons	Maximum Column Load in Newtons
		U_1 in cm	t_1 in sec	U_{m1} in cm	t_{m1} in sec	U_{m2} in cm	t_{m2} in sec	U_{m3} in cm	t_{m3} in sec		
11	U_o = .5 centimeters; c = 5000 Newtons per second	.647	1.0	.663	1.117	.657	1.213	.663	1.306	5000	11400
		.904	1.50	.930	1.601	.917	1.720	.922	1.814	7500	
		1.658	2.0	2.064	2.169	1.998	2.265	2.064	2.360	10000	
		2.801	2.270	3.619	2.580	3.588	2.676	3.619	2.772	11350	
12	U_o = .5 centimeters; c =10000 Newtons per second	.666	.50	.701	.581	.670	.709	.682	.802	5000	12500
		.876	.75	.970	.862	.932	.968	.955	1.063	7500	
		1.382	1.0	1.984	1.201	1.905	1.296	1.984	1.392	10000	
		3.287	1.24	8.600	1.699	8.454	1.796	8.599	1.893	12400	

TABLE 5 CONTINUED:

Column No.	Names and Values of Parameters Subjected to Variation	Position at the End of Phase 1		First Motion Reversal		Second Motion Reversal		Third Motion Reversal		P_o Final Constant Load in Newtons	Maximum Column Load in Newtons
		U_1 in cm	t_1 in sec	U_{m1} in cm	t_{m1} in sec	U_{m2} in cm	t_{m2} in sec	U_{m3} in cm	t_{m3} in sec		
13	c = 5000 Newtons per second V_o = .2 centimeters per second	-.00631	1.0	.0029	1.135	-.00024	1.228	.0029	1.321	5000	14900
		-.0083	1.5	.0056	1.687	-.00146	1.781	.0006	1.875	7500	
		.00194	2.0	-.00445	2.117	-.00212	2.229	-.0034	2.324	10000	
		-.2771	2.97	-1.215	3.39	-1.186	3.488	-1.215	3.586	14850	
14	c = 1000 Newtons per second U_o = .0001 centimeters	.000116	5.0	.000116	5.083	.000116	5.207	.000116	5.30	5000	14060
		.000144	7.5	.000145	7.59	.000144	7.728	.00145	7.823	7500	
		.000208	10.0	.000212	10.125	.000211	10.228	.000212	10.324	10000	
		-1.417	14.05	-1.686	14.426	-1.679	14.524	-1.686	14.622	14050	

TABLE 5 CONTINUED:

Column No.	Names and Values of Parameters Subjected to Variation	Position at the End of Phase 1		First Motion Reversal		Second Motion Reversal		Third Motion Reversal		P_o Final Constant Load in Newtons	Maximum Column Load in Newtons
		U_1 in cm	t_1 in sec	U_{m1} in cm	t_{m1} in sec	U_{m2} in cm	t_{m2} in sec	U_{m3} in cm	t_{m3} in sec		
15	c = 5000 Newtons per second U_o = .1 centimeters	.1286	1.0	.1314	1.136	.1305	1.229	.1314	1.322	5000	12650
		.1853	1.5	.1878	1.569	.1831	1.743	.1843	1.838	7500	
		.2941	2.0	.3680	2.168	.355	2.263	.368	2.359	10000	
		1.707	2.52	2.765	2.864	2.736	2.961	2.765	3.058	12600	
16	c = 2000 Newtons per second; g = 10 meters per second square (c.f. Column 4 above)	.00133	2.5	.00139	2.579	.00133	2.720	.00135	2.813	5000	13200
		.00202	3.75	.00214	3.843	.00206	3.98	.00209	4.073	7500	
		.00773	5.0	.0111	5.180	.0106	5.276	.0111	5.372	10000	
		1.418	6.59	1.871	7.107	1.867	7.205	1.871	7.302	13180	

TABLE 5 CONTINUED:

Column No.	Names and Values of Parameters Subjected to Variation	Position at the End of Phase 1		First Motion Reversal		Second Motion Reversal		Third Motion Reversal		P_o Final Constant Load in Newtons	Maximum Column Load in Newtons
		U_1 in cm	t_1 in sec	U_{m1} in cm	t_{m1} in sec	U_{m2} in cm	t_{m2} in sec	U_{m3} in cm	t_{m3} in sec		
17	c = 5000 Newtons per second U_o = .1 centimeters g = 10 meters per second square (c.f. Column 23, Table4A)	.144	1.0	.151	1.091	.146	1.215	.148	1.308	5000	11900
		.191	1.5	.201	1.623	.198	1.722	.2003	1.817	7500	
		.455	2.0	.682	2.189	.684	2.285	.682	2.380	10000	
		1.735	2.37	2.745	2.717	2.718	2.814	2.745	2.911	11850	
18	c = 5000 Newtons per second; U_o = .5 centimeters; g = 10 meters per second square (c.f. Column 11 above)	.712	1.0	..750	1.097	.729	1.214	.739	1.308	5000	10700
		.966	1.5	1.042	1.634	1.021	1.731	1.038	1.826	7500	
		2.223	2.0	2.673	2.168	2.599	2.264	2.673	2.360	10000	
		2.793	2.130	3.663	2.481	3.638	2.577	3.663	2.673	10650	

TABLE 5 CONTINUED:

Column No.	Names and Values of Parameters Subjected to Variation	Position at the End of Phase 1		First Motion Reversal		Second Motion Reversal		Third Motion Reversal		P_o Final Constant Load in Newtons	Maximum Column Load in Newtons
		U_1 in cm	t_1 in sec	U_{m1} in cm	t_{m1} in sec	U_{m2} in cm	t_{m2} in sec	U_{m3} in cm	t_{m3} in sec		
19	c = 5000 Newtons per second; U_o = .1 centimeters; g = 0; $\Delta\theta = .9\Delta\alpha$; P_{n1} = 10000 Newtons; P_{n2} = unrestricted (c.f. Column 23, Table4.A)	.129	1.0	.131	1.14	.131	1.23	.131	1.33	5000	17050
		.185	1.5	.188	1.57	.184	1.74	.185	1.83	7500	
		.294	2.0	.342	2.12	.323	2.23	.333	2.32	10000	
		.656	3.40	.702	3.52	.683	3.64	.692	3.73	17000	
20	c = 5000 Newtons per second; U_o = .5 centimeters; g = 0; $\Delta\theta = .9\Delta\alpha$; P_{n1} = 10000 Newtons; P_{n2} = unrestricted; (c.f. Column 11 above)	.647	1.0	.663	1.12	.657	1.22	.663	1.31	5000	13950
		.904	1.50	.929	1.61	.917	1.72	.923	1.81	7500	
		1.658	2.0	1.915	2.12	1.815	2.22	1.88	2.31	10000	
		2.739	2.78	2.731	2.85	2.759	3.08	2.755	3.17	13900	

TABLE 5 CONTINUED:

Column No.	Names and Values of Parameters Subjected to Variation	Position at the End of Phase 1		First Motion Reversal		Second Motion Reversal		Third Motion Reversal		P_o Final Constant Load in Newtons	Maximum Column Load in Newtons
		U_1 in cm	t_1 in sec	U_{m1} in cm	t_{m1} in sec	U_{m2} in cm	t_{m2} in sec	U_{m3} in cm	t_{m3} in sec		
21	c = 2000 Newtons per second; U_o = .001 centimeters g = 0; $\Delta\theta$ = .9$\Delta\alpha$; P_{n1} = 10000 Newtons; P_{n2} = unrestricted (c.f. Column 4 above)	.00122	2.5	.00129	2.59	.00125	2.70	.00128	2.79	5000	18180
		.00182	3.75	.00188	3.83	.00180	3.97	.00182	4.06	7500	
		.00284	5.0	.00321	5.10	.0030	5.22	.0031	5.31	10000	
		.00469	9.08	.00338	9.17	.00474	9.34	.00441	9.43	18160	
22	c = 5000 Newtons per second; U_o = .1 centimeters; g = 0; $\Delta\theta$ = .9$\Delta\alpha$; P_{n1} = 10000 Newtons P_{n2} = 12500 Newtons (c.f. Column 15 above)	.129	1.0	.131	1.136	.130	1.229	.131	1.322	5000	13000
		.185	1.5	.188	1.569	.183	1.743	.184	1.838	7500	
		.294	2.0	.352	2.142	.323	2.276	.336	2.37	10000	
		1.154	2.59	2.556	2.963	2.522	3.060	2.556	3.157	12950	

In the course of development of the concepts in Chapters 9 and 10, numerous examples of the buckling behaviour of Model 3 were presented for illustrating the general arguments. The following two illustrations may convey additional information on the buckling properties of the inelastic column:

Fig. 56 shows the load-deflection behaviour of Column No. 11 in Table 5. This column exhibits no oscillations simultaneous with loading.

Fig. 57 depicts the load-deflection behaviour of Column No. 4 in Table 5. This column attains 10 consecutive motion reversal positions during buckling phase 1 which all occur below 10 000 Newtons load level. In order to show this oscillatory behaviour simultaneous with loading, the load-deflection behaviour of the column up to 10 000 Newtons load level is separately drawn to the left of the diagram in Fig. 57, with a deflection scale which is hundred times larger than the corresponding scale to the right of the diagram.

A study of Figs. 56 and 57 shows that even for an axial load as near the maximum column load as possible, the final stable lateral motion of the column lies in a small closed interval between motion reversal Positions 2 and 3. This is a unique property which is observable in all illustrations of the buckling behaviour presented in the course of the foregoing chapters.

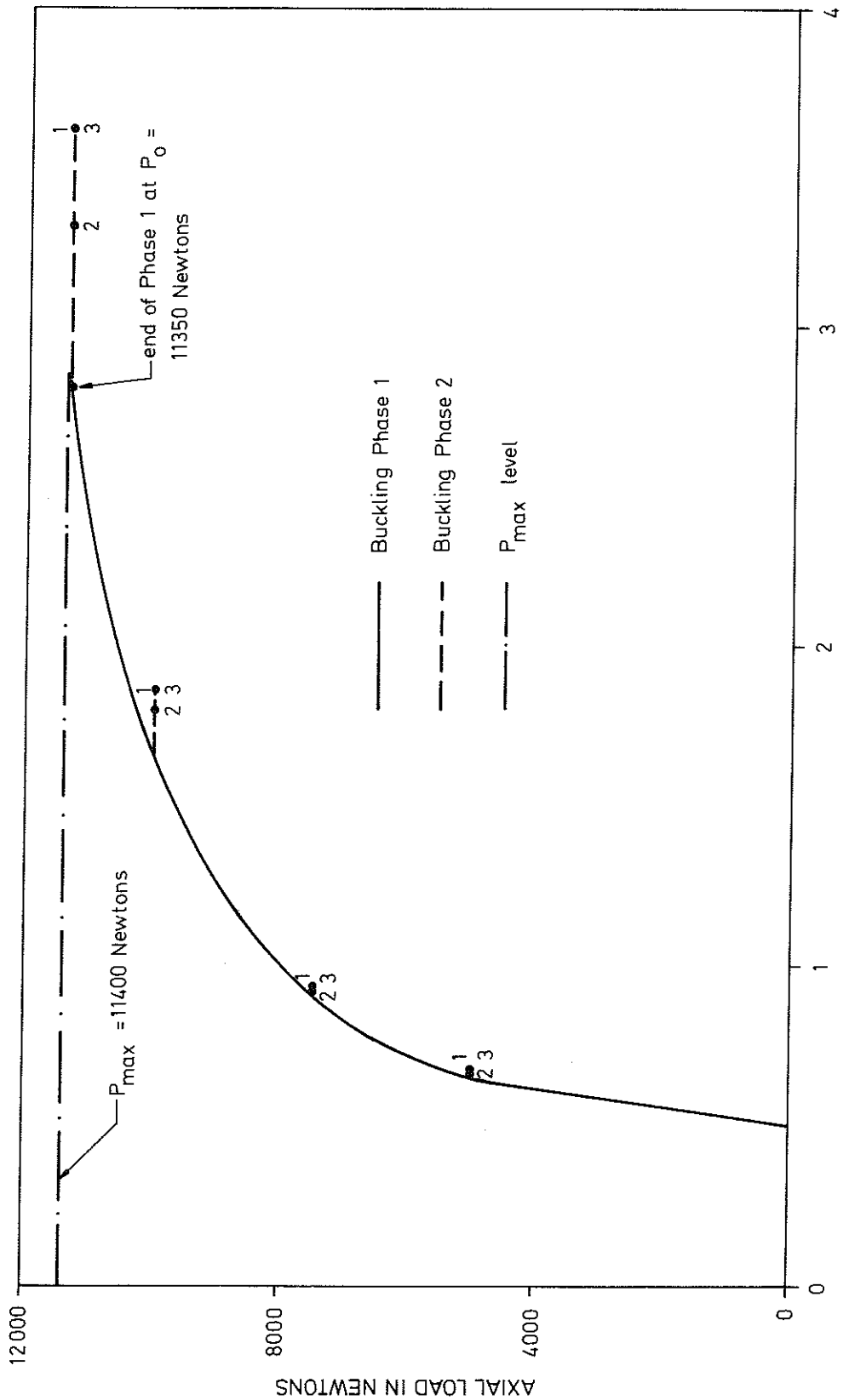

FIG. 56. BUCKLING BEHAVIOUR DURING BOTH PHASES FOR COLUMN No. 11 OF TABLE 5 WITH NO OSCILLATIONS SIMULTANEOUS WITH LOADING

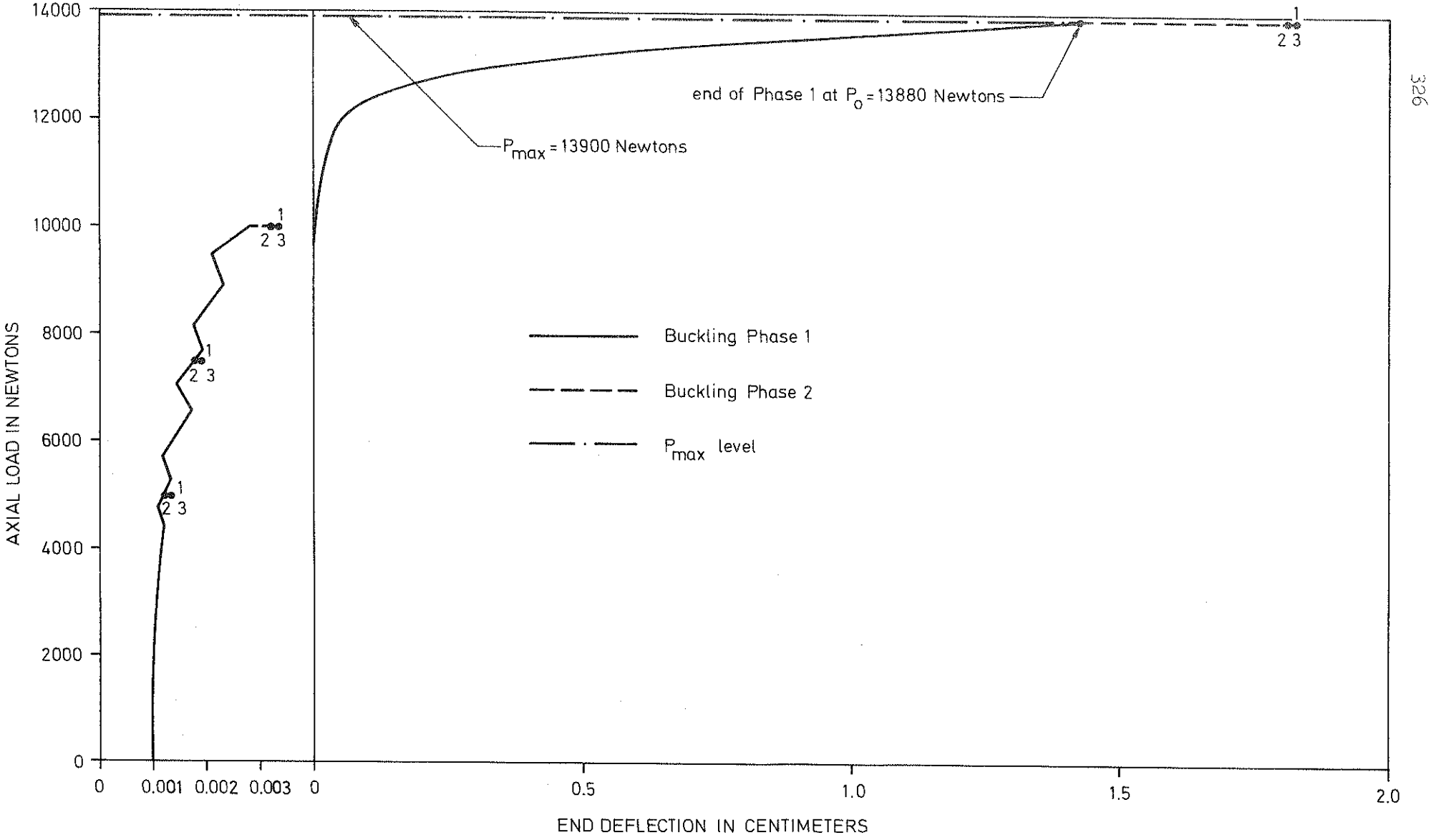

FIG. 57. BUCKLING BEHAVIOUR DURING BOTH PHASES FOR COLUMN No. 4 OF TABLE 5 WITH MILD OSCILLATIONS SIMULTANEOUS WITH LOADING

12. SUMMARY AND CONCLUSIONS

In the course of the foregoing discussions, the fundamental concepts of column stability were reexamined on the basis of physical ideas and geometrical concepts. Particular attention was paid to explore the buckling behaviour of an inelastic column with arbitrary stress strain diagram. A sequential chain of arguments were constructed to explain the various buckling phenomena in the context of a general dynamic theory. The following main results were acccmplished in the course of the present study:

In part I, the well-known concepts of elastic stability were reexamined, partly to refresh a knowledge of the existing fundamental principles, and partly to gain a clear understanding of the significance of the dynamic concept. The existence of a buckling load was proved on the basis of a predominantly geometrical argument. The static and dynamic behaviour of a simple perfect elastic column was studied according to the Small Displacement Theory for loads below or above the Euler load, and according to the Large Displacement Theory for loads above the Euler load; for loads above the Euler load, the temporary positions of the column simultaneous with loading were found to be dynamically unstable and if the axial load ceased to increase above the Euler load, the elastic column without energy losses was shown to move towards a lateral equilibrium position which would coincide with the static equilibrium position according to the Large Displacement Theory; a comparison of the results according to the Large and Small Displacement Theories verified the known fact that slight increases of axial load above the critical level would give rise to large lateral displacements, as a consequence of which it

was justified to use the Small Displacement Theory in subsequent discussion. In a next example, the buckling behaviour of a simple imperfect elastic column was studied for loads below the Euler load; the dynamically unstable positions of the column simultaneous with loading (buckling Phase 1) were determined, and subsequent motion towards a deflected equilibrium position under the influence of a constant axial load (buckling Phase 2) was studied.

In part II, two inelastic column models with bilinear stress strain diagram were analyzed. In the first model, the buckling behaviour of a perfect inelastic column simultaneous with the increase of axial load above the tangent modulus load was determined up to a point where either strain reversal begun to occur in the column, or the reduced modulus load was attained before the occurrence of strain reversal; the study of this model showed that in some situations considerable increase of the axial load above the tangent modulus load could take place without any strain reversal in the column; thus, deviations begun to emerge between the present dynamic approach and the static theory which assumes the occurrence of strain reversal in the column as soon as the axial load exceeds the tangent modulus load. In a second model, the complete buckling behaviour of a perfect inelastic column between the tangent modulus and the reduced modulus loads was studied during both buckling phases, taking into account the possibility of strain reversal simultaneous with loading; it was shown that for loads below the reduced modulus load, the motion of the column under constant axial load would turn into a simple harmonic motion around a delfected configuration, after three motion reversal positions subsequent to the end of buckling Phase 1; the amplitude of oscillation in the deflected

form was shown to be relatively small; for a number of loading rates, the lateral deflection zone according to the present approach was compared with the positions predicted by Shanley Theory; it was shown that this lateral deflection zone gets narrower and nearer to the positions envisaged by Shanley as the loading rate gets smaller and smaller values.

In part III, general concepts describing the buckling behaviour of an imperfect inelastic column with arbitrary stress strain diagram, were presented. Maximum column load was given a new definition, and a procedure for its determination was developed. For numerical results, a simple imperfect inelastic column with arbitrary stress strain diagram was thoroughly analyzed. The dependence of the maximum column load on the variations of dynamic parameters were proved, and the influence of parameter variations on the size of the maximum column load was fully determined. The following significant results were obtained:

The influence of velocity disturbance, imparted to the column simultaneously with the increase of axial load, could either increase or decrease the maximum column load; however, velocity disturbances imparted to the column at the start of buckling Phase 2 (under constant axial load) were shown to decrease the maximum column load.

An increase of the initial deflection was normally shown to result in a decrease of the maximum column load.

In most cases studied, an increase of the loading rate was shown to increase the maximum column load; the largest influence of the loading

rate was observed for columns with small initial imperfections; on a ceteris paribus basis, the loading rate was shown to have greater influence for longer columns with greater mass; an increase of the initial modulus of elasticity was shown to decrease the influence of the loading rate.

It was shown that under certain favourable conditions, it may be possible for a nearly perfect column which is originally deflected in a certain direction to permanently bow or fail in the reverse direction (backwards-inclined column); this phenomenon could either be induced due to favourable velocity disturbances, or self-generated due to a well-disposed parameter combination; this latter phenomenon, however, was shown to be sensitively dependent on the size of the time step corresponding to one computation cycle.

A backwards-inclined column was shown to behave abnormally in the sense that an increase of the initial deflection resulted in an increase of the maximum column load. This behaviour was observed during successive increases of the initial deflection, U_o, until at a certain value of U_o, the column turned into a normally behaving or forwards-inclined column.

Finally, the effect of the gravitational force and the influence of a possible change in the direction of application of the axial load on the buckling behaviour were numerically determined.

PART IV

APPENDICES

APPENDIX A

Discussion of Shanley Theory

Since the Shanley Theory has greatly influenced the development of inelastic stability since 1946, and since Shanley has eloquently stated the arguments in his original papers, the following paragraphs are directly quoted from Refs. 5 and 6. Thus, any misinterpretations of the original Shanley Theory are avoided.

1. Shanley's remarks and assumptions

Quotation from Ref. 5:

"But there is an implied assumption in the derivation of the reduced modulus theory that is open to question. It is in effect, assumed that something keeps the column straight while the strain increases from that predicted by the tangent modulus theory to the higher value derived from the reduced modulus theory. Actually, there is nothing (except the column's bending stiffness) to prevent the column from bending simultaneously with increasing axial loading ..... Evidently, the maximum column load will be reached somewhere between the loads predicted by the two theories. The entire problem should be reviewed on the basis that axial loading and bending can occur simultaneously. The use of the principle of superposition is not valid in this case ...."

2. Shanley's test data and his conclusions

It should be observed that Figs. A 1 - A 4 which are reproduced from Ref. 6, are given new numbers in this appendix.

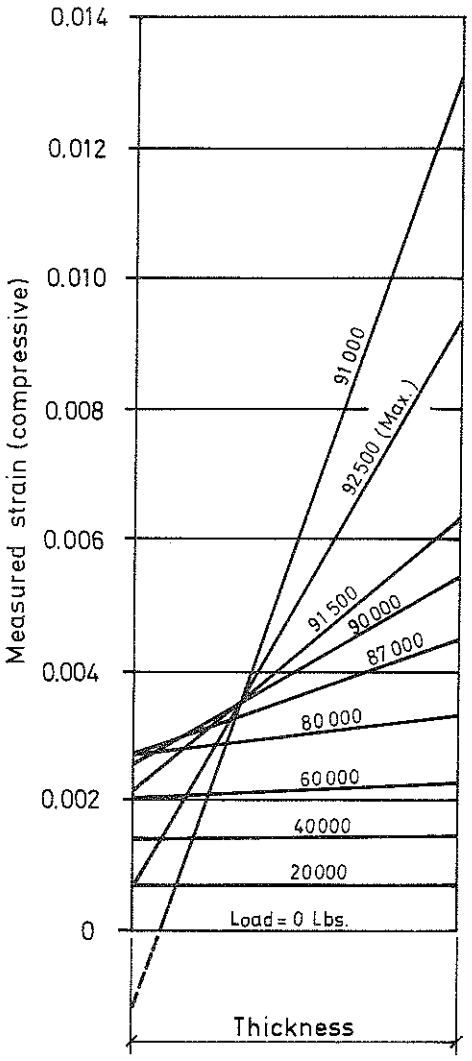

FIG. A1. STRAIN DISTRIBUTION AS DETERMINED IN A COLUMN TEST.

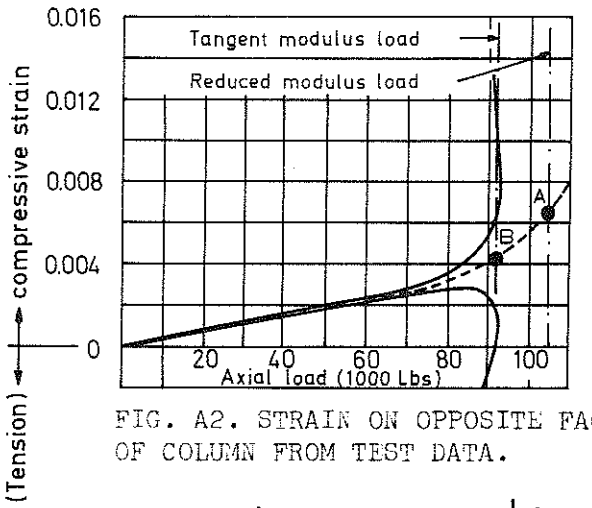

FIG. A2. STRAIN ON OPPOSITE FACES OF COLUMN FROM TEST DATA.

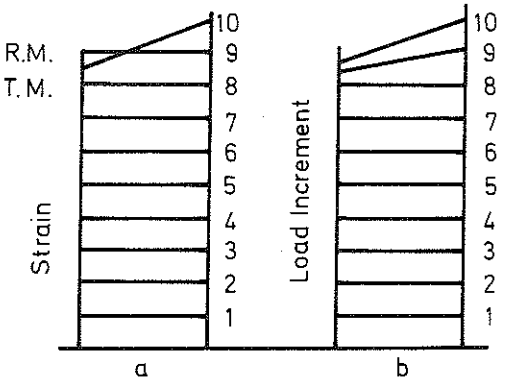

FIG. A3. ALTERNATIVE TYPES OF STRAIN DISTRIBUTION ACROSS COLUMN CROSS SECTI

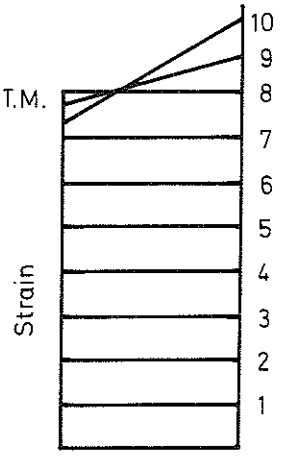

FIG. A4. TYPE OF STRAIN DISTRIBUTION NEEDED TO PERMIT LOADING BEYOND TANGENT-MODULUS LOAD.

Quotation from Ref. 6:

"Fig. A2 shows that if the column were to remain straight up to the reduced modulus load there could be no strain reversal below that load. What, then, can supply the extra effective value of E needed to prevent buckling beyond the tangent-modulus load?[1] The obvious answer is that the column cannot remain straight beyond the tangent modulus load; there must be a definite amount of strain reversal as soon as the load is further increased. This should cause the curves to separate at point B, one starting downward and the other upward. It can now be seen that in the derivation of the reduced modulus theory a questionable assumption was made. It was assumed, by implication at least, that the column remains straight while the axial load is increased to the predicted critical value, after which the column bends, or tries to bend. Actually the column is free to bend at any time. There is nothing to prevent it from bending simultaneously with increasing axial load. Under such a condition it is possible to obtain a nonuniform strain distribution without any stress reversal taking place. The difference between the two assumptions is shown diagrammatically in Fig. A3. Fig. A3(b), nowever, still represents a paradox. There is no strain reversal indicated; hence the value of E_t must apply over the entire cross-section; therefore, the column load cannot exceed the tangent-modulus value. If the load is to go any higher, some strain reversal must begin at the tangent-modulus load. The picture might then look something like Fig. A4 in which each succeeding increment of loading beyond the tangent-modulus load causes some additional strain reversal. The fact that this picture resembles the

---

1. The underlining does not occur in the original article. The statements underlined herein are intended to point out significant arguments.

actual distribution shown in Fig. A1 is significant.[2] ... on the basis of the foregoing reasoning the author predicted, in reference 1, (Ref. 5 herein), that (a) bending will begin as soon as the tangent-modulus load is exceeded; (b) the maximum column load will be reached somewhere between the loads predicted by the two theories."

From the above quotations and further study of Ref. 6, it may be inferred that Shanley Theory is based on the concept of a continuous sequence of equality between internal and external moments throughout the process of lateral deflection. However, the following discussion shows that the problem of inelastic buckling above the tangent modulus load is inherently dynamic as a consequence of which the duration of loading may exert considerable influence on the buckling behaviour.

In order to clearly visualize the significance of the dynamic concept, it is necessary to make a fundamental inquiry into the nature of buckling. For the purpose of the present discussion, it is sufficient to find out the behaviour of a perfect elastic column. Consider the column in Fig. A5 to be elastic and currently subjected to an axial load, equal to the Euler load. Under these circumstances and according to the small displacement theory, the column could be in equilibrium at any lateral deflection, U, corresponding to the free end of the column. This implies that at the Euler load, for any additional increment of lateral deflection, the extra increment of external moment is exactly balanced by the additional increment of internal moment.

---

2. Strain reversal for a given column may occur at any loading level depending on the loading rate, the size of initial disturbances, etc. The initial state must be specified for correctly interpreting the behaviour of the column for each particular case.

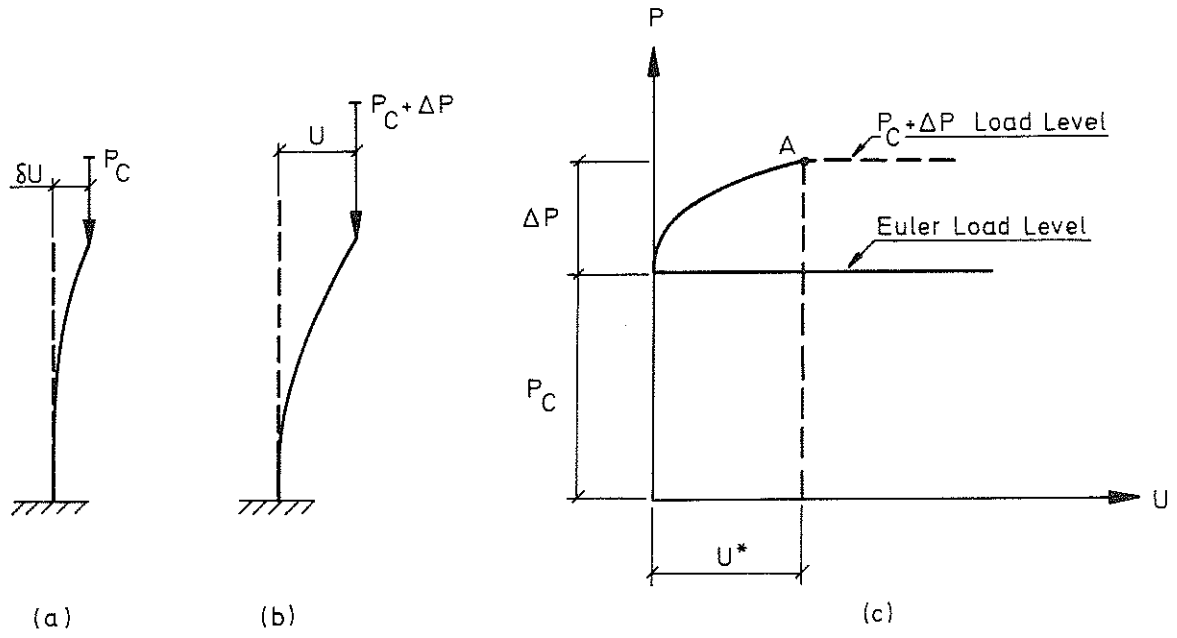

FIG. A 5. ILLUSTRATION OF THE CONCEPT OF ELASTIC BUCKLING: (a) INFINITESIMALLY DEFLECTED EQUILIBRIUM POSITION AT THE EULER LOAD; (b) DYNAMICALLY UNSTABLE POSITION OF THE COLUMN SIMULTANEOUS WITH LOADING ABOVE THE EULER LOAD; AND (c) LOAD-DEFLECTION BEHAVIOUR AT AND ABOVE THE EULER LOAD.

Now suppose that axial load of the column in Fig. A5 which is initially in equilibrium with an infinitesimal lateral deflection, δU, begins to increase by a finite increment, ΔP, above the Euler load. It is further assumed that at the load, $P = P_c + \Delta P$, the axial load remains constant. The question to be investigated now is what happens to the column by the time the axial load has reached the new constant level above the Euler load. Since, according to the small displacement theory, the additional external moment due to ΔP cannot be balanced by a corresponding increment of internal moment at the cross section of maximum strain (fixed end cross section), we may expect that the column quickly begins to bow with a rapidly growing lateral displacement. Thus, the phenomenon of buckling is intrinsically dynamic, involving the lateral

motion of the column as a function of time. The dynamic state of the column at the new load level above the Euler load will now be studied more closely as follows:

For a given column with certain dimensions and known mass per unit length, the magnitude of lateral deflection, U, at the time the axial load has exceeded the Euler load by an increment, ΔP, depends on two variable factors, namely, the initial infinitesimal deflection, δU, and the duration of loading, Δt, corresponding to the increase of axial load, ΔP. For a given δU, the larger the duration of loading, Δt, the greater would be the magnitude of the ensuing lateral deflection, U. On the other hand, for a given Δt, the smaller the initial deflection, δU, the smaller would be the time dependent lateral bowing which follows. Thus, for a given duration of loading, Δt, it is theoretically possible to choose δU sufficiently small or sufficiently large such that during the given interval of time, the column attains a lateral deflection, U^*, where U^* is any predetermined lateral deflection, see Fig. A5(c). This is a significant conclusion which will now be utilized below to examine the dynamic and static notions of buckling.

Fig. A6 is intended to show the alternative types of strain distribution simultaneous with an increase of axial load, ΔP, above the tangent modulus load.

Suppose that the axial load of an inelastic column increases by an increment, ΔP, just above the tangent modulus load. Thus, according to Shanley Theory some strain reversal must occur as depicted in Fig. A6(b). The amount of strain reversal predicted by Shanley Theory is predetermined for each given increment of axial load, ΔP. This implies

that for each specified increase of axial load above the tangent modulus load, the form and magnitude of strain distribution at each cross section and the corresponding deflected configuration of the column is uniquely determined.

FIG. A 6. ALTERNATIVE TYPES OF STRAIN DISTRIBUTION SIMULTANEOUS WITH AN INCREASE OF AXIAL LOAD, ΔP, ABOVE THE TANGENT MODULUS LOAD, AT THE CROSS SECTION OF THE COLUMN SUBJECTED TO MAXIMUM STRAIN: (a) WITH NO STRAIN REVERSAL; (b) WITH SOME STRAIN REVERSAL AS PREDICTED BY SHANLEY THEORY.

Now, if alternatively, the incremental strain distribution in Fig. A6(a) were to be applicable, the tangent modulus would govern the deformation throughout the column, whereby the column would be dynamically unstable analogous to the instability phenomenon discussed above in the case of an elastic column loaded above the Euler load. Furthermore, for the same duration of loading, Δt, the strain distribution in Fig. A6(a) would give rise to a lateral deflection less than the corresponding value due to the strain distribution in Fig. A6(b). Incidentally, there is a wide range of strain distributions of the type in Fig. A6(a) with no strain reversal, corresponding to various lateral deflections, all of which are smaller than the lateral bowing predicted by Shanley Theory.

The significance ofthe dynamic concept lies in the fact that there are infinite possibilities of lateral deflection simultaneous with

loading according to the incremental strain distribution in Fig. A6(a). Each different form of Fig. A6(a) would correspond to a different duration of loading. Strain reversal may occur in the column simultaneously with loading only when the rate of bending deformation becomes sufficiently large. Even after the occurrence of strain reversal, the column behaviour may differ from the static theory.

Thus, for a given column, the deflected configuration simultaneous with increase of load above the tangent modulus load is a funtion of the loading rate and the size of initial disturbances. Since both the loading rate and the magnitude of initial disturbances may widely vary, this would give rise to an equally wide range of variations of the deflected forms of the column simultaneous with the increase of axial load.

The present discussion was merely intended to show some qualitative difference between the static and dynamic concepts. The full significance of the ideas discussed herein may be found in the main body of the present work.

APPENDIX B

EQUATION OF MOTION OF PHASE 1 PRIOR TO STRAIN REVERSAL

a. The Particular Solution

The equation, see Eq. (52) in Sec. 5.4,

$$\frac{d^2\alpha}{dt^2} - St\alpha = 0, \quad S = \frac{3c}{ML} \tag{B1}$$

has the particular solutions

$$\alpha_i = t^{1/2} H^{(i)}_{1/3}(T) \quad (i = 1,2), \quad T = \frac{2}{3} j S^{1/2} t^{3/2} \tag{B2}$$

in which j = the pure imaginary number defined by the relation

$$j^2 = -1 \tag{B3}$$

and $H^{(i)}_{1/3}(T)$ = the Hankel functions of order one-third, see Ref. 19. The solution of Eq. (B1) is related to the Stokes equation

$$\frac{d^2u}{dz^2} + zu = 0 \tag{B4}$$

in the complex plane with the particular solutions

$$H1(z) = g + \frac{j\sqrt{3}}{3}(g - 2f) \tag{B5}$$

$$H2(z) = g - \frac{j\sqrt{3}}{3}(g - 2f) \tag{B6}$$

in which g and f are auxiliary functions of z defined by the equations

$$f(z) = a_o + a_1 z^3 + a_2 z^6 + \ldots a_m z^{3m} + \ldots \tag{B7}$$

$$g(z) = z(b_o + b_1 z^3 + b_2 z^6 + \ldots b_m z^{3m} + \ldots) \tag{B8}$$

in which a_m and b_m are real constants, see Ref. 19.

The general solution of Eq. (B1) may be put down in terms of the particular solutions of the Stokes equation:

$$\alpha = A_1 H1(z) + A_2 H2(z) \tag{B9}$$

in which A_1 and A_2 are complex constants and the argument, z, is related to the argument, T, of Equation (B2) by the relation

$$z = (\frac{3}{2}T)^{2/3}, \quad \arg z = \frac{2}{3} \arg T \tag{B10}$$

From Eqs. (B2) and (B10) and the mathemathical identity, $j = e^{j\pi/2}$, it follows that

$$z = e^{j\pi/3} s^{1/3} t \tag{B11}$$

Eq. (B11) shows that the argument, z, of the particular solutions of the Stokes equation appearing in Eq. (B9) must lie on the ray arg $z = \frac{\pi}{3}$ in the complex plane, z = x + jy, in which x and y denote the real and imaginary coordinates respectively.

By a computing program (see Appendix D, Program 3), the tabulated values given in Ref. 19 are used in the interpolation formulas given in the same reference:

$$Hi(z) = Hi(z_o)\left[1 - \frac{1}{2} z_o\Delta z^2 - \frac{1}{6}\Delta z^3 + \frac{1}{24} z_o^2\Delta z^4 + \frac{1}{30} z\Delta z^5 - \frac{1}{720} z_o^3\Delta z^6 + \right.$$

$$\left. + \frac{4}{720}\Delta z^6 + \ldots\right] + \overset{\prime}{Hi}(z_o)\left[\Delta z - \frac{1}{6} z_o\Delta z^3 - \frac{1}{12}\Delta z^4 + \frac{1}{120} z_o^2\Delta z^5 + \right.$$

$$\left. + \frac{1}{120} z_o\Delta z^6 + \ldots\right] \qquad \text{(B12)}$$

$$\overset{\prime}{Hi}(z) = Hi(z_o)\left[-z_o\Delta z - \frac{1}{2}\Delta z^2 + \frac{1}{6} z_o^2\Delta z^3 + \frac{1}{6} z_o\Delta z^4 - \frac{1}{120} z_o^3\Delta z^5 + \right.$$

$$\left. + \frac{4}{120}\Delta z^5 - \frac{1}{80} z_o^2\Delta z^6 + \ldots\right] + \overset{\prime}{Hi}(z)\left[1 - \frac{1}{2} z_o\Delta z^2 - \frac{1}{3}\Delta z^3 + \frac{1}{24} z_o^2\Delta z^4 + \right.$$

$$\left. + \frac{1}{20} z_o\Delta z^5 - \frac{1}{720} z_o^3\Delta z^6 + \frac{1}{72}\Delta z^6 + \ldots\right] \qquad \text{(B13)}$$

in which z = the desired argument, z_o = the argument nearest to z for which the functions $Hi(z_o)$ are already available, $\Delta z = z - z_o$ and the prime implies differentiation with respect to $\underline{z}$.

For arg $z = \frac{\pi}{3}$, the results of computations are given in Tables 1 and 2, in which R(Hi) and I(Hi) (i = 1,2) denote the real and the imaginary parts of the function Hi(z) respectively.

b. The General Solution

By expressing the complex functions in Eq. (B9) as the sum of real and imaginary parts, Eq. (B9) gets the form

$$R(\alpha) + jI(\alpha) = A_1 (R(H1) + jI(H1)) + A_2 (R(H2) + jI(H2)) \qquad (B14)$$

The complex constants A_1 and A_2 may also be written as the sum of real and imaginary parts:

$$A_1 = C_1 + jC_2, \quad A_2 = C_3 + jC_4 \qquad (B15)$$

in which C_1, C_2, C_3 and C_4 are arbitrary real constants.

From Eqs. (B3), (B14) and (B15) it follows that

$$R(\alpha) = C_1R(H1) - C_2I(H1) + C_3R(H2) - C_4I(H2) \qquad (B16)$$

and

$$I(\alpha) = C_1I(H1) + C_2R(H1) + C_3I(H2) + C_4R(H2) \qquad (B17)$$

The condition that the displacement function, α , must be a real function of time leads to

$$I(\alpha) = 0 \qquad (B18)$$

The complex functions g and f appearing in Eqs. (B5) and (B6) can also be expressed as the sum of the real and imaginary parts. Thus, from Eqs. (B5), (B6) and (B3), the real and imaginary parts of the function Hi(z) (i = 1,2), can be written in the form

$$R(h1) = R(g) - \frac{\sqrt{3}}{3} I(g) + \frac{2\sqrt{3}}{3} I(f) \tag{B19}$$

$$I(H1) = I(g) + \frac{\sqrt{3}}{3} R(g) - \frac{2\sqrt{3}}{3} R(f) \tag{B20}$$

$$R(H2) = R(g) + \frac{\sqrt{3}}{3} I(g) - \frac{2\sqrt{3}}{3} I(f) \tag{B21}$$

$$I(H2) = I(g) - \frac{\sqrt{3}}{3} R(g) + \frac{2\sqrt{3}}{3} R(f) \tag{B22}$$

From Eq. (B11) it can be concluded that

$$x^3 = e^{j\pi} St^3 = j^2 St^3 = -St^3 \tag{B23}$$

Thus the terms z^{3m} ($m = 1,2,3, \ldots$) in Eqs. (B7) and (B8) are all real whereby for $\arg z = \frac{\pi}{3}$, Eqs. (B7) and (B8) lead to

$$I(f) = 0 \text{ and } R(g) = \frac{\sqrt{3}}{3} I(g) \tag{B24}$$

Substitution of Eq. (B24) into Eqs. (B19) - (B22) and subsequent substitution into Eq. (B17) gives

$$I(\alpha) = \frac{2}{3} I(g)(2C_1 + C_3 + C_4\sqrt{3}) + \frac{2\sqrt{3}}{3} R(f)\,(C_3 - C_1) \tag{B25}$$

and

$$R(H1) = 0 \tag{B26}$$

From Eqs. (B18) and (B25) it follows that

$$C_1 = C_3 \text{ and } C_4 = -C_1\sqrt{3} \tag{B27}$$

Substitution of Eq. (B26) and (B27) into Eq. (B16) and the condition

expressed in Eq. (B18) lead to

$$\alpha = C_1(R(H2) + \sqrt{3}\, I(H2)) - C_2 I(H1) \tag{B28}$$

It is interesting to observe that Eq. (B26) serves as a check on the results of computations in Table 1.

From Eq. (B28) the angular velocity, α_1', can be expressed as the derivate of the deflection angle, α , with respect to time:

$$\alpha' = C_1 \frac{d}{dt} R(H2) + C_1\sqrt{3} \frac{d}{dt} I(H2) - C_2 \frac{d}{dt} I(H1) \tag{B29}$$

By definition, the derivative of the functions Hi(z) (i = 1,2) with respect to z can be written in the form

$$\frac{d}{dz} Hi(z) = R(Hi') + jI(Hi') \tag{B30}$$

Also for z = x + jy, the Cauchy-Riemann equations for analytic functions lead to

$$\frac{d}{dz} Hi(z) = \frac{\partial}{\partial x} R(Hi) + j \frac{\partial}{\partial x} I(Hi) \tag{B31}$$

and

$$\frac{d}{dz} Hi(z) = \frac{\partial}{\partial y} I(Hi) - j \frac{\partial}{\partial y} R(Hi) \tag{B32}$$

From Eqs. (B30) - (B32) it follows that

$$R(Hi') = \frac{\partial}{\partial x} R(Hi) = \frac{\partial}{\partial y} I(Hi) \tag{B33}$$

and

$$I(Hi') = \frac{\partial}{\partial x} I(Hi) = - \frac{\partial}{\partial y} R(Hi) \tag{B34}$$

From Eq. (B11) it can be concluded that

$$x = \frac{1}{2} S^{1/3} t \text{ and } y = \frac{\sqrt{3}}{2} S^{1/3} t \tag{B35}$$

which lead to

$$\frac{dx}{dt} = \frac{1}{2} S^{1/3} = \lambda \text{ and } \frac{dy}{dt} = \frac{\sqrt{3}}{2} S^{1/3} = \lambda\sqrt{3} \tag{B36}$$

The application of the chain rule

$$\frac{d}{dt} F(x,y) = \left(\frac{\partial F}{\partial x}\right)\left(\frac{dx}{dt}\right) + \left(\frac{\partial F}{\partial y}\right)\left(\frac{dy}{dt}\right) \tag{B37}$$

in which $F(x,y)$ stands for an arbitrary function of x and y, to all the derivatives in Eq. (B29) and substitution of Eqs. (B33), (B34), and (B36) in Eq. (B29) leads to

$$\dot{\alpha}' = 4C_1\gamma R(\dot{H}2) - C_2\gamma\left[I(\dot{H}1) + \sqrt{3}\, R(\dot{H}1)\right] \tag{B38}$$

Eq. (B35) results in the following relation between the time, t_1, elapsed during Phase 1 and the reference coordinate, y:

$$t_1 = \frac{2y}{\sqrt{3}\, S^{1/3}} \tag{B39}$$

APPENDIX C

EQUATIONS OF LATERAL AND AXIAL MOTION OF SIMPLE ELASTIC OR INELASTIC COLUMN

a. Multi-Cycle Computation Technique

In the following derivations, the motion of the simple column, see Fig. C 1, is sought during its entire loading period.

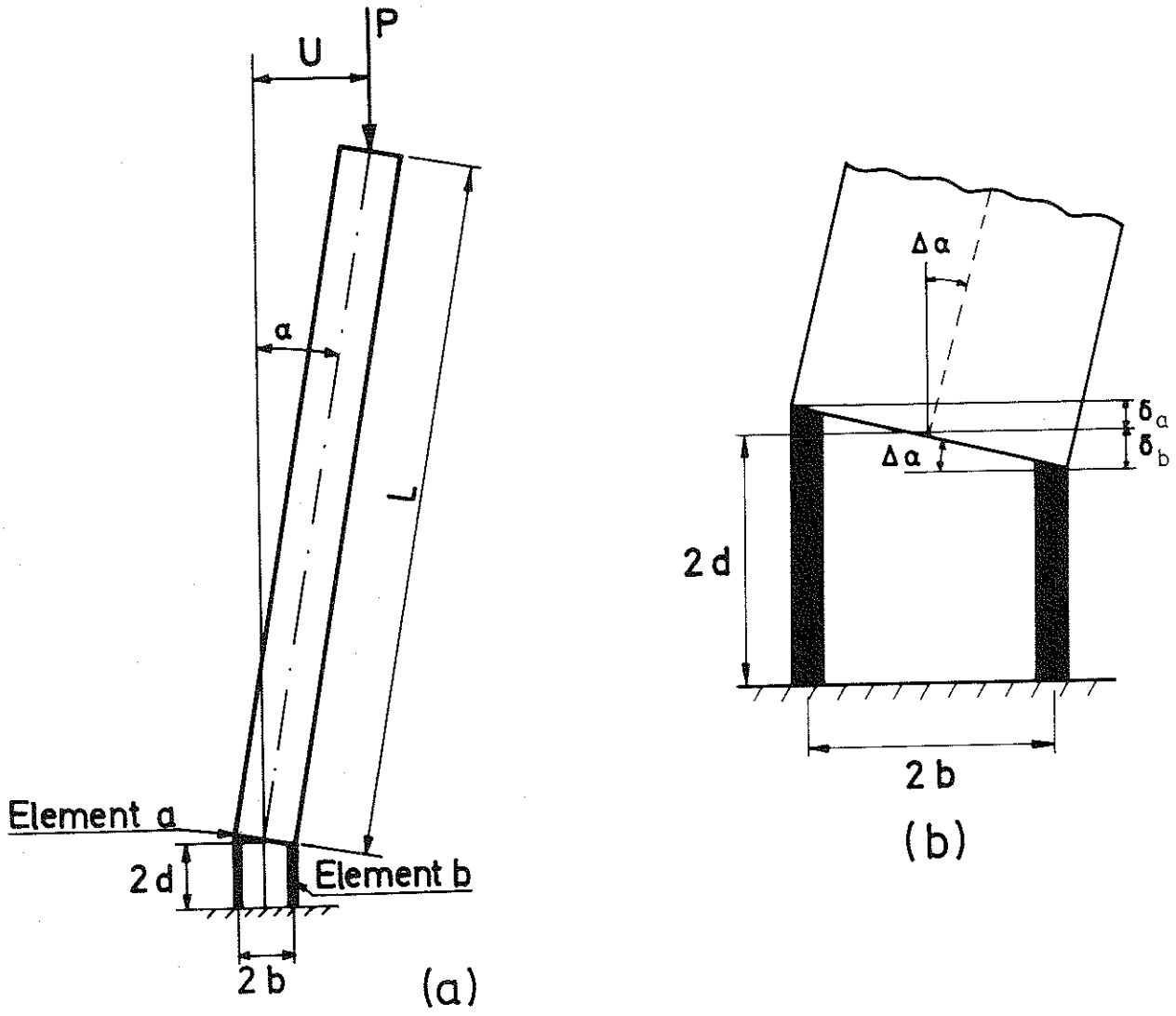

FIG. C 1. SIMPLE ELASTIC OR INELASTIC COLUMN; (a) THE ASSUMED MODEL; (b) THE HINGE

The column in Fig. C 1 is the same as Column B introduced in Sec. 1.3. The solution of the column problem during the whole loading history is obtained by dividing the given loading period into a sufficiently large number of loading intervals and applying the external load as concentrated increments at the beginning of each interval. Thus, starting from a known initial state, the equations of motion of the column are set up and the new state of the column is determined at the end of a short loading interval. Subsequent motion of the column during the next interval is found by considering the new state of the column as the initial state. Thus, the final state of the column at the end of the loading period may be obtained after a sufficiently large number of computation cycles, during which the state of the column at the end of a given cycle is regarded as the initial state for the next following cycle. Any desired degree of accuracy may be accomplished by controlling the time step corresponding to a computation cycle.

The following formulas are derived on the assumption of an inelastic column with an arbitrary stress strain diagram. However, the results are equally valid for an elastic column by replacing the tangent moduli of both column elements during all loading intervals by a single modulus of elasticity, E.

The stress strain relationship is in general approximated by a multilinear diagram, Fig. C 2.

The time step is assumed to be so short that the current values of the tangent moduli; E_a and E_b, corresponding to the two column elements, do not change during a computation cycle.

The details of treating the stress strain diagram in the numerical analysis of the problem is covered in the main text in Sec. 8.2. However, the stress strain diagram in fig. C 2 below is intended to illustrate the idea how it may be possible to maintain constant tangent moduli during the course of one computation cycle.

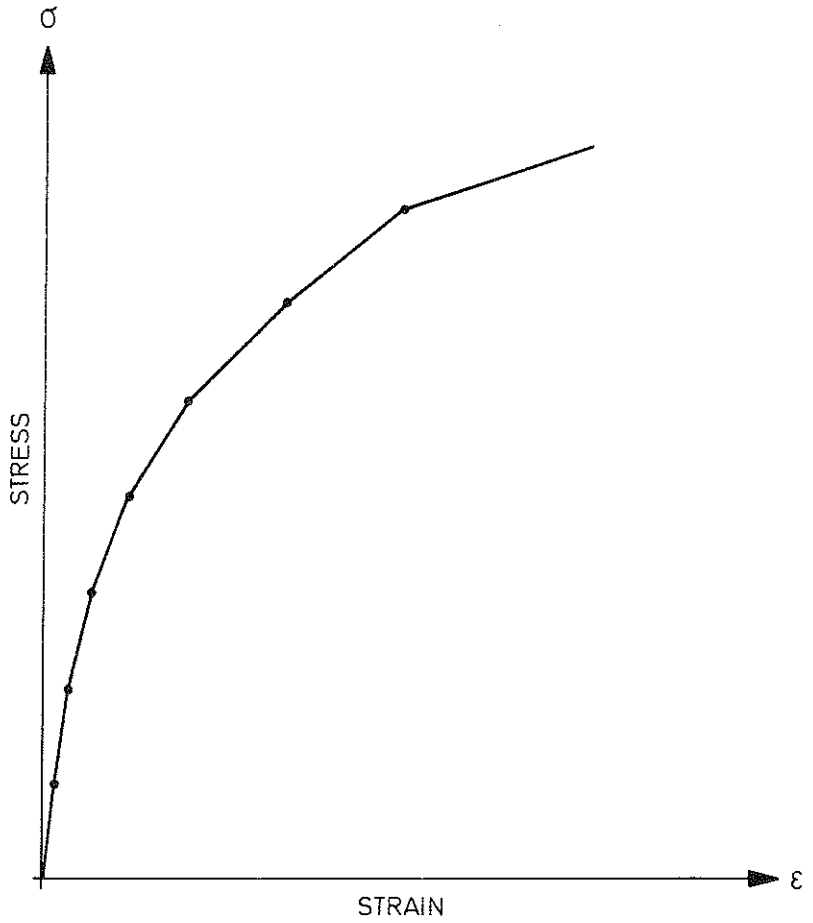

FIG. C 2. THE STRESS STRAIN RELATIONSHIP REPRESENTED BY A MULTILINEAR DIAGRAM

In the mathematical analysis which follows in the following section, the following facts should be observed:

1. The incremental stress and strain magnitudes are shown with two indices and each index may be either a or b. The first index refers to the type of the magnitude which can be either axial or bending, denoted by a and b respectively; and the second index refers to the actual column element which is denoted by the corresponding letter a or b. Thus, $\Delta\varepsilon_{ab}$ implies the axial strain increment corresponding to element b; $\Delta\varepsilon_{ba}$ indicates the bending strain increment in element a; $\Delta\varepsilon_{aa}$ refers to the axial strain element in element a; and $\Delta\varepsilon_{bb}$ means the bending strain increment in element b.

2. The incremental stress and strain magnitudes are always considered as absolute values; thus, the proper sign of a given magnitude is determined in each particular equation.

b. Equations of Lateral Motion

1. Incremental Magnitudes of Column Variables:

The strain increment, $\Delta\varepsilon_j$, in a column element, j, (j denotes either of the two elements a or b) is generally composed of an axial and a bending strain increment. Thus,

$$\Delta\varepsilon_j = \Delta\varepsilon_{aj} + \Delta\varepsilon_{bj} \qquad (C\ 1)$$

in which $\Delta\varepsilon_{aj}$ = the axial strain increment and $\Delta\varepsilon_{bj}$ = the bending strain increment.

Assuming that the column axially responds immediately to an increase of axial load, ΔP, see Secs. 3.1 and 3.2, the axial strain increment would be the same throughout the column such that

$$\Delta\varepsilon_{aa} = \Delta\varepsilon_{ab} \qquad (C\ 2)$$

and

$$\Delta\varepsilon_{aa} \cdot E_a \cdot A + \Delta\varepsilon_{ab} \cdot E_b \cdot A = \Delta P \qquad (C\ 3)$$

in which $\Delta\varepsilon_{aa}$, $\Delta\varepsilon_{ab}$, E_a, E_b = the axial strain increments and current deformation moduli[1] corresponding to elements a and b respectively; and A = area of one hinge element.

Using the notation

$$K = \frac{E_a}{E_b} \qquad (C\ 4)$$

---

1. The word deformation modulus is used herein interchangeably with the tangent modulus or the unloading modulus of elasticity as the case may be.

and substituting Eqs. (C 2) and (C 4) into Eq. (C 3) results in the following equation for the axial strain increments, $\Delta\varepsilon_{aa}$ and $\Delta\varepsilon_{ab}$ and the corresponding stresses $\Delta\sigma_{aa}$ and $\Delta\sigma_{ab}$:

$$\Delta\varepsilon_{aa} = \Delta\varepsilon_{ab} = \frac{\Delta P}{AE_b(K + 1)} \tag{C 5}$$

$$\Delta\sigma_{aa} = \frac{K \cdot \Delta P}{A(K + 1)} \tag{C 6a}$$

$$\Delta\sigma_{ab} = \frac{\Delta P}{A(K + 1)} \tag{C 6b}$$

The internal moment increment, ΔM_i, developed during one computation cycle is partly composed of an axially induced component, ΔM_{ia}, caused at the beginning of the computation cycle, due to the nonequality of the stress increments, Eqs. (C 6a) and (C 6b), and partly composed of a laterally induced component, ΔM_{ib}, due to subsequent lateral deflection of the column.

The axially induced internal moment increment, ΔM_{ia}, is found from the equation

$$\Delta M_{ia} = (\Delta\sigma_{ab} - \Delta\sigma_{aa}) \cdot A\, b \tag{C 7}$$

in which b = half of the hinge width; and all other symbols are already defined.

For the determination of the laterally induced internal moment increment, ΔM_{ib}, the relationship between the bending strain increment and the corresponding moment developed is found as follows:

The deformation increments, δ_a and δ_b, Fig. C 1(b), which are assumed to represent only the deformation due to bending, give rise to the following bending strain increments:

$$\Delta\varepsilon_{ba} = \frac{\delta_a}{2d} \quad , \quad \Delta\varepsilon_{bb} = \frac{\delta_b}{2d} \tag{C 8}$$

in which d = half of the depth of the hinge.

From the geometry of the bent column it follows that

$$\Delta\alpha = \lambda(\Delta\varepsilon_{ba} + \Delta\varepsilon_{bb}) \tag{C 9}$$

in which $\Delta\alpha$ = the lateral deflection angle increment; $\lambda = d/b$ and all other symbols are already defined.

Taking moment of the internal bending stresses with respect to the center of the hinge results in the following equation for the laterally induced internal moment increment, ΔM_{ib}:

$$\Delta M_{ib} = A\,b\,(E_a \cdot \Delta\varepsilon_{ba} + E_b \cdot \Delta\varepsilon_{bb}) \tag{C 10}$$

Multiplication of the right side of Eq. (C 10) by the unity factor $\Delta\alpha/\Delta\alpha$ and substitution of Eq. (C 9) into the denominator of the resulting equation gives

$$\Delta M_{ib} = \frac{A\,b\,(E_a \cdot \Delta\varepsilon_{ba} + E_b \cdot \Delta\varepsilon_{bb})}{\lambda(\Delta\varepsilon_{ba} + \Delta\varepsilon_{bb})} \cdot \Delta\alpha \tag{C 11}$$

writing $$\Delta M_{ib} = C \cdot \Delta\alpha \tag{C 12}$$

and comparing Eq. (C 12) with Eq. (C 11) leads to

$$C = \frac{A\,b\,(E_a \cdot \Delta\varepsilon_{ba} + E_b \cdot \Delta\varepsilon_{bb})}{\lambda(\Delta\varepsilon_{ba} + \Delta\varepsilon_{bb})} \qquad (C\ 13)$$

Since, the laterally induced bending increment results in no additional increase of axial load it follows that the bending stress increments, $\Delta\sigma_{ba}$ and $\Delta\sigma_{bb}$, corresponding to elements a and b respectively, are equal and opposite in sign, whereupon

$$E_a \cdot \Delta\varepsilon_{ba} = E_b \cdot \Delta\varepsilon_{bb} \qquad (C\ 14)$$

Substitution of Eqs. (C 4) and (C 14) into Eq. (C 13) leads to

$$C = \frac{2A \cdot b \cdot K \cdot E_b}{\lambda(K + 1)} \qquad (C\ 15)$$

The variable C, given by Eq. (C 15) defines the bending rigidity of the column.

Thus, the total moment increment, ΔM_i, during one computation cycle is the algebraic sum of the two components, ΔM_{ia} and ΔM_{ib}:

$$\Delta M_i = C \cdot \Delta\alpha + \Delta M_{ia} \qquad (C\ 16)$$

Substitution of Eqs. (C 6a) and (C 6b) into Eq. (C 7) and subsequent substitution of Eq. (C 8) into Eq. (C 16) leads to

$$\Delta M_i = C \cdot \Delta\alpha - \frac{\Delta P \cdot b(K - 1)}{(K + 1)} \qquad (C\ 17)$$

in which C is given by Eq. (C 15) and all the other variables are already defined.

From Eqs. (C 4), (C 9) and (C 14) it follows that

$$\Delta\varepsilon_{ba} = \frac{\Delta\alpha}{\lambda(K + 1)} \qquad \text{(C 18)}$$

$$\Delta\varepsilon_{bb} = \frac{K\Delta\alpha}{\lambda(K + 1)} \qquad \text{(C 19)}$$

The corresponding bending strain increments, $\Delta\sigma_{ba}$ and $\Delta\sigma_{bb}$, are found by substituting Eqs. (C 18) and (C 19) into Eq. (C 14). Thus,

$$\Delta\sigma_{ba} = \Delta\sigma_{bb} = \frac{KE_b \cdot \Delta\alpha}{\lambda(K + 1)} \qquad \text{(C 20)}$$

2. Total Magnitude of the Column Variables:

The incremental magnitudes of column variables are defined by Eqs. (C 1) - (C 20). The corresponding total magnitudes will now be determined below.

At a given instant of time during the current computation cycle, the total magnitudes of the internal moment, M_i, and the stresses, σ_a and σ_b, corresponding to elements a and b are obtained from the equations

$$M_i = M_{io} + \Delta M_i \qquad \text{(C 21)}$$

$$\sigma_a = \sigma_{ao} + \Delta\sigma_{aa} - \Delta\sigma_{ba} \qquad \text{(C 22)}$$

and

$$\sigma_b = \sigma_{bo} + \Delta\sigma_{ab} + \Delta\sigma_{bb} \qquad \text{(C 23)}$$

in which M_{io}, σ_{ao}, σ_{bo} = the total magnitudes at the beginning of the

current computation cycle corresponding to the internal moment and the stresses in elements a and b respectively; all other variables in Eqs. (C 21) - (C 23) are already defined.

For the determination of the total external moment, it is assumed that the axial load is updated at the beginning of the current computation cycle; furthermore any eventual change in the direction of the nonconservative axial load takes place at the beginning of the given cycle, so that the total external load, P, and its possible deviation from the vertical direction, θ, see Fig. C 3, are kept constant during the current computation cycle.

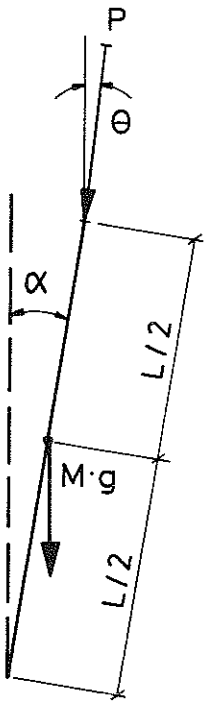

FIG. C 3. SCHEMATIC DIAGRAM SHOWING THE EXTERNAL FORCES, THE DEFLECTION ANGLE, α, AND THE DEVIATION ANGLE, θ

Thus, the total external moment, M_e, is found from the following equation:

$$M_e = (P + \frac{M \cdot g}{2}) \cdot L\alpha + P \cdot X_o - P\theta \cdot L \qquad (C\ 24)$$

in which g = gravitational acceleration; M = total mass of the column; and X_o = initial eccentricity in the application of the external load.

The equation of lateral motion of the column is governed by the equation

$$M_e - M_i = I\ddot{\alpha} \qquad (C\ 25)$$

in which I = the mass moment of inertia of the column; and $\ddot{\alpha}$ = the second derivative of the deflection angle, α, with respect to time.

The deflection angle increment, $\Delta\alpha$, may be written in the form

$$\Delta\alpha = \alpha - \alpha_o \qquad (C\ 26)$$

in which α_o = the initial deflection angle at the beginning of the current interval.

Substitution of Eq. (C 26) into Eq. (C 16), subsequent substitution of Eq. (C 16) into Eq. (C 21) followed by substitution of Eqs. (C 21) and (C 24) into Eq. (C 25) leads to the following differential equation for the determination of the lateral motion of the column:

$$\ddot{\alpha} + \frac{(C - P \cdot L - \frac{MgL}{2})}{I}\ \alpha = \frac{P \cdot X_o - M_{io} - \Delta M_{ia} + C\alpha_o - P\cdot\theta\cdot L}{I} \qquad (C\ 27)$$

Using the notations

$$\Delta M = C - P \cdot L - \frac{M \cdot g \cdot L}{2} \qquad (C\ 28)$$

$$H = P \cdot X_o - M_{io} - \Delta M_{ia} + C\alpha_o - P \cdot \theta \cdot L \qquad (C\ 29)$$

$$F = \frac{H}{\Delta M} \qquad (C\ 30)$$

and $$\omega = \sqrt{|\Delta M|/I} \qquad (C\ 31)$$

Then the deflection angle, α, and angular velocity, $\dot{\alpha}$, are found according to the following alternatives:

1. if $\Delta M < 0$ then the solutions are

$$\alpha = C_1 \sinh \omega t + C_2 \cosh \omega t + F \qquad (C\ 32)$$

and $$\dot{\alpha} = C_1 \omega \cosh \omega t + C_2 \omega \sinh \omega t \qquad (C\ 33)$$

2. if $\Delta M > 0$ then the solution of Eq. (27) leads to

$$\alpha = C_1 \sin \omega t + C_2 \cos \omega t + F \qquad (C\ 34)$$

and $$\dot{\alpha} = C_1 \omega \cos \omega t - C_2 \omega \sin \omega t \qquad (C\ 35)$$

The constants, C_1 and C_2, in the above equations are found from the initial condition at time, $t = 0$, at the beginning of the computation cycle:

$$C_1 = \frac{\dot{\alpha}_o}{\omega} \qquad (C\ 36)$$

and $$C_2 = \alpha_o - F \qquad (C\ 37)$$

3. if $\Delta M = 0$, then Eq. (C 27) leads to the solution

$$\alpha = \frac{H}{2I} t^2 + \dot{\alpha}_o \cdot t + \alpha_o \qquad (C\ 38)$$

$$\dot{\alpha} = \frac{H}{I} t + \dot{\alpha}_o \qquad (C\ 39)$$

c. Equations of Axial Motion[1]

Subjecting the column in Fig. C 1 to time dependent axial loading, the motion of the column in the axial direction would be governed by the equation

$$P_e - P_i = M \cdot \ddot{Z} \qquad (C\ 40)$$

in which P_e, P_i = the current values of the external and the internal axial loads respectively; M = mass of the column; and $\ddot{Z}$ = the second derivative of the axial deformation of the column hinge with respect to time.

The increment of internal load, ΔP_i, induced during the current computation cycle is found by the relation

$$\Delta P_i = 2AE_t \cdot \frac{\Delta Z}{2d} \qquad (C\ 41)$$

in which A = area of one hinge element; E_t = the current tangent modulus; d = half the depth of the hinge; and

$$\Delta Z = Z - Z_o \qquad (C\ 42)$$

where Z = the current value of the hinge axial deformation; and Z_o = the value of the axial deformation at the beginning of the current computation cycle.

---

1. Axial and lateral motions of the column are coupled and must be resolved simultaneously; however, since the axial inertia effects are found to be neglible for the loading rates considered herein (see Sec. 3.2), it has been justified to treat the two motions separately.

The current internal axial load, P_i, may be written as

$$P_i = P_{io} + \Delta P_i \tag{C 43}$$

in which P_{io} = the internal axial load at the beginning of the present computation cycle.

Substitution of Eq. (C 41) into Eq. (C 43) and subsequent substitution of Eqs. (C 43) and (C 42) into Eq. (C 40) leads to

$$\ddot{Z} + \frac{hZ}{M} = \frac{hZ_o - P_{io} + P_e}{M} \tag{C 44}$$

in which
$$h = \frac{AE_t}{d} \tag{C 45}$$

Using the notations

$$H_1 = hZ_o - P_{io} + P_e \tag{C 46}$$

$$F_1 = \frac{H_1}{h} \tag{C 47}$$

and
$$k^2 = \frac{h}{M} \tag{C 48}$$

Eq. (C 44) leads to the following solutions:

$$Z = A_1 \sin kt + A_2 \cos kt + F_1 \tag{C 49}$$

$$\dot{Z} = A_1 k \cos kt - A_2 k \sin kt \tag{C 50}$$

in which $\dot{Z}$ = the axial deformation rate and the constants A_1 and A_2 are

determined by the equations

$$A_1 = \frac{\dot{Z}_o}{k} \qquad (C\ 51)$$

and

$$A_2 = Z_o - F_1 \qquad (C\ 52)$$

in which $\dot{Z}_o$ = the deformation rate at the beginning of the present interval.

The value of the axial deformation, Z_s, according to the static theory is found to be

$$Z_s = \frac{P_e}{2AE} \cdot 2d = \frac{P_e}{h} \qquad (C\ 53)$$

d. Influence of Gravitational Force on the Motion of Simple Column

In the axial direction, the column's own weight may be replaced by an equal increment of axial load, provided that the directions of the axial load and the gravitational force coincide with each other. In the lateral direction, on the other hand, the column's own weight may in general exert some influence; however, for a perfect centrically loaded elastic or inelastic column whose initial state, at an increment of axial load below or above the critical load[1] is given, the gravitational force is shown below not to play any role in the ensuing lateral motion of the column. It is assumed that the axial load is conservative, i.e., it does not change direction simultaneous with the lateral motion, and that the disturbances which eventually give rise to lateral motion are vanishingly small.

Assume the column in Fig. C 1(a) to be an initially straight centrally loaded inelastic column which is currently deforming in the inelastic range under the influence of an axial load, P, such that

$$P = P_{cg} \pm \Delta P \qquad (C\ 54)$$

in which P_{cg} = the critical axial load which represents a load below which the deviation of the column from the straight configuration is vanishingly small; ΔP = the increment of load beyond the critical load, P_c; and the plus or minus sign correspond to an increment of load

---

1. The critical load in this discussion alludes to the axial load which takes into account the influence of the gravitational force. This explains the use of the index g in connection with the critical load in the equations of this section.

above or below the critical load respectively.

At the critical load, the internal moment, M_i, due to a small lateral deflection under the influence of constant axial load, is expressed by the equation

$$M_i = C_c \cdot \alpha_c \qquad (C\ 55)$$

in which C_c, α_c = the bending rigidity, respective deflection angle at the critical load, P_c.

Equating the expression for internal moment from Eq. (C 55) with the corresponding expression for the external moment

$$M_e = (P_c + \frac{M \cdot g}{2}) \cdot L \cdot \alpha_c \qquad (C\ 56)$$

results in the following equation for the critical axial load, P_{cg}:

$$P_{cg} = \frac{C_c}{L} - \frac{M \cdot g}{2} \qquad (C\ 57)$$

in which P_{cg} = the critical axial load carried by the column in excess of its own dead weight.

Substitution of Eq. (C 57) into Eq. (C 54) followed by substitution of Eq. (C 54) into Eq. (C 27), and observing that the deviation angle, θ, and the initial eccentricity, X_o, are both equal to zero, leads to the following equation of lateral motion of the simple column subjected to vanishingly small disturbances, according to the small displacement theory:

$$\ddot{\alpha} + \frac{(C - C_c \pm \Delta P)}{I} \cdot \alpha = \frac{-M_{io} - \Delta M_{ia} + C\alpha_o}{I} \qquad (C\ 58)$$

in which the variables C, M_{io}, ΔM_{ia} and α_o correspond to the beginning of the current computation cycle; and the plus or minus sign correspond to the increment of load, ΔP, below or above the critical load respectively.

Eq. (C 58) shows that the lateral motion of the initially straight centrally loaded, simple inelastic column above or below a certain critical load is independent of the gravitational force. This is, specifically true in the case of bending of the perfect simple inelastic column simultaneous with loading above the tangent modulus load. This simplifies the procedure for the determination of lateral motion of perfect columns, since the terms containing the gravitational force could, altogether, be omitted from the formulations. However, it should be observed that the gravitational force reduces the size of the critical axial load, see Eq. (C 57).

APPENDIX D

COMPUTER PROGRAMS

COMPUTER PROGRAMS

8 computer programs are developed herein for the purpose of the numerical illustration of the various buckling phenomena explored in this work. The following is a description of the task performed by each computer program:

1. Program 1 calculates the lateral deflection of a simple perfect elastic column simultaneous with the increase of axial load above the Euler load according to the Small Displacement Theory; furthermore, it determines the static lateral equilibrium positions of the column above the Euler load according to the Large Displacement Theory.

2. Program 2 calculates the axial and lateral motions of a simple imperfect elastic column simultaneous with the increase of axial load below the Euler load[1].

3. Program 3 computes the values of Hankel functions and their derivatives on the ray Arg $z = \pi/3$, in the complex plane. The computed values are then utilized in Program 4 below for the exact determination of the motion of the unstable column simultaneous with the increase of axial load above the tangent modulus load, see further Appendix B and Sec. 5.4.

4. Program 4 determines the motion of the simple perfect inelastic column with constant tangent modulus simultaneosly with the increase of axial load above the tangent modulus load, before the occurrence of strain reversal and below the reduced modulus load. The calculations are performed both according to an exact mathematical method (see Appendix B) and according to an approximate procedure (see Appendix C).

---

1. Throughout the calculations in Programs 2 - 8, the Small Displacement Theory is assumed, and the column simulated refers to the simple column in Fig. C 1, in Appendix C.

5. Program 5 determines the load deflection behaviour of the simple perfect inelastic column according to Shanley Theory.

6. Program 6 calculates the complete buckling behaviour of the simple inelastic column with constant tangent modulus between the tangent modulus and the reduced modulus loads. The possibility of strain reversal simultaneous with loading is taken into accont, and the oscillatory behaviour under the influence of constant axial load is thoroughly analyzed.

7. Program 7 and 8 are alternative programs for determination of the complete buckling behaviour of a simple imperfect inelastic column with arbitrary stress strain diagram. Program 8 is computationally more efficient; however, it cannot treat disturbances introduced at an arbitrary instant of time during buckling Phase 2 (under constant axial load); on the other hand, Program 7 takes more computer time, but it can deal with the disturbances during buckling Phase 2.

Program 1 is written in BASIC and run on HP 2116 C Computer at the Division of Building Technology and Structural Engineering, Lund; Programs 4 and 5 are written in special programming language and run on HP 9820 A desk computer, at the Department of Civil Engineering, Lund; Programs 2, 3, 6, 7, and 8 are executed on Univac 1100 digital computer located at the University of Lund Computing Center; Program 3 is written in Algol, whereas programs 2, 6, 7 and 8 are written in Univac BASIC.

Beginning with program 4, the symbols used in the programs are defined in this appendix; programs 1 and 2 perform simple tasks and most of the symbols used are identical to those of programs 6, 7 and 8; program 3 calculates other tabular values in addition to Tables 1 and 2 needed in the present work; thus, the symbols used in programs 1, 2 and 3 are not separately defined in this appendix.

```
100  REM                              PROGRAM 1:
110  REM.- THIS PROGRAM CALCULATES LARGE DEFORMATIONS OF SIMPLE COLUMN
120  PRINT "SAMPLE CALCULATIONS ACCORDING TO PROGRAM 1 :"
130  PRINT
150  PRINT
160  READ C0,L,A1,A4,M,X,U0,V0,A5,Y,A7
162  LET P1=C0/L
164  PRINT "EULER LOAD=",P1;"NEWTONS"
166  PRINT
168  PRINT
170  LET P0=3.14159
172  PRINT TAB(25),"A. STATIC ANALYSIS :"
174  PRINT
180  LET A0=P0/A1
190  PRINT TAB(15),"AXIAL LOAD","ALPHA","END DEFLECTION"
200  PRINT TAB(15),"IN NEWTONS","IN RADIANS","IN CENTIMETERS"
210  PRINT
220  LET L1=T=P2=L4=0
250  LET B1=1
260  LET L1=L1+A0
270  LET A3=L1/SIN(L1)-1
280  LET P=P1*L1/SIN(L1)
290  LET U=L*SIN(L1)*100
300  PRINT TAB(15),P,L1,U
302  PRINT
310  IF A3<A5 AND L1<P0/2 THEN 260
320  PRINT
330  PRINT
340  PRINT TAB(25),"B. DYNAMIC ANALYSIS :"
350  PRINT
360  PRINT "AXIAL LOAD","TIME","ALPHA","ALPHA RATE","DEFLECTION"
362  PRINT "IN NEWTONS","IN SECONDS","IN RADIANS","IN RAD/SEC","IN CM"
370  PRINT
380  LET I=M*L↑2/3
390  LET L0=L1=U0/(100*L)
400  LET L2=L3=V0/(100*L)
410  LET C=A4
412  LET A6=Y
420  LET L0=L1
430  LET L2=L3
440  LET T=T+X
450  LET P2=P2+C*X
460  LET P=P1+P2
470  LET G=SQR(3*P2/(M*L))
480  LET D1=(EXP(G*X)-EXP(-G*X))/2
490  LET D2=(EXP(G*X)+EXP(-G*X))/2
500  LET C1=L2/G
510  LET C2=L0
520  LET L1=C1*D1+C2*D2
530  LET L3=G*C1*D2+G*C2*D1
532  IF P <= P1*L1/SIN(L1) AND C>1 THEN 536
534  GOTO 540
536  PRINT "EXCESSIVE LATERAL DEFLECTION"
537  PRINT
```

```
 538  GOSUB 810
 539  STOP
 540  IF C<1 AND P>P1*L1/SIN(L1) THEN 420
 550  IF C<1 THEN 630
 560  LET A6=A6-1
 564  IF A6=0 THEN 570
 568  GOTO 590
 570  GOSUB 810
 580  LET A6=Y
 590  IF P2<A7*P1 THEN 420
 592  PRINT
 594  PRINT "LATERAL DEFLECTION CONTINUES UNDER CONSTANT AXIAL LOAD :"
 596  PRINT
 600  GOSUB 810
 610  LET C=0
 620  GOTO 420
 630  PRINT
 632  PRINT "EQUILIBRIUM POSITION ACCORDING TO LARGE DISPLACEMENT THEORY"
 634  PRINT
 640  GOSUB 810
 740  STOP
 800  REM.- SUBROUTINE PRINT :
 810  PRINT P,T,L1,L3,100*L*SIN(L1)
 820  PRINT
 830  RETURN
1500  REM                              DATA BLOCK :
1510  REM (C0=SPRING COEFFICIENT)
1520  DATA 25000
1530  REM (L=LENGTH)
1540  DATA 2.5
1550  REM (A1=P1/A0 ; A0=STATIC DEFLECTION ANGLE INCREMENT)
1560  DATA 10
1570  REM (A4=LOADING RATE)
1580  DATA 1000
1590  REM (M=MASS)
1600  DATA 100
1610  REM (X=TIME INTERVAL)
1620  DATA 1.00000E-02
1630  REM (U0=INITIAL END DEFLECTION)
1640  DATA 1.00000E-03
1650  REM (V0=INITIAL END VELOCITY)
1660  DATA 0
1670  REM (A5=DELTA(P)/P(EULER)=FINAL EQUILIBRIUM LOAD RATIO)
1680  DATA 1
1690  REM (Y=NO. OF CYCLES IN EACH PRINTING INTERVAL)
1700  DATA 100
1710  REM (A7=P2(FINAL)/P(EULER)=FINAL DYNAMIC LOAD RATIO)
1720  DATA .3
2000  END
```

```
100  REM                          PROGRAM 2 :
110  REM.- THIS PROGRAM INVESTIGATES INERTIA EFFECTS
120  PRINT 'SAMPLE CALCULATIOS ACCORDING TO PROGRAM 2 :'
130  PRINT
140  PRINT
150  READ A,B,E,X,U0,V0,D,L,M,G9,J,C,Y,B0
152 LET M2=B*A*1E-6*E*B/D
154  LET P9=M2/L-M*G9/2
156  PRINT 'EULER LOAD=';P9;'NEWTONS'
158  PRINT
159  PRINT
160  LET H0=A*E*1.00000E-04/D
162  READ X0
170  LET P=P1=Z=M0=T=Z2=Z1=0
180  PRINT 'P','TIME','Z(DYNAMIC)','Z(STATIC)'
190  PRINT
200  PRINT TAB(15),'ALPHA RATE','U(DYNAMIC)','U(STATIC)'
210  PRINT
212  PRINT
220  LET A9=Y
230  LET I=M*L**2/3
240  LET L0=L1=L9=U0/(100*L)
250  LET L2=L3=V0/(100*L)
280  IF J<.5 THEN 340
290  LET L4=M2*L0/(M2-M*G9*L/2)
300  LET M0=M2*(L4-L0)
310  LET L0=L1=L4
330  LET Z=M*G9*D/(A*E*1.00000E-04)
340  LET Z0=Z
350  LET Z2=Z1
360  LET L0=L1
370  LET L2=L3
380  LET T=T+X
390  LET P=P+C*X
400  LET H1=H0*Z0-P1+P
410  LET F1=H1/H0
420  LET K=SQR(H0/M)
430  LET A1=Z2/K
440  LET A2=Z0-F1
450  LET Z=A1*SIN(K*X)+A2*COS(K*X)+F1
460  LET Z1=A1*K*COS(K*X)-A2*K*SIN(K*X)
470  LET Z4=Z-Z0
480  LET P1=P1+H0*Z4
490  LET M3=M2-P*L-M*G9*L/2
500  LET H=P*X0/100+M2*L0-M0
510  LET F=H/M3
520  LET G=SQR(M3/I)
530  LET C1=L2/G
540  LET C2=L0-F
550  LET L1=C1*SIN(G*X)+C2*COS(G*X)+F
560  LET L3=C1*G*COS(G*X)-C2*G*SIN(G*X)
570  LET A7=L1-L0
580  LET M0=M0+M2*A7
581  GOTO 590
582  IF L2*L3>0 THEN 590
584  GOSUB 810
590  LET A9=A9-1
600  IF A9>.5 THEN 620
610  GOSUB 810
620  IF P >= B0*P9 THEN 640
630  GOTO 340
640  GOSUB 810
650  STOP
```

```
800  REM.- SUBROUTINE 1 :
810  LET Z3=(P+G9*M)/H0
820  LET U1=100*L*(P*X0/100+M2*L9)/M3
830  LET U=100*L*L1
840  PRINT P,T,Z,Z3
850  PRINT
860  PRINT TAB(15),L3,U,U1
862  IF P >= .8*P9 THEN 866
864  GOTO 870
866  LET A9=Y/4
868  GOTO 872
869  IF A9>.5 THEN 872
870  LET A9=Y
872  PRINT
874  PRINT
880  RETURN
1500  REM                          DATA BLOCK :
1510  REM (A=AREA OF ONE HINGE ELEMENT)
1520  DATA 5
1530  REM (B=HALF OF HINGE WIDTH)
1540  DATA 5
1550  REM (E=ELASTIC MODULUS)
1560 DATA 1E10
1570  REM (X=TIME INTERVAL)
1580  DATA 1.00000E-02
1590  REM (U0=INITIAL END DEFLECTION)
1600 DATA 0
1610  REM (V0=INITIAL END VELOCITY)
1620  DATA 0
1630  REM (D=HALF HINGE DEPTH)
1640 DATA 10
1650  REM (L=LENGTH)
1660 DATA 5
1670  REM (M=MASS)
1680 DATA 500
1690  REM (G9=GRAVITATIONAL ACCELERATION)
1700  DATA 10
1710  REM (J=0 IF G9=0,J=1 OTHERWISE)
1720  DATA 1
1730 REM (LOADING RATE,Y)
1740 DATA 2000,200
1770  REM (B0=P/P EULER)
1780 DATA .98
1790  REM (X0=INITIAL ECCENTRICITY)
1800 DATA .1
2000  END
```

PROGRAM 3

```
1       BEGIN
2             INTEGER I,N,M,G $
3             REAL ARRAY A(1:8,1:4),A10(1:8)$
4             I=0 $
5             A(1,1)=1.0 $
6             A(2,1)=-1/2 $
7             A(3,1)=-1/6 $
8             A(4,1)=1/24 $
9             A(5,1)=1/30 $
10            A(6,1)=-1/720 $
11            A(7,1)=4/720 $
12            A(8,1)=0 $
13            A(1,2)=1.0 $
14            A(2,2)=-1/6 $
15            A(3,2)=-1/12 $
16            A(4,2)=1/120 $
17            A(5,2)=1/120 $
18            A(6,2)=A(7,2)=A(8,2)=0 $
19            A(1,3)=0 $
20            A(2,3)=-1.0 $
21            A(3,3)=-1/2 $
22            A(4,3)=1/6 $
23            A(5,3)=1/6 $
24            A(6,3)=-1/120 $
25            A(7,3)=4/120 $
26            A(8,3)=-1/180 $
27            A(1,4)=1.0 $
28            A(2,4)=-1/2 $
29            A(3,4)=-1/3 $
30            A(4,4)=1/24 $
31            A(5,4)=1/20 $
32            A(6,4)=-1/720 $
33            A(7,4)=1/72 $
34            A(8,4)=0 $
35            READ (A10)$
36            M=50 $
37      BEGIN
38            INTEGER J,J1 $
39            REAL X,Y,XS,T,E,SID,COD $
40            REAL ARRAY A1(1:8),B,SIC,COC(1:4),X0(0:M),
41                        F,H(1:4,1:8),SUM(1:8,1:2,0:8),
42                        A0,FUN(1:8,0:M) $
43            FORMAT
44            F01(X51,I1,A0.0),
45            F02(X42,I1,A0.0),
46            F03(X48,I1,A0.0),
47            F04(X62,I2,A0.0),
48            FORM(X31,D4.2,D6.2,4D15.8,A1.1),
49            FORM1(X46,'TABLE .-COORDINATES X AND Y,',
50            'THE NEAREST',A0.1),
51            FORM2(X46,'TABULATED COORDINATES X0 AND Y0',X1,
52            'AND THE',A0.1),
53            FORM3(X46,'DIFFERENCE DELTA X=',
54            'X-X0',A0.3),
55            FORM41(X30,'TABLE  .-THE REAL AND'
56            ,X1,'IMAGINARY PARTS OF ',X1,
57            'FUNCTION H1 AND THE',A0.1),
58            FORM42(X30,'TABLE  .-THE REAL AND'
59            ,X1,'IMAGINARY PARTS OF ',X1,
60            'FUNCTION H2 AND THE',A0.1),
61            FORM04(X57,'TABLE   CONTINUED:',A0,3),
```

```
 62          FORM5(X36,'CORRESPONDING DERIVATIVES'
 63          ,X1,'FOR THE GIVEN VALUES OF',X1
 64          ,'Z0=X0+J*Y0',A0.3),
 65          FORM6(X81,'*',X14,'*',A0.1),
 66          FORM71(X32,'Y0',X4,'X0',X9,
 67          'R(H1)',X10,'I(H1)',X10,'R(H1)',
 68          X10,'I(H1)',A0.1),
 69          FORM72(X32,'Y0',X4,'X0',X9,
 70          'R(H2)',X10,'I(H2)',X10,'R(H2)',
 71          X10,'I(H2)',A0.1),
 72          FORM8(X31,'(1)',X3,'(2)',X10,
 73          '(3)',X12,'(4)',X12,'(5)',
 74          X12,'(6)',A0.1),
 75          FORM9(X43,'TABLE .-RESULTS OF',X1,
 76          'COMPUTATION OF THE REAL AND',A0.1),
 77          FORM01(X43,'IMAGINARY PARTS OF',X1,
 78          'FUNCTION H1 AND THE CORRES-',A0.1),
 79          FORM02(X43,'IMAGINARY PARTS OF',X1,
 80          'FUNCTION H2 AND THE CORRES-',A0.1),
 81          FORM10(X43,'PONDING DERIVATIVES',X1,
 82          'FOR Z ON THE RAY ARG Z= /3',A0.3),
 83          F0(X32,D4.2,4D16.8,A1.1),
 84          F1(X43,'Y=Y0',X11,'X',X11,'X0',
 85          X9,'DELTA X',A0.1),
 86          F10(X43,'(1)',X11,'(2)',X9,'(3)',
 87          X11,'(4)',A0.1),
 88          F2(X43,D4.2,D16.8,D16.8,D16.8,A1.1),
 89          F3(X79,'*',X15,'*',A0.1),
 90          F4(X33,'Y',X11,'R(H1)',X11,'I(H1)',X11,
 91          'R(H1)',X11,'I(H1)',A0.1),
 92          F40(X32,'(1)',X11,'(2)',X13,'(3)',
 93          X13,'(4)',X13,'(5)',A0.1),
 94          F5(X33,'Y',X11,'R(H2)',X11,'I(H2)',X11,
 95          'R(H2)',X11,'I(H2)',A0.1),
 96          NP(E3) $
 97          SWITCH S:=L3,L4,L5,L6,L8,L9,L10,L11 $
 98          MARGIN(66,2,65) $
 99          FOR N:=(1,1,5)DO FUN(N,0):=A10(N) $
100          J1:=4 $
101          WRITE(NP) $
102          WRITE(F01,J1) $
103          WRITE(FORM1) $
104          WRITE(FORM2) $
105          WRITE(FORM3) $
106          WRITE(F1) $
107          WRITE(F10) $
108          GO TO L $
109       L0:WRITE(NP) $
110          WRITE(F04,J1) $
111          WRITE(FORM04) $
112          WRITE(F1) $
113          WRITE(F10) $
114        L:READ (X,Y,T,A1) $
115          FOR N:=(1,1,8)DO H0(N,I):=A1(N) $
116          X0(I):=X $
117          XS:=X+T $
118          IF I EQL 0 THEN GO TO L1 $
119          E:=SQRT(X**2+Y**2) $
120          SID:=Y/E $
121          COD:=X/E $
122          FOR N:=(1,1,4)DO
123          BEGIN
124            B(N):=SQRT(A1(2*N-1)**2+A1(2*N)**2) $
125            SIC(N):=A1(2*N)/B(N) $
```

```
126             COC(N)=A1(2*N-1)/B(N) $
127             F(N,1)=COC(N) $
128             F(N,2)=T**2*E*(COC(N)*COD-SIC(N)*SID) $
129             F(N,3)=T**3*COC(N) $
130             F(N,4)=T**4*E**2*(COC(N)*(COD**2-SID**2)
131                   -2*SIC(N)*SID*COD) $
132             F(N,5)=T**5*E*(COC(N)*COD-SIC(N)*SID) $
133             F(N,6)=T**6*E**3*(COC(N)*(4*COD**3-3*COD)-
134                   SIC(N)*(3*SID-4*SID**3)) $
135             F(N,7)=T**6*COC(N) $
136             F(N,8)=T**7*E**2*(COC(N)*(COD**2-SID**2)
137                   -2*SIC(N)*SID*COD) $
138             H(N,1)=SIC(N) $
139             H(N,2)=T**2*E*(SIC(N)*COD+COC(N)*SID) $
140             H(N,3)=T**3*SIC(N) $
141             H(N,4)=T**4*E**2*(SIC(N)*(COD**2-SID**2)
142                   +2*COC(N)*SID*COD) $
143             H(N,5)=T**5*E*(SIC(N)*COD+COC(N)*SID) $
144             H(N,6)=T**6*E**3*(SIC(N)*(4*COD**3-3*COD)+
145                   COC(N)*(3*SID-4*SID**3)) $
146             H(N,7)=T**6*SIC(N) $
147             H(N,8)=T**7*E**2*(SIC(N)*(COD**2-SID**2)
148                   +2*COC(N)*SID*COD) $
149          END $
150          FOR N=(1,1,8)DO FOR G=1,2 DO
151          BEGIN
152             SUM(N,G,0)=0 $
153             SUM(1,G,N)=SUM(1,G,N-1)+A(N,1)*F(2*G-1,N) $
154             SUM(2,G,N)=SUM(2,G,N-1)+A(N,2)*F(2*G,N) $
155             SUM(3,G,N)=SUM(3,G,N-1)+A(N,3)*F(2*G-1,N) $
156             SUM(4,G,N)=SUM(4,G,N-1)+A(N,4)*F(2*G,N) $
157             SUM(5,G,N)=SUM(5,G,N-1)+A(N,1)*H(2*G-1,N) $
158             SUM(6,G,N)=SUM(6,G,N-1)+A(N,2)*H(2*G,N) $
159             SUM(7,G,N)=SUM(7,G,N-1)+A(N,3)*H(2*G-1,N) $
160             SUM(8,G,N)=SUM(8,G,N-1)+A(N,4)*H(2*G,N)
161          END $
162          FUN(1,I)=B(1)*SUM(1,1,8)+B(2)*T*SUM(2,1,8) $
163          FUN(2,I)=B(1)*SUM(5,1,8)+B(2)*T*SUM(6,1,8) $
164          FUN(3,I)=B(1)/T*SUM(3,1,8)+B(2)*SUM(4,1,8) $
165          FUN(4,I)=B(1)/T*SUM(7,1,8)+B(2)*SUM(8,1,8) $
166          FUN(5,I)=B(3)*SUM(1,2,8)+B(4)*T*SUM(2,2,8) $
167          FUN(6,I)=B(3)*SUM(5,2,8)+B(4)*T*SUM(6,2,8) $
168          FUN(7,I)=B(3)/T*SUM(3,2,8)+B(4)*SUM(4,2,8) $
169          FUN(8,I)=B(3)/T*SUM(7,2,8)+B(4)*SUM(8,2,8) $
170       L1:WRITE(F2,Y,XS,X,T) $
171          I=I+1 $
172          IF I EQL 26 THEN GO TO LL $
173          IF I LEQ M THEN GO TO L $
174          G=1 $
175          J=1 $
176          J1=J1+1 $
177          GO TO L2 $
178       LL:WRITE(NP) $
179          WRITE(F04,J1) $
180          WRITE(FORM04) $
181          WRITE(FORM6) $
182          IF G EQL 1 THEN WRITE(FORM71)
183          ELSE WRITE(FORM72) $
184          WRITE(FORM8) $
185          GO TO S(J) $
186       L2:WRITE(NP) $
187          WRITE(F02,J1) $
188          IF G EQL 1 THEN WRITE(FORM41)
189          ELSE WRITE(FORM42) $
```

```
190           WRITE(FORM5) $
191           WRITE(FORM6) $
192           IF G EQL 1 THEN WRITE(FORM71)
193           ELSE WRITE(FORM72) $
194           WRITE(FORM8) $
195           GO TO S(J) $
196        L3:FOR I=(0,1,25)DO
197           BEGIN
198             Y=I*0.1 $
199           WRITE(FORM,Y,X0(I),FOR N=(1,1,4)DO H0(N,I)) $
200           END $
201           J=J+1 $
202           GO TO LL $
203        L4:FOR I=(26,1,M)DO
204           BEGIN
205             Y=I*0.1 $
206           WRITE(FORM,Y,X0(I),FOR N=(1,1,4)DO H0(N,I)) $
207           END $
208           J=J+1 $
209           J1=J1+1 $
210           G=2 $
211           GO TO L2 $
212        L5:FOR I=(0,1,25)DO
213           BEGIN
214             Y=I*0.1 $
215           WRITE(FORM,Y,X0(I),FOR N=(5,1,8)DO H0(N,I)) $
216           END $
217           J=J+1 $
218           GO TO LL $
219        L6:FOR I=(26,1,M)DO
220           BEGIN
221             Y=I*0.1 $
222           WRITE(FORM,Y,X0(I),FOR N=(5,1,8)DO H0(N,I)) $
223           END $
224           J=J+1 $
225           J1=J1+1 $
226           G=1 $
227           GO TO L7 $
228        NN:WRITE(NP) $
229           WRITE(F04,J1) $
230           WRITE(FORM04) $
231           WRITE(F3) $
232           IF G EQL 1 THEN WRITE(F4)
233           ELSE WRITE(F5) $
234           WRITE(F40) $
235           GO TO S(J) $
236        L7:WRITE(NP) $
237           WRITE(F03,J1) $
238           WRITE(FORM9) $
239           IF G EQL 1 THEN WRITE(FORM01)
240           ELSE WRITE(FORM02) $
241           WRITE(FORM10) $
242           WRITE(F3) $
243           IF G EQL 1 THEN WRITE(F4)
244           ELSE WRITE(F5) $
245           WRITE(F40) $
246           GO TO S(J) $
247        L8:FOR I=(0,1,25)DO
248           BEGIN
249             Y=I*0.1 $
250             WRITE(FO,Y,FOR N=(1,1,4)DO FUN(N,I)) $
251           END $
252           J=J+1 $
253           GO TO NN $
```

```
254          L9:FOR I=(26,1,M)DO
255              BEGIN
256                Y=I*0.1 $
257                WRITE(FO,Y,FOR N=(1,1,4)DO FUN(N,I)) $
258              END $
259              J=J+1 $
260              J1=J1+1 $
261              L=2 $
262              GO TO L7 $
263          L10:FOR I=(0,1,25)DO
264              BEGIN
265                Y=I*0.1 $
266                WRITE(FO,Y,FOR N=(5,1,8)DO FUN(N,I)) $
267              END $
268              J=J+1 $
269              GO TO NN $
270          L11.FOR I=(26,1,M)DO
271              BEGIN
272                Y=I*0.1 $
273                WRITE(FO,Y,FOR N=(5,1,8)DO FUN(N,I)) $
274              END $
275              WRITE(NP) $
276        END OF CALCULATIONS
277        END OF PROGRAM $
COMPILATION COMPLETE
```

PROGRAM 4

a. Description

This program determines the load deflection behaviour of the column in Model 1 during buckling Phase 1, before the occurrence of strain reversal. The calculations are carried out for both exact and approximate methods. The exact method utilizes the function values in Tables 1 and 2 at intervals corresponding to y = 0.02. The respective time interval, t_1, is calculated by means of Eq. (57), see Sec. 5.4 and the corresponding deflection angle and angular velocity is determined by Eqs. (55) and (56) in which the constants C_1 and C_2 are found by Eqs. (58) and (59) respectively.

The approximate method uses the procedure described in Appendix C The time spacing, Δt, for the approximate method, is chosen in such a way that the time interval, t, for the exact method is an integer multiple of the time spacing, Δt. Thus, the printing interval for both methods could be made to coincide at time intervals corresponding to increments of y equal to 0.2.

This program is written in special programming language and run on HP 9820 A Calculator.

b. Names of Variables

Name in the program	Name in the actual model
R0	1
R1 - R120	20 x 6 sets of Hankel functions: R(H1), I(H2), I(H1), R($\dot{H}$2), R($\dot{H}$1), I($\dot{H}$1)
R121 - R160	Registers reserved for storing additional H-functions
A	Area
B	b
C	c
X	Δt
Y	No. of calculation cycles between two consecutive printouts
R161	U_o, α_o,α
R162	V_o, $\dot{\alpha}_o$,$\dot{\alpha}$
R163	E_o
R164	E_t
R165	M, saf, see Eq. (121)
R166	L
R167	y = imaginary part of z
R168	S = 3 c/ML
R169	$\gamma = 1/2\ S^{1/3}$
R170	C_{1h} a)
R171	C_{2h}
R172	$K_o = E_o/E_t$, ΔP_{max}
R173	P_t
R174	t = time in seconds
R175	ω = (3ct/ML)
R176	$C_1 = \dot{\alpha}_o/\omega$

a) Index h implies correspondence to the exact method using Hankel functions

Name in the program	Name in the actual model
R177	Sinh ($\omega\Delta t$)
R178	Cosh ($\omega\Delta t$)
R179	α_h
R180	C_2
R181	$\dot{\alpha}_h$
R182	Variable integer controlling the printing interval
R183	$\Delta P/\Delta P_{max}$
R184	d
R185	λ
R200	The desired value of y at which the first information is printed

PROGRAM 4

c. List

```
0:
TBL 2;FXD 7;1→R0
⊢
1:
ENT "U0",R161,"V
0",R162,"E0",R16
3,"ET",R164,B,"D
",R184,A⊢
2:
ENT "M",R165,"L"
,R166,C,"PIN",Y,
"Y0",R200⊢
3:
PRT "U0=",R161,"
V0=",R162,"E0=",
R163,"ET=",R164,
"B=",B,"A=",A⊢
4:
PRT "M=",R165,"L
=",R166,"C=",C,"
PIN=",Y,"D/B=",R
184/B;SPC 2⊢
5:
R184/B→R185⊢
6:
0→R167;(3C/R165R
166→R168)↑(1/3)/
2→R169;0→X⊢
7:
R161/100R166→R16
1;R162/100R166→R
162⊢
8:
R162/R169(7R4+ƒ3
R6→R170)+R161(R6
+ƒ3R4)/R170R2→R1
70⊢
9:
R161/R2-ƒ3R170→R
171;I⊢ R167>0;
GTO +6⊢
10:
R163/R164→R172⊢
11:
(1E-6*BAR164/R16
6R185→R173)(R172
-1)/(R172+1)→R17
2⊢
12:
PRT "FT=",R173,"
DELTA PMAX=",R17
2;SPC 3⊢
13:
Y→R182;0→R183→R1
74;PRT "INITIAL
STATE :";SPC 1;
GSB "2"⊢
14:
GSB "4"⊢
15:
R167/(Y-1)ƒ3R169
→X;PRT "DELTA T=
",X;SPC 3⊢
16:
PRT "MAIN","CALC
ULATIONS :";SPC
2⊢
17:
R174→X→R174;ƒ(R1
68R174)→R175⊢
18:
R162/R175→R176;R
161→R1d0⊢
19:
(EXP (R175X)-
EXP (-R175X))/2→
R177⊢
20:
(EXP (R175X)+
EXP (-R175X))/2→
R178⊢
21:
R176R177→R180R17
8→R181⊢
22:
R176R175R178+R18
0R175R177→R182⊢
23:
1E-4*ĿR164R162B/
R184C→R165⊢
24:
IF (R182-1→R182)
=1;GSB "2"⊢
25:
IF R182=1;Y→R182
⊢
26:
IF 1=(I>R165)*(R
200>R167);GTO +2
⊢
27:
IF R182=Y;GSB "1
"⊢
28:
IF 1≤R165;PRT "S
RB";GSB "1"⊢
29:
IF 1≤(CR174/R172
→R183);PRT "DPMA
X";GSB "1"⊢
30:
IF 1≤(1≤R165)+(1
≤R183);STP ⊢
31:
IF INT (R167+.9)
=6;PRT "Y=",R167
;STP ⊢
32:
IF R182=Y;GSB "4
"⊢
33:
GTO 17⊢
34:
"1";PRT "APPROXI
MATE","SOLUTION
:";SPC 1;GSB "3"
⊢
35:
PRT "U=",100R166
R161⊢
36:
PRT "V=",100R166
R162;SPC 3;RET ⊢
37:
"2";R170(RR0+ƒ3R
(R0+1))-R171R(R0
+2)→R179⊢
38:
4R170R169R(R0+3)
-R171R169(ƒ3R(R0
+4)+R(R0+5))→R18
1⊢
39:
IF 1=(I>R165)*(R
200>R167);GTO 44
⊢
40:
PRT "EXACT SOLUT
ION :";SPC 1;
GSB "3"⊢
41:
PRT "U=",100R179
R166⊢
42:
PRT "V=",100R181
R166⊢
43:
SPC 3⊢
44:
R0+6→R0⊢
45:
RET ⊢
46:
"3";PRT "Y=",R16
7,"LOAD RATIO=",
R183,"DELTA T=",
R174;RET ⊢
47:
"4";R167+.2→R167
;RET ⊢
48:
END ⊢
R222
```

PROGRAM 5

```
0:
FXD 7;SPC 2⊢
1:
ENT "AREA=?",A,"
B=?",B,"L=?",C,"
E0=?",X,"ET=?",Y
,"U0=?",R0,"D=?"
,R12⊢
2:
PRT "AREA=",A,"B
=",B,"L=",C,"E0=
",X,"ET=",Y,"U0=
",R0,"D=",R12⊢
3:
X/Y→R1⊢
4:
1E-6*ABYB/CR12→R
2;PRT "PT=",R2;
SPC 3⊢
5:
R2(R1-1)/(R1+1)→
R3⊢
6:
.1→R7⊢
7:
R0/100C→R4⊢
8:
R7(R1-1)/(R1+1)→
R10⊢
9:
(1E-2*BR10(R1-1)
+CR4(R1-1))/C(R1
-1-R10(1+R1))→R5
⊢
10:
100CR5→R6⊢
11:
PRT "LOAD RATIO=
",R7,"U=",R6;
SPC 2⊢
12:
R7+.1→R7⊢
13:
IF R7<.9;GTO 8⊢
14:
END ⊢
```

The above program calculates the buckling behaviour according to Shanley Theory.

Name in the program	Name in the actual model
A	A
B	b
C	L
X	E_o
Y	E_t
R0	U_o
R1	$E_o/E_t = K$
R2	P_t
R3	ΔP_{max}

Name in the program	Name in the actual model
R4	α_o
R5	α
R6	U
R7	.1
R10	.1(K - 1)/(K + 1)
R12	d

PROGRAM 6

a. Description

This program is developed to determine the influence of parameter variations on the buckling behaviour of column Model 2. The axial load is continuously increasedup to any desired level, whereafter the state space variables are stored at the end of Phase 2. During Phase 2, the motion of the column is followed up to three motion reversal positions. For determining the stable lateral configurations for a new load level, the state space variables are restored and the computation continued up to the new load level. The procedure is then followed in the same way as for the previous load level. Information about the state of the column is given by the current values of the eight variables, $\Delta P/\Delta P_{max}$, U, t, $\dot{\alpha}$, E_a, E_a, E_b, σ_a and σ_b, with four values printed at a line. This information is printed in either of the following cases:

1. When the axial load increases by certain predetermined increment above the axial load.
2. When the strain reversal begins to occur of begins to end in a certain direction.
3. When the column attains a position of motion reversal.

b. Names of Variables

The array of variable names in this program is a subset of the

corresponding arrays for Programs 7 and 8, which are presented in Sections b of the two programs.

```
100 REM                          PROGRAM 6
110 PRINT '       SAMPLE CALCULATIONS CORRESPONDING TO MODEL 2 :'
120 DIM S(20),C(20)
130 PRINT
140 PRINT
150 READ E0
160 READ E5
170 PRINT
180 PRINT
190 PRINT
200 READ J6
210 FOR J5=1 TO J6
220 READ C(J5)
230 NEXT J5
240 LET J5=1
250 READ U0,V0,X,L,M,A,B,D0,V1,A5,D
260 DIM P(20)
270 READ N4
280 FOR N3=1 TO N4
290 READ P(N3)
300 NEXT N3
310 LET F1=U0/(100*L)
320 LET F2=V0/(100*L)
330 LET C=C(J5)
340 LET N3=1
350 LET U=U0
360 LET K=1
370 LET Y=1000/(C*X)
380 LET E=E1=E5
390 LET P=B*A*1E-6*E5*B/(D0*L)
400 LET P8=P*(E0/E5-1)/(E0/E5+1)
410 LET Y1=Y
420 LET A9=Y
430 LET P7=P
440 LET S0=S2=Z2=Z3=E2=E3=T=0
450 LET Z=Z1=P/(2*A*1.00000E-04)
460 LET L1=F1
470 LET L3=F2
480 LET S=L3*A*1E-4*E1/C
490 LET S1=-S
500 LET M0=P*L1*L
510 LET Z8=M0/(2*A*B*1.00000E-06)
520 LET Z=Z-Z8
530 LET Z1=Z+Z8
540 LET Z7=P7/(2*A*1.00000E-04)
550 LET I=M*L**2/3
560 PRINT'TANGENT MODULUS LOAD=',P7
570 PRINT 'MAXIMUM LOAD INCREMENT=',P8
580 PRINT
590 PRINT
600 PRINT'P','U','TIME','ALPHA RATE'
610 PRINT
620 PRINT 'E OF A','E OF B','SIGMA A','SIGMA B'
630 PRINT
640 PRINT
650 GOSUB 2440
660 LET Z9=.8*Z7
670 REM.-MAIN LOOP IN PHASE 1 BEGINS HERE :
680 LET C=C(J5)
690 LET Y=Y1
700 LET N1=N2=1
710 REM.- MULTI-CYCLE SEARCH LOOP RESTARTS HERE :
720 LET L0=L1
```

```
730 LET L2=L3
740 LET T=T+X
750 IF C<1 THEN 800
760 LET S0=S
770 LET S2=S1
780 LET P=P+C*X
790 LET P5=P5+C*X
800 LET K=E/E1
810 LET M2=2*B*A*1E-6*K*E1*B/D0/(K+1)
820 LET M0=M0-C*X*B*(K-1)*1E-2/(K+1)
830 LET M3=M2-P*L
840 LET H=M2*L0-M0
850 LET F=H/M3
860 IF 0>M3 THEN 880
870 GOTO 900
880 LET M1=M3
890 LET M3=-M3
900 LET O=SQR(M3/I)
910 LET C1=L2/O
920 LET C2=L0-F
930 IF C2+C1=0THEN 970
940 LET R2=(C2-C1)/(C2+C1)
950 IF  -Z>Z9 AND R2<1 THEN 1240
960 IF -Z1>Z9 AND R2<1  THEN 1240
970 IF 0>M1 THEN 1010
980 LET L1=C1*SIN(O*X)+C2*COS(O*X)+F
990 LET L3=O*C1*COS(O*X)-O*C2*SIN(O*X)
1000 GOTO 1050
1010 LET D1=(EXP(O*X)-EXP(-O*X))/2
1020 LET D2=(EXP(O*X)+EXP(-O*X))/2
1030 LET L1=C1*D1+C2*D2+F
1040 LET L3=O*C1*D2+O*C2*D1
1050 LET M1=0
1060 LET A7=L1-L0
1070 IF D <= (P-P7)/P8 THEN 1090
1080 GOTO 1120
1090 LET L3=L3+V1/(100*L)
1100 LET V1=0
1110 LET D=1
1120 LET Z4=C*X/(A*(1+K)*1.00000E-04)
1130 LET Z5=K*E1*A7*B/D0/(K+1)
1140 LET M0=M0+M2*A7
1150 LET Z1=Z1+Z4+Z5
1160 LET Z=Z+K*Z4-Z5
1170 IF -Z>Z9 THEN 1190
1180 GOTO 1200
1190 LET E=E5
1200 IF -Z1>Z9 THEN 1220
1210 GOTO 1270
1220 LET E1=E5
1230 GOTO 1270
1240 PRINT TAB(28),'UNSTABLE STATE'
1250 GOSUB 2590
1260 GO TO 3060
1270 LET U=100*L*L1
1280 IF 0>L3 OR L2>0 AND L3=0 THEN 1370
1290 IF C<1 THEN 1320
1300 LET S=L3*A*1E-4*E1*B/D0/C
1310 IF 1>S THEN 1370
1320 IF Z2>Z THEN 1400
1330 LET E2=E
1340 LET Z2=Z
1350 LET E=E0
1360 GOTO 1400
```

```
1370 IF Z2<.1 OR Z2>Z THEN 1400
1380 LET E=E2
1390 LET Z2=0
1400 IF L3>0 OR 0>L2 AND L3=0 THEN 1490
1410 IF C<1 THEN 1440
1420 LET S1=-K*L3*A*1E-4*E1*B/D0/C
1430 IF 1>S1 THEN 1490
1440 IF Z3>Z1 THEN 1520
1450 LET E3=E1
1460 LET Z3=Z1
1470 LET E1=E0
1480 GO TO 1520
1490 IF Z3<.1 OR Z3>Z1 THEN 1520
1500 LET E1=E3
1510 LET Z3=0
1520 IF C>1 OR N1<0 THEN 1550
1530 LET N1=-1
1540 GOTO 720
1550 LET K=E/E1
1560 GOTO 1580
1570 GOSUB 2440
1580 IF L2*L3 <= 0 THEN 1600
1590 GOTO 1620
1600 PRINT TAB(23),'TEMPORARY END POSITION'
1610 GOSUB 2590
1620 IF C<1 THEN 1750
1630 LET A9=A9-1
1640 IF A9=0 THEN 1660
1650 GO TO 1680
1660 GOSUB 2590
1670 LET A9=Y
1680 IF (P-P7)/P8<A5 THEN 720
1690 LET Y=2*Y
1700 IF I0>.5 THEN 1750
1710 PRINT TAB(27),'PHASE 2 BEGUN :'
1720 LET I0=1
1730 GOSUB 2590
1740 GOTO 1770
1750 IF L2*L3>0 THEN 720
1760 GOTO 2130
1770 LET S(1)=S
1780 LET S(2)=L1
1790 LET S(3)=S1
1800 LET S(4)=L3
1810 LET S(5)=E
1820 LET S(6)=E1
1830 LET S(7)=E2
1840 LET S(8)=E3
1850 LET S(9)=Z
1860 LET S(10)=Z1
1870 LET S(11)=Z2
1880 LET S(12)=Z3
1890 LET S(13)=M0
1900 LET S(17)=T
1910 LET S(18)=A9
1920 LET S(19)=Y1
1930 LET A9=A9-INT(A9/10)*10
1940 LET C=0
1950 GOTO 1280
1960 LET S=S(1)
1970 LET L1=S(2)
1980 LET S1=S(3)
1990 LET L3=S(4)
2000 LET E=S(5)
```

```
2010 LET E1=S(6)
2020 LET E2=S(7)
2030 LET E3=S(8)
2040 LET Z=S(9)
2050 LET Z1=S(10)
2060 LET Z2=S(11)
2070 LET Z3=S(12)
2080 LET M0=S(13)
2090 LET T=S(17)
2100 LET A9=S(18)
2110 LET Y1=S(19)
2120 GOTO 680
2130 LET N2=N2+1
2140 IF L2>0 THEN 2160
2150 GOTO 2210
2160 LET L6=L1
2170 LET T1=T
2180 IF N2>3.5 THEN 2260
2190 LET N1=1
2200 GOTO 1280
2210 LET L7=L1
2220 LET T2=T
2230 IF N2>3.5 THEN 2260
2240 LET N1=1
2250 GOTO 1280
2260 PRINT TAB(30),'END POSITION'
2270 PRINT
2280 PRINT
2290 PRINT 'UMAX','TMAX','UMIN','TMIN'
2300 PRINT
2310 PRINT L6*100*L,T1,L7*100*L,T2
2320 PRINT
2330 LET N3=N3+1
2340 IF N3>N4+.1 THEN 3060
2350 PRINT
2360 PRINT
2370 LET A5=P(N3)
2380 PRINT 'CALCULATIONS CONTINUE FOR A HIGHER LOAD RATIO =',A5
2390 PRINT
2400 LET I0=0
2410 GOTO 1960
2420 REM                          SUBROUTINES :
2430 REM .-SUBROUTINE 1 :
2440 IF 1 <= S AND 1>S0 THEN 2490
2450 IF S <= 1 AND S0>1 THEN 2510
2460 IF 1 <= S1 AND 1>S2 THEN 2530
2470 IF S1 <= 1 AND S2>1 THEN 2550
2480 GOTO 2570
2490 PRINT TAB(19),'STRAIN REVERSAL FORWARDS BEGUN'
2500 GOTO 2560
2510 PRINT TAB(19),'STRAIN REVERSAL FORWARDS ENDED'
2520 GOTO 2560
2530 PRINT TAB(18),'STRAIN REVERSAL BACKWARDS BEGUN'
2540 GOTO 2560
2550 PRINT TAB(18),'STRAIN REVERSAL BACKWARDS ENDED'
2560 GOSUB 2590
2570 RETURN
2580 REM.- SUBROUTINE 2 :
2590 PRINT '     '
2600 PRINT P,U,T,L3
2610 PRINT
2620 PRINT E,E1,Z,Z1
2630 PRINT
2640 PRINT
```

```
2650 PRINT
2660 RETURN
2670 REM                          DATA BLOCK :
2680 REM (E-MODULI)
2690 DATA 2E10
2700 DATA 1E10
2710 REM (J6=NUMBER OF LOADING RATES)
2720 DATA 5
2730 REM.- VALUES OF LOADING RATES :
2740 DATA 5000
2750 DATA 1000
2760 DATA 500
2770 DATA 100
2780 DATA 50
2790 REM (U0)
2800 DATA 1E-3
2810 REM V0
2820 DATA 0
2830 REM (DELTA T)
2840 DATA 1.00000E-02
2850 REM (L)
2860 DATA 5
2870 REM (M)
2880 DATA 500
2890 REM (A)
2900 DATA 5
2910 REM (B,D0)
2920 DATA 5,10
2930 REM (V1)
2940 DATA 0
2950 REM (A5=FINAL LOAD LEVEL WHEN FINDING EQUILIBRIUM COFIGURATIONS)
2960 DATA .4
2970 REM (D=LOAD RATIO CORRESPONDING TO VELOCITY DISTURBANCE)
2980 DATA 1
2990 REM N4=NUMBER OF LOAD RATIOS AT WHICH EQUILIBRIUM STATE IS FOUND
3000 DATA 4
3010 REM .- VALUES OF LOAD RATIOS :
3020 DATA .4
3030 DATA .6
3040 DATA .8
3050 DATA .9
3060 PRINT
3070 PRINT
3080 PRINT
3090 IF J5+.1>J6 THEN 3180
3100 LET J5=J5+1
3110 PRINT'CALCULATIONS CONTINUE FOR A NEW LOADING RATE=',C(J5)
3120 LET I0=0
3130 PRINT
3140 PRINT
3150 LET N3=1
3160 LET A5=P(N3)
3170 GO TO 330
3180 END
```

PROGRAM 7

a. Description

This program is entitled Multi-Cycle Search method, a description of which is presented in Section 8.3. Sample calculations for this program can be found herein in the illustration of the reliability of numerical results in Sec. 8.8. The information about the state of the column printed in the computations for this program correspond to the same state variables as for Program 8, see Sec. 8.4.

b. Name of Variables

The array of variable names in this program is, with the exception of the following variables, a subset of the corresponding array for Program 5, which is presented in Section b of the previous program.

Name in the program	Actual name or description
L6 and L7	α_{max} and α_{min}
N1	An integer which transfers control to the part of the program which assigns the initial elastic modulus, E_o, to the proper column element during buckling phase 2
N3	Variable integer used as array index
N4	Number of load levels for which equilibrium configurations are sought
O	ω
T1 and T2	t_{max} and t_{min}

```
100 REM                          PROGRAM 7
110 REM .- THIS PROGRAM DEVELOPS THE CONCEPT OF MULTI-CYCLE SEARCH METHOD
120 PRINT 'SAMPLE CALCULATIONS ACCORDING TO MULTI-CYCLE SEARCH METHOD :'
130 DIM S(30)
140 PRINT
150 PRINT
160 DIM A(100)
170 READ N
180 FOR I=1 TO N
190 READ A(I)
200 NEXT I
210 PRINT 'P','U','TIME','ALFA-RATE'
220 PRINT
230 PRINT 'E OF A','E OF B','SIGMA A','SIGMA B'
240 PRINT
250 PRINT
260 PRINT
270 LET A0=A1=A2=A3=B0=K=1
280 READ U0,V0,X0,X,Y,E0,A4,L,M,A,B,D0,V1,A5,D5,D6,D,J
290 DIM P(20)
300 READ N4
310 FOR N3=1 TO N4
320 READ P(N3)
330 NEXT N3
340 LET N3=1
342 LET D4=D0/B
344 LET A6=E0*B/(D5*(D6+1)*100*L*D4)
346 LET P0=A6*D5*2*A*1E-4
348 LET P8=INT(DIG(P0)+.5)*P0/DIG(P0)
350 LET R2=M6=1
370 LET U=U0
380 READ G9,J2,J3,J4,B1,B3
390 READ V2,X2
400 LET E=E1=A(0)=E0
410 LET Y1=Y
420 LET A9=Y
430 LET X1=X
440 LET L0=L1=U0/(100*L)
450 LET L2=L3=V0/(100*L)
460 IF J2<.5 THEN 480
470 GOSUB 3990
480 LET I=M*L**2/3
490 LET S=L3*A*1E-4*E0/D4/A4
500 LET S1=-S
510 GOSUB 2870
520 REM.-MAIN LOOP IN PHASE 1 BEGINS HERE :
530 LET C=A4
540 LET Y=Y1
550 LET N1=N2=1
560 REM.- MULTI-CYCLE SEARCH LOOP RESTARTS HERE :
570 LET X=X1
580 LET L0=L1
590 IF C>1 THEN 600
600 LET L2=L3
610 LET T=T+X
620 IF C<1 THEN 660
630 LET S0=S
640 LET S2=S1
650 LET P=P+C*X
660 LET K=E/E1
670 LET M2=2*B*A*1E-6*K*E1/D4/(K+1)
680 LET M0=M0-C*X*B*(K-1)*1.00000E-02/(K+1)
690 LET M3=M2-P*L
```

```
700 LET H=P*X0/100+M2*L0-M0-P*T0*L
710 IF M3=0 THEN 920
720 LET F=H/M3
730 LET M1=M3
740 IF 0>M3 THEN 760
750 GOTO 770
760 LET M3=-M3
770 LET O=SQR(M3/I)
780 LET C1=L2/O
790 LET C2=L0-F
800 IF C>1 THEN 830
810 LET R2=(C2-C1)/(C2+C1)
820 IF M1<0 AND R2<1 THEN 2250
830 IF 0>M1 THEN 870
840 LET L1=C1*SIN(O*X)+C2*COS(O*X)+F
850 LET L3=O*C1*COS(O*X)-O*C2*SIN(O*X)
860 GOTO 940
870 LET D1=(EXP(O*X)-EXP(-O*X))/2
880 LET D2=(EXP(O*X)+EXP(-O*X))/2
890 LET L1=C1*D1+C2*D2+F
900 LET L3=O*C1*D2+O*C2*D1
910 GOTO 940
920 LET L1=X**2*H/(2*I)+X*L2+L0
930 LET L3=X*H/I+L2
940 LET A7=L1-L0
950 IF J3<.5 OR B1>P/P8 THEN 970
960 GOSUB 3840
970 IF D <= P/P8 THEN 990
980 GOTO 1020
990 LET L3=L3+V1/(100*L)
1000 LET V1=0
1010 LET D=1
1020 LET Z4=C*X/(A*(1+K)*1.00000E-04)
1030 IF U<100 THEN 1060
1040 PRINT'EXCESSIVE DEFLECTION'
1050 STOP
1060 LET Z5=K*E1*A7/D4/(K+1)
1070 LET M0=M0+M2*A7
1080 LET Z1=Z1+Z4+Z5
1090 LET Z=Z+K*Z4-Z5
1100 IF Z<0 OR Z1<0 THEN 1120
1110 GOTO 1210
1120 IF A3>N OR B0>N THEN 1210
1130 IF -A3*A6 >= Z THEN 1160
1140 IF -B0*A6 >= Z1 THEN 1190
1150 GO TO 1210
1160 LET E=A(A3)*E0
1170 LET A3=A3+1
1180 GOTO 1210
1190 LET E1=A(B0)*E0
1200 LET B0=B0+1
1210 IF Z<0 OR A1>N THEN 1260
1220 IF A1*A6 <= Z THEN 1240
1230 GOTO 1260
1240 LET E=A(A1)*E0
1250 LET A1=A1+1
1260 IF A2>N THEN 1310
1270 IF A2*A6 <= Z1 THEN 1290
1280 GOTO 1310
1290 LET E1=A(A2)*E0
1300 LET A2=A2+1
1310 LET K=E/E1
1320 LET U=100*L*L1
1330 IF 0>L3 OR L2>0 AND L3=0 THEN 1420
```

```
1340 IF C<1 THEN 1370
1350 LET S=L3*A*1E-4*E1/D4/C
1360 IF 1>S THEN 1420
1370 IF Z2>Z THEN 1450
1380 LET E2=E
1390 LET Z2=Z
1400 LET E=E0
1410 GOTO 1450
1420 IF Z2<1 OR Z2>Z THEN 1450
1430 LET E=E2
1440 LET Z2=0
1450 IF L3>0 OR 0>L2 AND L3=0 THEN 1540
1460 IF C<1 THEN 1490
1470 LET S1=-K*L3*A*1E-4*E1/D4/C
1480 IF 1>S1 THEN 1540
1490 IF Z3>Z1 THEN 1570
1500 LET E3=E1
1510 LET Z3=Z1
1520 LET E1=E0
1530 GOTO 1570
1540 IF Z3<1 OR Z3>Z1 THEN 1570
1550 LET E1=E3
1560 LET Z3=0
1570 IF C>1 OR N1<0 THEN 1600
1580 LET N1=-1
1590 GOTO 580
1600 LET K=E/E1
1610 IF C<1 AND J>.5 THEN 2210
1620 IF C<1 THEN 1920
1630 REM SCAPE NEXT LINE WHEN FINDING EQUILIBRIUM COFIGURATIONS
1640 IF T>1.1*X THEN 1700
1650 GOSUB 2870
1660 IF L2*L3 <= 0 THEN 1680
1670 GOTO 1700
1680 PRINT TAB(23),'TEMPORARY END POSITION'
1690 GOSUB 3020
1700 IF A9=1 THEN 1750
1710 LET A9=A9-1
1720 IF A9>=1 THEN 1770
1730 LET Y=Y-1
1740 GOTO 1760
1750 GOSUB 3020
1760 LET A9=Y
1770 IF(P+.01)/P8<A5 THEN 580
1780 LET Y=20
1790 IF I0>.5 THEN 1870
1800 IF J>.5 THEN 1830
1810 PRINT TAB(27),'PHASE 2 BEGUN :'
1820 GOTO 1840
1830 PRINT TAB(22),'MULTI-CYCLE SEARCH BEGUN :'
1840 LET I0=1
1850 GOSUB 3020
1860 IF J<.5 THEN 1940
1870 IF J>.5 THEN 1890
1880 GOTO 1920
1890 GOSUB 3760
1900 IF Q>0 THEN 1940
1910 GOTO 580
1920 IF L2*L3>0 THEN 580
1930 GOTO 2560
1940 LET S(1)=S
1950 LET S(2)=L1
1960 LET S(3)=S1
1970 LET S(4)=L3
```

```
1980 LET S(5)=E
1990 LET S(6)=E1
2000 LET S(7)=E2
2010 LET S(8)=E3
2020 LET S(9)=Z
2030 LET S(10)=Z1
2040 LET S(11)=Z2
2050 LET S(12)=Z3
2060 LET S(13)=M0
2070 LET S(14)=A1
2080 LET S(15)=A2
2090 LET S(16)=A3
2100 LET S(17)=T
2110 IF J>.5 THEN 2150
2120 LET S(18)=A9
2130 LET S(19)=Y1
2140 LET A9=A9-INT(A9/10)*10
2150 LET S(20)=B0
2160 LET S(21)=T0
2170 LET C=0
2180 LET L3=L3+V2/(100*L)
2190 LET X=X1/X2
2200 GO TO 1330
2210 GOSUB 3760
2220 IF Q>0 AND N1>0 THEN 1330
2230 IF Q>0 THEN 580
2240 GOTO 2320
2250 IF L3<0 THEN 2280
2260 PRINT TAB(22),'PMAX IN FORWARD DIRECTION'
2270 GOTO 2290
2280 PRINT TAB(22),'P MAX IN REVERSE DIRECTION'
2290 GOSUB 3020
2300 PRINT 'NO. OF TRIALS ABOVE THE FIRST P0 LEVEL =',A0
2310 STOP
2320 LET S=S(1)
2330 LET L1=S(2)
2340 LET S1=S(3)
2350 LET L3=S(4)
2360 LET E=S(5)
2370 LET E1=S(6)
2380 LET E2=S(7)
2390 LET E3=S(8)
2400 LET Z=S(9)
2410 LET Z1=S(10)
2420 LET Z2=S(11)
2430 LET Z3=S(12)
2440 LET M0=S(13)
2450 LET A1=S(14)
2460 LET A2=S(15)
2470 LET A3=S(16)
2480 LET A0=A0+1
2490 LET T=S(17)
2500 IF J>.5 THEN 2530
2510 LET A9=S(18)
2520 LET Y1=S(19)
2530 LET B0=S(20)
2540 LET T0=S(21)
2550 GOTO 530
2560 LET N2=N2+1
2570 IF L2>0 THEN 2590
2580 GOTO 2640
2590 LET L6=L1
2600 LET T1=T
2610 IF N2>3.5 THEN 2690
```

```
2620 LET N1=1
2630 GOTO 1330
2640 LET L7=L1
2650 LET T2=T
2660 IF N2>3.5 THEN 2690
2670 LET N1=1
2680 GOTO 1330
2690 PRINT TAB(30),'END POSITION'
2700 PRINT
2710 PRINT
2720 PRINT 'UMAX','TMAX','UMIN','TMIN'
2730 PRINT
2740 PRINT L6*100*L,T1,L7*100*L,T2
2750 PRINT
2760 LET N3=N3+1
2770 IF N3>N4+.1 THEN 4280
2780 PRINT
2790 PRINT
2800 LET A5=P(N3)
2810 PRINT 'CALCULATIONS CONTINUE FOR A HIGHER LOAD RATIO =',A5
2820 PRINT
2830 LET I0=0
2840 GOTO 2320
2850 REM                          SUBROUTINES :
2860 REM .-SUBROUTINE 1 :
2870 IF 1 <= S AND 1>S0 THEN 2920
2880 IF S <= 1 AND S0>1 THEN 2940
2890 IF 1 <= S1 AND 1>S2 THEN 2960
2900 IF S1 <= 1 AND S2>1 THEN 2980
2910 GOTO 3000
2920 PRINT TAB(19),'STRAIN REVERSAL FORWARDS BEGUN'
2930 GOTO 2990
2940 PRINT TAB(19),'STRAIN REVERSAL FORWARDS ENDED'
2950 GOTO 2990
2960 PRINT TAB(18),'STRAIN REVERSAL BACKWARDS BEGUN'
2970 GOTO 2990
2980 PRINT TAB(18),'STRAIN REVERSAL BACKWARDS ENDED'
2990 GOSUB 3020
3000 RETURN
3010 REM.- SUBROUTINE 2 :
3020 PRINT '* * * * *'
3030 PRINT INT(P+.5),U,T,L3
3040 PRINT
3050 PRINT E,E1,Z,Z1
3060 PRINT
3070 PRINT
3080 RETURN
3090 REM                        DATA BLOCK :
3100 REM NUMBER OF S-LEVELS
3110 DATA 79
3120 REM (E-MODULI)
3130 DATA 1,1,1,1,.667,.572,.5,.445,.4,.308
3140 DATA .268,.236,.23,.222,.218,.208,.2,.193,.185,.178
3150 DATA .17,.167,.167,.167,.167,.165,.164,.163,.162,.154
3160 DATA .148,.143,.138,.134,.111,.111,.111,.111,.111,.111
3170 DATA .11,.11,.11,.109,.1,.1,.1,.1,.1,.1
3180 DATA .1,.1,.1,.1,.1,.1,.1,.1,.1
3190 DATA 8.40000E-02,7.70000E-02,6.30000E-02,6.10000E-02,5.70000E-02
3200 DATA 5.30000E-02,5.00000E-02,4.80000E-02,4.60000E-02,4.40000E-02
3210 DATA 4.00000E-02,3.30000E-02,2.80000E-02,2.60000E-02,2.40000E-02
3220 DATA 1.70000E-02,1.50000E-02,1.30000E-02,1.10000E-02,1.00000E-02
3230 REM (U0)
3240 DATA 2
3250 REM V0
```

```
3260 DATA 0
3270 REM (X0)
3280 DATA 0
3290 REM (DELTA T)
3300 DATA 1.00000E-02
3310 REM (Y=NO. OF CYCLES DURING EACH PRINTING INTERVAL)
3320 DATA 1000
3330 REM (E0)
3340 DATA 1E11
3350 REM (LOADING RATE)
3360 DATA 500
3370 REM (L)
3380 DATA 5
3390 REM (M)
3400 DATA 500
3410 REM (A)
3420 DATA 5
3430 REM (B,D0)
3440 DATA 5,10
3450 REM (V1)
3460 DATA 0
3470 REM (A5=STARTING LOAD LEVEL WHEN SEARCHING FOR PMAX)
3480 REM (A5=FINAL LOAD LEVEL WHEN FINDING EQUILIBRIUM COFIGURATIONS)
3490 DATA .46
3500 REM.- (D5,D6=STRESS LEVEL INTEGER AND K AT PR LEVEL)
3510 DATA 60,10
3520 REM (D=LOAD RATIO CORRESPONDING TO VELOCITY DISTURBANCE)
3530 DATA 1
3540 REM (J=1 WHEN SEARCHING FOR PMAX)
3550 REM (J=0 WHEN FINDING EQUILIBRIUM CONFIGURATIONS)
3560 DATA 1
3570 REM N4=NUMBER OF LOAD RATIOS AT WHICH EQUILIBRIUM STATE IS FOUND
3580 DATA 4
3590 REM .- VALUES OF LOAD RATIOS :
3600 DATA .25
3610 DATA .375
3620 DATA .5
3630 DATA .8725
3640 REM (G9=GRAVITATIONAL ACCELERATION)
3650 REM (J2=0 WHEN G9=0,J2=1 OTHERWISE)
3660 REM (J3=0 FOR CONSERVATIVE AXIAL LOAD,J3=1 OTHERWISE)
3670 REM (J4=0 FOR POSITIVE DEVIATION ANGLE ,J4=1 OTHERWISE)
3680 REM (B1=LOAD RATIO AT WHICH P BECOMES NONCONSERVATIVE)
3690 REM (B3=NO. OF CYCLES DURING WHICH DEVIATION ANGLE IS INCREASING)
3700 DATA 0,0
3710 DATA 0,0
3720 DATA .5,1E6
3730 REM (V2,X2)
3740 DATA 0,10
3750 REM.- SUBROUTINE 3 :
3760 IF L2*L3>0 THEN 3810
3770 IF L1*L2<0 THEN 3800
3780 LET Q=-1
3790 RETURN
3800 LET N1=Q=1
3810 LET Q=1
3820 RETURN
3830 REM.- SUBROUTINE 4 :
3840 IF B4>=B3 THEN 3920
3850 IF J4<.5 THEN 3880
3860 LET T0=T0-.9*A7
3870 GOTO 3890
3880 LET T0=T0+.9*A7
3890 LET B2=B4=B2+1
```

```
3900 LET T1=T0/B3
3910 RETURN
3920 IF B2<.5 THEN 3960
3930 LET T0=T0-T1
3940 LET B2=B2-1
3950 RETURN
3960 LET T0=J3=0
3970 RETURN
3980 REM.- SUBROUTINE 5 :
3990 LET Z=Z1=Z2=G9*M/2/(A*1.00000E-04)
4000 LET A1=A2=INT(Z/A6)+1
4010 LET E2=E1=A(A1-1)+1
4020 LET Z8=A1*A6-Z
4030 LET E=E0
4040 LET K=E/E1
4050 LET M2=2*B*A*1E-6*K*E1/D4/(K+1)
4060 LET L4=Z8*D4*(K+1)/(K*E1)
4070 LET Z8=A6
4080 LET L5=(M*G9*L1*L/2)/(M2-M*G9*L/2)
4090 IF L5 <= L4 THEN 4150
4100 IF A2>N THEN 4150
4110 LET E1=A(A2)*E0
4120 LET A2=A2+1
4130 GOSUB 4220
4140 GOTO 4040
4150 LET L4=L5
4160 GOSUB 4220
4170 PRINT TAB(27),'INITIAL STATE'
4180 PRINT
4190 GOSUB 3020
4200 RETURN
4210 REM.- SUBROUTINE 6 :
4220 LET L1=L0=L1+L4
4230 LET M0=M0+M2*L4
4240 LET Z9=K*E1*L4/D4/(K+1)
4250 LET Z=Z-Z9
4260 LET Z1=Z1+Z9
4270 RETURN
4280 END
```

PROGRAM 8

a. Description

This program is entitled Single-Cycle Search method, a complete description of which is given herein in Section 8.4. Sample calculations of this program can be found in the various illustrations of the maximum column load herein in Chapters 8 and 9.

b. Names of Variables

Name in the program	Actual name or description
A(...)	One-dimensional array of β-values
A	A
A0	Integer counting the number of trials for P_{max}
A1	Integer controlling the current number of breaking-point stress levels corresponding to compressive stress in Element a of the column
A2	Integer controlling the current number of breaking-point stress levels corresponding to compressive stress in Element b of the column
A3	Integer controlling the current number of breaking-point stress levels corresponding to possible tensile stress in Element a of the column
A4	Non-zero loading rate
A5	P_o-level in Phase 2
A6	$\Delta\sigma$
A7	$\Delta\sigma$
A9	Integer controlling the number of cycles in each printing interval

Name in the program	Actual name or description
B	b
B0	Integer controlling the current number of breaking-point stress levels corresponding to possible tensile stress in Elemnet b of the column
B1	$b_1 = P_{nl}/P_a$ = Load ratio at which the axial load may become nonconservative
B2	b_2 = integer ccunting the number of computation cycles during which the axial load may be nonconservative
B3	b_3 = number of computation cycles during which the deviation of the axial load from the original direction is increasing
B4	$b_4 = b_2$ (see description for b_2 above)
C	c
C1, C2 and C3	C_1, C_2 and C_3 ($C_3 = C_2/C_1$)
D, D0	P_d/P_{max}, d
D1 and D2	Sinh ($\omega\Delta t$), and cosh ($\omega\Delta t$)
D3, D4, D5, D6	$D_3 = (\alpha_b - F)/C_1$, λ, D_5, D_6 = number of limiting stress levels and the value of K at $P = P_r$
E, E1, E2 and E3	E_a, E_b, E_{as} and E_{bs}
F	F
G	ω
G9	g = gravitational acceleration
H	H
I	Integer used as variable array index; I
I0	Integer for controlling first entry to Phase 2
J	Integer controlling the twofold objective of the program: J=0 for determination of maximum column load, J=0 for finding stable lateral equilibrium configuration
J1, J2	Integers controlling the influence of gravitation force: J_1=0 if the axial load begins to increase before the column reaches a lateral equilibrium configuration under the influence of gravitational force, J_1=1 ohherwise; and J_2=0 if the gravitational acceleration, g=0, J_2=1 otherwise

Name in the program	Actual name or description
J3, J4 vative axial	Integers controlling the influence of deviation in the original direction of application of the axial load: J_3=0 for conservative axial load, J_3=1 otherwise; and J_4==0 if the deviation opposes the effect of initial imperfection of the column, J_4=1 otherwise
K	K
L, L0, L1, L2, L3, L4, L5 and L9	L, α_o, α, $\dot{\alpha}_o$, $\dot{\alpha}$, $\Delta\alpha_b$, $\Delta\alpha_e$, α_c
M	M
M0	M_i
M1	ΔM
M2	C
M3	$\lvert\Delta M\rvert$ = absolute value of ΔM
N	Number of breaking-point stress levels on the stress strain diagram
N1	Integer controlling the number of motion reversal positions in Phase 2
N3	Integer controlling the transfer to Left or Right Block in Phase 2
P(...)	One-dimensional array containing the values of final load increment ratios
P, P0	P, P_r = reduced modulus load
P8	An arbitrary axial load greater than or equal to the reduced modulus load
Q0	$1/(C_3 + D_3)$
Q1	$(C_3 - D_3)/(C_3 + D_3)$
Q8	An integer controlling the exact zero value of C_1 at a motion reversal position
Q9	The number π
R2	$R_2 = (C_2 - C_1)/(C_2 + C_1)$
R1	$R_1 = (\alpha_b - F)/(C_1 + C_2)$
R3	$R_3 = -\dot{\alpha}_o/H$
R4	$R_4 = 2(\alpha_o - \alpha_b)/(H \cdot I)$

Name in the program	Actual name or description
R5	R_5 = Integer controlling the criterium for motion reversal: If R_5=0, motion reversal occurs during the current stress interval; motion of the column diverges if R_5=1
S(...)	One-dimensional array containing state space variables
S, S0, S1 and S2	saf, saf_o, sbb and sbb_o
T, T0, T3, T8 and T9	t, θ, $\Delta\theta$, t_b and t_r
U and U0	U and U_o
V, V0 and V1	V, V_o and V_1
X	Variable time step, Δt, in Phases 1 and 2
X0	X_o
X1	Constant time step, Δt, in Phase 1
Y	Number of computation cycles between each two printouts
Y1	A real variable controlling the relationship between t_b and t_r
Z0	σ_j
Z, Z1, Z2 and S3	σ_a, σ_b, σ_{as} and σ_{bs}
Z4	σ_{ab}
Z5	$\sigma_{ba} = \sigma_{bb}$
Z6 and Z7	σ_c and $\Delta\sigma_c$
Z8	$\Delta\sigma_{cg}$ = stress increment corresponding to the next breaking-point stress level due to column deflection under the influence, of the gravititional force
Z9	$\Delta\sigma_{cg}$ (see above), or $\Delta\sigma_{eg}$ (stress increment corresponding to the equilibrium of the column in the last stress interval due to column deflection under the influence of the gravitational force

```
100 REM                                   PROGRAM 8
110 REM.- THIS PROGRAM DEVELOPS THE CONCEPT OF SINGLE-CYCLE SEARCH METHOD
120 PRINT 'SAMPLE CALCULATIONS ACCORDING TO SINGLE-CYCLE SEARCH METHOD :'
130 DIM S(20),A(100),P(20)
140 PRINT
150 PRINT
160 READ N,E0
170 FOR I=1 TO N
180 READ A(I)
190 NEXT I
200 PRINT 'P','U','TIME','ALPHA RATE'
210 PRINT
220 PRINT 'E OF A','E OF B','SIGMA A','SIGMA B'
230 PRINT
240 PRINT
250 PRINT
260 LET A0=A1=A2=A3=B0=K=Q8=Y1=1
270 LET Q9=3.14159
280 READ U0,V0,X0,X,Y,A4,L,M,A,B,D0,D,V1,A5,D5,D6,J,N5
290 FOR N4=1 TO N5
300 READ P(N4)
310 NEXT N4
320 LET N4=1
322 LET D4=D0/B
330 LET A6=E0*B/(D5*(D6+1)*100*L*D4)
332 LET P0=A6*D5*2*A*1E-4
334 LET P8=INT(DIG(P0)+.5)*P0/DIG(P0)
340 READ G9,J2,J3,J4,B1,B3
350 LET U=U0
360 LET E=E1=A(0)=E0
370 LET X1=X
380 LET A9=Y
390 LET L0=L1=U0/(100*L)
400 LET L2=L3=V0/(100*L)
410 IF J2<.5 THEN 430
420 GOSUB 3420
430 LET I=M*L**2/3
440 LET S=L3*A*1E-4*E0/D4/A4
450 LET S1=-S
460 GOSUB 4230
470 REM.-MAIN LOOP IN PHASE 1 :
480 LET C=A4
490 GOSUB 3650
500 GOSUB 1960
510 GOSUB 2740
520 IF U<100 THEN 550
530 PRINT'EXCESSIVE DEFLECTION'
540 STOP
550 GOSUB 2850
560 IF D <= P/P8 THEN 580
570 GOTO 610
580 LET L3=L3+V1/(100*L)
590 LET V1=0
600 LET D=1
610 LET K=E/E1
620 GOSUB 3970
622 IF T>1.1*X THEN 680
630 GOSUB 4230
640 IF L2*L3 <= 0 THEN 660
650 GOTO 680
660 PRINT TAB(23),'TEMPORARY END POSITION'
670 GOSUB 3340
680 IF A9=1 THEN 710
```

```
690 LET A9=A9-1
700 GOTO 730
710 GOSUB 3340
720 LET A9=Y
730 IF (P+.01)/C8<A5 THEN 490
740 LET S(1)=S
750 LET S(2)=L1
760 LET S(3)=S1
770 LET S(4)=L3
780 LET S(5)=E
790 LET S(6)=E1
800 LET S(7)=E2
810 LET S(8)=E3
820 LET S(9)=Z
830 LET S(10)=Z1
840 LET S(11)=Z2
850 LET S(12)=Z3
860 LET S(13)=M0
870 LET S(14)=A1
880 LET S(15)=A2
890 LET S(16)=A3
900 LET S(17)=T
910 LET S(18)=B0
920 REM- SINGLE-CYCLE SEARCH METHOD BEGINS HERE :
930 LET C=0
940 IF J>.98 THEN 970
950 PRINT TAB(27),'PHASE 2:'
960 GOTO 990
970 IF A0>1.5 THEN 1000
980 PRINT TAB(20),'SINGLE-CYCLE SEARCH BEGUN :'
990 GOSUB 3340
1000 IF L3>0 OR L2<0 AND L3=0 THEN 1780
1010 REM.-LEFT BLOCK IN PHASE 2 (LB2) BEGINS HERE:
1020 LET N3=1
1030 LET L0=L1
1040 LET L2=L3
1050 GOSUB 3970
1060 GOSUB 1960
1070 LET Q8=1
1080 IF Z2<1 THEN 1200
1090 LET Z6=Z2
1100 LET Z0=Z
1110 GOSUB 3740
1120 IF R5>.9 THEN 1440
1130 IF Y1<0 OR T9<T8 THEN 1470
1140 GOSUB 3870
1150 GOSUB 3650
1160 LET E=E2
1170 REM.-MIDDLE BLOCK IN PHASE 2 (MB2) BEGINS HERE:
1180 GOSUB 1960
1190 REM.-MB2 LOOP BEGINS HERE:
1200 IF N3>.5 THEN 1230
1210 IF A2 <= N THEN 1290
1220 GOTO 1240
1230 IF A1 <= N THEN 1260
1240 GOSUB 2560
1250 GOTO 1470
1260 LET Z6=A6*A1
1270 LET Z0=Z
1280 GOTO 1310
1290 LET Z6=A6*A2
1300 LET Z0=Z1
1310 GOSUB 3740
1320 IF R5>.9 THEN 1440
```

```
1330 IF Y1<0 OR T9<T8 THEN 1470
1340 GOSUB 3870
1350 IF N3>.5 THEN 1390
1360 LET E1=A(A2)*E0
1370 LET A2=A2+1
1380 GOTO 1410
1390 LET E=A(A1)*E0
1400 LET A1=A1+1
1410 GOSUB 3650
1420 GOSUB 1960
1430 IF M1>0 OR R5<.9 THEN 1200
1440 GOSUB 4380
1450 STOP
1460 REM.- MOTION REVERSAL BLOCK IN PHASE 2 BEGINS HERE :
1470 LET X=T9
1480 LET T=T+X
1490 GOSUB 2740
1500 LET Q8=0
1510 GOSUB 2850
1520 IF J>.98 THEN 1590
1530 IF N3>.5 THEN 1560
1540 PRINT TAB(24),'RIGHT EXTREME POSITION'
1550 GOTO 1570
1560 PRINT TAB(24),'LEFT EXTREME POSITION'
1570 GOSUB 3340
1580 GOTO 1630
1590 IF N3<.5 AND L1<0 THEN 1020
1600 IF N3>.5 AND L1>0 THEN 1780
1610 GOSUB 4470
1620 GOTO 480
1630 LET N1=N1+1
1640 IF N1>2.5 THEN 1670
1650 IF N3>.5 THEN 1780
1660 GOTO 1020
1670 LET N4=N4+1
1680 IF N4>N5+.1 THEN 1760
1690 PRINT
1700 PRINT
1710 LET A5=P(N4)
1720 PRINT 'CALCULATIONS CONTINUE FOR A HIGHER LOAD RATIO=',A5
1730 PRINT
1740 GOSUB 4470
1750 GOTO 480
1760 STOP
1770 REM.-RIGHT BLOCK IN PHASE 2(RB2) BEGINS HERE:
1780 LET N3=0
1790 LET L0=L1
1800 LET L2=L3
1810 GOSUB 3970
1820 GOSUB 1960
1830 LET Q8=1
1840 IF Z3<1 THEN 1200
1850 LET Z6=Z3
1860 LET Z0=Z1
1870 GOSUB 3740
1880 IF R5>.9 THEN 1440
1890 IF Y1<0 OR T9<T8 THEN 1470
1900 GOSUB 3870
1910 GOSUB 3650
1920 LET E1=E3
1930 GOTO 1180
1940 REM                          SUBROUTINES :
1950 REM.- SUBROUTINE 1 :
1960 LET K=E/E1
```

```
1970 LET M2=2*B*A*1E-6*K*E1/D4/(K+1)
1980 LET M3=M2-P*L-M*G9*L/2
1990 LET M0=M0-C*X*B*(K-1)*1.00000E-02/(K+1)
2000 LET H=P*X0/100+M2*L0-M0-P*T0*L
2010 LET M1=M3
2020 IF M3=0 THEN 2120
2030 LET F=H/M3
2040 IF M3>0 THEN 2060
2050 LET M3=-M3
2060 LET G=SQR(M3/I)
2070 IF Q8>.5 THEN 2100
2080 LET C1=0
2090 GOTO 2110
2100 LET C1=L2/G
2110 LET C2=L0-F
2120 RETURN
2130 REM.- SUBROUTINE 2 :
2140 IF C1><0 THEN 2240
2150 IF C2+L9-F=0 THEN 2170
2160 GOTO 2200
2170 IF C2-L9+F<0 THEN 2470
2180 LET T8=Q9/G
2190 GOTO 2480
2200 LET Y1=(C2-L9+F)/(C2+L9-F)
2210 IF Y1<0 THEN 2480
2220 LET T8=2*ATN(SQR(Y1))/G
2230 GOTO 2480
2240 LET C3=C2/C1
2250 LET D3=(L9-F)/C1
2260 IF C3+D3><0 THEN 2330
2270 IF D3<0 THEN 2290
2280 GOTO 2310
2290 LET T8=2*(Q9-ATN(-D3))/G
2300 GOTO 2480
2310 LET T8=2*ATN(D3)
2320 GOTO 2480
2330 LET Q0=1/(C3+D3)
2340 LET Q1=(C3-D3)/(C3+D3)
2350 LET Y1=Q0**2+Q1
2360 IF Y1<0 THEN 2480
2370 IF Q0<0 AND Q1 <= 0 THEN 2390
2380 GOTO 2410
2390 LET T8=2*Q9/G-2*ATN(-Q0-SQR(Y1))/G
2400 GOTO 2480
2410 IF Q0>0 AND Q1 <= 0 THEN 2430
2420 GOTO 2450
2430 LET T8=2*ATN(Q0-SQR(Y1))/G
2440 GOTO 2480
2450 LET T8=2*ATN(Q0+SQR(Y1))/G
2460 GOTO 2480
2470 LET Y1=-1
2480 GOSUB 2560
2490 RETURN
2500 REM.- SUBROUTINE 3 :
2510 LET L3=C1*G*COS(G*X)-C2*G*SIN(G*X)
2520 LET L1=L9
2530 GOSUB 2850
2540 RETURN
2550 REM.- SUBROUTINE 4 :
2560 IF M1>0 THEN 2620
2570 IF M1=0 THEN 2600
2580 GOSUB 4940
2590 GOTO 2720
2600 GOSUB 5210
```

```
2610 GOTO 2720
2620 IF C1=0 THEN 2690
2630 IF C2><0 THEN 2660
2640 LET T9=Q9/(2*G)
2650 GOTO 2720
2660 IF C1/C2>0 THEN 2710
2670 LET T9=(Q9-ATN(-C1/C2))/G
2680 GOTO 2720
2690 LET T9=Q9/G
2700 GOTO 2720
2710 LET T9=ATN(C1/C2)/G
2720 RETURN
2730 REM.-SUBROUTINE 5 :
2740 IF M1<0 THEN 2790
2750 IF M1=0 THEN 2820
2760 LET L1=C1*SIN(G*X)+C2*COS(G*X)+F
2770 LET L3=C1*G*COS(G*X)-C2*G*SIN(G*X)
2780 GOTO 2830
2790 GOSUB 4710
2800 GOSUB 4750
2810 GOTO 2830
2820 GOSUB 5290
2830 RETURN
2840 REM.- SUBROUTINE 6:
2850 LET A7=L1-L0
2860 IF J3<.5 OR B1>P/P8 THEN 2880
2870 GOSUB 3190
2880 LET U=100*L*L1
2890 LET Z4=C*X/(A*(K+1)*1.00000E-04)
2900 LET M0=M0+M2*A7
2910 LET Z5=K*E1*A7/D4/(K+1)
2920 LET Z1=Z1+Z4+Z5
2930 LET Z=Z+K*Z4-Z5
2940 IF Z<0 OR Z1<0 THEN 2970
2950 IF C<1 THEN 3170
2960 GOTO 3070
2970 IF A3>N OR B0>N THEN 3060
2980 IF -A3*A6 >= Z THEN 3010
2990 IF -B0*A6 >= Z1 THEN 3040
3000 GO TO 3060
3010 LET E=A(A3)*E0
3020 LET A3=A3+1
3030 GOTO 3060
3040 LET E1=A(B0)*E0
3050 LET B0=B0+1
3060 IF C<1 THEN 3170
3070 IF Z<0 OR A1>N THEN 3120
3080 IF A1*A6 <= Z THEN 3100
3090 GOTO 3120
3100 LET E=A(A1)*E0
3110 LET A1=A1+1
3120 IF A2>N THEN 3170
3130 IF A2*A6 <= Z1 THEN 3150
3140 GOTO 3170
3150 LET E1=A(A2)*E0
3160 LET A2=A2+1
3170 RETURN
3180 REM.- SUBROUTINE 7 :
3190 IF B4>=B3 THEN 3270
3200 IF J4<.5 THEN 3230
3210 LET T0=T0-.9*A7
3220 GOTO 3240
3230 LET T0=T0+.9*A7
3240 LET B4=B2=B2+1
```

```
3250 LET T1=T0/B3
3260 RETURN
3270 IF B2<.5 THEN 3310
3280 LET T0=T0-T1
3290 LET B2=B2-1
3300 RETURN
3310 LET J3=T0=0
3320 RETURN
3330 REM.- SUBROUTINE 8 :
3340 PRINT '* * * * *'
3350 PRINT P,U,T,L3
3360 PRINT
3370 PRINT E,E1,Z,Z1
3380 PRINT
3390 PRINT
3400 RETURN
3410 REM.-SUBROUTINE 9 :
3420 LET Z=Z1=Z2=G9*M/2/(A*1.00000E-04)
3430 LET A1=A2=INT(Z/A6)+1
3440 LET E1=E2=A(A1-1)*E0
3450 LET Z8=A1*A6-Z
3460 LET E=E0
3470 LET K=E/E1
3480 LET M2=2*B*A*1E-6*E1*K/D4/(K+1)
3490 LET L4=Z8*D4*(K+1)/(K*E1)
3500 LET Z8=A6
3510 LET L5=(M*G9*L1*L/2-M0)/(M2-M*G9*L/2)
3520 IF L5 <= L4 THEN 3580
3530 IF A2>N THEN 3580
3540 LET E1=A(A2)*E0
3550 LET A2=A2+1
3560 GOSUB 5380
3570 GOTO 3470
3580 LET L4=L5
3590 GOSUB 5380
3600 PRINT TAB(27),'INITIAL STATE :'
3610 PRINT
3620 GOSUB 3340
3630 RETURN
3640 REM.- SUBROUTINE 10 :
3650 LET T=T+X
3660 IF C<1 THEN 3700
3670 LET P=P+C*X
3680 LET S0=S
3690 LET S2=S1
3700 LET L0=L1
3710 LET L2=L3
3720 RETURN
3730 REM.- SUBROUTINE 11 :
3740 LET Z7=Z6-Z0
3750 IF N3<.9 THEN 3770
3760 LET Z7=-Z7
3770 LET L9=Z7*D4*(K+1)/(K*E1)+L0
3780 IF M1>0 THEN 3840
3790 IF M1<0 THEN 3820
3800 GOSUB 5070
3810 GOTO 3850
3820 GOSUB 4790
3830 GOTO 3850
3840 GOSUB 2140
3850 RETURN
3860 REM.- SUBROUTINE 12 :
3870 LET X=T8
3880 IF M1=0 THEN 3920
```

```
3890 IF M1>0 THEN 3940
3900 GOSUB 5010
3910 RETURN
3920 GOSUB 5330
3930 RETURN
3940 GOSUB 2510
3950 RETURN
3960 REM.- SUBROUTINE 13 :
3970 IF N3>.5 THEN 4060
3980 IF C<1 THEN 4010
3990 LET S=L3*A*1E-4*E1/D4/C
4000 IF 1>S THEN 4060
4010 IF Z2>Z THEN 4090
4020 LET E2=E
4030 LET Z2=Z
4040 LET E=E0
4050 GOTO 4090
4060 IF Z2<=0 OR Z2>Z THEN 4090
4070 LET E=E2
4080 LET Z2=0
4090 IF C<1 AND N3<.5 THEN 4180
4100 IF C<1 THEN 4130
4110 LET S1=-K*L3*A*1E-4*E1/D4/C
4120 IF 1>S1 THEN 4180
4130 IF Z3>Z1 THEN 4210
4140 LET E3=E1
4150 LET Z3=Z1
4160 LET E1=E0
4170 GOTO 4210
4180 IF Z3<=0 OR Z3>Z1 THEN 4210
4190 LET E1=E3
4200 LET Z3=0
4210 RETURN
4220 REM.- SUBROUTINE 14 :
4230 IF 1 <= S AND 1>S0 THEN 4280
4240 IF S <= 1 AND S0>1 THEN 4300
4250 IF 1 <= S1 AND 1>S2 THEN 4320
4260 IF S1 <= 1 AND S2>1 THEN 4340
4270 GOTO 4360
4280 PRINT TAB(19),'STRAIN REVERSAL FORWARDS BEGUN'
4290 GOTO 4350
4300 PRINT TAB(19),'STRAIN REVERSAL FORWARDS ENDED'
4310 GOTO 4350
4320 PRINT TAB(18),'STRAIN REVERSAL BACKWARDS BEGUN'
4330 GOTO 4350
4340 PRINT TAB(18),'STRAIN REVERSAL BACKWARDS ENDED'
4350 GOSUB 3340
4360 RETURN
4370 REM.- SUBROUTINE 15 :
4380 IF N3>.5 THEN 4410
4390 PRINT TAB(22),'P MAX IN FORWARD DIRECTION'
4400 GOTO 4420
4410 PRINT TAB(22),'P MAX IN REVERSE DIRECTION'
4420 PRINT
4430 GOSUB 3340
4440 PRINT 'NO. OF TRIALS ABOVE THE FIRST P0 LEVEL =',A0
4450 RETURN
4460 REM.- SUBROUTINE 16 :
4470 LET S=S(1)
4480 LET L1=S(2)
4490 LET S1=S(3)
4500 LET L3=S(4)
4510 LET E=S(5)
4520 LET E1=S(6)
```

```
4530 LET E2=S(7)
4540 LET E3=S(8)
4550 LET Z=S(9)
4560 LET Z1=S(10)
4570 LET Z2=S(11)
4580 LET Z3=S(12)
4590 LET M0=S(13)
4600 LET A1=S(14)
4610 LET A2=S(15)
4620 LET A3=S(16)
4630 LET A0=A0+1
4640 LET X=X1
4650 LET Q8=Y1=1
4660 LET T=S(17)
4670 LET B0=S(18)
4680 LET N1=0
4690 RETURN
4700 REM.- SUBROUTINE 17 :
4710 LET D1=(EXP(G*X)-EXP(-G*X))/2
4720 LET D2=(EXP(G*X)+EXP(-G*X))/2
4730 RETURN
4740 REM.- SUBROUTINE 18 :
4750 LET L1=C1*D1+C2*D2+F
4760 LET L3=G*C1*D2+G*C2*D1
4770 RETURN
4780 REM.- SUBROUTINE 19 :
4790 LET R1=(L9-F)/(C2+C1)
4800 LET R2=(C2-C1)/(C2+C1)
4810 LET Y1=R1**2-R2
4820 IF R1<0 THEN 4900
4830 IF Y1<0 THEN 4910
4840 IF R1-SQR(Y1)<1 THEN 4870
4850 LET T8=LOG(R1-SQR(Y1))/G
4860 GOTO 4910
4870 IF R1+SQR(Y1)<1 THEN 4900
4880 LET T8=LOG(R1+SQR(Y1))/G
4890 GOTO 4910
4900 LET Y1=-1
4910 GOSUB 4940
4920 RETURN
4930 REM.- SUBROUTINE 20 :
4940 LET R2=(C2-C1)/(C2+C1)
4950 IF R2<1 THEN 4980
4960 LET T9=LOG(SQR(R2))/G
4970 GOTO 4990
4980 LET R5=1
4990 RETURN
5000 REM.- SUBROUTINE 21 :
5010 GOSUB 4710
5020 LET L3=C1*G*D2+C2*G*D1
5030 LET L1=L9
5040 GOSUB 2850
5050 RETURN
5060 REM.- SUBROUTINE 22 :
5070 IF H=0 THEN 5180
5080 LET R3=-L2/H
5090 IF R3<0 THEN 5180
5100 LET R4=2*(L0-L9)/(H*I)
5110 LET Y1=R3**2-R4
5120 IF Y1<0 THEN 5180
5130 IF R4 >= 0 AND R3 >= 0 THEN 5160
5140 LET T8=(R3+SQR(Y1))*I
5150 GOTO 5180
5160 LET T8=(R3-SQR(Y1))*I
```

```
5170 GOTO 5180
5180 GOSUB 5210
5190 RETURN
5200 REM.- SUBROUTINE 23 :
5210 IF H=0 THEN 5260
5220 LET R3=-L2/H
5230 IF R3<0 THEN 5260
5240 LET T9=R3*I
5250 GOTO 5270
5260 LET R5=1
5270 RETURN
5280 REM.- SUBROUTINE 24 :
5290 LET L1=X**2*H/(2*I)+X*L2+L0
5300 LET L3=X*H/I+L2
5310 RETURN
5320 REM.- SUBROUTINE 25 :
5330 LET L3=X*H/I+L2
5340 LET L1=L9
5350 GOSUB 2850
5360 RETURN
5370 REM.- SUBROUTINE 26 :
5380 LET L1=L0=L1+L4
5390 LET M0=M0+M2*L4
5400 LET Z9=K*E1*L4/D4/(K+1)
5410 LET Z=Z-Z9
5420 LET Z1=Z1+Z9
5430 RETURN
5440 REM                    DATA BLOCK :
5450 REM.- (NO.OF STRESS LEVELS,E0)
5460 DATA 79,1E11
5470 REM.-E-MODULI
5480 DATA 1,1,1,1,.667,.572,.5,.445,.4,.308
5490 DATA .268,.236,.23,.222,.218,.208,.2,.193,.185,.178
5500 DATA .17,.167,.167,.167,.167,.165,.164,.163,.162,.154
5510 DATA .148,.143,.138,.134,.111,.111,.111,.111,.111,.111
5520 DATA .11,.11,.11,.109,.1,.1,.1,.1,.1,.1
5530 DATA .1,.1,.1,.1,.1,.1,.1,.1,.1,.1
5540 DATA 8.40000E-02,7.70000E-02,6.30000E-02,6.10000E-02,5.70000E-02
5550 DATA 5.30000E-02,5.00000E-02,4.80000E-02,4.60000E-02,4.40000E-02
5560 DATA 4.00000E-02,3.30000E-02,2.80000E-02,2.60000E-02,2.40000E-02
5570 DATA 1.70000E-02,1.50000E-02,1.30000E-02,1.10000E-02,1.00000E-02
5580 REM.- (U0,V0,X0)
5590 DATA .002,0,0
5600 REM.- DELTA T
5610 DATA 1.00000E-02
5620 REM.- (Y,LOADING RATE)
5630 DATA 40,5000
5640 REM.- (L,M,A,B,D0)
5650 DATA 5,500,5,5,10
5660 REM.- (D=LOAD RATIO CORRESPONDING TO VELOCITY DISTURBANCE,V1)
5670 DATA 1,0
5680 REM (A5=STARTING LOAD LEVEL WHEN SEARCHING FOR PMAX)
5690 REM (A5=FINAL LOAD LEVEL WHEN FINDING EQUILIBRIUM CONFIGURATIONS)
5700 DATA .6
5710 REM.- (D5,D6=STRESS LEVEL INTEGER AND K AT PR LEVEL)
5720 DATA 60,10
5730 REM.- (J=1 WHEN SEARCHING FOR P MAX)
5740 REM (J=0 WHEN FINDING EQUILIBRIUM CONFIGURATIONS)
5750 DATA 1
5760 REM NUMBER AND VALUES OF EQUILIBRIUM STATE LOAD RATIOS :
5770 DATA 4,.25,.375,.5
5780 REM LAST EQUILIBRIUM STATE LOAD RATIO :
5790 DATA .75
5800 REM.- (G9=GRAVITATIONAL ACCELERATION)
```

```
5810 REM.- (J2=0 WHEN G9=0 , J2=1 OTHERWISE)
5820 REM.- (J3=0 FOR CONSERVATIVE AXIAL LOAD , J3=1 OTHERWISE)
5830 REM.- (J4=0 FOR POSITIVE DEVIATION ANGLE,J4=1 OTHERWISE)
5840 REM.- (B1=LOAD RATIO AT WHICH P BECOMES NONCONSERVATIVE)
5850 REM.- (B3=NO. OF CYCLES DURING WHICH P-DEVIATION IS INCREASING)
5860 DATA 0,0
5870 DATA 0,0
5880 DATA .25,50
5890 END
```

APPENDIX E

SINGLE-CYCLE SEARCH METHOD:

FLOW DIAGRAMS

MAIN PROGRAM

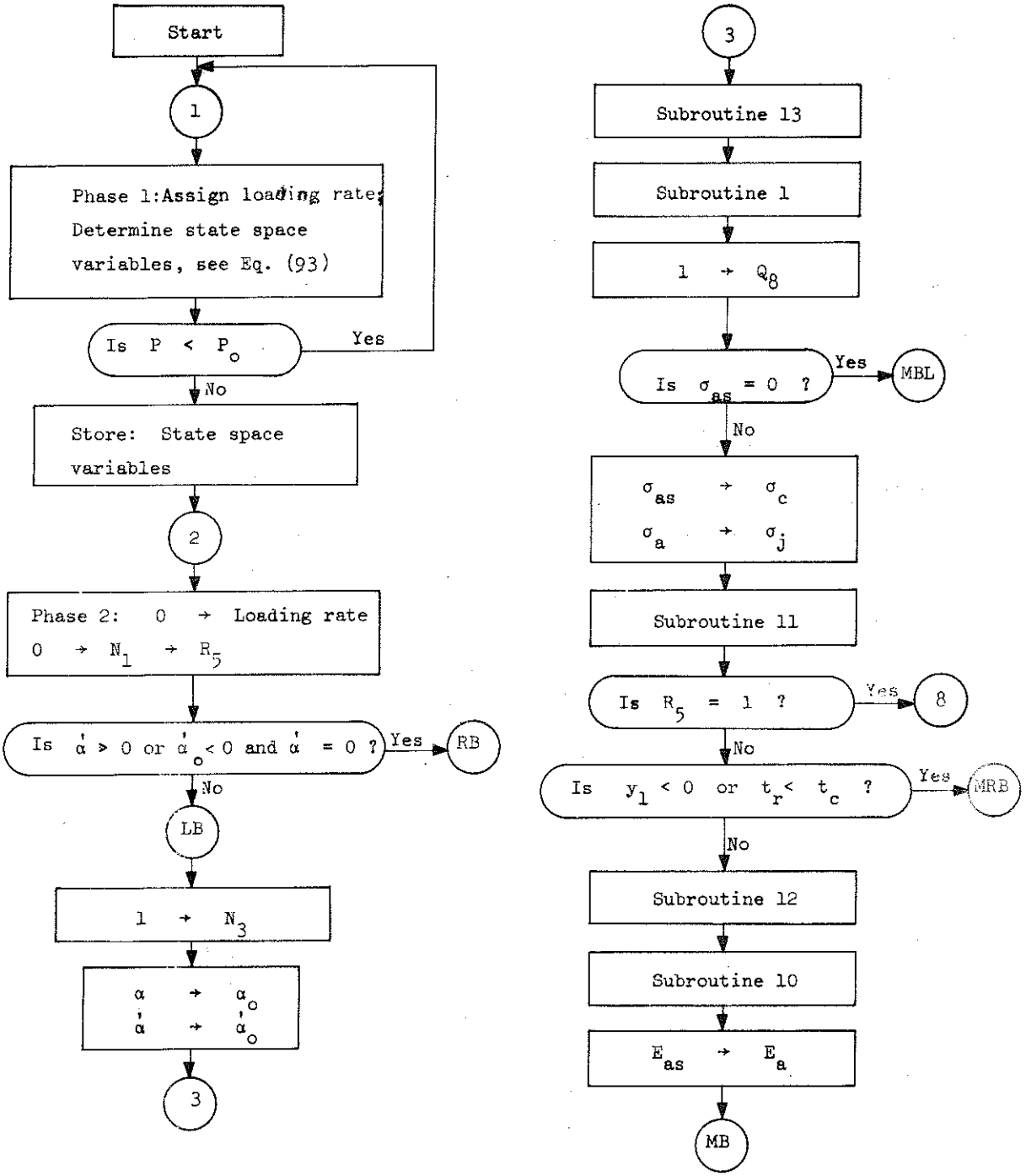

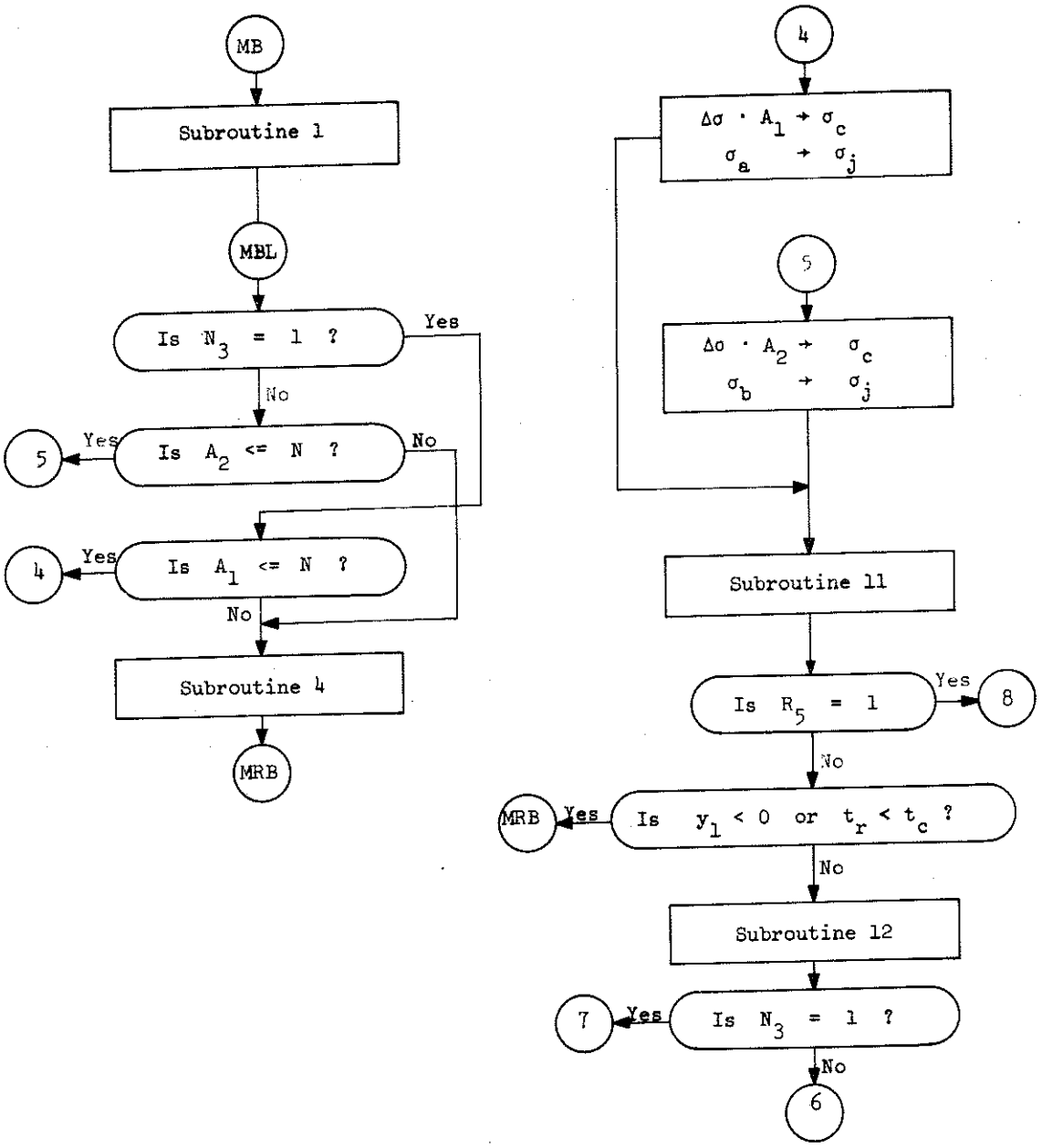
MB
Subroutine 1
MBL
Is N_3 = 1 ?
Yes
No
5
Yes
Is A_2 <= N ?
No
4
Yes
Is A_1 <= N ?
No
Subroutine 4
MRB
4
$\Delta\sigma \cdot A_1 \rightarrow \sigma_c$
$\sigma_a \rightarrow \sigma_j$
5
$\Delta\sigma \cdot A_2 \rightarrow \sigma_c$
$\sigma_b \rightarrow \sigma_j$
Subroutine 11
Is R_5 = 1
Yes
8
No
MRB
Yes
Is $y_1 < 0$ or $t_r < t_c$?
No
Subroutine 12
7
Yes
Is N_3 = 1 ?
No
6

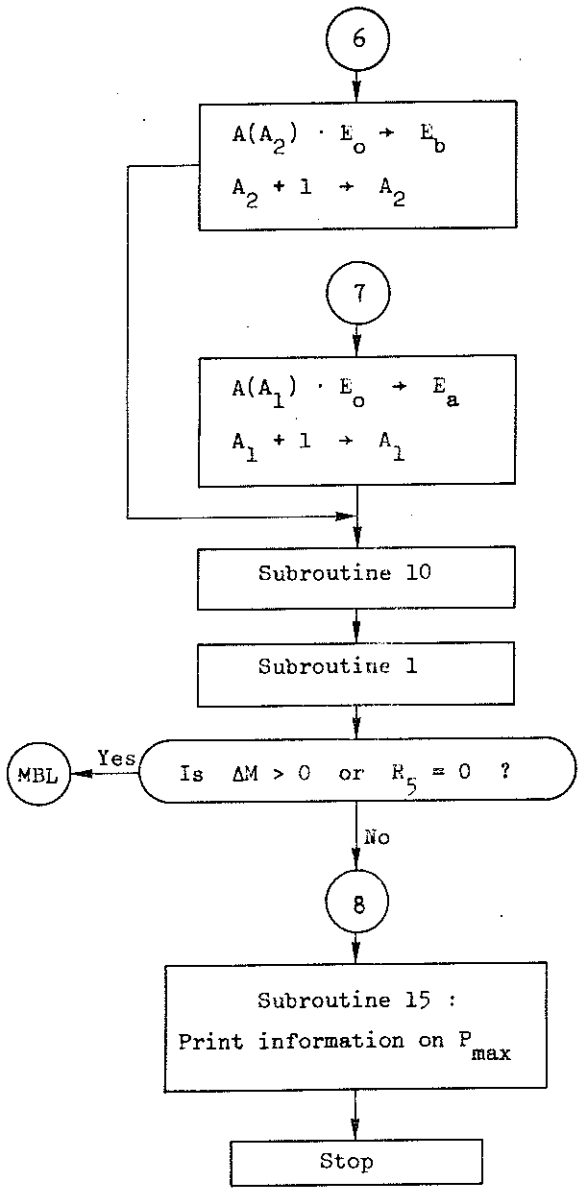
6
A(A2) · Eo → Eb
A2 + 1 → A2
7
A(A1) · Eo → Ea
A1 + 1 → A1
Subroutine 10
Subroutine 1
MBL
Yes
Is ΔM > 0 or R5 = 0 ?
No
8
Subroutine 15 :
Print information on Pmax
Stop

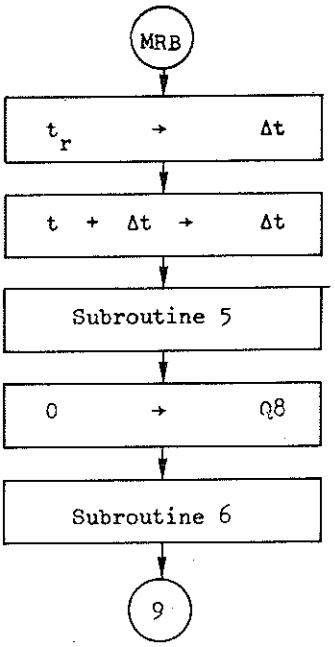
MRB
tr → Δt
t + Δt → Δt
Subroutine 5
0 → Q8
Subroutine 6
9

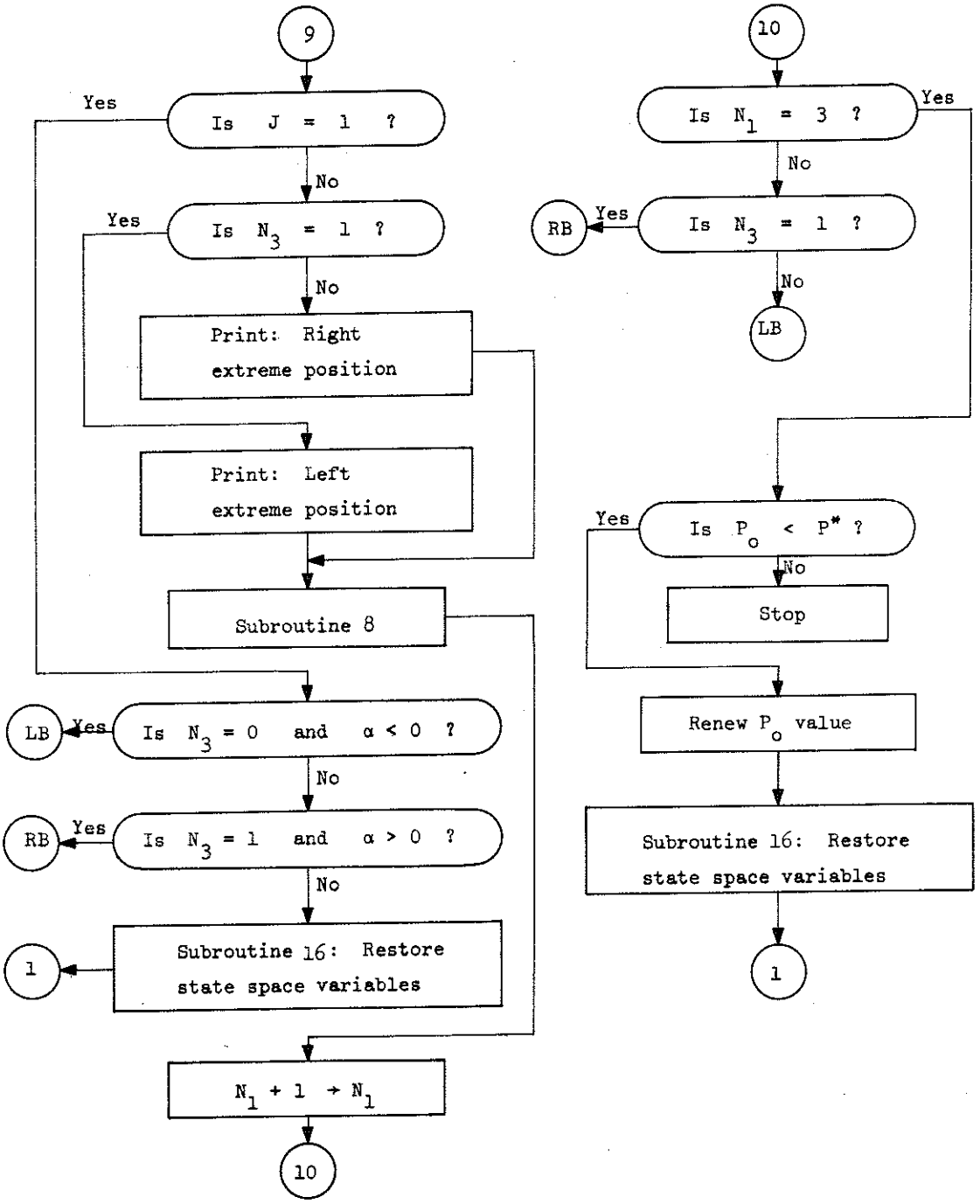
9
Yes
Is J = 1 ?
No
Yes
Is N_3 = 1 ?
No
Print: Right extreme position
Print: Left extreme position
Subroutine 8
LB
Yes
Is N_3 = 0 and α < 0 ?
No
RB
Yes
Is N_3 = 1 and α > 0 ?
No
1
Subroutine 16: Restore state space variables
N_1 + 1 → N_1
10
10
Is N_1 = 3 ?
Yes
No
RB
Yes
Is N_3 = 1 ?
No
LB
Yes
Is P_o < P^* ?
No
Stop
Renew P_o value
Subroutine 16: Restore state space variables
1

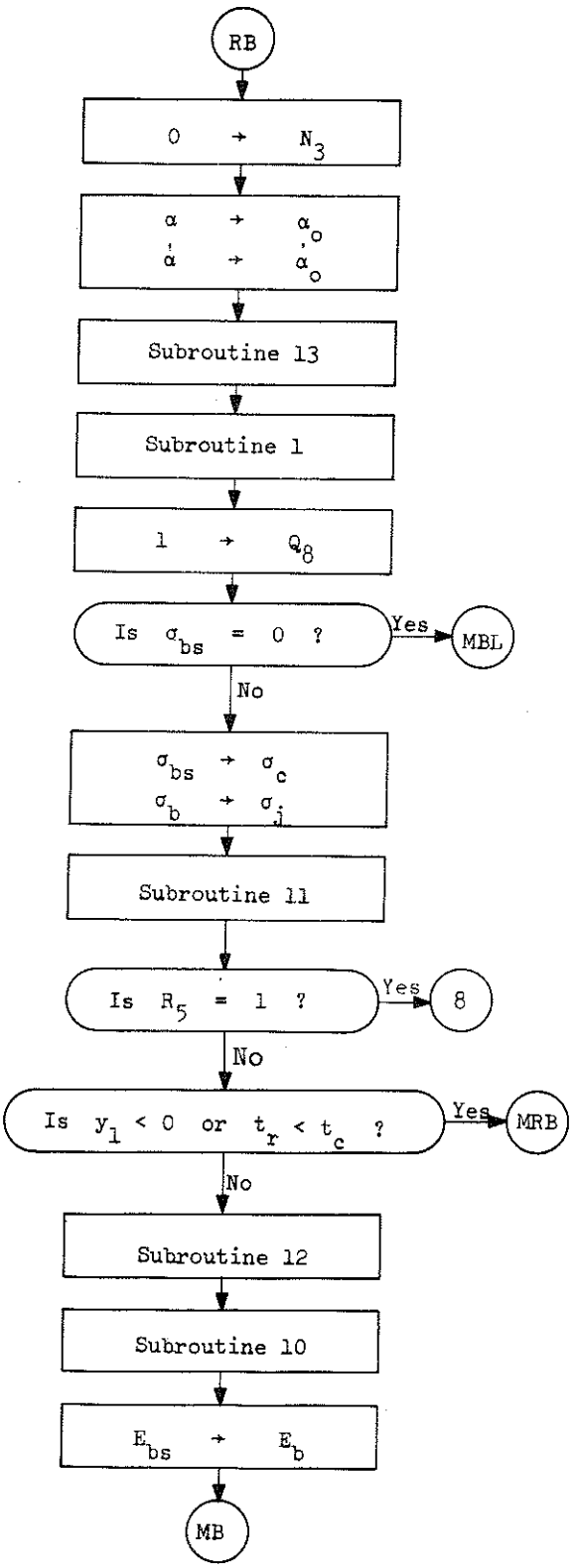
RB
0 → N_3
$\alpha \rightarrow \alpha_o$
$\dot{\alpha} \rightarrow \dot{\alpha}_o$
Subroutine 13
Subroutine 1
1 → Q_8
Is $\sigma_{bs} = 0$?
Yes
MBL
No
$\sigma_{bs} \rightarrow \sigma_c$
$\sigma_b \rightarrow \sigma_j$
Subroutine 11
Is $R_5 = 1$?
Yes
8
No
Is $y_1 < 0$ or $t_r < t_c$?
Yes
MRB
No
Subroutine 12
Subroutine 10
$E_{bs} \rightarrow E_b$
MB

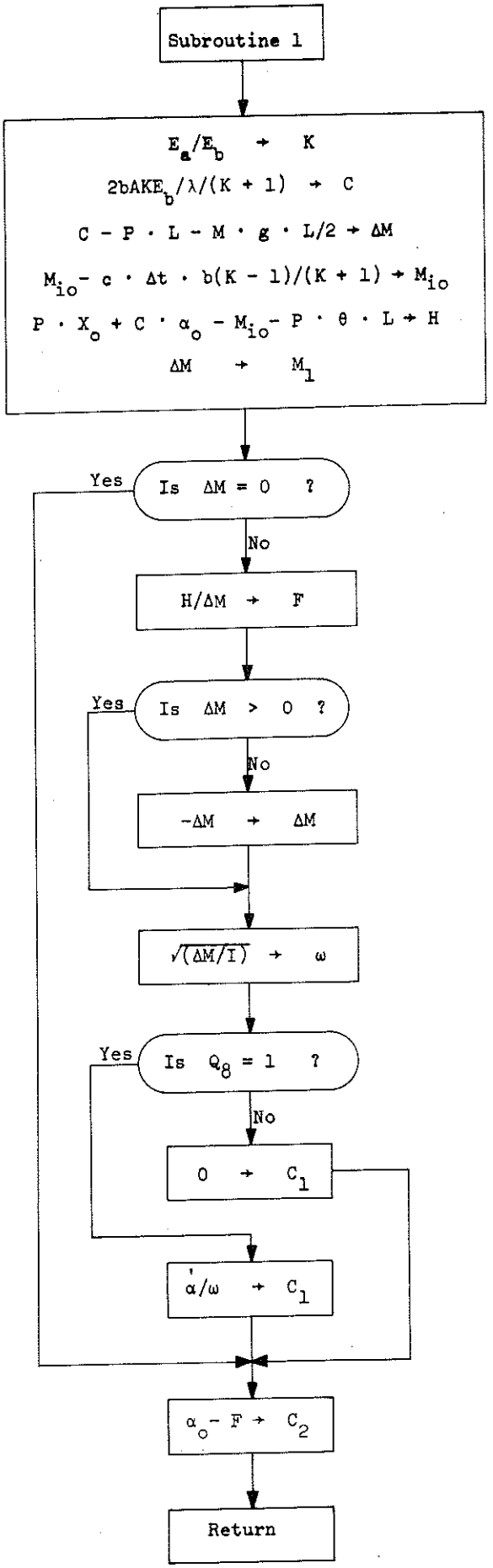
Subroutine 1
$E_a/E_b \rightarrow K$
$2bAKE_b/\lambda/(K+1) \rightarrow C$
$C - P \cdot L - M \cdot g \cdot L/2 \rightarrow \Delta M$
$M_{io} - c \cdot \Delta t \cdot b(K-1)/(K+1) \rightarrow M_{io}$
$P \cdot X_o + C \cdot \alpha_o - M_{io} - P \cdot \theta \cdot L \rightarrow H$
$\Delta M \rightarrow M_1$
Yes
Is $\Delta M = 0$?
No
$H/\Delta M \rightarrow F$
Yes
Is $\Delta M > 0$?
No
$-\Delta M \rightarrow \Delta M$
$\sqrt{(\Delta M/I)} \rightarrow \omega$
Yes
Is $Q_8 = 1$?
No
$0 \rightarrow C_1$
$\alpha'/\omega \rightarrow C_1$
$\alpha_o - F \rightarrow C_2$
Return

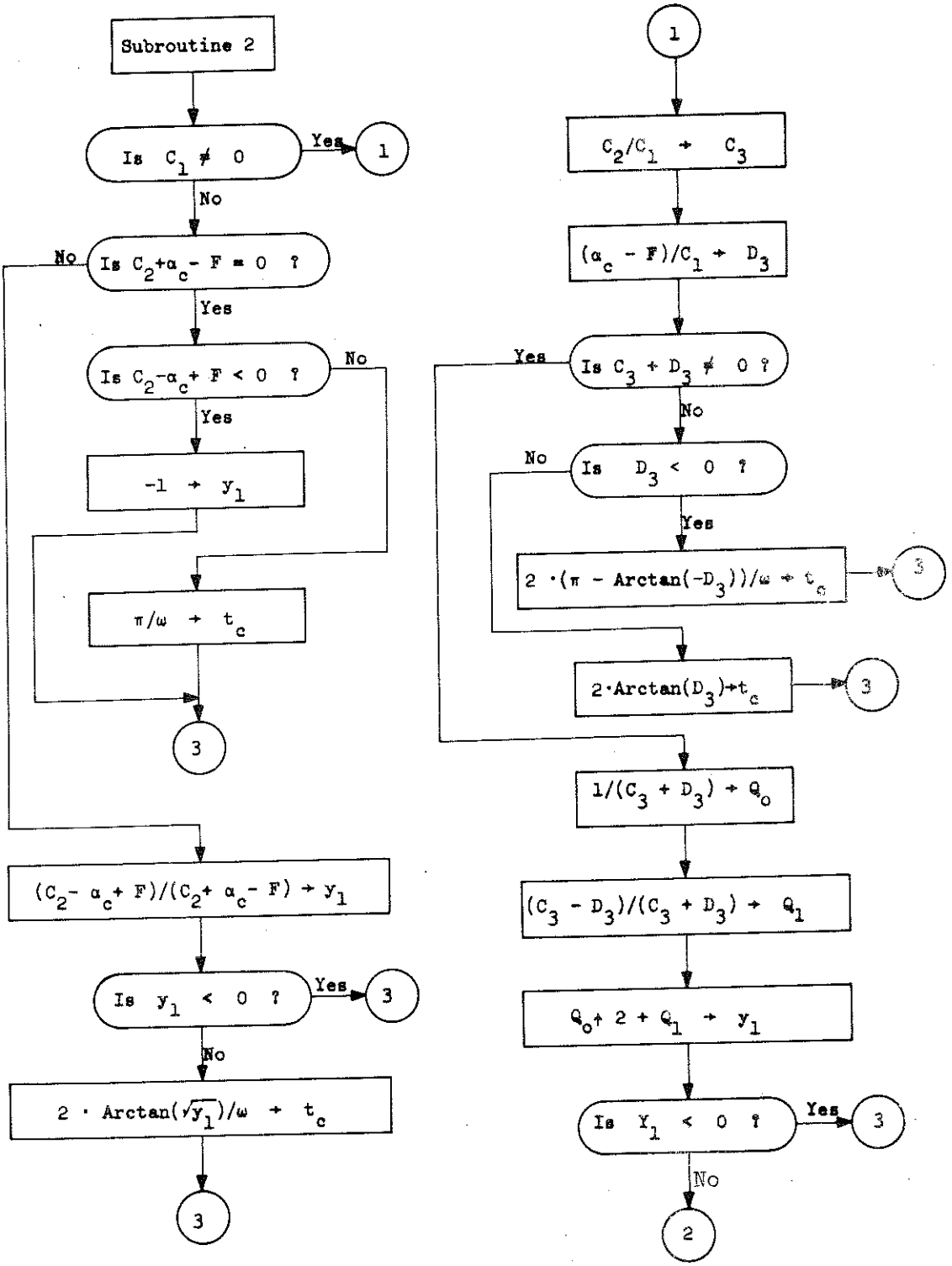
Subroutine 2
Is $C_1 \neq 0$
Yes
1
No
Is $C_2+\alpha_c-F=0$?
No
Yes
Is $C_2-\alpha_c+F<0$?
No
Yes
$-1 \rightarrow y_1$
$\pi/\omega \rightarrow t_c$
3
$(C_2-\alpha_c+F)/(C_2+\alpha_c-F) \rightarrow y_1$
Is $y_1 < 0$?
Yes
3
No
$2 \cdot \text{Arctan}(\sqrt{y_1})/\omega \rightarrow t_c$
3
1
$C_2/C_1 \rightarrow C_3$
$(\alpha_c - F)/C_1 \rightarrow D_3$
Yes
Is $C_3 + D_3 \neq 0$?
No
No
Is $D_3 < 0$?
Yes
$2 \cdot(\pi - \text{Arctan}(-D_3))/\omega \rightarrow t_c$
3
$2 \cdot \text{Arctan}(D_3) \rightarrow t_c$
3
$1/(C_3 + D_3) \rightarrow Q_o$
$(C_3 - D_3)/(C_3 + D_3) \rightarrow Q_1$
$Q_o \uparrow 2 + Q_1 \rightarrow y_1$
Is $Y_1 < 0$?
Yes
3
No
2

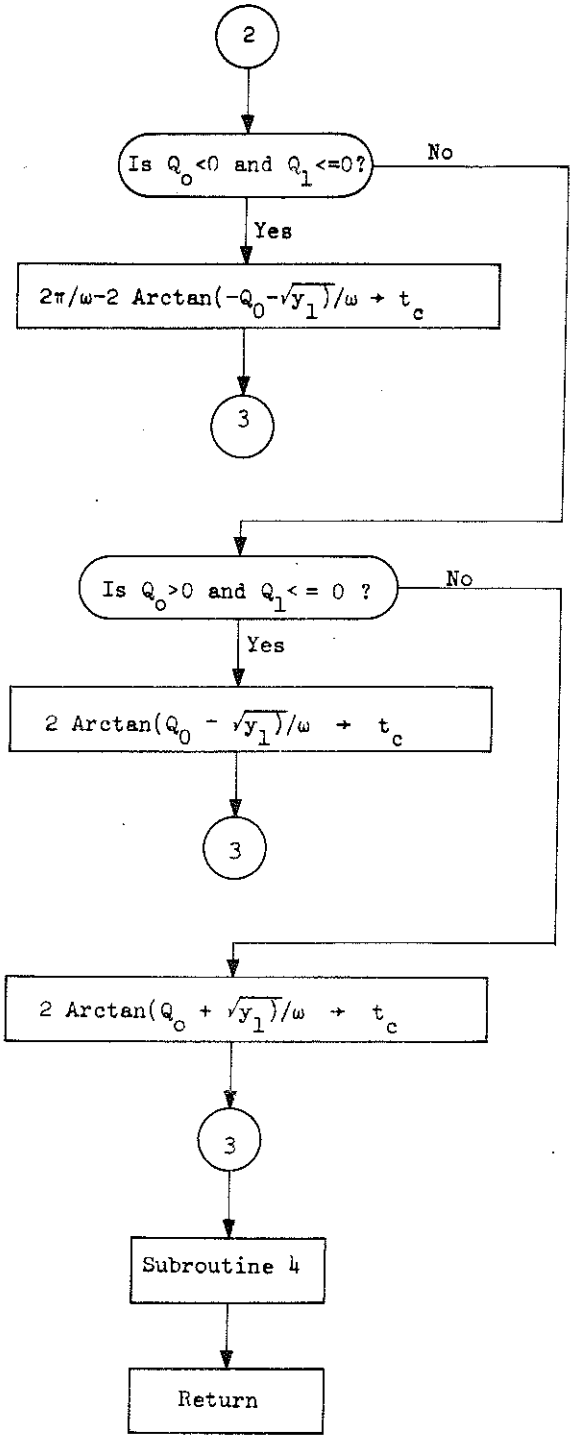
2
Is Q_o<0 and Q_1<=0?
No
Yes
$2\pi/\omega-2$ Arctan$(-Q_0-\sqrt{y_1})/\omega \rightarrow t_c$
3
Is Q_o>0 and Q_1< = 0 ?
No
Yes
2 Arctan$(Q_0 - \sqrt{y_1})/\omega \rightarrow t_c$
3
2 Arctan$(Q_o + \sqrt{y_1})/\omega \rightarrow t_c$
3
Subroutine 4
Return

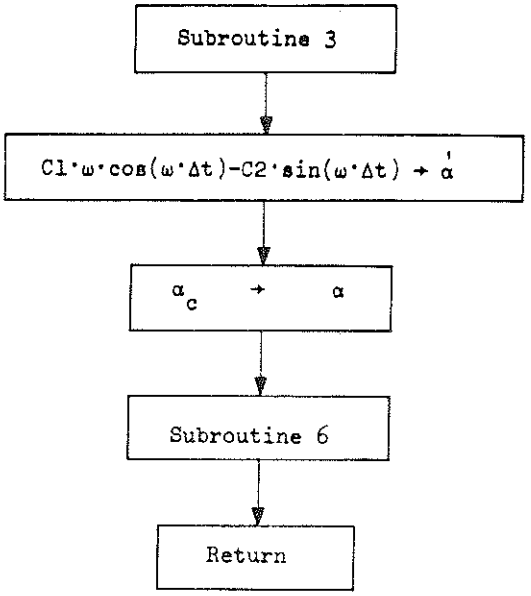
Subroutine 3
$C1\cdot\omega\cdot\cos(\omega\cdot\Delta t)-C2\cdot\sin(\omega\cdot\Delta t) \rightarrow \dot{\alpha}$
$\alpha_c \rightarrow \alpha$
Subroutine 6
Return

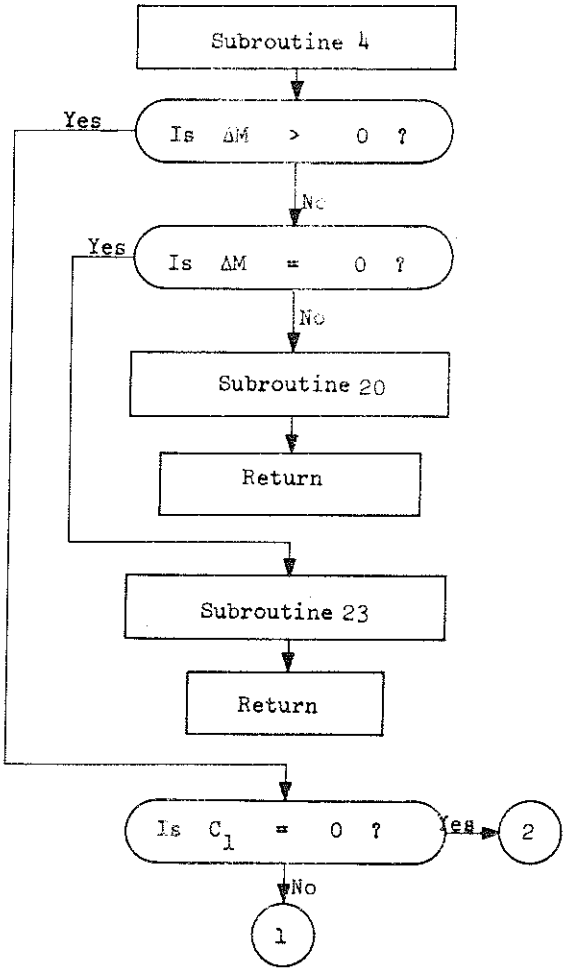
Subroutine 4
Yes
Is ΔM > 0 ?
No
Yes
Is ΔM = 0 ?
No
Subroutine 20
Return
Subroutine 23
Return
Is C_1 = 0 ?
Yes
2
No
1

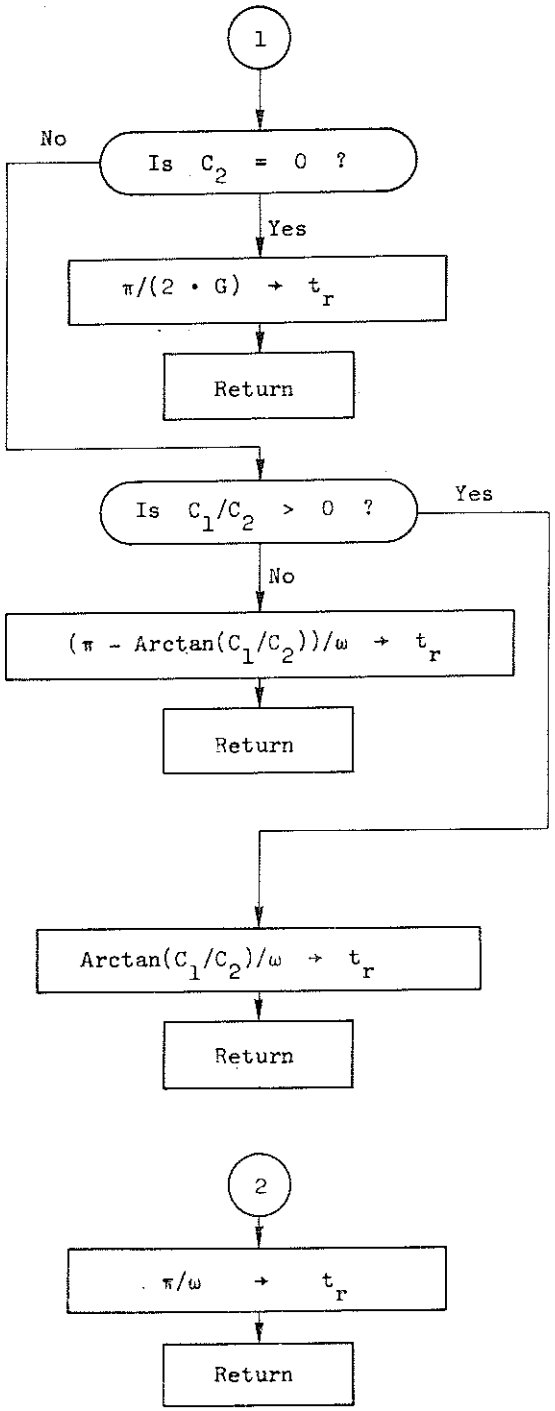
1
No
Is $C_2 = 0$?
Yes
$\pi/(2 \cdot G) \rightarrow t_r$
Return
Is $C_1/C_2 > 0$?
Yes
No
$(\pi - \text{Arctan}(C_1/C_2))/\omega \rightarrow t_r$
Return
$\text{Arctan}(C_1/C_2)/\omega \rightarrow t_r$
Return
2
$\pi/\omega \rightarrow t_r$
Return

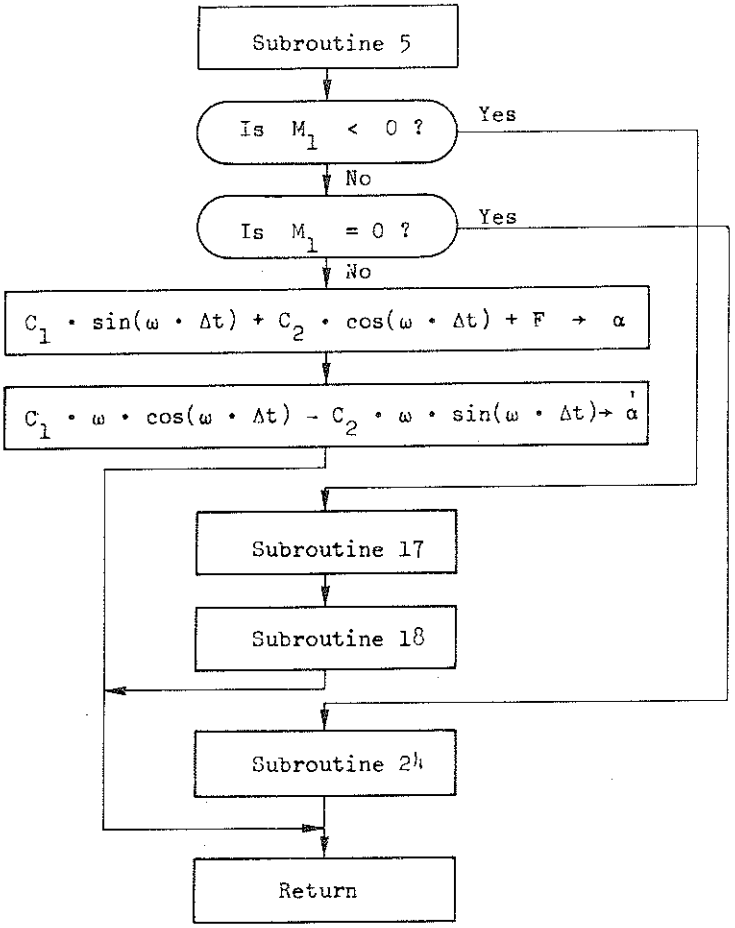
Subroutine 5
Is $M_1 < 0$?
Yes
No
Is $M_1 = 0$?
Yes
No
$C_1 \cdot \sin(\omega \cdot \Delta t) + C_2 \cdot \cos(\omega \cdot \Delta t) + F \rightarrow \alpha$
$C_1 \cdot \omega \cdot \cos(\omega \cdot \Delta t) - C_2 \cdot \omega \cdot \sin(\omega \cdot \Delta t) \rightarrow \alpha'$
Subroutine 17
Subroutine 18
Subroutine 24
Return

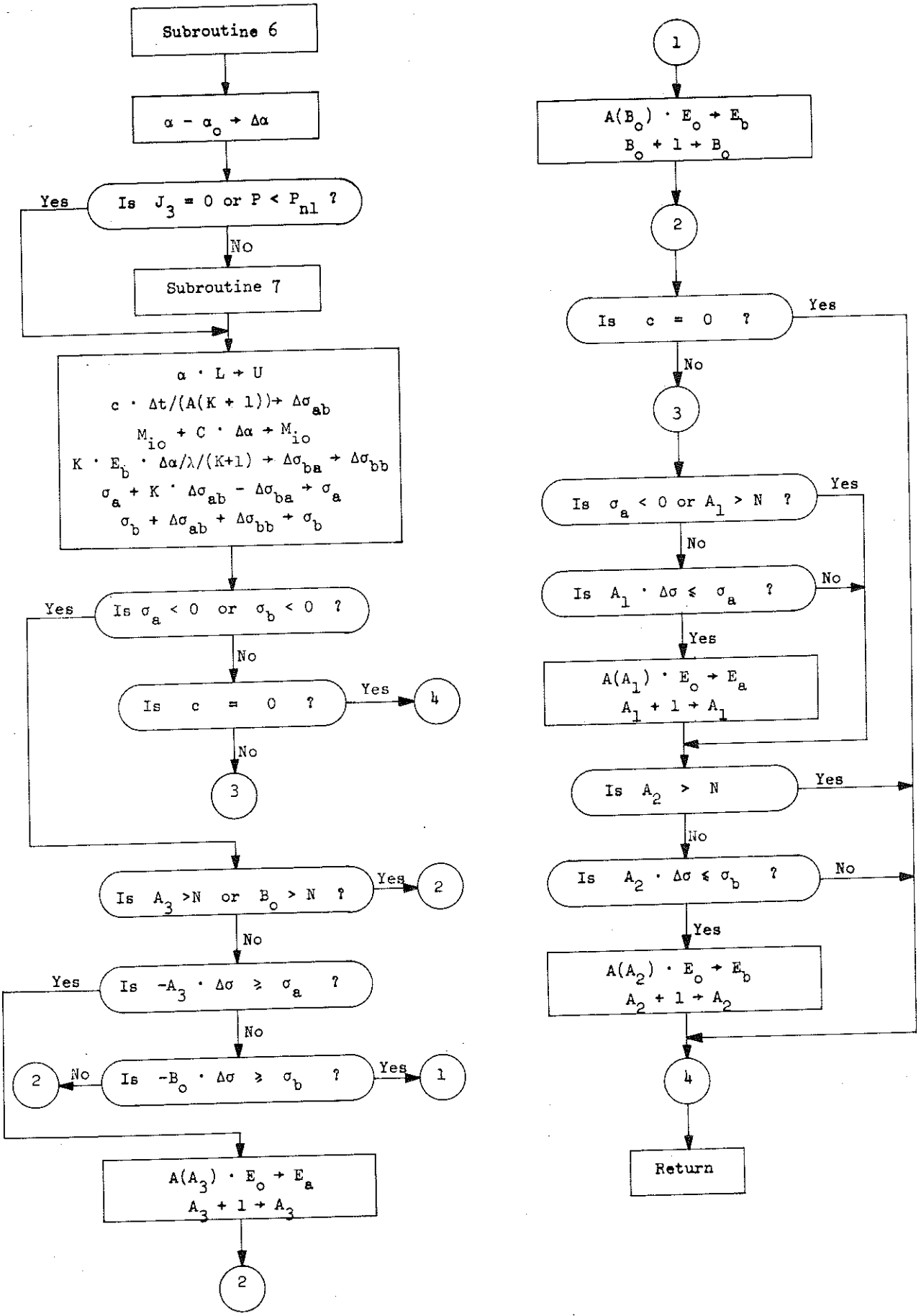
Subroutine 6
α - α_o → Δα
Yes
Is J_3 = 0 or P < P_nl ?
No
Subroutine 7
α · L → U
c · Δt/(A(K + 1)) → Δσ_ab
M_io + C · Δα → M_io
K · E_b · Δα/λ/(K+1) → Δσ_ba → Δσ_bb
σ_a + K · Δσ_ab - Δσ_ba → σ_a
σ_b + Δσ_ab + Δσ_bb → σ_b
Yes
Is σ_a < 0 or σ_b < 0 ?
No
Is c = 0 ?
Yes
4
No
3
Is A_3 >N or B_o > N ?
Yes
2
No
Yes
Is -A_3 · Δσ ≥ σ_a ?
No
2
No
Is -B_o · Δσ ≥ σ_b ?
Yes
1
A(A_3) · E_o → E_a
A_3 + 1 → A_3
2
1
A(B_o) · E_o → E_b
B_o + 1 → B_o
2
Is c = 0 ?
Yes
No
3
Is σ_a < 0 or A_1 > N ?
Yes
No
Is A_1 · Δσ ≤ σ_a ?
No
Yes
A(A_1) · E_o → E_a
A_1 + 1 → A_1
Is A_2 > N
Yes
No
Is A_2 · Δσ ≤ σ_b ?
No
Yes
A(A_2) · E_o → E_b
A_2 + 1 → A_2
4
Return

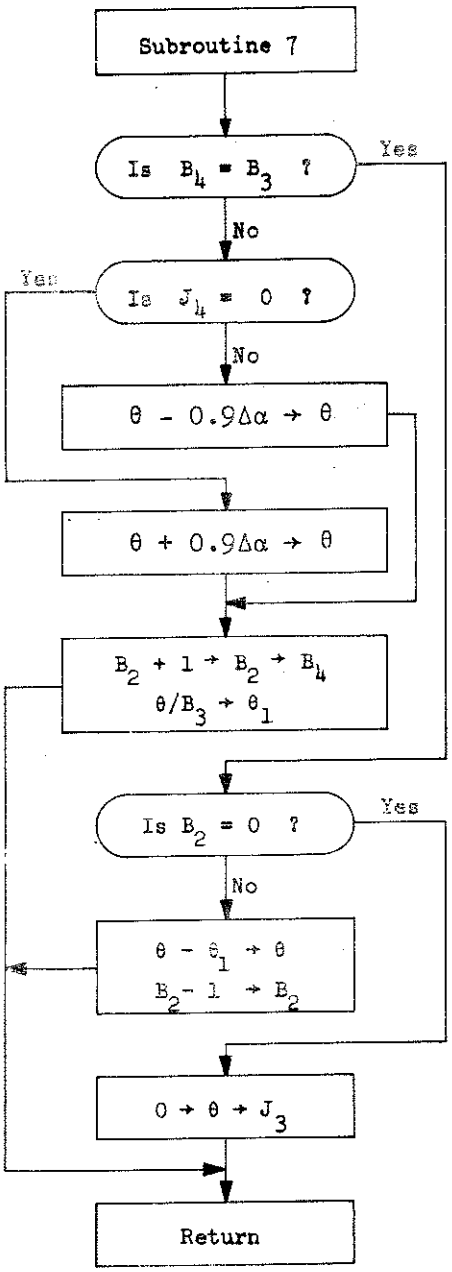
Subroutine 7
Is $B_4 = B_3$?
Yes
No
Is $J_4 = 0$?
Yes
No
$\theta - 0.9\Delta\alpha \rightarrow \theta$
$\theta + 0.9\Delta\alpha \rightarrow \theta$
$B_2 + 1 \rightarrow B_2 \rightarrow B_4$
$\theta/B_3 \rightarrow \theta_1$
Is $B_2 = 0$?
Yes
No
$\theta - \theta_1 \rightarrow \theta$
$B_2 - 1 \rightarrow B_2$
$0 \rightarrow \theta \rightarrow J_3$
Return

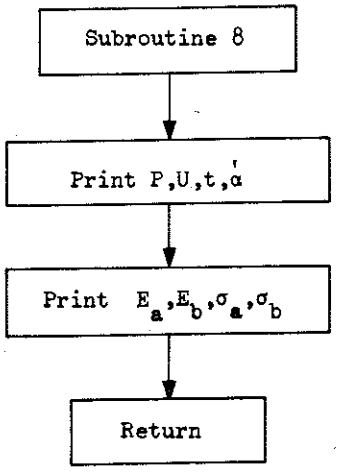
Subroutine 8
Print P,U,t,α'
Print $E_a, E_b, \sigma_a, \sigma_b$
Return

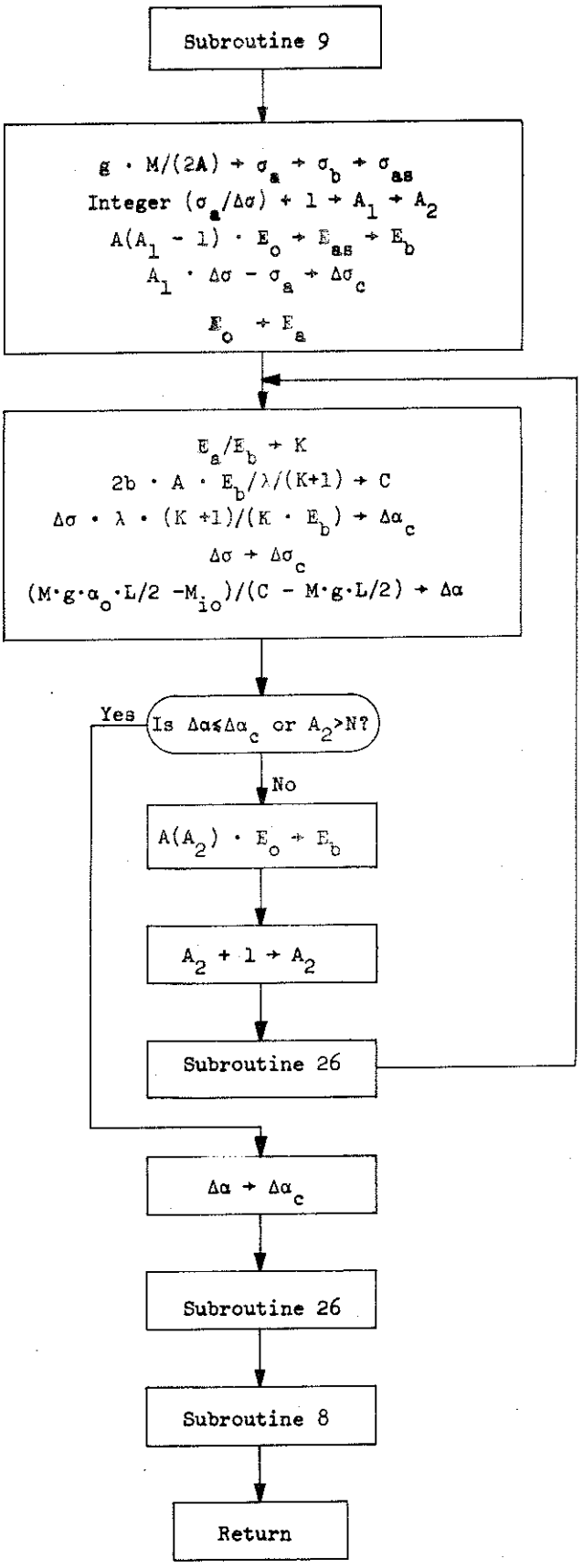
Subroutine 9
$g \cdot M/(2A) \rightarrow \sigma_a \rightarrow \sigma_b \rightarrow \sigma_{as}$
Integer $(\sigma_a/\Delta\sigma) + 1 \rightarrow A_1 \rightarrow A_2$
$A(A_1 - 1) \cdot E_o \rightarrow E_{as} \rightarrow E_b$
$A_1 \cdot \Delta\sigma - \sigma_a \rightarrow \Delta\sigma_c$
$E_o \rightarrow E_a$
$E_a/E_b \rightarrow K$
$2b \cdot A \cdot E_b/\lambda/(K+1) \rightarrow C$
$\Delta\sigma \cdot \lambda \cdot (K+1)/(K \cdot E_b) \rightarrow \Delta\alpha_c$
$\Delta\sigma \rightarrow \Delta\sigma_c$
$(M \cdot g \cdot \alpha_o \cdot L/2 - M_{io})/(C - M \cdot g \cdot L/2) \rightarrow \Delta\alpha$
Yes
Is $\Delta\alpha \leq \Delta\alpha_c$ or $A_2 > N$?
No
$A(A_2) \cdot E_o \rightarrow E_b$
$A_2 + 1 \rightarrow A_2$
Subroutine 26
$\Delta\alpha \rightarrow \Delta\alpha_c$
Subroutine 26
Subroutine 8
Return

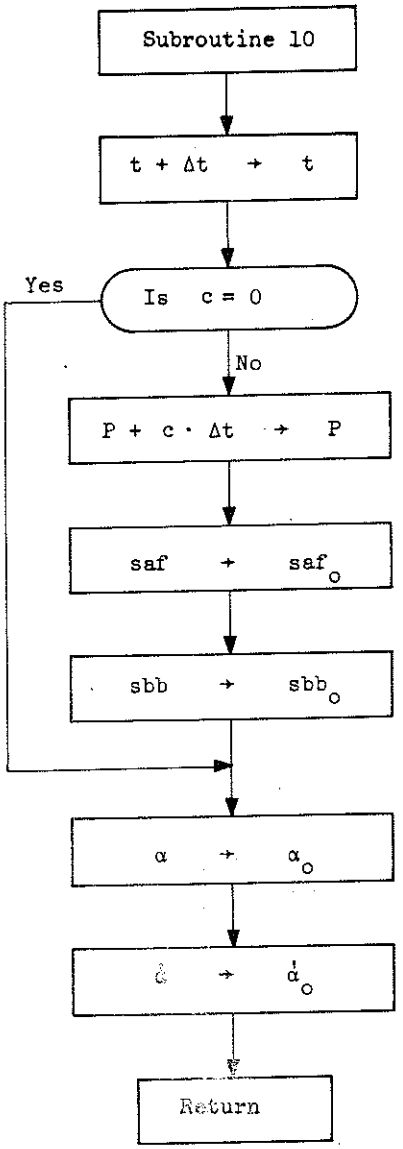
Subroutine 10
t + Δt → t
Yes
Is c = 0
No
P + c · Δt → P
saf → saf$_o$
sbb → sbb$_o$
α → α$_o$
α̇ → α̇$_o$
Return

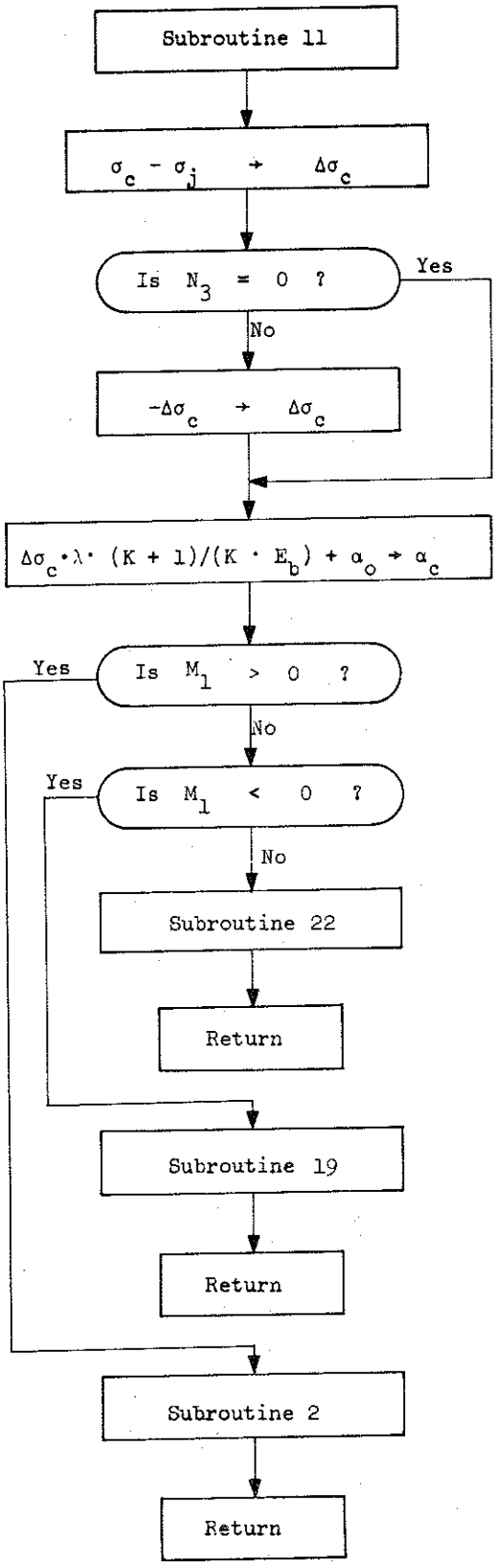
Subroutine 11
σ$_c$ - σ$_j$ → Δσ$_c$
Is N$_3$ = 0 ?
Yes
No
-Δσ$_c$ → Δσ$_c$
Δσ$_c$·λ·(K + 1)/(K · E$_b$) + α$_o$ → α$_c$
Yes
Is M$_1$ > 0 ?
No
Yes
Is M$_1$ < 0 ?
No
Subroutine 22
Return
Subroutine 19
Return
Subroutine 2
Return

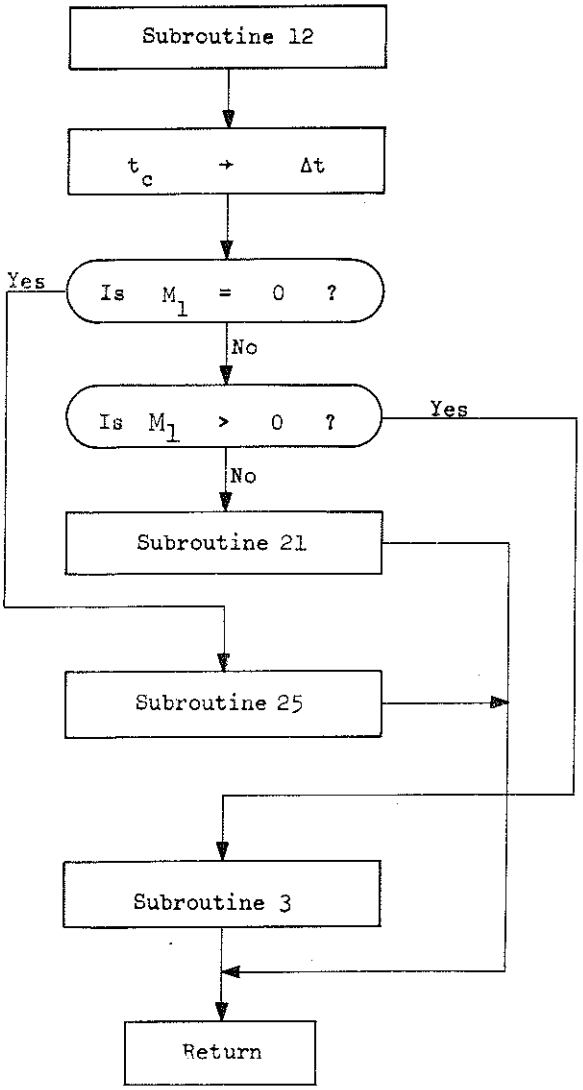
Subroutine 12
t_c → Δt
Yes
Is M_1 = 0 ?
No
Is M_1 > 0 ?
Yes
No
Subroutine 21
Subroutine 25
Subroutine 3
Return

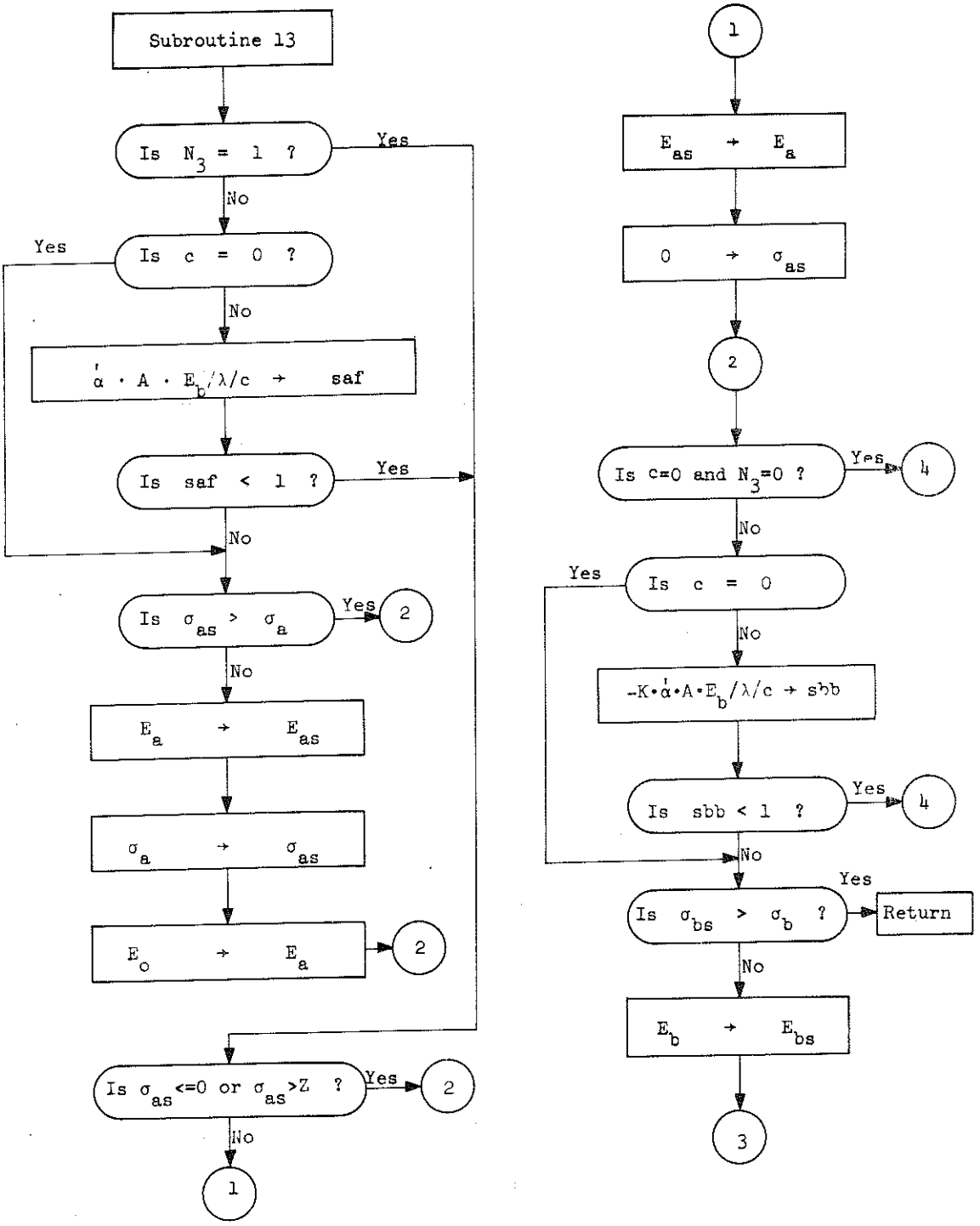
Subroutine 13
Is N_3 = 1 ?
Yes
No
Yes
Is c = 0 ?
No
$\alpha' \cdot A \cdot E_b/\lambda/c \rightarrow$ saf
Is saf < 1 ?
Yes
No
Is $\sigma_{as} > \sigma_a$
Yes
2
No
$E_a \rightarrow E_{as}$
$\sigma_a \rightarrow \sigma_{as}$
$E_o \rightarrow E_a$
2
Is $\sigma_{as} <= 0$ or $\sigma_{as} > Z$?
Yes
2
No
1
1
$E_{as} \rightarrow E_a$
$0 \rightarrow \sigma_{as}$
2
Is c=0 and N_3=0 ?
Yes
4
No
Yes
Is c = 0
No
$-K \cdot \alpha' \cdot A \cdot E_b/\lambda/c \rightarrow$ sbb
Is sbb < 1 ?
Yes
4
No
Yes
Is $\sigma_{bs} > \sigma_b$?
Return
No
$E_b \rightarrow E_{bs}$
3

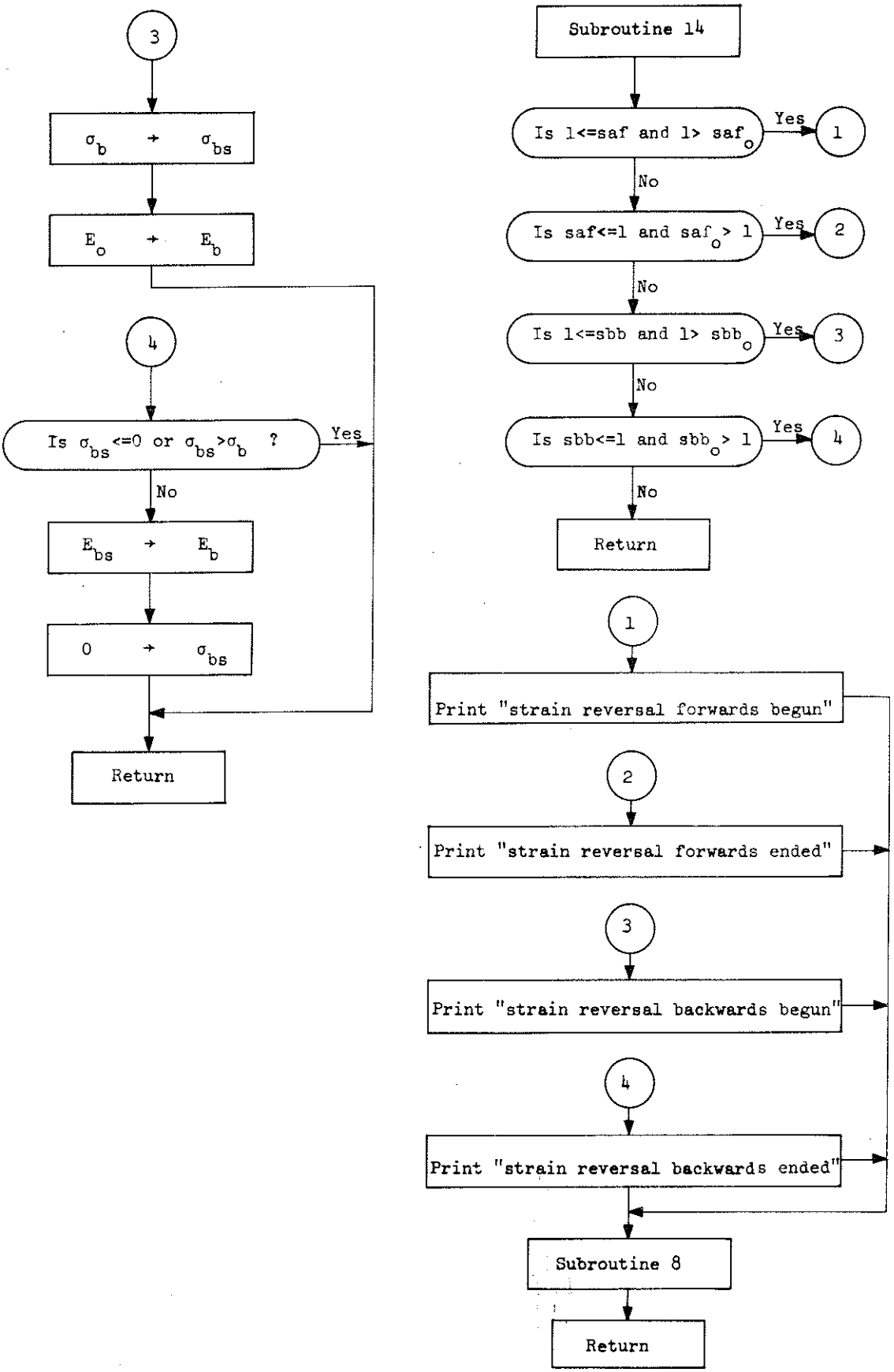
Subroutine 14
Is 1<=saf and 1> saf$_o$
Yes
1
No
Is saf<=1 and saf$_o$> 1
Yes
2
No
Is 1<=sbb and 1> sbb$_o$
Yes
3
No
Is sbb<=1 and sbb$_o$> 1
Yes
4
No
Return
1
Print "strain reversal forwards begun"
2
Print "strain reversal forwards ended"
3
Print "strain reversal backwards begun"
4
Print "strain reversal backwards ended"
Subroutine 8
Return
3
σ_b → σ_{bs}
E_o → E_b
4
Is σ_{bs}<=0 or σ_{bs}>σ_b ?
Yes
No
E_{bs} → E_b
0 → σ_{bs}
Return

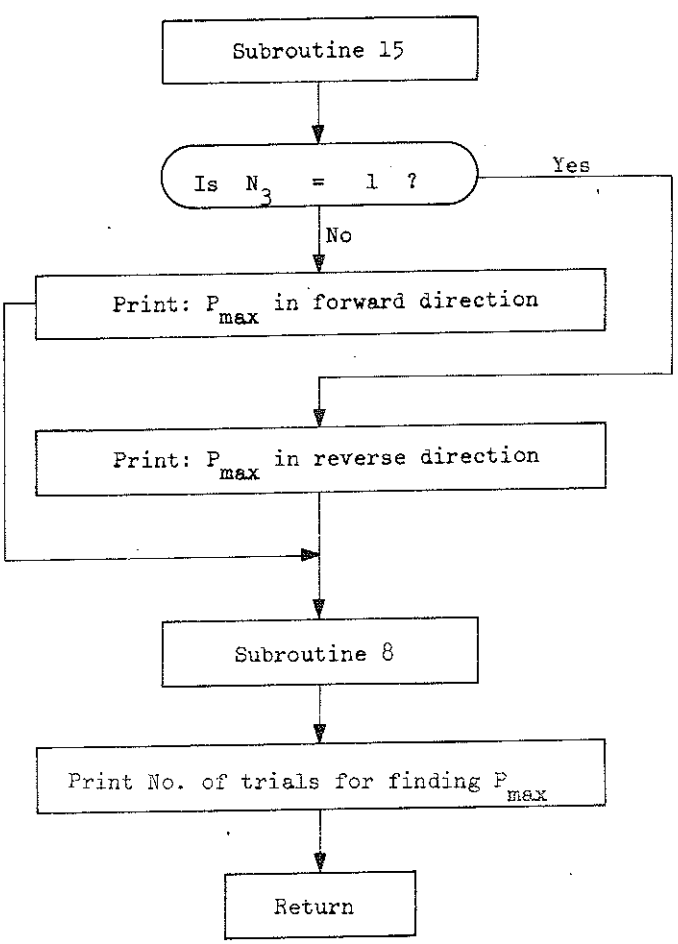
Subroutine 15
Is N_3 = 1 ?
Yes
No
Print: P_{max} in forward direction
Print: P_{max} in reverse direction
Subroutine 8
Print No. of trials for finding P_{max}
Return

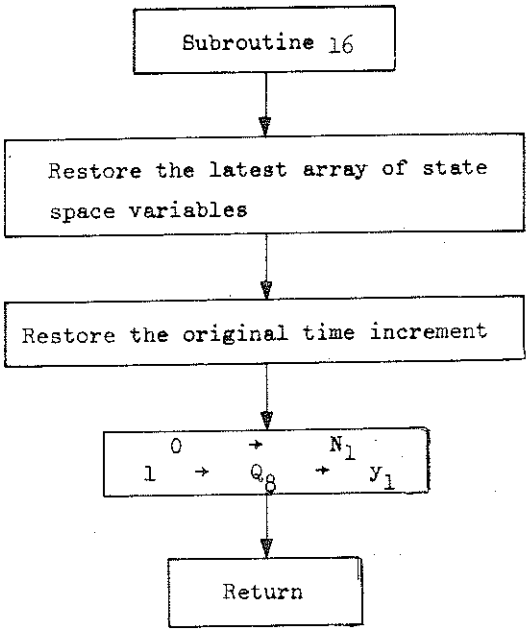
Subroutine 16
Restore the latest array of state space variables
Restore the original time increment
0 → N_1
1 → Q_8 → y_1
Return

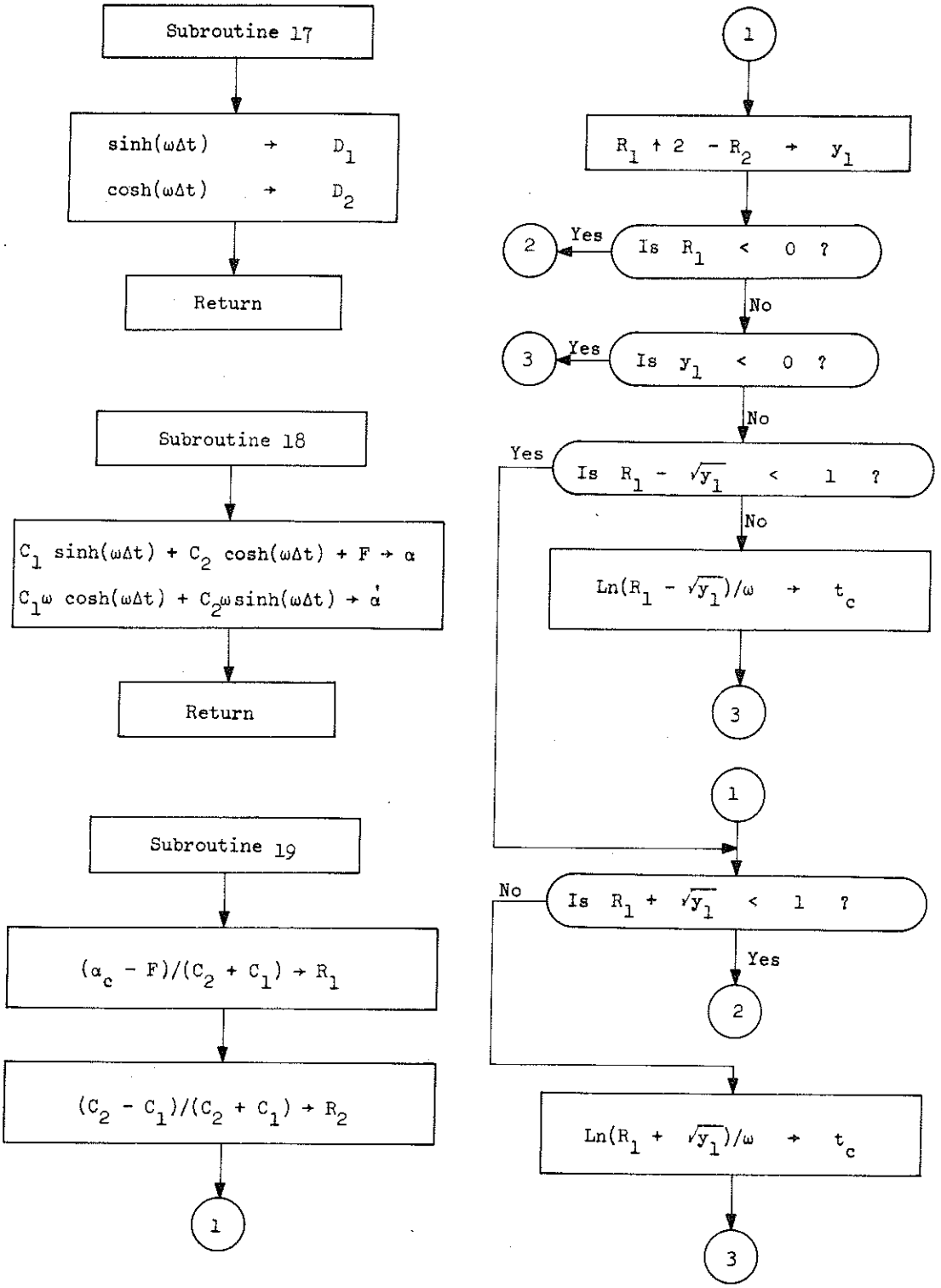
Subroutine 17
sinh(ωΔt) → D1
cosh(ωΔt) → D2
Return
Subroutine 18
C1 sinh(ωΔt) + C2 cosh(ωΔt) + F → α
C1ω cosh(ωΔt) + C2ω sinh(ωΔt) → α'
Return
Subroutine 19
(αc - F)/(C2 + C1) → R1
(C2 - C1)/(C2 + C1) → R2
1
1
R1 ↑ 2 - R2 → y1
Is R1 < 0 ?
Yes
2
No
Is y1 < 0 ?
Yes
3
No
Is R1 - √y1 < 1 ?
Yes
No
Ln(R1 - √y1)/ω → tc
3
1
Is R1 + √y1 < 1 ?
No
Yes
2
Ln(R1 + √y1)/ω → tc
3

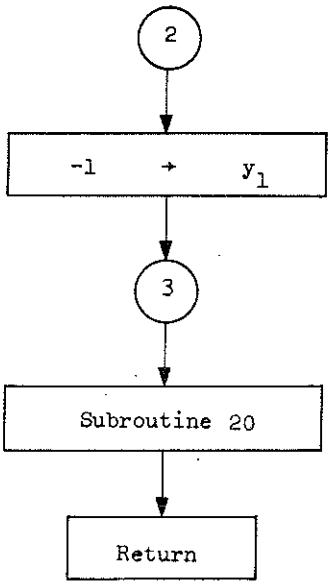
2
-1 → y_1
3
Subroutine 20
Return

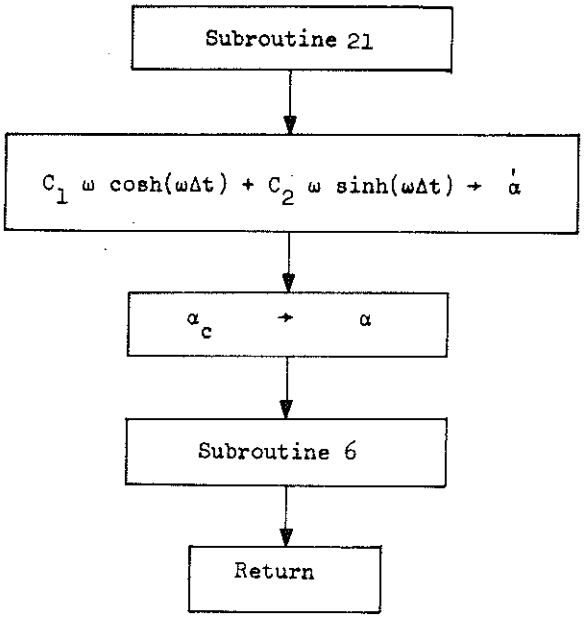
Subroutine 21
$C_1 \omega \cosh(\omega\Delta t) + C_2 \omega \sinh(\omega\Delta t) \rightarrow \dot{\alpha}$
$\alpha_c \rightarrow \alpha$
Subroutine 6
Return

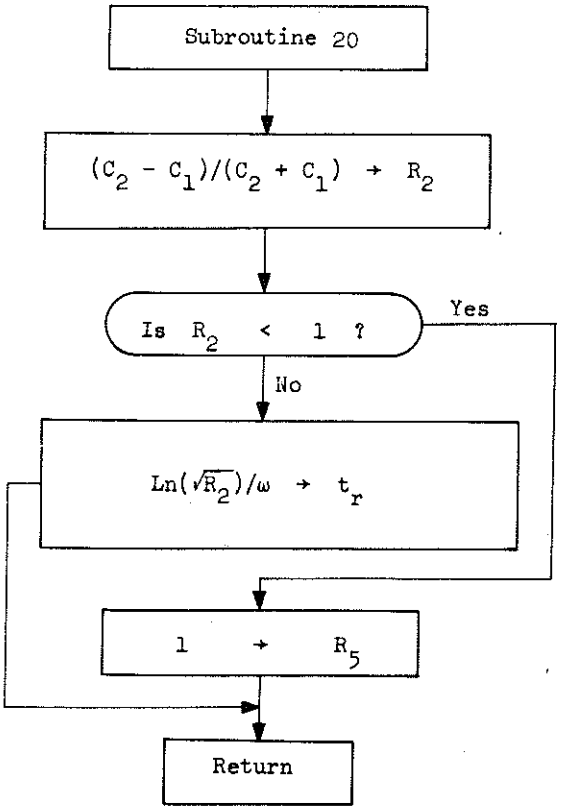
Subroutine 20
$(C_2 - C_1)/(C_2 + C_1) \rightarrow R_2$
Is R_2 < 1 ?
Yes
No
$\mathrm{Ln}(\sqrt{R_2})/\omega \rightarrow t_r$
1 → R_5
Return

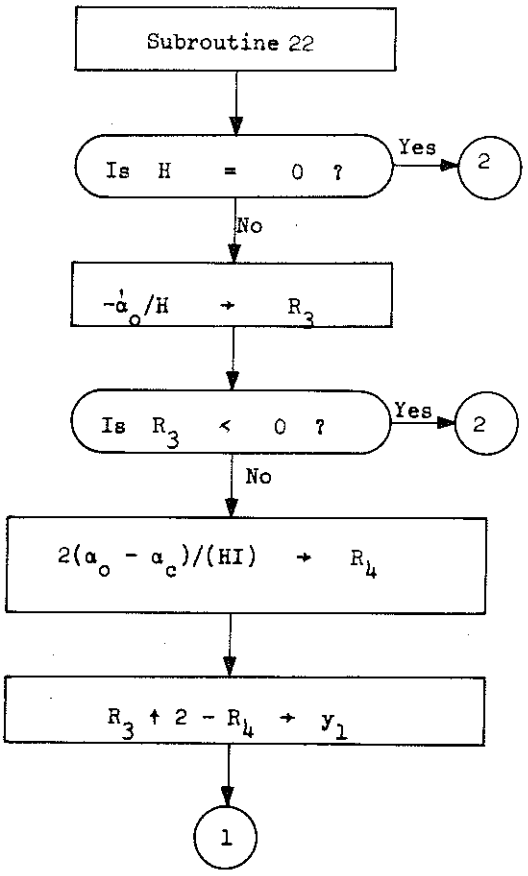
Subroutine 22
Is H = 0 ?
Yes
2
No
$-\dot{\alpha}_o/H \rightarrow R_3$
Is R_3 < 0 ?
Yes
2
No
$2(\alpha_o - \alpha_c)/(HI) \rightarrow R_4$
$R_3 + 2 - R_4 \rightarrow y_1$
1

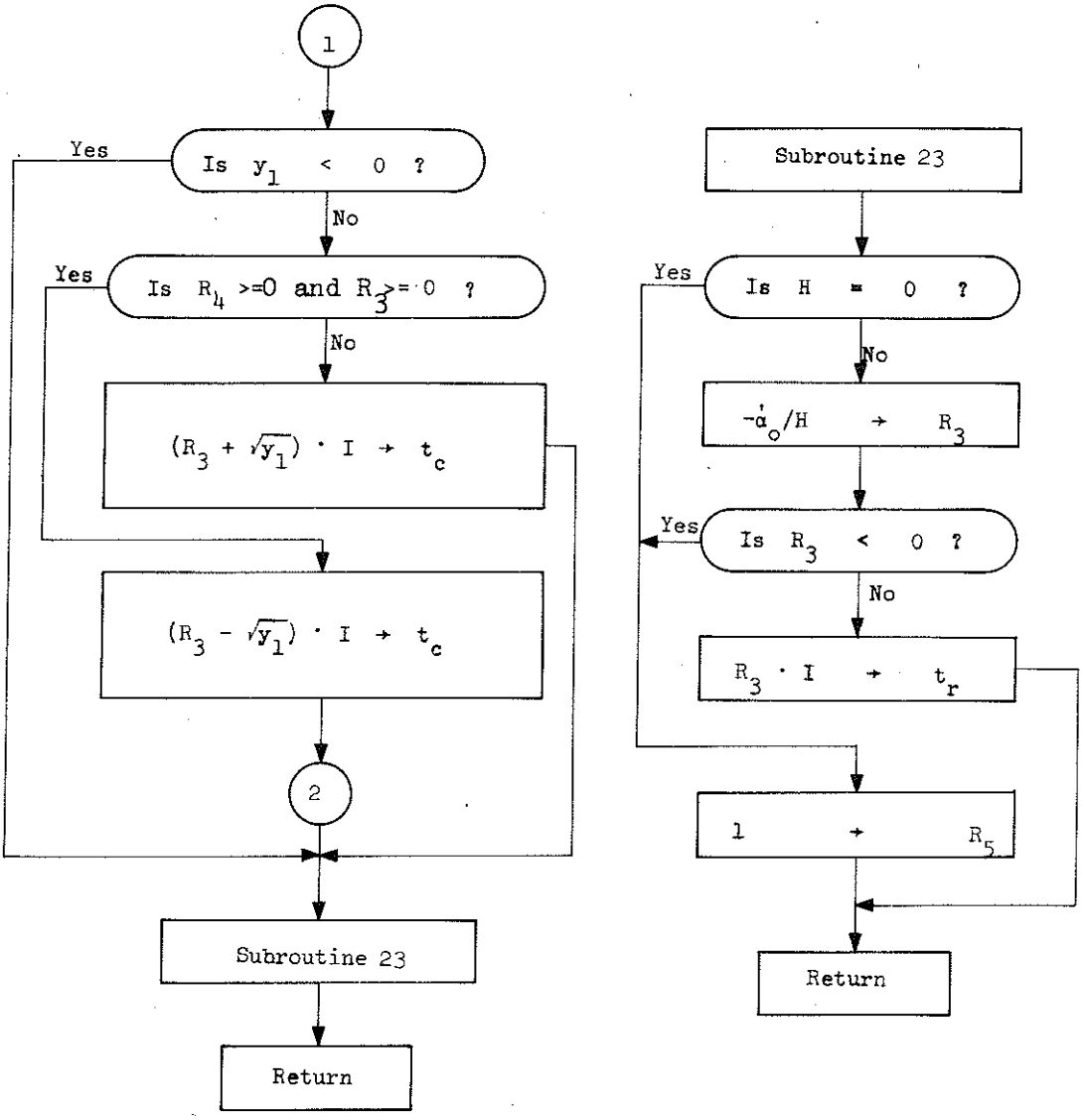
1
Yes
Is y_1 < 0 ?
No
Yes
Is R_4 >=0 and R_3 >= 0 ?
No
$(R_3 + \sqrt{y_1}) \cdot I \rightarrow t_c$
$(R_3 - \sqrt{y_1}) \cdot I \rightarrow t_c$
2
Subroutine 23
Return
Subroutine 23
Yes
Is H = 0 ?
No
$-\dot{a}_o/H \rightarrow R_3$
Yes
Is R_3 < 0 ?
No
$R_3 \cdot I \rightarrow t_r$
1 → R_5
Return

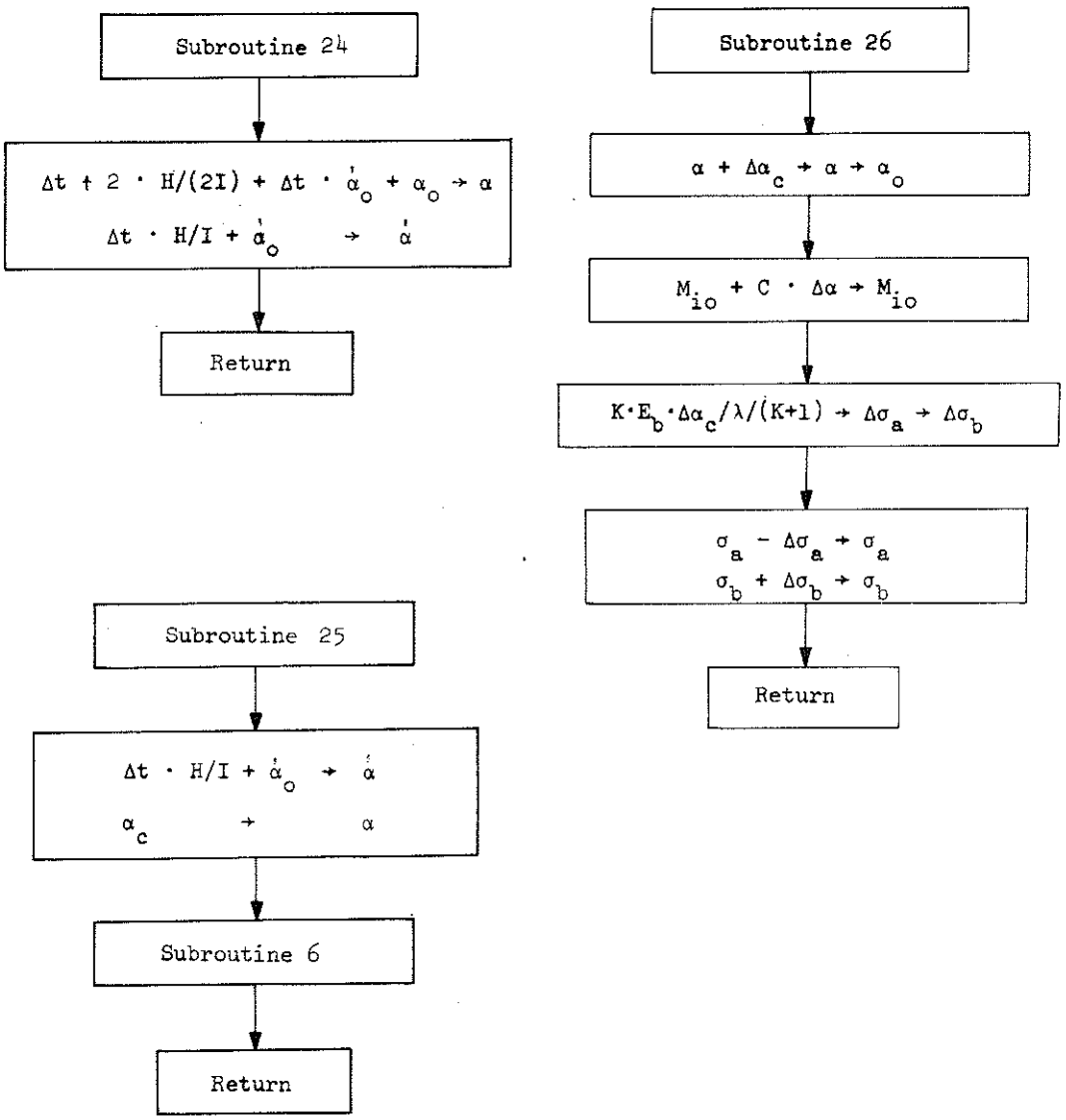
Subroutine 24
Δt + 2 · H/(2I) + Δt · α̇o + αo → α
Δt · H/I + α̇o → α̇
Return
Subroutine 26
α + Δαc → α → αo
Mio + C · Δα → Mio
K·Eb·Δαc/λ/(K+1) → Δσa → Δσb
σa − Δσa → σa
σb + Δσb → σb
Return
Subroutine 25
Δt · H/I + α̇o → α̇
αc → α
Subroutine 6
Return

REFERENCES

1. Considère, A., "Resistance de pièce comprimés," Congrès International des Procédés de Construction, Vol. 3, Paris, 1891, p. 371.

2. Jasinski, F., "Noch ein Wort zu den Knickfragen," Schweizerische Bauzeitung, Vol. XXV, No. 25, June 22, 1895, p. 172.

3. Engesser, Fr., "Ueber Knickfragen," Schweizerische Bauzeitung, Vol. XXVI, No. 4, July 27, 1895, p.24.

4. Kármán, T.V., "Untersuchungen über Knickfestigkeit," Forschungsarbeiten, No. 81, Berlin, 1910.

5. Shanley, F.R., "The Column Paradox," Journal of the Aeronautical Sciences, Vol. 13, No. 12, December, 1946.

6. Shanley, F.R., "Inelastic Column Theory," Journal of the Aeronautical Sciences, Vol. 14, No. 5, May, 1947.

7. Chi-Teh, Wong, "Inelastic Column Theories and an Analysis of Experimental Observations," Journal of the Aeronautical Sciences, Vol. 15, May, 1948, pp. 283-292.

8. Duberg, J.E., and Wilder, T.W., "Column Behaviour in the Plastic Stress Range," Journal of the Aeronautical Sciences, Vol. 17, No. 6, June, 1950, pp. 323-327.

9. Tung-Hua, Lin, "Inelastic Column Buckling," Journal of the Aeronautical Sciences, Vol. 17, March, 1950, pp. 159-172.

10. Cicala, P., "Column Buckling in the Elastoplastic Range," Journal of the Aeronautical Sciences, Vol. 17, August, 1950, pp. 508-512.

11. Schleicher, F., "Zur Theorie der plastischen Knickung," Der Bauingenieur, Vol. 26, No. 5, 1951, pp. 139-141, Part I; Vol. 26, July, 1950, pp. 197-201, Part II.

12. Pearson, C.E., "Bifurcation Criterion and Plastic Buckling of Plates and Columns," Journal of the Aeronautical Sciences, Vol. 17, No. 7, July, 1950, pp. 417-421.

13. Pflüger, A., "Zur plastischen Knickung gerader Stäbe," Ingenieur-Archiv, Vol. 20, No. 5, 1952, pp. 291-301.

14. Malvick, A.J., and Lee, L.H.N., "Buckling Behaviour of an Inelastic Column," Journal of the Engineering Mechanics Division, ASCE, Vol. 91, No. EM3, Proc. Paper 4372, June, 1965, pp. 113-127.

15. Hill, R., and Sewell, M.J., "A General Theory of Inelastic Column Failure," J. Mech. Phys. Solids, Vol. 8, 1960, pp. 105-111, Part I; Vol. 8, 1960, pp. 112-118, Part II; Vol. 10, 1962, pp. 285-300, Part III.

16. Lee, L.H.N., "Inelastic Column Stability Subjected to Time-Dependent Load," Int. J. Solids Structures, Vol. 3, 1967, pp. 853-864.

17. Timoshenko, S.P., and Gere, J.M., "Theory of Elastic Stability," 2:nd ed., Mc Graw-Hill, New York, 1961.

18. Chajes, A., "Stability Behaviour Illustrated by Simple Models," Journal of the Structural Division, ASCE, Vol. 95, ST 6, proc. paper 6598, June, 1969, pp. 1153-1171.

19. The Staff of the Computation Laboratory, "Tables of the modified Hankel Functions of Order One-Third and of their Derivatives," The Annals of the Computation Laboratory of Havard University, Vol. 2, Cambridge, Massachusetts, 1945.

20. McIvor, I.K., and Bernard, J.E., "The Dynamic Response of Columns Under Short Duration Axial Loads," Journal of Applied Mechanics, September, 1973, pp. 688-692.

21. Pettersson, O., "Ett icke-konservativt knäckningsproblem", Festskrift till Professor Carl Forssell, Stockholm, 1956.

22. Cf. Timoshenko, S.P., "History of Strength of Materials," McGraw-Hill Book Company, Inc., New York, 1953, pp 28-34.

23. Hurty, W.C., and Rubinstein, M.F., "Dynamics of Structures", Prentice-Hall, Inc., Englewood Cliffs, New Jersey, 1964.